
PH.D. DISSERTATION

Presented by
Aralar ERDOZAIN

Submitted to
Université de Pau et des Pays de l'Adour
and
Universidad del País Vasco - Euskal Herriko Unibertsitatea

Defended on December 15, 2016

Model Reduction Techniques for the Fast Inversion of Borehole Resistivity Measurements

Reviewers:

Serge NICAISE	Professeur Université de Valenciennes et du Hainaut-Cambrésis
Grégory VIAL	Professeur Ecole Centrale de Lyon

Defense Committee:

Hélène BARUCQ	Directrice de Recherches INRIA	Advisor
Abderrahmane BENDALI	Professeur INSA de Toulouse	Examiner
Gilles CARBOU	Professeur UPPA	President
Rabia DJELLOULI	Professor California State University Northridge	Examiner
Ignacio MUGA	Professor Pontificia Universidad de Valparaíso	Examiner
David PARDO	Professor Euskal Herriko Unibertsitatea	Advisor
Victor PERON	Maître de Conférences UPPA	Advisor
Grégory VIAL	Professeur Ecole Centrale de Lyon	Reviewer

A mis padres.

ACKNOWLEDGEMENTS

I would like to begin by thanking the people that have contributed academically in the development of this project. I thank H el ene Barucq, my supervisor at the University of Pau and head of the team Magique 3D, for giving me the opportunity of being part of this team and for welcoming me from the very first day. I would also like to thank Victor P eron, my co-supervisor in the University of Pau, for the time he has dedicated to me, and the patience he has had during this whole process. I also thank David Pardo, my supervisor in the University of the Basque Country, for welcoming me at Bilbao during each of my stays and for the time he has dedicated to me during these periods. To sum up, I thank the three of them for giving me the opportunity to learn from and with them.

Secondly, I would like to thank the many researchers and collaborators that contributed in some way to the development of this project or helped me in any way during this period. In particular, I thank Dr.  ngel Rodr iguez-Rozas, his experience and advices where really helpful when I developed my code. Special mention goes also to Professor Ignacio Muga. I thank him for the welcome he gave me in Valparaiso and the work we have done together. Finally, I thank Professor Marc Duruff e. My work with him was brief but it was really helpful and his welcome at Bordeaux was very nice.

I would like to continue by thanking the people of the team Magique 3D. I thank all the permanent researchers of the team for their help and advices. I also thank the rest of Ph.D. students, engineers, and "stagiaires" that have worked side by side with me. I could not think of better colleagues to accompany me during this Ph.D.. You are the ones that understand best what performing this kind of work is and it is thank to you that work has become something enjoyable during this period. During my stays at Bilbao, I had the opportunity to meet some old colleagues and to meet other new ones, I thank you all for making my stays at Bilbao so pleasant. Finally, I thank the people I met in Chile for being so friendly and for teaching me their language, which is basically also the same as mine, but sometimes it does not seem so.

Moving to a more personal level, I thank my friends from the Bachelor's degree of mathematics. I gave my first steps in mathematics with you in Bilbao and you were the ones that made this experience so great that I got the motivation to continue with a master and then a Ph.D.. Eskerrik asko denoi! In the same way, I would like to thank my colleagues of the master. This period was much more brief,

but from the very first moment all of us got along very well. Thanks for the good relationship we had and the good moments we spent in the three different cities the master took place.

I would like to continue by thanking my oldest friends, the ones from my hometown Tafalla. It is really great to have friends like you. You cannot image how important it is for a person like me, who lives abroad, to know that he can always count with friends like you when he comes back home. Friends that welcome you with open arms as if you had never left, even if they did not have any news from you for months.

To finish thanking my friends, I would like to mention the people that has been the most present in my life during these last years, my friends in Pau. You have been the best friends anyone could wish. You have been there in the good and in the bad moments. Believe me when I say that it is thanks to you that I have been able to muster the courage to finish this Ph.D. and that it is the moments I have spent with all of you that have made these last years worthwhile.

In general, no one wants to be in the last place, but in this case I have left the most important people for the end. Valentina, thank you for supporting me all along the way. You are the only one that truly knows how I have felt at every moment. Thank you for being there for me.

Lastly, I would like to thank those who have been there for me since ever, for every decision I have had to make in my life, my parents. You have always known how to guide me through the best path in life and you have always pushed me forward to give the best of myself. Everything that I have accomplished and everything that I am today, I owe it to you. I cannot think of anything you could have made better. Thank you for everything.

ABSTRACT

Through-casing borehole resistivity measurements are commonly acquired in order to characterize the Earth's subsurface. The use of a casing surrounding the borehole highly complicates numerical simulations of the electric potential due to its thinness and a large contrast between casing conductivity and surrounding rock formation conductivity. In this work, we model the casing as a thin cylindrical layer of uniform thickness. Motivated by realistic scenarios, we realize that the conductivity of the case is typically proportional to its thickness to the power of minus three.

In this Ph.D. Dissertation, we focus on the above problem to derive Impedance Transmission Conditions (ITCs) in order to replace the metallic casing. To do so, we start by considering a 2D model in Cartesian coordinates that serves as an initial approximation to solve the more realistic 3D axi-symmetric model (using cylindrical coordinates) considered in most realistic through casing borehole simulations. We start by considering the static (zero frequency) case, and we also derive ITCs for nonzero frequencies, which are important to understand certain physical phenomena occurring in through casing borehole measurements, namely, the so-called Delaware and Groningen effects. Then, we analyze these models by proving stability and convergence results, and we assess the numerical performance of these models by employing a Finite Element Method. Finally, we derive semi-analytical solutions for such models, which provide a more efficient way of evaluating our approximate models as in comparison with full numerical solutions.

RÉSUMÉ

Les mesures de résistivité en forage sont communément utilisées pour obtenir une meilleure caractérisation du sous-sol. L'utilisation d'un tube métallique pour couvrir le puits complique énormément les simulations numériques pour le potentiel électrique à cause de la faible épaisseur du tube et de sa conductivité élevée par rapport à celle des formations du sous-sol. Dans ce travail, motivé par des configurations réalistes, le tube est modélisé par une couche mince cylindrique d'épaisseur uniforme et la résistivité du tube est proportionnelle au cube de son épaisseur.

Dans cette thèse, on se concentre sur ce problème pour obtenir des Conditions de transmission (ITCs) approchées pour le potentiel électrique à travers le tube métallique. Pour ce faire, on considère dans une première approche, un modèle 2D en coordonnées cartésiennes, puis on résout le problème 3D axisymétrique qui est considéré dans la majorité des simulations de mesures de résistivité en forage à travers un tube. On considère d'abord le cas statique (fréquence nulle), puis on obtient des ITCs pour des fréquences non-nulles, lesquelles sont importantes pour comprendre certains phénomènes physiques, comme les effets Delaware et Groningen. Ensuite, on analyse les modèles en prouvant des résultats de stabilité et convergence, et on évalue la performance numérique de ces modèles en utilisant la méthode des éléments finis. Enfin, on construit des solutions semi-analytiques pour ces modèles, lesquelles nous fournissent une manière plus efficace d'évaluer nos modèles approchés par rapport aux solutions numériques (éléments finis).

RESUMEN

Las medidas de resistividad en perforaciones a través de tubos se utilizan de manera común para obtener una mejor caracterización del subsuelo de la tierra. El uso de un tubo que cubre el pozo complica enormemente las simulaciones numéricas debido a su finura y al gran contraste entre la conductividad del tubo y la de las formaciones rocosas. En este trabajo, modelizamos el tubo como una membrana cilíndrica fina de grosor uniforme. Basándonos en configuraciones realistas, consideramos que la conductividad del tubo es proporcional a su grosor a la potencia de menos tres.

En esta tesis doctoral, nos concentramos en el problema anterior para obtener condiciones de transmisión de impedancia (ITCs) que sirvan para reemplazar el tubo metálico. Para ello, empezamos por considerar un modelo 2D en coordenadas cartesianas, que sirve como una primera aproximación para resolver el problema 3D con simetría axial (empleando coordenadas cilíndricas) considerado en la mayoría de las simulaciones realistas de perforaciones con tubos. Empezamos por considerar el caso estático (frecuencia nula), y más tarde obtenemos ITCs para frecuencias no nulas, las cuales son importantes para entender ciertos fenómenos físicos que ocurren al obtener medidas de resistividad en pozos a través de tubos, como por ejemplo, los efectos de Delaware y Groningen. Después, analizamos estos modelos demostrando resultados de estabilidad y convergencia, y evaluamos el rendimiento numérico de estos modelos empleando el método de elementos finitos. Por último, obtenemos soluciones semi-analíticas para dichos modelos, las cuales proporcionan una manera más eficiente de evaluar las soluciones a nuestros modelos aproximados en comparación con soluciones puramente numéricas.

LABURPENA

Hobietan egindako erresistibitate neurketak sarri erabiltzen dira lurrazpiaren geruza ezberdinak identifikatzeko. Hobia hodi metaliko batez inguratuta dagoenean, potentzial elektrikoarentzako zenbakizko simulazioak izugarri konplikatu egiten dira hodiaren izaera mehea eta eroankortasun altua direla eta, zeina inguruko lur geruzena baino askoz altuagoa da. Lan honetan, hodi metalikoa forma zilindrikoa duen geruza mehe bat bezala modelizatzen dugu. Konfigurazio errealistetan oinarrituta, hodiaren eroankortasuna bere lodieraren kubo negativoarekiko proportzionala kontsideratzen dugu.

Tesi honetan, azalduko problema kontzentratzen gara hodi metalikoa transmisio kondizio baliokideekin (ITCs) ordezkatzeko. Hau burutzeko, 2D eredu bat kontsideratzen dugu koordenatu kartesiarretan, zeina lehendabiziko hurbilpen bat bezala erabiltzen dugun ardatz bertikalarekiko simetria duen eta errealistagoa den 3D eredu bat ebazteko (koordenatu zilindrikoetan). Hasteko, kasu estatikoa (frekuentzia nuloa) kontsideratzen dugu, eta gero, era berean, frekuentzia ez nulotarako ITCs-ak garatzen ditugu, zeinak hainbat fenomeno fisiko ulertzeko garrantzitsuak diren, adibidez, Delaware eta Groningen efektuak. Ondoren, modelo hauen analisi bat egiten dugu hainbat estabilitate eta konbergentzia emaitza frogatuz, eta modelo hauen zenbakizko errendimendua aztertzen dugu Elementu Finituen Metodoa erabiliz. Azkenik, soluzio semi-analitikoak garatzen ditugu modelo hauentzako, zeinak gure modelo hurbilduak ebaluatzeko modu eraginkorrago bat eskeintzen diguten zenbakizko soluzio hutsekin konparatuta.

CONTENTS

Introduction	13
Introducción	17
Sarrera	23
Introduction	29
1 ITCs with Dirichlet boundary conditions	45
1.1 Introduction	45
1.2 Static 2D configuration: model problem and scaling	46
1.3 Static 2D configuration: first class of ITCs	49
1.3.1 Construction of a multiscale expansion	49
1.3.2 Equivalent models	59
1.4 Static 2D configuration: second class of ITCs	62
1.4.1 Construction of a multiscale expansion	62
1.4.2 Equivalent models	72
1.4.3 Artificial boundaries	77
1.5 Time-harmonic problem in a 2D configuration	79
1.5.1 Model problem	80
1.5.2 First class of ITCs: construction of a multiscale expansion	80
1.5.3 First class of ITCs: equivalent models	81
1.5.4 Second class of ITCs: construction of a multiscale expansion	82
1.5.5 Second class of ITCs: equivalent models	83
1.6 3D axisymmetric configuration	84
1.6.1 Model problem and scaling	85
1.6.2 First class of ITCs: construction of a multiscale expansion	90
1.6.3 First class of ITCs: equivalent models	100
1.6.4 Second class of ITCs: construction of a multiscale expansion	102
1.6.5 Second class of ITCs: equivalent models	105

2	ITCs with mixed boundary conditions	107
2.1	Introduction	107
2.2	Static 2D configuration: first class of ITCs	108
2.2.1	Construction of a multiscale expansion	108
2.2.2	Equivalent models	120
2.3	Static 2D configuration: second class of ITCs	122
2.3.1	Construction of a multiscale expansion	122
2.3.2	Equivalent models	130
3	Analysis of the ITCs	133
3.1	Introduction	133
3.2	The reference model	133
3.3	Convergence of the asymptotic expansion	138
3.4	Validation: first class of ITCs	144
3.4.1	Second-order model: variational formulation	144
3.4.2	Fourth-order model: variational formulation	145
3.4.3	Stability results	148
3.4.4	Convergence results	153
3.5	Validation: second class of ITCs	156
3.5.1	First-order model: variational formulation	156
3.5.2	Second-order model: variational formulation	157
3.5.3	Stabilized δ -order two model: variational formulation	158
3.5.4	Stability results	159
3.5.5	Convergence results	164
4	Numerical results	169
4.1	Introduction	169
4.2	2D configuration	169
4.2.1	Dirichlet conditions	169
4.2.2	Mixed boundary conditions	180
4.3	2D time-harmonic configuration	183
4.4	3D Axisymmetric configuration	184
4.5	Application	188
4.5.1	One rock layer with varying conductivity	191
4.5.2	Two rock layers with fixed conductivity	191
4.5.3	Several rock layers with fixed conductivity	193
5	Semi-analytical solutions	195
5.1	Introduction	195
5.2	Framework	195
5.3	Dirichlet conditions	196

5.4	Robin conditions	202
5.5	Impedance Transmission conditions	204
Conclusions		213
Conclusions		217
Conclusiones		219
Ondorioak		223
Appendix A Additional results		227
A.1	Introduction	227
A.2	3D axisymmetric configuration	227
A.2.1	Model problem and scaling	228
A.2.2	First class of ITCs: construction of a multiscale expansion	231
A.2.3	First class of ITCs: equivalent models	241
A.2.4	Second class of ITCs: equivalent models	243
A.3	Variational formulations for the time-harmonic problem	245
A.3.1	Reference model	245
A.3.2	First class of ITCs	245
A.3.3	Second class of ITCs	246
A.4	3D axisymmetric variational formulations	247
A.4.1	Reference model	247
A.4.2	First class of ITCs	248
A.4.3	Second class of ITCs	251
A.5	Numerical results for 3D Electromagnetism	252
A.5.1	Introduction	252
A.5.2	Model problem	254
A.5.3	Approximate model	256
A.5.4	Numerical results	256
A.6	Unified notation for Equivalent Conditions	257
A.7	Comparison with other models	263
A.8	Asymptotic expansion in a geometry independent of ε	264
A.8.1	Introduction	264
A.8.2	Construction of a multiscale expansion	267
A.8.3	Comparison	271
Appendix B Finite Element Method implementation		273
B.1	Introduction	273
B.2	Model problem: strong and weak formulations	274
B.2.1	Homogeneous Dirichlet boundary conditions	275

B.2.2	Non-homogeneous Dirichlet boundary conditions	275
B.2.3	Robin boundary conditions	276
B.3	Discrete formulation	278
B.3.1	Dirichlet boundary conditions	278
B.3.2	Robin boundary conditions	279
B.4	Domain discretization	280
B.5	Meshes	282
B.5.1	Nodes coordinates	282
B.5.2	Connectivity matrix	283
B.5.3	Robin nodes	284
B.5.4	Dirichlet nodes	285
B.6	Shape functions of degree p and basis functions	286
B.7	Local stiffness matrix	288
B.8	Local force vector	288
B.9	Robin boundary conditions	289
B.10	Dirichlet boundary conditions	291
B.11	Transmission conditions	291
B.12	Numerical integration	293

INTRODUCTION

Les mesures de résistivité en forage sont communément utilisées pour obtenir une meilleure caractérisation du sous-sol. Une procédure standard pour obtenir de telles mesures consiste à utiliser plusieurs transmetteurs et antennes réceptrices. Ces transmetteurs et récepteurs sont des instruments situés dans un puits qui permettent de transmettre et d'enregistrer des ondes électromagnétiques qui se propagent vers différentes couches de formations rocheuses du sous-sol. Conformément aux résultats exposés dans [28, 29], la deuxième différence du potentiel électrique dans la direction verticale peut être utilisée pour déterminer la conductivité des diverses couches de formations rocheuses. Cette technique a été largement utilisée dans la littérature pour obtenir des mesures de résistivité en forage, on renvoie le lecteur aux travaux [11, 31, 34–38, 50] à ce sujet.

Ce type de procédé a un intérêt particulier lorsqu'il met en jeu un tube métallique pour couvrir le puits. L'utilisation de ce tube permet de protéger le forage et d'éviter d'éventuelles ruptures. Mais ce procédé induit aussi des complications lorsqu'il s'agit d'effectuer des simulations numériques du potentiel électrique à cause de la faible épaisseur du tube et de la conductivité élevée du tube par rapport à celle des formations du sous-sol. De fait, dans ce type d'étude, les résultats sont souvent imprécis ou simplement trop coûteux pour les effectuer en temps réel.

Ces problèmes ont déjà été abordés de deux façons différentes, par des méthodes analytiques et des méthodes numériques. L'utilisation de méthodes analytiques [25, 30, 39] limite les types de géométries que l'on peut considérer, elles ne sont donc pas très pratiques pour modéliser des configurations physiques réalistes. L'utilisation de méthodes numériques semble le meilleur moyen pour traiter des configurations complexes. Il existe une grande variété de techniques, comme par exemple la méthode de Petrov-Galerkin Discontinue [17, 61], l'analyse Isogéométrique [26, 51], ou encore la Méthode des Éléments Finites [32–34, 58]. Cependant, cette option peut aussi engendrer de nombreuses instabilités numériques à cause des forts contrastes de conductivité, et aussi à cause de la faible épaisseur du tube. Tout

cela conduit inévitablement à une augmentation du coût de calcul.

Pour surmonter cette difficulté, on adopte une méthode asymptotique afin de traiter des configurations réalistes [38] dans lesquelles la conductivité du tube prend des valeurs beaucoup plus élevées que celle des formations rocheuses. Notre but est de travailler dans le contexte de cette application, pour laquelle on suppose que la conductivité du tube est de l'ordre suivant

$$\sigma_{\text{lay}} \approx \varepsilon^{-3},$$

où ε désigne l'épaisseur du tube. Dans ce contexte, notre objectif est de développer des Conditions de Transmission d'Impédance (ITCs) principalement pour le potentiel électrique, ainsi que pour le champ électromagnétique. Le concept de Conditions d'Impédance (ICs) et de ITCs est assez classique dans la modélisation des phénomènes de propagation d'ondes; une telle condition peut-être obtenue en effectuant un développement asymptotique et elle est conçue pour remplacer une partie du domaine de calcul. Les techniques asymptotiques sont largement utilisées dans le domaine de la propagation d'ondes, citons par exemple les travaux [6, 8, 9, 23, 24, 27, 43] sur des problèmes de couches limites en électromagnétisme (effet de peau et courant de Foucault).

Les travaux [2, 13, 22, 48, 49, 57] correspondent à des études similaires associées à l'obtention de ICs obtenues pour remplacer une couche mince placée au bord du domaine. La question des ITCs est plus proche avec le travail présent, mais elle est plus délicate que la question des ICs. Tout de même on peut trouver une grande variété de travaux liés à ce sujet, [12, 15, 19–21, 40, 44, 47, 49, 52, 53, 55, 56].

Cette étude a été réalisée dans le contexte de milieux fortement contrastés, dans lesquels les paramètres physiques dépendent de l'épaisseur de la couche mince. On trouve plusieurs travaux qui ont des similitudes par rapport à ce sujet, par exemple, dans [54], les auteurs développent des ITCs pour des modèles de courant de Foucault dans lesquels on trouve une conductivité d'ordre ε^{-1} ou ε^{-2} où ε est l'épaisseur de la couche mince. De même, dans [45], on trouve un problème de couche mince pour les équations en temps de Maxwell, où la conductivité est d'ordre ε^{-2} dans une couche mince de taille ε . On peut citer enfin les travaux [46] et [20], pour un problème pour le potentiel électrique statique et un problème électromagnétique respectivement en présence d'une couche mince résistive.

Il existe aussi des études similaires en ce qui concerne l'obtention de ITCs pour d'autres modèles physiques, par exemple on peut mentionner [5] concernant l'étude de l'élasto-dynamique, [41, 42] dans le domaine de l'élasto-acoustique et [16] dans le domaine de l'acoustique. Il existe aussi des modèles dans lesquels d'autres paramètres physiques sont reliés à l'épaisseur de la couche mince: [3] effectue une

étude sur le problème d'une inclusion élastique en forme de coque avec une rigidité d'ordre ε^{-1} ou ε^{-3} .

Dans ce travail, on considère des domaines de calcul qui ne sont pas lisses. Ce cadre de travail peut compliquer largement l'analyse asymptotique par rapport au cas lisse (voir par exemple [14]) et la présence de singularités géométriques (comme des coins) peut réduire la performance des conditions d'impédance standards, voir par exemple [6, 7, 59, 60]. Dans ce travail on considère principalement un problème de transmission pour le potentiel électrique

$$\operatorname{div}[(\sigma - i\epsilon_0\omega)\nabla u] = f \quad \text{dans } \Omega,$$

avec des conditions de frontière de Dirichlet ou mixtes (Dirichlet et Neumann). On commence par considérer le domaine Ω comme un domaine rectangulaire dans \mathbb{R}^2 , puis on considère le domaine Ω comme un domaine axisymétrique en forme de puits dans \mathbb{R}^3 . Ce domaine est composé par trois sous-domaines $\Omega_{\text{int}}^\varepsilon$, $\Omega_{\text{ext}}^\varepsilon$ et $\Omega_{\text{lay}}^\varepsilon$, où ce dernier correspond au tube qui est représenté par une couche mince d'épaisseur uniforme ε . Dans ces équations ω représente la fréquence et ϵ_0 représente la permittivité électrique. Le paramètre σ correspond à la conductivité, qui est constante dans chaque sous-domaine. Finalement f représente une source de courant qui est nulle dans le tube.

Dans ce contexte, on développe des ITCs adaptées au potentiel u quand ε tend vers zéro. On développe deux classes de ITCs en utilisant deux approches. La première approche consiste à écrire les ITCs à travers le tube, tandis que la deuxième approche consiste à écrire les ITCs à travers une interface artificielle située au milieu du tube. Les deux classes ont leurs propres avantages et inconvénients, ce sujet est discuté dans ce travail. On présente aussi des justifications mathématiques pour ces ITCs et on étudie la performance numérique des modèles développés. Les ITCs de la première classe se comportent comme des approximations du second ordre et du quatrième ordre, tandis que les ITCs pour la deuxième classe sont obtenues pour les quatre premiers ordres.

La méthode asymptotique adoptée se résume ainsi. D'abord on effectue un chagement d'échelle dans le sous-domaine qui correspond au tube métallique, $\Omega_{\text{lay}}^\varepsilon$, dans la direction normale à la couche mince afin de se ramener à une géométrie indépendante de ε . Ensuite, on effectue un *Ansatz* sous forme d'un développement puissances de ε et on obtient une collection de problèmes élémentaires à résoudre successivement. Puis on tronque la série et on sélectionne les premiers termes du développement pour en déduire des conditions équivalentes en négligeant des termes résiduels. Finalement on prouve des résultats de convergence pour ces modèles. On suit cette méthode pour les deux configurations (2D et 3D).

Le manuscrit est structuré de la manière suivante. Dans le premier chapitre

développe des ITCs pour le potentiel électrique statique dans une configuration avec des conditions de frontière de Dirichlet, on décrit la procédure pour obtenir ces ITCs. On considère la configuration 2D et la configuration 3D axisymétrique pour le potentiel électrique statique, ainsi que le problème à fréquence non-nulle. Le chapitre 2 présente des résultats similaires au chapitre 1 pour le potentiel électrique statique en 2D, mais pour un problème des conditions de frontière mixtes (Dirichlet et Neumann). Dans le chapitre 3 on effectue une analyse mathématique des modèles asymptotiques obtenues dans le chapitre 1, on présente des résultats de stabilité (existence, unicité et estimations uniformes) et convergence. Le chapitre 4 est consacré à l'analyse numérique et à la simulation des modèles asymptotiques obtenus dans les chapitres précédents. On vérifie les ordres de convergence et on présente plusieurs applications pour ces modèles. Dans le chapitre 5 on développe des solutions semi-analytiques pour certains modèles en utilisant la transformé de Fourier. Finalement, on présente des résultats complémentaires aux premiers chapitres dans l'Annexe A. Pour obtenir les résultats numériques du Chapitre 4, on a implémenté un code d'éléments finis. On explique les différentes caractéristiques de ce code dans le Annexe B.

INTRODUCCIÓN

Las medidas de resistividad se utilizan de manera común para obtener una mejor caracterización del subsuelo de la tierra. El procedimiento estándar para la obtención de dichas medidas de resistividad consiste en emplear uno o varios transmisores y antenas receptoras. Estos transmisores y receptores, a los que denominamos el instrumento, se sitúan dentro de un pozo, donde se utilizarán para transmitir ondas electromagnéticas hacia las diferentes capas de formaciones rocosas del subsuelo para más tarde registrar las ondas entrantes. Conforme a los resultados expuestos en [28, 29], la segunda derivada del potencial eléctrico en la dirección vertical puede ser utilizada para determinar la conductividad de las diversas capas de formaciones que componen el subsuelo de la tierra. Esta técnica ha sido extensamente utilizada en la literatura para obtener medidas de resistividad en pozos de sondeo, remitimos al lector a los trabajos [11, 31, 34–38, 50] para más información sobre este tema.

Este tipo de procedimientos son de especial interés cuando se realizan a través de una cobertura metálica, ya que a menudo se emplea un tubo hecho de metal para cubrir el pozo. Por un lado, el uso de dicho tubo metálico permite proteger la perforación y evitar los posibles colapso, pero por otro lado también crea enormes complicaciones a la hora de realizar simulaciones numéricas para el potencial eléctrico debido a la delgadez y alta conductividad del tubo comparado a la de las formaciones del subsuelo. Por lo tanto, al realizar este tipo de estudios, los resultados a menudo son imprecisos o simplemente demasiado costosos para realizarlos en tiempo real.

Este tipo de problemas han sido abordados mediante dos enfoques diferentes, los métodos analíticos y los métodos numéricos. El uso de métodos analíticos [25, 30, 39] limita los tipos de geometrías que pueden considerarse, por lo tanto no es muy adecuado para modelizar configuraciones físicas realistas. El uso de métodos numéricos parece ser la mejor respuesta para lidiar con configuraciones complejas. Podemos encontrar una gran variedad de técnicas en lo que se refiere a métodos numéricos. El método de Petrov-Garlerkin Discontinuo [17, 61], el análisis

Isogeométrico [26, 51] y el Método de Elementos Finitos hp [32–34, 58] son ejemplos de técnicas que merecen ser mencionadas. No obstante, esta opción también puede acarrear numerosas dificultades debido al gran contraste de conductividad eléctrica entre el tubo metálico y las capas del subsuelo, así como el minúsculo grosor del tubo. En particular, cuando tratamos este tipo de membranas finas, el coste computacional aumenta cuando intentamos mallarlas. Además, los métodos numéricos utilizados para resolver este tipo de problemas, no funcionan como es debido cuando se consideran medios con altos contrastes. Estos hechos conllevan un inevitable aumento en el coste de computación, por tanto, es esencial evitar la membrana fina mediante el uso de técnicas matemáticas que permitan construir problemas reducidos compuestos por condiciones de transmisión o de frontera apropiadas.

Para superar esta dificultad adoptamos un método asintótico motivado por configuraciones realistas [38], en el cual la conductividad en el tubo toma valores mucho más altos que los de las formaciones rocosas. Nuestro propósito es trabajar en el contexto de esta aplicación, para la cual suponemos que la conductividad en el tubo toma la siguiente forma

$$\sigma_{\text{lay}} \approx \varepsilon^{-3},$$

donde ε denota el grosor del tubo, el cual es presentado como una membrana fina de grosor uniforme. Podemos motivar esta elección mediante el artículo [38], en el cual podemos observar los siguientes valores para la conductividad y para el grosor del tubo metálico

$$\begin{cases} \varepsilon = 1.27 \cdot 10^{-2} \text{ m} , \\ \sigma_{\text{lay}} = 4.34 \cdot 10^6 \Omega^{-1} \text{ m}^{-1}. \end{cases}$$

De estos valores, inferimos la siguiente relación entre estos parámetros físicos

$$\sigma_{\text{lay}} = 8.89 \cdot \varepsilon^{-3}.$$

En este contexto nuestro objetivo es desarrollar Condiciones de Transmisión de Impedancia (ITCs) principalmente para el potencial eléctrico, y más tarde para el campo electromagnético, a través de dicho tubo. El pequeño grosor del tubo, que viene dado de forma natural por el problema, comparado con el resto del dominio permite que este tipo de método sea ideal para este problema. El concepto de Condiciones de Impedancia (ICs) y ITCS es bastante clásico en el modelizado de fenómenos de propagación de ondas. Dicha condición es obtenida por medio de la realización de una expansión asintótica y está diseñada para reemplazar una parte del dominio computacional. Las técnicas asintóticas se emplean ampliamente en el campo de la propagación de ondas, por ejemplo mencionamos los trabajos [6, 8, 9,

[23, 24, 27, 43] relacionados con el fenómeno de capa límite en Electromagnetismo (efecto pelicular y corriente de Foucault).

Los trabajos [2, 13, 22, 48, 49, 57] corresponden a estudios similares relacionados con la obtención de ICs para el electromagnetismo, en los cuales se obtienen ICs para sustituir una membrana fina que se encuentra en un borde del dominio. La cuestión de las ITCs está más relacionada con el presente trabajo, pero también es más delicada que la cuestión de las ICs. De todas maneras, podemos encontrar una extensa variedad de trabajos relacionados con este tema, [12, 15, 19–21, 40, 44, 47, 49, 52, 53, 55, 56].

Este estudio se ha realizado en el contexto de medios de alto contraste, en los cuales los parámetros físicos tienen una dependencia del grosor de la membrana fina. Podemos encontrar varios trabajos con similitudes en este tema, por ejemplo, en [54], los autores desarrollan ITCs para modelos de corriente de Foucault donde encontramos una conductividad dependiente del grosor de la membrana fina de órdenes ε^{-1} y ε^{-2} . Del mismo modo, en [45], encontramos un problema de membrana fina para las ecuaciones armónicas de Maxwell, cuya conductividad depende del grosor de la membrana fina con orden ε^{-2} . En [46] y [20], se consideran un problema para el potencial estático y un problema electromagnético respectivamente, estando presente en ambos trabajos una membrana fina resistiva.

También existen estudios similares respecto a la obtención de ITCs para otros modelos físicos, por ejemplo podemos mencionar [5] en cuanto a el estudio de la Elasto-dinámica, [41, 42] en lo que refiere al estudio de un problema con medios acústicos y elásticos y [16] en el campo de la Acústica. También existen modelos en los que los parámetros físicos dependen del grosor de la membrana fina, [3] realiza un estudio sobre el problema de una inclusión elástica con forma de cascarón con una rigidez de órdenes ε^{-1} y ε^{-3} .

En este trabajo, consideramos dominios computacionales que no son suaves e incluyen vértices y bordes. En general, este contexto complica enormemente el análisis comparado con el caso suave (ver por ejemplo [14]) y la presencia de singularidades geométricas (como esquinas) reduce el rendimiento de las condiciones de impedancia estándares, ver por ejemplo [6, 7, 59, 60]. En este trabajo consideramos principalmente un problema de transmisión para el potencial eléctrico

$$\operatorname{div}[(\sigma - i\varepsilon_0\omega)\nabla u] = f \quad \text{en } \Omega,$$

con condiciones de frontera de Dirichlet o mixtas (Dirichlet y Neumann). Empezamos considerando el dominio Ω como un dominio con forma rectangular en \mathbb{R}^2 , y luego consideramos el dominio Ω como un dominio con simetría axial en forma de pozo en \mathbb{R}^3 . Este dominio está compuesto de tres subdominios $\Omega_{\text{int}}^\varepsilon$, $\Omega_{\text{ext}}^\varepsilon$ y $\Omega_{\text{lay}}^\varepsilon$, donde este último corresponde a el tubo y es una membrana fina de grosor

uniforme. En estas ecuaciones ω representa la frecuencia y ϵ_0 representa la permitividad. El parámetro σ corresponde a la conductividad, que es una función constante a trozos que toma un valor diferente en cada subdominio. Finalmente f es una función que se anula en el tubo.

En este contexto, abordamos el problema de las ITCs para u cuando ϵ tiende a cero. Desarrollamos dos clases diferentes de ITCs mediante dos enfoques diferentes. El primero consiste en obtener las ITCs a través del tubo mismo, mientras que el segundo enfoque aborda el problema obteniendo las ITCs a través de una interfaz artificial situada en el medio del tubo. Ambas clases tienen sus ventajas et inconvenientes, tema que desarrollaremos en este trabajo. También presentamos las justificaciones matemáticas para estas ITCs y estudiamos el rendimiento numérico de los modelos que hemos desarrollado. Las ITCs de la primera clase se comportan como aproximaciones de segundo y cuarto orden, mientras que las ITCs de segunda clase son obtenidas desde el primer hasta el cuarto orden.

El método asintótico que seguimos puede ser resumido en los siguientes pasos. Primero de todo realizamos un escalado en el subdominio correspondiente al tubo metálico, $\Omega_{\text{lay}}^\epsilon$, en la dirección normal a la membrana fina. Entonces realizamos un *Ansatz* en forma de expansión de potencias de ϵ y obtenemos una colección de problemas. Éstos pueden ser resueltos de forma alterna para determinar los problemas elementales satisfechos por cada término de la expansión asintótica. Más tarde, truncamos la serie y seleccionamos los primeros términos de la expansión para inferir condiciones equivalentes omitiendo los términos residuales dependiendo de ϵ . Finalmente demostramos los resultados de convergencia para los modelos asintóticos que hemos obtenido. Seguimos esta metodología tanto para la configuración 2D, como para la configuración 3D.

El manuscrito está estructurado de la siguiente manera. En el primer capítulo explicamos como obtenemos las ITCs para el potencial eléctrico estático en una configuración con condiciones de frontera de Dirichlet, presentamos el problema modelo y describimos el procedimiento para obtener las ITCs de primera y segunda clase. Consideramos la configuración 2D y la 3D con simetría axial para el potencial eléctrico estático y una configuración 2D para el caso armónico. El capítulo 2 presenta resultados similares a el capítulo 1 para el potencial eléctrico estático en 2D pero en este caso consideramos condiciones de frontera mixtas (Dirichlet y Neumann). Más tarde, en el capítulo 3, realizamos un análisis matemático de los modelos asintóticos que hemos derivado en el capítulo 1, presentamos los resultados correspondientes a la estabilidad (existencia, unicidad y estimaciones uniformes) y a la convergencia de las soluciones de los modelos obtenidos. El capítulo 4 está destinado al análisis numérico del rendimiento de los modelos asintóticos obtenidos en los capítulos anteriores. Analizamos los órdenes de convergencia numéricos y

comprobamos si concuerdan con los órdenes de convergencia teóricos. Finalmente, presentamos varias aplicaciones para estos modelos. En el capítulo 5 desarrollamos soluciones semi-analíticas para varios de los modelos estudiados mediante el uso de una transformada de Fourier. Finalmente, podemos encontrar dos anexos. Primero, en el Anexo A, presentamos resultados similares a los mostrados en los capítulos anteriores para otras configuraciones adicionales, como las formulaciones variacionales para el caso 3D con simetría axial y el caso armónico, resultados numéricos preliminares para el Electromagnetismo en 3D, una notación unificada para las condiciones equivalentes obtenidas en este documento y una comparación de los resultados obtenidos en este documento respecto a otros modelos en la literatura. Por último, para obtener los resultados numéricos del capítulo 4, hemos implementado un código de elementos finitos y en el Anexo B explicamos las diferentes características de este código, como los tipos de problemas que resuelve y como funciona.

SARRERA

Erresistibitate neurketak sarri erabiltzen dira lurrazpiaren karakterizazio hobe bat lortzeko orduan. Erresistibitate neurketa hauek lortzeko prozedura estandarrak transmisore eta antena errezeptore bat edo zenbait erabiltzean datza. Transmisore eta errezeptore hauek, instrumentu bezala izendatuko ditugunak, hobi baten barnean kokatzen dira, non lurrazpiaren geruzetarantz uhin elektromagnetikoak bidaltzeko eta era berean, iristen diren uhinak erregistratzeko, erabiliko diren. [28, 29] lanetan azaltzen diren emaitzen arabera, potentzial elektrikoaren bigarren deribatua norabide bertikalean erabilia izan daiteke lurrazpia osatzen duten geruza ezberbinen eroankortasuna zehazteko. Teknika hau oso erabilia izan da literaturan hobietako erresistibitate neurketak eskuratzeko, irakurlea [11, 31, 34–38, 50] lanetara igortzen dugu gai honen inguruan informazio gehiago eskuratzeko.

Mota honetako prozedurek interes berezia daukate estalki metaliko batean zehar egiten direnean, izan ere maiz metalez egindako hodi bat erabiltzen da hobiak estaltzeko. Alde batetik, aipaturiko hodi honen erabilerak, zulaketa babebestea eta kolapso posibleak sahiestea baimentzen ditu, baina bestalde, zailtasun izugarriak sortzen ditu potentzial elektrikoarentzako zenbakizko simulazioak egiterakoan hodiaren mehetasun eta eroankortasun altua direla eta. Beraz, horrelako analisiak egiterakoan, sarritan emaitzak ez dira zehatzak izaten edo besterik gabe kostu konputazionala oso altua da denbora errealean burutzeko.

Mota honetako problemei bi ikuspuntu desberdinetatik aurre egin izan zaie, metodo analitikoak erabiliz eta zenbakizko metodoak erabiliz. Metodo analitikoan erabilerak [25, 30, 39] kontsideratu daitezkeen geometriak mugatzen ditu, beraz, ez da oso aproposa konfigurazio fisiko errealistak modelizatzeko. Zenbakizko metodoen erabilerak konfigurazio komplexuei ekiteko erantzunik aproposena ematen du. Teknika ugari aurkitu daitezke zenbakizko metodoen inguruan. Petrov-Galerkin ez-jarraitua [17, 61], analisi Isogeometrikoa [26, 51] eta hp Elementu Finituen Metodoa [32–34, 58] aipatzea merezi duten tekniken adibideak dira. Dena den, aukera honekin ere zailtasun ugari aurkitu ditzakegu metalezko hodiaren eta lurrazpi-

aren geruzen eroankortasunen arteko kontrastea eta hodiaren lodiera txikia dela eta. Bereziki, mota honetako geruza meheekin lan egiterakoan, kostu konputazionalaren igoera handi bat gertatzen da sare bat sortzerako orduan. Gainera, problema hauek ebazteko erabiltzen diren zenbakizko metodoek ez dute ongi funtzionatzen kontraste altuko ingurunueak kontsideratzen direnean. Arrazoi hauek kostu konputazionalaren igoera saihestezin bat dakarte, beraz, geruza mehea saihestea ez-inbestekoa da transmisio kondizioak dituzten eredu murriztuak garatzea bideratzen duten teknika matematikoak erabiliz.

Zailtasun hauek gainditzeko, konfigurazio errealistetan [38] oinarritutako metodo asintotiko bat proposatzen dugu, zeinean hodiaren eroankortasunak balio askoz handiagoak hartzen dituen lurrazpiko geruzekin konparatuta. Gure helburua aplikazio honen testuinguruan lan egitea da, zeinean hodiaren eroankortasunak hurrengo itxura hartzen duen

$$\sigma_{\text{lay}} \approx \varepsilon^{-3},$$

non ε -ek hodiaren lodiera izendatzen duen, zeina lodiera uniformeko geruza mehe bat bezala aurkezten den. Aukera hau motibatatu dezakegu [38] lanean oinarrituz, non ondorengo balioak aurkitzen ditugun hodiaren eroankortasun eta lodierarentzako

$$\begin{cases} \varepsilon = 1.27 \cdot 10^{-2} \text{ m} , \\ \sigma_{\text{lay}} = 4.34 \cdot 10^6 \Omega^{-1} \text{ m}^{-1}. \end{cases}$$

Balio hauetatik hurrengo erlazioa ondorioztatzen dugu bi parametro fisiko hauen artean

$$\sigma_{\text{lay}} = 8.89 \cdot \varepsilon^{-3}.$$

Testuinguru honetan gure helburua batez ere hodi horren zehar potentzial elektrikoarentzat Inpedantzia Transmisio Kondizioak (ITCs) garatzea da, eta geroago eremu elektromagnetikoarentzat. Naturalki txikia den hodiaren lodierak, gainerako eremuarekin konparatuta, metodo hau problema mota hauentzako aukera ezin hobea izatea baimentzen du. Inpedantzia Kondizioen kontzeptua (ICs) eta ITCs-ena nahiko klasikoa da uhinen hedapenaren modelizazioan. Holako kondizio bat hedapen asintotiko bat eginez lortzen da eta eremu konputazionalaren zati bat ordezkatzeko bereziki diseinatuta dago. Teknika asintotikoak oso erabiliak dira uhinen hedapenaren eremuan, adibidez [6, 8, 9, 23, 24, 27, 43] lanak aurki ditzakegu elektromagnetismoaren eremuan geruza limitearen fenomenoarekin erlazionatuta (azal efektua eta Foucault-en korrrontea).

[2, 13, 22, 48, 49, 57] lanak elektromagnetismoarentzako garatutako ICs-en inguruan egindako estudio antzekoak dira, zeinetan eremuaren bazter batean kokatuta dagoen geruza mehe bat ordezkatzeko ICs-ak garatzen diren. ITCs-en gaia erlazionatuagoa dago lan honekin, baina gai delikautagoa da ICs-ena

baino. Dena den, lan sorta handi bat aurki dezakegu gai honen inguruan, [12, 15, 19–21, 40, 44, 47, 49, 52, 53, 55, 56].

Lan hau kontraste altuko inguruneen testuinguruan eginda dago, zeinetan parametro fisikoek geruza mehearen lodierarekiko mendekotasun bat duten. Lan ezberdin batzuk aurki ditzakegu gai honen inguruan antzekotasunak dituztenak, adibidez, [54] lanean, egileek ITC-ak garatzen dituzte Foucault-en korrontearen ereduentzako, non aurkitzen dugun eroankortasunak geruza mehearen lodierarekiko ε^{-1} eta ε^{-2} ordeneko menpekotasuna daukan. Era berean, [45] lanean, geruza mehe bat duen problema bat aurkitzen dugu Maxwell-en ekuazio harmonikoentzat, non eroankortasunak geruza mehearen lodierarekiko ε^{-2} ordeneko mendekotasuna duen. [46] eta [20] lanetan, potentzial estatikoarentzako problema bat eta problema elektromagnetiko bat kontsideratzen dira hurrenez hurren, bi lanetan geruza mehe erresistibo bat aurkitzen dugularik.

Beste eredu fisikoetarako estudio antzekoak ere existitzen dira, adibidez [5] aipa dezakegu elasto-dinamikaren arloan, [41, 42] ingurune elastiko eta akustikoen eremuan eta [16] akustikaren arloan. Era berean, badaude ereduak zeinetan parametro fisikoek geruza mehearen lodierarekiko menpekotasuna duten, [3] lanean, egileak oskol itsura duen inklusio elastiko baten analisia egiten du, non zurruntasuna ε^{-1} eta ε^{-3} ordenekoa den.

Lan honetan, leunak ez diren eremu komputazionalak kontsideratzen ditugu, zeinek erpin eta ertzak dituzten. Orokorrean, textuinguru honek analisia izugarri zaildu egiten du kasu leunarekin konparatuta (ikus adibidez [14]) eta singularitasun geometrikoen presentziak (erpinak adibidez) inpendantzia kondizio estandarren errendimendua murriztu egiten du, ikusi adibidez [6, 7, 59, 60]. Lan honetan bereziki potentzial elektrikoarentzako transmisio problema bat kontsideratzen dugu

$$\operatorname{div}[(\sigma - i\epsilon_0\omega)\nabla u] = f \quad \Omega\text{-an} ,$$

Dirichlet edo muga baldintza mixtoekin (Dirichlet eta Neumann). Hasteko Ω eremua laukizuzen formako eremu bezala kontsideratzen dugu \mathbb{R}^2 -n, eta gero Ω eremua ardatz bertikalarekiko simetrikoa den hobi itxurako eremu bezala kontsideratzen dugu \mathbb{R}^3 -n. Eremu hau hiru azpieremuz osatuta dago, $\Omega_{\text{int}}^\varepsilon$, $\Omega_{\text{ext}}^\varepsilon$ eta $\Omega_{\text{lay}}^\varepsilon$, non azkenengo hau hodi metalikoari dagokion eta lodiera uniformeko geruza bezala kontsideratzen dugun. Ekuazio hauetan ω -k frekuentzia eta ϵ_0 -k permitibitatea adierazten du. σ parametroa eroankortasunari dagokio eta zatika konstatea den funtzio bat da zeinak azpieremu bakoitzean balio ezberdin bat hartzen duen. Amaitzeko f funtzio bat da zeina hodian ezeztatu egiten den.

Testuinguru hontan, u -rentzako ITC-en problemari ekiten diogu ε zerorantz doanean. Bi ITCs klase ezberdin garatzen ditugu bi ikuspegi ezberdin erabiliz. Lehenengoak ITCs-ak hodian zehar garatzean datza, bigarrenak berriz, ITCs-ak

hodiaren erdian kokatzen den interfaze batean zehar garatuz ekiten dio problemari. Klase bakoitzak bere abantaila eta eragozpenak ditu, zeinak lan honetan azaldu egiten diren. Lan honetan ITCs hauentzako justifikazio matematikoak ematen ditugu eta era berean garatutako eredu matematikoen zenbakizko errendimendua aztertu egiten dugu. Lehenengo klaseko ITC-ak bigarren eta laugarren ordeneko hurbilketa moduan aurkitzen ditugu, ostera bigarren klaseko ITCs-ak lehenengo ordenetik laugarren ordenerarte garatzen ditugu.

Jarraitzen dugun metodo asintotikoa hurrengo urratsetan laburtua izan daiteke. Lehendabizi, hodi metalikoari dagokion azpierzemuan, $\Omega_{\text{lay}}^\varepsilon$, eskalatze bat egiten dugu geruza mehearen norabide normalean. Orduan, ε -en berreturen serie moduko *Ansatz* bat eraikitzen dugu eta oinarrizko problema bilduma bat lortzen dugu, zeinak txandaka ebatzi behar diren. Gero, seriea trunkatzen dugu eta lehenengo gaiak aukeratzen ditugu kondizio baliokideak lortzeko ε -en menpe dagoen hondarra mespresatuz. Amaitzeko, garatu ditugun ereduentzako konbergentzia emaitzak frogatu egiten ditugu. Metodologia hay jarraitzen dugu bai 2D konfigurazioarentzat, bai 3D konfigurazioarentzat.

Textuak hurrengo egitura jarraitzen du. Lehenengo kapituluak potentzial elektriko estatikoarentzat ITCs-ak nola garatzen ditugun azaltzen dugu Dirichlet muga baldintzak kontsideratuz, eredu problema aurkezten dugu eta lehenengo eta bigarren klaseko ITCs-ak garatzeko prozesua deskribatzen dugu. 2D konfigurazioa eta ardatz bertikalarekiko simetria duen 3D konfigurazioa kontsideratzen ditugu potentzial elektriko estatikoarentzat, eta baita 2D konfigurazio bat kasu harmonikoarentzako. 2 kapituluak, 1 kapituluak aurkeztutako emaitza antzekoak erakusten ditu potentzial elektriko estatikoarentzat 2D konfigurazioan, baina kasu honetan muga baldintza mixtoak (Dirichlet eta Neumann) kontsideratzen ditugu. Ondoren, 3 kapituluak, 1 kapituluak garatutako eredu asintotikoen analisi matematiko bat egiten dugu. Hain zuzen ere, estabilitate (existentzia, bakartasun eta estimazio uniformeak) eta konbergentziari buruzko emaitzak aurkezten ditugu. 4 kapituluak aurreko kapituluetan garatutako eredu asintotikoen zenbakizko errendimendua aztertzeraz zuzendua dago. Zenbakizko konbergentzia ordenak aztertzen ditugu eta konbergentzia orden teorikoekin bat egiten duten egiaztatzen dugu. Amaitzeko eredu hauentzako hainbat aplikazio aurkezten ditugu. 5 kapituluak, garatutako hainbat ereduentzako soluzio semi-analitikoak eraikitzen ditugu Fourier-en transformada bat erabiliz. Azkenik, bi eranskin aurkitzen ditugu. Lehenengo A eranskina daukagu, non aurreko kapituluak antzeko emaitzak aurkitu daitezkeen beste konfigurazio osagarri batzuetarako, adibidez, ardatz bertikalarekiko simetria duen 3D konfigurazioarentzako eta kasu harmonikoarentzako formulazio ahula, 3D Elektromagnetismoarentzako zenbakizko probak, dokumentu honetan garatutako kondizio baliokideentzako notazio bateratu bat eta hemen lortutako emaitzen eta literaturan aurkitutako beste eredu batzuen arteko konparazio bat. Amaitzeko, 4

kapituluan aurkeztutako zenbakizko emaitzak lortzeko elementu finituen kode bat garatu dugu eta hain zuzen ere **B** eranskinean kode honen ezaugarri ezberdinak azaltzen ditugu, adibidez ze problema ebazten dituen eta nola funtzionatzen duen.

INTRODUCTION

Borehole resistivity measurements are commonly used when trying to obtain a better characterization of the Earth's subsurface. The standard procedure for acquiring borehole resistivity measurements consists in employing a logging instrument equipped with one or several transmitters and receiver antennas. The logging instrument moves along a given well while electromagnetic measurements are recorded at each logging position. Electrical logging through casing is of special interest because the well is often surrounded by a steel-made casing. On one hand, the use of such casings allows to protect the well and avoid possible collapses, but on the other hand it also highly complicates the numerical simulations for the electric potential due to the thinness and high conductivity of the casing compared to those of the layer formations. Thus, when performing through casing resistivity simulations, the numerical results are often inaccurate or simply too costly to be performed in real time.

According to the results shown in [28, 29], the second vertical derivative of the electric potential, measured at the receiving antennas can be employed to determine the conductivity of the different layer formations composing the Earth's subsurface. This technique has been widely employed in the literature for acquiring borehole resistivity measurements. See, for instance, [11, 31, 34–38, 50].

These kind of problems have already been faced by two different approaches, the use of semi-analytical methods and the use of numerical methods. The use of semi-analytical methods [25, 30, 39] limits the types of subsurface models that one can consider, severely limiting the number of real problem configurations that one can solve. The use of numerical methods seems the best answer for dealing with complex geometries. A wide range of techniques can be found regarding such numerical methods, including Discontinuous Petrov-Galerkin methods [17, 61], Isogeometric analysis [26, 51], and hp-adaptive Finite Element Methods [32–34, 58]. However, tackling this problem with numerical methods becomes challenging too due to the high electrical conductivity contrast between the metallic casing and the

layer formations, as well as the small thickness of the casing. In particular, when dealing with thin layers, the computational cost greatly increases due to the need of a heavily refined mesh. Traditional numerical methods employed to solve these problems do not perform well when high contrast materials are considered. As a result, the computational cost dramatically increases.

To overcome these difficulties, in this Ph.D. dissertation we replace the thin layer occupied by the casing by a novel Impedance Transmission Condition (ITC). For that, we adopt an asymptotic method which is motivated by a realistic configuration [38], where the casing conductivity takes much higher values than those in the layer formations. We further assume that the conductivity in the casing has the following form

$$\sigma_{\text{lay}} \approx \varepsilon^{-3},$$

where ε denotes the casing thickness, which is expressed in terms of a thin layer of uniform thickness. The above assumption is indeed realistic, since in real scenarios we have (see [38]):

$$\begin{cases} \varepsilon = 1.27 \cdot 10^{-2} \text{ m}, \\ \sigma_{\text{lay}} = 4.34 \cdot 10^6 \text{ } \Omega^{-1} \text{ m}^{-1}. \end{cases}$$

From these values we infer the following relation between these physical parameters

$$\sigma_{\text{lay}} = 8.89 \cdot \varepsilon^{-3}.$$

In this framework, our aim is to derive Impedance Transmission Conditions (ITCs) mainly for the electric potential, and eventually for the electromagnetic field, across the aforementioned casing. The naturally small thickness of the casing compared to the rest of the domain makes it ideal for applying this kind of method. The concept of Impedance Conditions (ICs) and ITCs is classical in the modelling of wave propagation phenomena. Such conditions are derived by performing an asymptotic expansion and are designed to replace one part of the computational domain (in our case, the subdomain occupied by the casing). Asymptotic techniques are widely employed in the field of wave propagation problems, for instance, [6, 8, 9, 23, 24, 27, 43] related to boundary layer phenomena in Electromagnetism (skin effect and eddy current problem).

Similar studies regarding the derivation of ICs for Electromagnetism include [2, 13, 22, 48, 49, 57], where ICs are derived to substitute a thin layer present in one side of the domain. ITCs are more suitable for our present work, but their derivation is also more complex than that of ICs. There also exists a wide variety of works related to this topic, e.g., [12, 15, 19–21, 40, 44, 47, 49, 52, 53, 55, 56].

This study is performed in the framework of high-contrast material properties, where the conductivity has a dependence on the thickness of a thin layer. Several

works can be found with similarities in this matter. For instance, in [54], the authors derive ITCs for eddy current models with a dependence on the conductivity parameter of the thin layer of the form ε^{-1} and ε^{-2} . In the same way, in [45], we find a thin layer problem for the time-harmonic Maxwell's equations, whose conductivity depends on the thickness of the thin layer in the form of ε^{-2} . In [46] and [20], a problem for the static potential and an electromagnetic problem are considered, and in both works a thin resistive layer is present.

There also exist similar studies regarding the derivation of ITCs for other physical models. For example in [5] they focus on Elastodynamics, [41, 42] study a problem with elastic and acoustic media, and [16] considers the field of Acoustics. There also exists other models where the physical parameters depend on the thickness of the a layer. For instance [3] perfoms a study about the problem of an elastic shell-like inclusion with a rigidity of the form ε^{-1} and ε^{-3} .

In this work, we consider non-smooth computational domains, which include vertices and edges. In general, this framework greatly complicates the analysis compared to the smooth case (see for example [14]) and the presence of geometrical singularities (such as corners) may reduce the performance of standard impedance conditions, see for example [6, 7, 59, 60]. In this work, we consider mainly a transmission problem for the electric potential, reading as

$$\operatorname{div}[(\sigma - i\epsilon_0\omega)\nabla u] = f \quad \text{in } \Omega,$$

with Dirichlet or mixed (Dirichlet and Neumann) boundary conditions. We first consider the domain Ω to be a rectangular shaped domain in \mathbb{R}^2 , and then we consider the domain Ω to be an axi-symmetric borehole shaped domain in \mathbb{R}^3 . This domain is composed of three subdomains $\Omega_{\text{int}}^\varepsilon$, $\Omega_{\text{ext}}^\varepsilon$, and $\Omega_{\text{lay}}^\varepsilon$, where the last one corresponds to the casing and is a thin layer of uniform thickness ε . Here, ω represents the frequency and ϵ_0 is the electrical permittivity. The parameter σ corresponds to the conductivity and it is a piecewise constant function that takes different values in each subdomain. Function f corresponds to the right-hand side and it is a function that vanishes in the casing.

In this framework, we address the issue of ITCs for u as ε tends to zero. We derive two different classes of ITCs employing different approaches. The first one consists in deriving ITCs across the casing itself, whereas the second approach tackles the problem by deriving ITCs on an artificial interface located on the middle of the casing. Both classes have their advantages and drawbacks, which are described in this work. We shall present the mathematical justification for these ITCs and we shall also concentrate on studying the numerical performance of the derived models. A first class of ITCs provide second and fourth order approximations whereas a second class of ITCs deliver order one up to order four approximations.

The asymptotic method consists of the following steps. First, we scale the subdomain occupied by the casing, $\Omega_{\text{lay}}^\varepsilon$, along the direction perpendicular to the vertical casing in order to obtain a geometry independent of ε . Then, we select an *Ansatz* for the electric potential u in the form of power expansion of ε . We obtain a collection of problems that can be alternately solved to determine the elementary problems satisfied by each term of the asymptotic expansion. Then, we truncate the resulting series and collect the first terms of the expansion to infer equivalent conditions by neglecting residual terms depending on ε . Finally, we prove convergence results for the derived asymptotic models. We follow this methodology for both the 2D and the 3D axi-symmetric configurations.

The outline of the dissertation consists of the following. In the next chapter, we derive the ITCs for the static (zero frequency) electric potential in a configuration with Dirichlet boundary conditions. We also introduce a model problem and we describe the procedure to derive ITCs of the first and second classes. We consider a 2D and a 3D axi-symmetric configurations for the static electric potential and a 2D configuration for the time-harmonic case. Chapter 2 expands the results of Chapter 1 to the case of mixed (Dirichlet and Neumann) boundary conditions. Then, in Chapter 3 we perform a mathematical analysis of the asymptotic models we have derived in Chapter 1. We present stability (existence, uniqueness and uniform estimates) and convergence results for the solution of the derived models. Chapter 4 is devoted to the numerical performance assessment of the asymptotic models derived in the previous chapters. We analyze the numerical order of convergence and we verify they match with the theoretical orders of convergence. Finally we present several applications to these models. Then, in Chapter 5 we derive semi-analytical solutions for some of the obtained 3D axi-symmetric models by employing a Hankel transform. We also provide two appendixes. First, in Appendix A, similar results to the ones of the previous chapters are presented for some additional configurations, like variational formulations for the 3D axi-symmetric configuration and the time-harmonic case, preliminary numerical test for 3D Electromagnetism, a unified notation for the Equivalent Conditions derived in this document and a comparison of the results presented here with other models in the literature. Lastly, to obtain the numerical results of Chapter 4 a finite element code has been implemented and in Appendix B we explain the different features of this code, including what type of problems it solves and how it works.

Rather than moving on the content of the dissertation, we have decided to give an overview of the main results we have obtained. The following part of this introduction provides the reader a detailed abstract of the thesis. We will concentrate ourselves on presenting the results for the problem of the static electric potential with homogeneous Dirichlet conditions and we refer to Chapters 2 and 4 for results regarding the problem with mixed conditions.

2D ITCs derivation

Here we concentrate on presenting the results for the static case but we also derive ITCs for time-harmonic case in Section 1.5. We begin by performing an asymptotic expansion of the solution, which has the following form for the first approach (see Proposition 1)

$$\begin{cases} u_{\text{int}}(x, y) = u_{\text{int}}^0(x, y) + \varepsilon^2 u_{\text{int}}^2(x, y) + r_{\text{int}}^3(x, y) & \text{in } \Omega_{\text{int}}^\varepsilon, \\ u_{\text{ext}}(x, y) = u_{\text{ext}}^0(x, y) + \varepsilon^2 u_{\text{ext}}^2(x, y) + r_{\text{ext}}^3(x, y) & \text{in } \Omega_{\text{ext}}^\varepsilon, \\ u_{\text{lay}}(x, y) = \varepsilon^2 U^2(\varepsilon^{-1}(x - x_0), y) + r_{\text{lay}}^3(x, y) & \text{in } \Omega_{\text{lay}}^\varepsilon, \end{cases}$$

and the following form for the second approach (see Proposition 2), which is given by

$$\begin{cases} u_{\text{int}}(x, y) = u_{\text{int}}^0(x, y) + \varepsilon u_{\text{int}}^1(x, y) + r_{\text{int}}^1(x, y) & \text{in } \Omega_{\text{int}}, \\ u_{\text{ext}}(x, y) = u_{\text{ext}}^0(x, y) + \varepsilon u_{\text{ext}}^1(x, y) + r_{\text{ext}}^1(x, y) & \text{in } \Omega_{\text{ext}}, \\ u_{\text{lay}}(x, y) = r_{\text{lay}}^1(x, y) & \text{in } \Omega_{\text{lay}}^\varepsilon. \end{cases}$$

where the terms r^N represent the residue (see (0.6) for precise estimates). Then, we truncate the series and collect the first terms of the expansion to infer equivalent conditions by neglecting residual terms depending on ε . We derive asymptotic models of different orders¹ for the first class of problems, which can be summarized as follows

Order two (Dirichlet conditions)

$$\begin{cases} u_{\text{int}}^{[1]} = 0 & \text{on } \Gamma_{\text{int}}^\varepsilon, \\ u_{\text{ext}}^{[1]} = 0 & \text{on } \Gamma_{\text{ext}}^\varepsilon. \end{cases}$$

¹Let $u^{[k]}$ be the solution to an asymptotic model, and let u be the solution to the reference problem. We say that the asymptotic model is of order $k + 1$, if there exists a constant C independent of ε , such that $\|u - u^{[k]}\|_{1, \Omega^\varepsilon} \leq C\varepsilon^{k+1}$ for ε sufficiently small, where $\Omega^\varepsilon = \Omega_{\text{int}}^\varepsilon \cup \Omega_{\text{ext}}^\varepsilon$.

Order four

$$\begin{cases} [u^{[3]}]_{\Gamma^\varepsilon} = 0, \\ [\sigma \partial_n u^{[3]}]_{\Gamma^\varepsilon} = -\frac{\hat{\sigma}_0}{\varepsilon^2} \frac{d^2}{dy^2} \{u^{[3]}\}_{\Gamma^\varepsilon}. \end{cases}$$

The asymptotic conditions derived for the second class of problems are summarized as follows

Order one (Dirichlet conditions)

$$\begin{cases} u_{\text{int}}^{[0]} = 0 & \text{on } \Gamma, \\ u_{\text{ext}}^{[0]} = 0 & \text{on } \Gamma. \end{cases}$$

Order two (Robin conditions)

$$\begin{cases} u_{\text{int}}^{[1]} = \frac{\varepsilon}{2} \partial_n u_{\text{int}}^{[1]} & \text{on } \Gamma, \\ u_{\text{ext}}^{[1]} = -\frac{\varepsilon}{2} \partial_n u_{\text{ext}}^{[1]} & \text{on } \Gamma. \end{cases}$$

When numerically solving this model, it presents some instability problems due to a non-coercive term that appears in the variational formulation of the problem. This fact causes the numerical solutions to present big oscillations near the thin layer, behaviour which is not desirable. However, this issue can be solved by employing artificial boundaries [15, 16] and rewriting the transmission conditions across them. Doing so we obtain the following model (see Section 3.5 for more details)

$$\begin{cases} u_{\delta,\text{int}}^{[1]} = \frac{\varepsilon(1-2\delta)}{2} \partial_n u_{\delta,\text{int}}^{[1]} & \text{on } \Gamma_{\text{int}}^\delta, \\ u_{\delta,\text{ext}}^{[1]} = -\frac{\varepsilon(1-2\delta)}{2} \partial_n u_{\delta,\text{ext}}^{[1]} & \text{on } \Gamma_{\text{ext}}^\delta, \end{cases} \quad (0.1)$$

which is stable for $\delta > 0.5$.

Order three

$$\left\{ \begin{array}{l} [u^{[2]}]_{\Gamma} + \varepsilon \{ \partial_n u^{[2]} \}_{\Gamma} + \frac{\varepsilon^2}{8} [\partial_n^2 u^{[2]}]_{\Gamma} = 0, \\ \frac{\varepsilon^2}{\widehat{\sigma}_0} [\sigma \partial_n u^{[2]}]_{\Gamma} + \frac{\varepsilon^2}{8} \frac{d^2}{dy^2} \{ \partial_n^2 u^{[2]} \}_{\Gamma} + \frac{\varepsilon}{4} \frac{d^2}{dy^2} [\partial_n u^{[2]}]_{\Gamma} + \frac{d^2}{dy^2} \{ u^{[2]} \}_{\Gamma} = 0. \end{array} \right.$$

Order four

$$\left\{ \begin{array}{l} [u^{[3]}]_{\Gamma} + \varepsilon \{ \partial_n u^{[3]} \}_{\Gamma} + \frac{\varepsilon^2}{8} [\partial_n^2 u^{[3]}]_{\Gamma} + \frac{\varepsilon^3}{24} \{ \partial_n^3 u^{[3]} \}_{\Gamma} = 0, \\ \frac{\varepsilon^2}{\widehat{\sigma}_0} [\sigma \partial_n u^{[3]}]_{\Gamma} + \frac{\varepsilon^3}{\widehat{\sigma}_0} \{ \sigma \partial_n u^{[3]} \}_{\Gamma} + \frac{\varepsilon^3}{96} \frac{d^2}{dy^2} [\partial_n^3 u^{[3]}]_{\Gamma} \\ + \frac{\varepsilon^2}{8} \frac{d^2}{dy^2} \{ \partial_n^2 u^{[3]} \}_{\Gamma} + \frac{\varepsilon}{4} \frac{d^2}{dy^2} [\partial_n u^{[3]}]_{\Gamma} + \frac{d^2}{dy^2} \{ u^{[3]} \}_{\Gamma} = 0. \end{array} \right.$$

Classical conditions and comparison with equivalent conditions

In this section we show the results we obtain when we no longer consider the conductivity in the thin layer to be dependent on its thickness to remark the different results we obtain with our approach compared to the classical one. The model problem remains the same, but now the conductivity inside the casing, σ_{lay} , is just a constant and not dependent on ε any more. Considering this model and applying the same asymptotic method to derive approximate models of the first class, we obtain a first-order model and a third-order model. The expression of the impedance conditions for these models are the following.

First-order model

$$\left\{ \begin{array}{ll} \sigma_{\text{int}} \Delta u_{\text{int}}^{[0]} = f_{\text{int}} & \text{in } \Omega_{\text{int}}^{\varepsilon}, \\ \sigma_{\text{ext}} \Delta u_{\text{ext}}^{[0]} = f_{\text{ext}} & \text{in } \Omega_{\text{ext}}^{\varepsilon}, \\ [u^{[0]}]_{\Gamma^{\varepsilon}} = 0, \\ [\sigma \partial_n u^{[0]}]_{\Gamma^{\varepsilon}} = 0, \\ u^{[0]} = 0 & \text{on } \partial\Omega \cap \partial\Omega^{\varepsilon}. \end{array} \right. \quad (0.2)$$

Third-order model

$$\left\{ \begin{array}{ll} \sigma_{\text{int}} \Delta u_{\text{int}}^{[2]} = f_{\text{int}} & \text{in } \Omega_{\text{int}}^{\varepsilon}, \\ \sigma_{\text{ext}} \Delta u_{\text{ext}}^{[2]} = f_{\text{ext}} & \text{in } \Omega_{\text{ext}}^{\varepsilon}, \\ [u^{[2]}]_{\Gamma^{\varepsilon}} = \frac{\varepsilon}{\sigma_{\text{lay}}} \{ \sigma \partial_n u^{[2]} \}_{\Gamma^{\varepsilon}}, \\ [\sigma \partial_n u^{[2]}]_{\Gamma^{\varepsilon}} = -\varepsilon \sigma_{\text{lay}} \frac{d^2}{dy^2} \{ u^{[2]} \}_{\Gamma^{\varepsilon}}, \\ u^{[2]} = 0 & \text{on } \partial\Omega \cap \partial\Omega^{\varepsilon}. \end{array} \right. \quad (0.3)$$

We notice that these models are different from (1.18) and (1.19). A main difference comparing with our approach (i.e. when $\sigma_{\text{lay}} = \hat{\sigma}_0 \varepsilon^{-3}$) comes from the fact that now the lower order model (0.2) is coupled, whereas model (1.18) is governed by two independent problems. Moreover, the lower order model (0.2) is of order one, whereas model (1.18) is of order two. In the same way, the higher order model (0.3) is of order three, whereas model (1.19) is of order four.

In the same way, applying the asymptotic method to derive approximate models of the second class, we obtain a first-order model and a second-order model. The expression of the impedance conditions for these models are the following.

First-order model

$$\left\{ \begin{array}{ll} \sigma_{\text{int}} \Delta u_{\text{int}}^{[0]} = f_{\text{int}} & \text{in } \Omega_{\text{int}}, \\ \sigma_{\text{ext}} \Delta u_{\text{ext}}^{[0]} = f_{\text{ext}} & \text{in } \Omega_{\text{ext}}, \\ [u^{[0]}]_{\Gamma} = 0, \\ [\sigma \partial_n u^{[0]}]_{\Gamma} = 0, \\ u^{[0]} = 0 & \text{on } \partial\Omega. \end{array} \right. \quad (0.4)$$

Second-order model

$$\left\{ \begin{array}{ll} \sigma_{\text{int}} \Delta u_{\text{int}}^{[1]} = f_{\text{int}} & \text{in } \Omega_{\text{int}}, \\ \sigma_{\text{ext}} \Delta u_{\text{ext}}^{[1]} = f_{\text{ext}} & \text{in } \Omega_{\text{ext}}, \\ [u^{[1]}]_{\Gamma} = \frac{\varepsilon}{\sigma_{\text{lay}}} \left\{ \sigma \partial_n u^{[1]} \right\}_{\Gamma} - \varepsilon \left\{ \partial_n u^{[1]} \right\}_{\Gamma}, \\ [\sigma \partial_n u^{[1]}]_{\Gamma} = -\varepsilon \sigma_{\text{lay}} \frac{d^2}{dy^2} \left\{ u^{[1]} \right\}_{\Gamma} - \varepsilon \left\{ \sigma \partial_n^2 u^{[1]} \right\}_{\Gamma}, \\ u^{[1]} = 0 & \text{on } \partial\Omega. \end{array} \right. \quad (0.5)$$

We notice that these models are different from (1.36) and (1.38). A main difference comparing with our approach (i.e. when $\sigma_{\text{lay}} = \hat{\sigma}_0 \varepsilon^{-3}$) comes from the fact that now both models are coupled, whereas employing our approach, the models are uncoupled, given thus by two independent problems. In this case, contrary to the first class of ITCs, the order of these models, (0.4) and (0.5), coincide with the one of the models (1.36) and (1.38).

3D axisymmetric ITCs derivation

In this configuration, the meridian domain corresponds to the 2D configuration (see Figure 1), but in the variables (r, z) instead of the variables (x, y) . We follow the same methodology for this configuration, we begin by performing an asymptotic expansion of the solution. Here, even though they are different, for the sake of simplicity we employ the same notation as in the 2D configuration for the terms

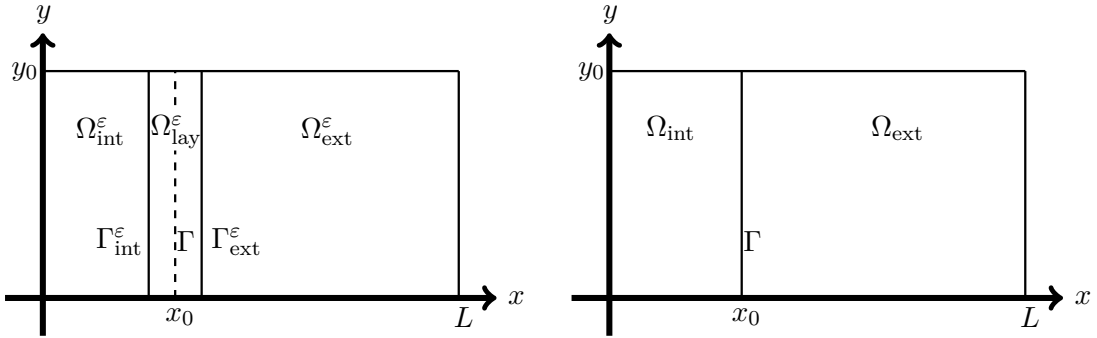
of the asymptotic expansion. The asymptotic expansion has the following form for the first approach (see Proposition 3)

$$\begin{cases} u_{\text{int}}(r, z) = u_{\text{int}}^0(r, z) + \varepsilon^2 u_{\text{int}}^2(r, z) + \varepsilon^3 u_{\text{int}}^3(r, z) + r_{\text{int}}^3(r, z) & \text{in } \Omega_{\text{int}}^\varepsilon, \\ u_{\text{ext}}(r, z) = u_{\text{ext}}^0(r, z) + \varepsilon^2 u_{\text{ext}}^2(r, z) + \varepsilon^3 u_{\text{ext}}^3(r, z) + r_{\text{ext}}^3(r, z) & \text{in } \Omega_{\text{ext}}^\varepsilon, \\ u_{\text{lay}}(r, z) = \varepsilon^2 U^2(\varepsilon^{-1}(r - r_0), z) + \varepsilon^3 U^3(\varepsilon^{-1}(r - r_0), z) + r_{\text{lay}}^3(r, z) & \text{in } \Omega_{\text{lay}}^\varepsilon, \end{cases}$$

and the following form for the second approach (see Proposition 4)

$$\begin{cases} u_{\text{int}}(r, z) = u_{\text{int}}^0(r, z) + \varepsilon u_{\text{int}}^1(r, z) + r_{\text{int}}^1(r, z) & \text{in } \Omega_{\text{int}}, \\ u_{\text{ext}}(r, z) = u_{\text{ext}}^0(r, z) + \varepsilon u_{\text{ext}}^1(r, z) + r_{\text{ext}}^1(r, z) & \text{in } \Omega_{\text{ext}}, \\ u_{\text{lay}}(r, z) = r_{\text{lay}}^1(r, z) & \text{in } \Omega_{\text{lay}}^\varepsilon, \end{cases}$$

where the terms r^N represent the residue. Then, we truncate the series and collect the first terms of the expansion to infer equivalent conditions by neglecting residual terms depending on ε . The asymptotic conditions we have derived for the first class of problems can be summarized as follows



(a) Reference problem domain.

(b) Domain for the second class of ITCs.

Figure 1: Domains for the reference model and the second class of asymptotic models.

Order two (Dirichlet conditions)

$$\begin{cases} u_{\text{int}}^{(1)} = 0 & \text{on } \Gamma_{\text{int}}^\varepsilon, \\ u_{\text{ext}}^{(1)} = 0 & \text{on } \Gamma_{\text{ext}}^\varepsilon. \end{cases}$$

Order three

$$\begin{cases} [u^{[2]}]_{\Gamma^\varepsilon} = 0, \\ \frac{d^2}{dz^2} \{u^{[2]}\}_{\Gamma^\varepsilon} + \varepsilon^2 \frac{1}{\widehat{\sigma}_0} [\sigma \partial_n u^{[2]}]_{\Gamma^\varepsilon} = 0. \end{cases}$$

Order four

$$\begin{cases} [u^{[3]}]_{\Gamma^\varepsilon} = 0, \\ \varepsilon^2 \frac{1}{\widehat{\sigma}_0} [\sigma \partial_n u^{[3]}]_{\Gamma^\varepsilon} + \varepsilon^3 \frac{1}{\widehat{\sigma}_0 r_0} \{\sigma \partial_n u^{[3]}\}_{\Gamma^\varepsilon} = -\frac{d^2}{dz^2} \{u^{[3]}\}_{\Gamma^\varepsilon}. \end{cases}$$

The asymptotic conditions derived for the second class of problems are summarized as follows

Order one (Dirichlet conditions)

$$\begin{cases} u_{\text{int}}^{[0]} = 0 & \text{on } \Gamma, \\ u_{\text{ext}}^{[0]} = 0 & \text{on } \Gamma. \end{cases}$$

Order two (Robin conditions)

$$\begin{cases} u_{\text{int}}^{[1]} = \frac{\varepsilon}{2} \partial_n u_{\text{int}}^{[1]} & \text{on } \Gamma, \\ u_{\text{ext}}^{[1]} = -\frac{\varepsilon}{2} \partial_n u_{\text{ext}}^{[1]} & \text{on } \Gamma. \end{cases}$$

We remark that these conditions coincide with the ITCs derived for the 2D problem up to the second order of approximations.

Stability and convergence results

These asymptotic models approximate the solution to the reference model and converge to it with a determined order. We perform the mathematical proves of existence, uniqueness, and uniform estimates for the reference problem and the

asymptotic models. Then, we prove the order of convergence of the asymptotic models. We begin by proving the following optimal estimates for the residue (see Proposition 2)

$$\|r_{\text{ext}}^N\|_{1,\Omega_{\text{ext}}^\varepsilon} + \|r_{\text{int}}^N\|_{1,\Omega_{\text{int}}^\varepsilon} + \sqrt{\varepsilon} \|r_{\text{lay}}^N\|_{1,\Omega_{\text{lay}}^\varepsilon} \leq C\varepsilon^{N+1}, \quad (0.6)$$

and then, we obtain the following convergence results for the solutions to the asymptotic models of the first class (see Proposition 6 and Proposition 7)

$$\begin{aligned} \|u_{\text{int}} - u_{\text{int}}^{[1]}\|_{1,\Omega_{\text{int}}^\varepsilon} + \|u_{\text{ext}} - u_{\text{ext}}^{[1]}\|_{1,\Omega_{\text{int}}^\varepsilon} &\leq k\varepsilon^2, \\ \|u_{\text{int}} - u_{\text{int}}^{[3]}\|_{1,\Omega_{\text{int}}^\varepsilon} + \|u_{\text{ext}} - u_{\text{ext}}^{[3]}\|_{1,\Omega_{\text{int}}^\varepsilon} &\leq k\varepsilon^4, \end{aligned}$$

and the following for the asymptotic models of the second class (see Proposition 10 and Proposition 11)

$$\begin{aligned} \|u_{\text{int}} - u_{\text{int}}^{[0]}\|_{1,\Omega_{\text{int}}^\varepsilon} + \|u_{\text{ext}} - u_{\text{ext}}^{[0]}\|_{1,\Omega_{\text{int}}^\varepsilon} &\leq k\varepsilon, \\ \|u_{\text{int}} - u_{\delta,\text{int}}^{[1]}\|_{1,\Omega_{\text{int}}^\delta} + \|u_{\text{ext}} - u_{\delta,\text{ext}}^{[1]}\|_{1,\Omega_{\text{ext}}^\delta} &\leq k\varepsilon^2. \end{aligned}$$

When considering the second class of ITCs, the model of order two presents some instability problems. However, this issue can be solved by employing artificial boundaries [15, 16] and rewriting the transmission conditions across them. This is the reason we denote the solution to this asymptotic model as $u_\delta^{[1]}$ (see Section 3.5 for more details).

Numerical results and application

Numerical results show that theoretical order of convergence coincide with the convergence rates obtained with simulations. When measuring the error in L^2 norm we recover the theoretical order of convergence for all the models, including the second-order model of the second class in the 2D configuration, despite the instabilities it has. On the other hand, when measuring the error in the H^1 norm, the order of convergence is recovered for all the models except for this one, due to the instabilities. However, when employing a technique based on the use of artificial boundaries, the order of convergence is recovered for the H^1 norm with this model too. We observe the numerical convergence rates for the different models we have derived in Figure 2. In the same way, we have derived similar results for the 3D axisymmetric configuration by obtaining convergence curves for the different models employing the H^1 norm.

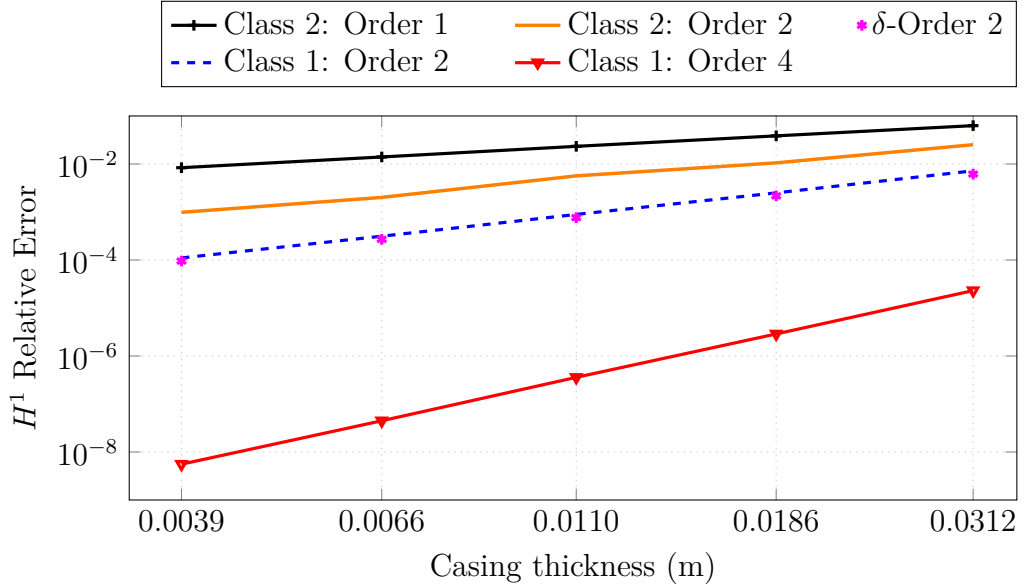


Figure 2: H^1 relative error of the different asymptotic models for different values of ε

Comparison between the equivalent models

We would like to show a brief comparison of the models derived employing the two approaches we have considered. Both approaches have their advantages and drawbacks. Table 1 summarizes some of these points for the different models we have derived.

Model	Numerical order	Stability	ε -independent domain
Class 1: Order 2	2	✓	✗
Class 1: Order 4	4	✓	✗
Class 2: Order 1	1	✓	✓
Class 2: Order 2	1-2	✗	✓
δ -Order 2	2	✓	✗

Table 1: Comparison of the four models we have derived.

As we observe in Table 1, the models obtained for the first class of problems have a higher order of convergence than those derived for the second class. On the

other hand, one of the models of the second class presents some instability issues, even though we present a technique for solving these problems in Section 1.4.3. An advantage of the second class ITCs in comparison with the first class ITCs is that the domain of the obtained models does not depend on ε , while it does for the models of the first class. This makes these models much more practical, specially when considering a curved thin layer. Concerning the models derived for the 3D axisymmetric configuration, we remark that the models obtained for the first class of problems are different from those obtained in the 2D configuration for the first class, the main difference being the derivation of an additional third-order model and an extra term in the fourth-order model.

Application

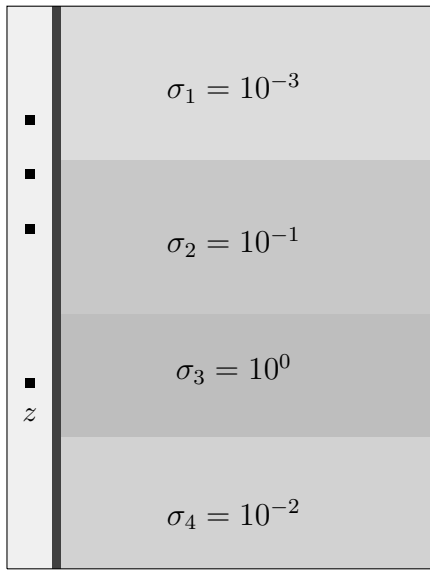
Here we present an application for the derived models. We consider a three dimensional axisymmetric borehole surrounded by several rock layers of different conductivities. We introduce a transmitter and three receivers inside the borehole, and we approximate the second derivative of potential in the axis direction by employing the second difference of potential measured at the receivers. The second difference of potential is characterized by the following formula

$$\partial_z^2 u(r_1, z_2) \approx \frac{u(r_1, z_3) - 2u(r_1, z_2) + u(r_1, z_1)}{h^2},$$

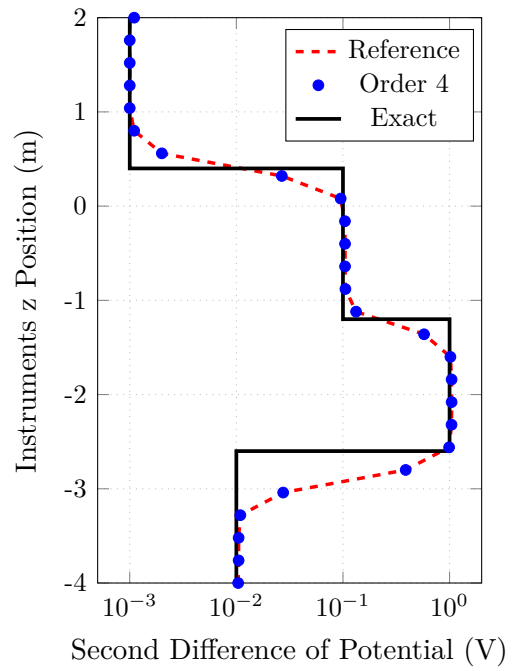
where (r_1, z_1) , (r_1, z_2) , and (r_1, z_3) are the positions of the three receivers. This expression approximates the value of second derivative of potential in the vertical direction up to an error of order $O(h)$, where h denotes the distance between the receivers, $h = z_3 - z_2 = z_2 - z_1$. This calculi allows us to determine the conductivity of the rock formations. We observe such a configuration in Figure 3a and in Figure 3b we observe the result of measuring the second difference of potential at the receivers. We observe that the results for the reference model and the asymptotic model of order four are almost identical.

Semi-analytical solutions

In this section we present the results obtained in the form of semi-analytical solutions. We consider several of the derived asymptotic models and we obtain semi-analytical solutions for them by applying a Hankel transform, more specifically, we consider problems (1.84), (1.85), and (1.77). In order to be able to perform this kind of analysis, we assume that in these problems the domain is infinite along the



(a) Domain with a four layered rock formation.



(b) Second difference of potential for different positions of the instrument in a four layered formation.

Figure 3: Borehole surrounded by a four layered formation and second difference of potential measured at the receivers for the reference model and the approximate model of order four.

z direction. The employed Hankel transform has the following form

$$\hat{u}_k(r, \xi) = \frac{1}{2\pi} \int_{(-\pi, \pi) \times \mathbb{R}} u(r, \theta, z) \cos(k\theta) e^{i\xi z} d\theta dz.$$

Once the expression of \hat{u} is found, we employ the following inverse Hankel transform to obtain the expression of u

$$u(r, \theta, z) = \sum_{k=0}^{\infty} \frac{\zeta_k}{2\pi} \int_{\mathbb{R}} \hat{u}_k(r, \xi) e^{i\xi z} d\xi \cos(k\theta),$$

where

$$\zeta_k = \begin{cases} 1 & k = 0, \\ 2 & k > 0. \end{cases}$$

The main result concerning this section corresponds to the semi-analytical expression of the solution to Problem (1.77), defined over the domain showed in Figure 1.4, which has the form

$$\begin{cases} \hat{u}_k(r, |\xi|) = C_1^k(|\xi|)I_k(|\xi|r), & r \in (0, r_t), \\ \hat{u}_k(r, |\xi|) = C_3^k(|\xi|)I_k(|\xi|r) + C_4^k(|\xi|)K_k(|\xi|r), & r \in (r_t, r_{0,\varepsilon}^-), \\ \hat{u}_k(r, |\xi|) = C_5^k(|\xi|)I_k(|\xi|r) + C_6^k(|\xi|)K_k(|\xi|r), & r \in (r_t, r_{0,\varepsilon}^+), \end{cases}$$

where functions I_k and K_k correspond to the modified Bessel function of first and second kind respectively. The coefficients C_1^k , C_3^k , C_4^k , C_5^k , and C_6^k are determined by employing the boundary and transmission conditions of Problem (1.77).

DERIVATION OF ITCS WITH DIRICHLET EXTERNAL BOUNDARY CONDITIONS

1.1 Introduction

This chapter is devoted to the study of a transmission problem for the electric potential. In all considered configurations, the domain includes a highly conductive thin layer of uniform thickness ε and Dirichlet boundary conditions. The objective of this chapter is to derive equivalent transmission conditions when ε tends to zero. For this purpose we adopt two different approaches that deliver two different classes of ITCS. The first approach consists in deriving equivalent conditions across the thin layer itself, whereas on the second approach we derive the equivalent conditions across an artificial interface located in the middle of the thin layer.

This chapter is structured as follows. Section 1.2 states the model problem for a 2D transmission problem for the static electric potential. Then, we present the scaling we perform as a first step towards deriving a multiscale expansion in terms of powers of ε for the solution to the model problem. This part is common to the two approaches we consider, which are explained in Sections 1.3 and 1.4 respectively. Both sections consist of the derivation of ITCS for each of the considered approaches. Additionally, at the end of Section 1.4, we present a technique, based on some artificial boundaries, for solving a stability problem occurring in one of the derived models.

Finally, Sections 1.5 and 1.6 present similar results for a 2D time-harmonic problem and a 3D axi-symmetric problem. The derivation of the ITCS for these configurations is similar to the one presented in the previous sections. Thus, we summarize the procedure and we concentrate on showing the main results, concerning the asymptotic expansion of the solution and the derivation of the asymptotic models.

1.2 Static 2D configuration: model problem and scaling

The main objective of this section is to present the model problem we are interested in and to explain the first step towards the derivation of asymptotic models. This first step consists in a scaling performed in the subdomain corresponding to the thin layer. The objective of these asymptotic models is to replace a thin layer by proper transmission or boundary conditions.

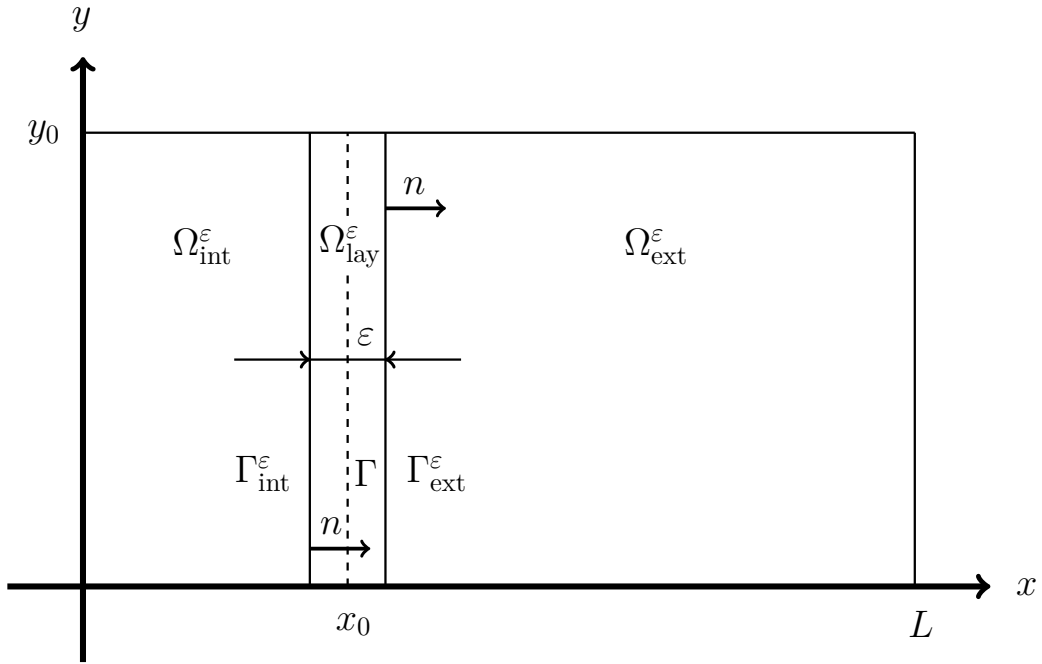


Figure 1.1: Domain of interest, composed of a thin layer, an interior domain, and an exterior domain.

Let $\Omega \subset \mathbb{R}^2$ be the domain of interest described in Figure 1.1. Domain Ω is rectangular shaped and is composed of three rectangular shaped subdomains $\Omega_{\text{int}}^\varepsilon$, $\Omega_{\text{ext}}^\varepsilon$, and $\Omega_{\text{lay}}^\varepsilon$. The subdomain $\Omega_{\text{lay}}^\varepsilon$ is a thin layer of uniform thickness $\varepsilon > 0$. We denote the interface between $\Omega_{\text{int}}^\varepsilon$ and $\Omega_{\text{lay}}^\varepsilon$ by $\Gamma_{\text{int}}^\varepsilon$, and the interface between $\Omega_{\text{lay}}^\varepsilon$ and $\Omega_{\text{ext}}^\varepsilon$ by $\Gamma_{\text{ext}}^\varepsilon$. In this domain, we study the equations of the static electric potential, which read as follows

$$\operatorname{div}(\sigma \nabla u) = f. \quad (1.1)$$

Here, u represents the electric potential, σ is the conductivity, and f stands for a current source. The conductivity is a piecewise constant function, with a different

value in each subdomain. Specifically, the value of the conductivity inside the thin layer $\Omega_{\text{lay}}^\varepsilon$ is much larger than the one in the other subdomains and we assume that it depends on the parameter ε . We consider a conductivity of the following form

$$\sigma = \begin{cases} \sigma_{\text{int}} & \text{in } \Omega_{\text{int}}^\varepsilon, \\ \sigma_{\text{lay}} = \widehat{\sigma}_0 \varepsilon^{-3} & \text{in } \Omega_{\text{lay}}^\varepsilon, \\ \sigma_{\text{ext}} & \text{in } \Omega_{\text{ext}}^\varepsilon, \end{cases}$$

where $\widehat{\sigma}_0 > 0$ is a given constant. We assume that the right-hand side f is a piecewise smooth function that is independent of ε and it vanishes inside the layer $\Omega_{\text{lay}}^\varepsilon$.

$$f = \begin{cases} f_{\text{int}} & \text{in } \Omega_{\text{int}}^\varepsilon, \\ f_{\text{lay}} = 0 & \text{in } \Omega_{\text{lay}}^\varepsilon, \\ f_{\text{ext}} & \text{in } \Omega_{\text{ext}}^\varepsilon. \end{cases}$$

It is possible to prove that Problem (1.1) has a unique solution $u \in H_0^1(\Omega)$. Representing this solution u in each subdomain as follows

$$u = \begin{cases} u_{\text{int}} & \text{in } \Omega_{\text{int}}^\varepsilon, \\ u_{\text{lay}} & \text{in } \Omega_{\text{lay}}^\varepsilon, \\ u_{\text{ext}} & \text{in } \Omega_{\text{ext}}^\varepsilon, \end{cases}$$

the Problem (1.1) becomes

$$\left\{ \begin{array}{ll} \sigma_{\text{int}} \Delta u_{\text{int}} = f_{\text{int}} & \text{in } \Omega_{\text{int}}^\varepsilon, \\ \sigma_{\text{ext}} \Delta u_{\text{ext}} = f_{\text{ext}} & \text{in } \Omega_{\text{ext}}^\varepsilon, \\ \Delta u_{\text{lay}} = 0 & \text{in } \Omega_{\text{lay}}^\varepsilon, \\ u_{\text{int}} = u_{\text{lay}} & \text{on } \Gamma_{\text{int}}^\varepsilon, \\ u_{\text{lay}} = u_{\text{ext}} & \text{on } \Gamma_{\text{ext}}^\varepsilon, \\ \sigma_{\text{int}} \partial_n u_{\text{int}} = \widehat{\sigma}_0 \varepsilon^{-3} \partial_n u_{\text{lay}} & \text{on } \Gamma_{\text{int}}^\varepsilon, \\ \widehat{\sigma}_0 \varepsilon^{-3} \partial_n u_{\text{lay}} = \sigma_{\text{ext}} \partial_n u_{\text{ext}} & \text{on } \Gamma_{\text{ext}}^\varepsilon, \\ u = 0 & \text{on } \partial\Omega, \end{array} \right. \quad (1.2)$$

where ∂_n represents the normal derivative in the direction of the normal vector, inwardly directed to $\Omega_{\text{ext}}^\varepsilon$ on $\Gamma_{\text{ext}}^\varepsilon$, and outwardly directed to $\Omega_{\text{int}}^\varepsilon$ on $\Gamma_{\text{int}}^\varepsilon$ (see Figure 1.1).

Introduction of a scaling

A key point for the derivation of a multiscale expansion for the solution to Problem (1.2) consists in performing a scaling along the direction normal to the thin layer. We begin by describing domain $\Omega_{\text{lay}}^\varepsilon$ in the following way

$$\Omega_{\text{lay}}^\varepsilon = \left\{ \gamma(y) + \varepsilon X n : \gamma(y) \in \Gamma, X \in \left(-\frac{1}{2}, \frac{1}{2} \right) \right\},$$

where γ is a parametrization of the curve Γ (see Figure 1.1), which is defined as

$$\gamma(y) = (x_0, y), \text{ for all } y \in (0, y_0)$$

and $n = (1, 0)$ is the normal vector to the curve Γ . This domain geometry induces the following scaling

$$x = x_0 + \varepsilon X \quad \Leftrightarrow \quad X = \varepsilon^{-1} (x - x_0).$$

As a consequence, we have

$$\partial_X^k = \varepsilon^k \partial_x^k, \quad k \in \mathbb{N}.$$

This scaling allows us to write the Laplace operator in the following way

$$\Delta = \partial_x^2 + \partial_y^2 = \varepsilon^{-2} \partial_X^2 + \partial_y^2.$$

On the interfaces $\Gamma_{\text{int}}^\varepsilon$ and $\Gamma_{\text{ext}}^\varepsilon$, we rewrite the normal derivative in the following form $\partial_n = \partial_x = \varepsilon^{-1} \partial_X$. Finally, we denote by U the function that satisfies

$$u_{\text{lay}}(x, y) = u_{\text{lay}}(x_0 + \varepsilon X, y) = U(X, y), \quad (X, y) \in \left(-\frac{1}{2}, \frac{1}{2} \right) \times (0, y_0).$$

We rewrite System (1.2) with the newly defined variables and functions and

we obtain

$$\left\{ \begin{array}{ll} \sigma_{\text{int}} \Delta u_{\text{int}} = f_{\text{int}} & \text{in } \Omega_{\text{int}}^\varepsilon, \\ \sigma_{\text{ext}} \Delta u_{\text{ext}} = f_{\text{ext}} & \text{in } \Omega_{\text{ext}}^\varepsilon, \\ \varepsilon^{-2} \partial_X^2 U + \partial_y^2 U = 0 & \text{in } \left(\frac{-1}{2}, \frac{1}{2} \right) \times (0, y_0), \\ u_{\text{int}} \left(x_0 - \frac{\varepsilon}{2}, y \right) = U \left(-\frac{1}{2}, y \right) & y \in (0, y_0), \\ u_{\text{ext}} \left(x_0 + \frac{\varepsilon}{2}, y \right) = U \left(\frac{1}{2}, y \right) & y \in (0, y_0), \\ \sigma_{\text{int}} \partial_n u_{\text{int}} \left(x_0 - \frac{\varepsilon}{2}, y \right) = \hat{\sigma}_0 \varepsilon^{-4} \partial_X U \left(-\frac{1}{2}, y \right) & y \in (0, y_0), \\ \sigma_{\text{ext}} \partial_n u_{\text{ext}} \left(x_0 + \frac{\varepsilon}{2}, y \right) = \hat{\sigma}_0 \varepsilon^{-4} \partial_X U \left(\frac{1}{2}, y \right) & y \in (0, y_0), \\ u = 0 & \text{on } \partial\Omega, \end{array} \right. \quad (1.3)$$

1.3 Static 2D configuration: first class of ITCs

1.3.1 Construction of a multiscale expansion

In the following, we asymptotically expand the solution in a power series of ε . Then, by truncating this series and neglecting higher order terms in ε , we derive approximate models composed of equivalent transmission conditions across the thin layer described in Section 1.3.2.

We start by defining the jump and mean value of a function across a thin layer.

Definition 1. *Let u be a smooth function defined over Ω . We define its jump and mean value across a thin layer as*

$$\left\{ \begin{array}{l} [u]_{\Gamma^\varepsilon} = u_{\text{ext}}|_{\Gamma_{\text{ext}}^\varepsilon} - u_{\text{int}}|_{\Gamma_{\text{int}}^\varepsilon}, \\ \{u\}_{\Gamma^\varepsilon} = \frac{1}{2} \left(u_{\text{ext}}|_{\Gamma_{\text{ext}}^\varepsilon} + u_{\text{int}}|_{\Gamma_{\text{int}}^\varepsilon} \right). \end{array} \right.$$

Now we proceed to derive an asymptotic expansion of u . We first perform an *Ansatz* in the form of power series expansion of ε for the solution to Problem (1.3),

i.e. we look for solutions

$$\begin{cases} u_{\text{int}}(x, y) \approx \sum_{k \geq 0} \varepsilon^k u_{\text{int}}^k(x, y) & \text{in } \Omega_{\text{int}}^\varepsilon, \\ u_{\text{ext}}(x, y) \approx \sum_{k \geq 0} \varepsilon^k u_{\text{ext}}^k(x, y) & \text{in } \Omega_{\text{ext}}^\varepsilon, \\ U(X, y) \approx \sum_{k \geq 0} \varepsilon^k U^k(X, y) & \text{in } \left(-\frac{1}{2}, \frac{1}{2}\right) \times (0, y_0). \end{cases} \quad (1.4)$$

Equations for the coefficients of the electric potential

Substituting the previous expressions (1.4) into the Equations (1.3) and collecting the terms with the same powers in ε , for every $k \in \mathbb{N}$ we obtain the following set of equations

$$\begin{cases} \sigma_{\text{int}} \Delta u_{\text{int}}^k(x, y) = f_{\text{int}}(x, y) \delta_0^k & \text{in } \Omega_{\text{ext}}^\varepsilon, & (1.5a) \\ \sigma_{\text{ext}} \Delta u_{\text{ext}}^k(x, y) = f_{\text{ext}}(x, y) \delta_0^k & \text{in } \Omega_{\text{ext}}^\varepsilon, & (1.5b) \\ \partial_X^2 U^k(X, y) = -\partial_y^2 U^{k-2}(X, y) & \text{in } \left(-\frac{1}{2}, \frac{1}{2}\right) \times (0, y_0), & (1.5c) \end{cases}$$

along with the following transmission conditions

$$\begin{cases} U^k\left(-\frac{1}{2}, y\right) = u_{\text{int}}^k\left(x_0 - \frac{\varepsilon}{2}, y\right) & y \in (0, y_0), & (1.6a) \\ U^k\left(\frac{1}{2}, y\right) = u_{\text{ext}}^k\left(x_0 + \frac{\varepsilon}{2}, y\right) & y \in (0, y_0), & (1.6b) \\ \hat{\sigma}_0 \partial_X U^k\left(-\frac{1}{2}, y\right) = \sigma_{\text{int}} \partial_n u_{\text{int}}^{k-4}\left(x_0 - \frac{\varepsilon}{2}, y\right) & y \in (0, y_0), & (1.6c) \\ \hat{\sigma}_0 \partial_X U^k\left(\frac{1}{2}, y\right) = \sigma_{\text{ext}} \partial_n u_{\text{ext}}^{k-4}\left(x_0 + \frac{\varepsilon}{2}, y\right) & y \in (0, y_0), & (1.6d) \end{cases}$$

and the following boundary conditions

$$\left\{ \begin{array}{ll} u^k(0, y) = u^k(L, y) = 0 & y \in (0, y_0), \quad (1.7a) \\ u^k(x, 0) = u^k(x, y_0) = 0 & x \in \left(0, x_0 - \frac{\varepsilon}{2}\right) \cup \left(x_0 + \frac{\varepsilon}{2}, L\right), \quad (1.7b) \\ U^k(X, 0) = \bar{U}^k(X, y_0) = 0 & X \in \left(-\frac{1}{2}, \frac{1}{2}\right), \quad (1.7c) \end{array} \right.$$

where δ_0^k represents the Kronecker symbol. For determining the elemental problem satisfied by each of the terms of the expansion, we will also need the following equation obtained by applying the fundamental theorem of calculus for a smooth function U^k ,

$$\int_{-\frac{1}{2}}^{\frac{1}{2}} \partial_X^2 U^k(X, y) dX = \partial_X U^k\left(\frac{1}{2}, y\right) - \partial_X U^k\left(-\frac{1}{2}, y\right). \quad (1.8)$$

If we replace Equation (1.5c) on the left-hand side of the above equation, and Equations (1.6c) and (1.6d) on the right-hand side, we obtain the following compatibility condition

$$-\int_{-\frac{1}{2}}^{\frac{1}{2}} \partial_y^2 U^{k-2}(X, y) dX = \frac{1}{\hat{\sigma}_0} \left[\sigma \partial_n u^{k-4} \right]_{\Gamma^\varepsilon}(y). \quad (1.9)$$

We adopt the convention that the terms with negative indices in Equations (1.5) - (1.9) are equal to zero. Employing equations (1.5) - (1.9) we deduce the elementary problems satisfied outside and inside the layer for any $k \in \mathbb{N}$. For that purpose, we employ the following algorithm composed of three steps.

Algorithm for the determination of the coefficients

We assume that the first terms of the expansion (1.4) up to the order ε^{k-1} have already been calculated, and we derive the equations for the k -th term. The first two steps are intended to determine U^k and the third step determines u_{int}^k and u_{ext}^k . For every $k = 0, 1, 2, \dots$, we perform the following steps:

First step:

We select Equation (1.5c), along with Equations (1.6c) and (1.6d), and we build the following differential problem in the variable X for U^k (the variable y

plays the role of a parameter)

$$\begin{cases} \partial_X^2 U^k(X, y) = -\partial_y^2 U^{k-2}(X, y) & X \in \left(-\frac{1}{2}, \frac{1}{2}\right), \\ \widehat{\sigma}_0 \partial_X U^k \left(-\frac{1}{2}, y\right) = \sigma_{\text{int}} \partial_n u_{\text{int}}^{k-4} \left(x_0 - \frac{\varepsilon}{2}, y\right), \\ \widehat{\sigma}_0 \partial_X U^k \left(\frac{1}{2}, y\right) = \sigma_{\text{ext}} \partial_n u_{\text{ext}}^{k-4} \left(x_0 + \frac{\varepsilon}{2}, y\right). \end{cases} \quad (1.10)$$

There exists a solution U^k of (1.10) provided the compatibility condition (1.9) is satisfied. We deduce the expression of U^k up to a function in the variable y , denoted by $\varphi_0^k(y)$. The function U^k has the following form

$$U^k(X, y) = V^k(X, y) + \varphi_0^k(y),$$

where V^k represents the part of U^k that is determined at this step and has the form (see Proposition 1)

$$V^k(X, y) = \begin{cases} 0 & \text{if } k = 0, 1, 2, 3, \\ \varphi_{k-2}^k(y)X^{k-2} + \varphi_{k-3}^k(y)X^{k-3} + \dots + \varphi_1^k(y)X & \text{if } k > 3. \end{cases}$$

Function φ_0^k is determined at the second step.

Second step:

We employ the compatibility condition (1.9) for the $k + 2$ term, along with Equation (1.7c) to write the following differential problem in the variable y for function φ_0^k , involved into the expression of U^k .

$$\begin{cases} \frac{d^2}{dy^2} \varphi_0^k(y) = -\frac{1}{\widehat{\sigma}_0} [\sigma \partial_n u^{k-2}]_{\Gamma^\varepsilon}(y) - \int_{-\frac{1}{2}}^{\frac{1}{2}} \partial_y^2 V^k(X, y) dX & y \in (0, y_0), \\ \varphi_0^k(0) = 0, \\ \varphi_0^k(y_0) = 0. \end{cases} \quad (1.11)$$

Solving this differential equation, we obtain function φ_0^k and thus, the complete expression of U^k .

Third step:

We derive the equations outside the layer by employing Equations (1.5a), (1.5a), (1.6a), (1.6b), (1.7a), and (1.7b). We infer that u_{int}^k and u_{ext}^k are defined independently in the two subdomains $\Omega_{\text{int}}^\varepsilon$ and $\Omega_{\text{ext}}^\varepsilon$ by the following differential problems

$$\left\{ \begin{array}{ll} \sigma_{\text{int}} \Delta u_{\text{int}}^k = f_{\text{int}} \delta_0^k & \text{in } \Omega_{\text{int}}^\varepsilon, \\ u_{\text{int}}^k \left(x_0 - \frac{\varepsilon}{2}, y \right) = U^k \left(-\frac{1}{2}, y \right), \\ u_{\text{int}}^k = 0 & \text{on } \partial\Omega \cap \partial\Omega_{\text{int}}^\varepsilon. \end{array} \right. \quad (1.12)$$

$$\left\{ \begin{array}{ll} \sigma_{\text{ext}} \Delta u_{\text{ext}}^k = f_{\text{ext}} \delta_0^k & \text{in } \Omega_{\text{ext}}^\varepsilon, \\ u_{\text{ext}}^k \left(x_0 + \frac{\varepsilon}{2}, y \right) = U^k \left(\frac{1}{2}, y \right), \\ u_{\text{ext}}^k = 0 & \text{on } \partial\Omega \cap \partial\Omega_{\text{ext}}^\varepsilon. \end{array} \right.$$

We now define u^k , for $k \in \mathbb{N}$, as

$$u^k = \begin{cases} u_{\text{int}}^k & \text{in } \Omega_{\text{int}}^\varepsilon, \\ u_{\text{ext}}^k & \text{in } \Omega_{\text{ext}}^\varepsilon. \end{cases}$$

We will now employ this algorithm to determine the first terms of the expansion.

First terms of the asymptotics

Terms of order zero

We consider Problem (1.10) for U^0

$$\left\{ \begin{array}{l} \partial_X^2 U^0(X, y) = 0 \quad X \in \left(-\frac{1}{2}, \frac{1}{2} \right), \\ \partial_X U^0 \left(-\frac{1}{2}, y \right) = 0, \\ \partial_X U^0 \left(\frac{1}{2}, y \right) = 0. \end{array} \right.$$

The solution to the above equation has the form $U^0(X, y) = \varphi_0^0(y)$. Then, we

employ (1.11) and build the following problem for φ_0^0

$$\begin{cases} \frac{d^2}{dy^2}\varphi_0^0(y) = 0 & y \in (0, y_0), \\ \varphi_0^0(0) = 0, \\ \varphi_0^0(y_0) = 0. \end{cases}$$

We deduce that $\varphi_0^0(y) = 0$ and thus, $U^0(X, y) = 0$. Finally, employing (1.12), we obtain that the limit solution u^0 satisfies homogeneous Dirichlet boundary conditions on $\Gamma_{\text{int}}^\varepsilon$ and $\Gamma_{\text{ext}}^\varepsilon$. Thus, we write the problem satisfied by u^0 as

$$\begin{cases} \sigma_{\text{int}}\Delta u_{\text{int}}^0 = f_{\text{int}} & \text{in } \Omega_{\text{int}}^\varepsilon, \\ u_{\text{int}}^0 = 0 & \text{on } \partial\Omega_{\text{int}}^\varepsilon. \end{cases} \quad (1.13)$$

$$\begin{cases} \sigma_{\text{ext}}\Delta u_{\text{ext}}^0 = f_{\text{ext}} & \text{in } \Omega_{\text{ext}}^\varepsilon, \\ u_{\text{ext}}^0 = 0 & \text{on } \partial\Omega_{\text{ext}}^\varepsilon. \end{cases}$$

Terms of order one

We consider Problem (1.10) for U^1

$$\begin{cases} \partial_X^2 U^1(X, y) = 0 & X \in \left(-\frac{1}{2}, \frac{1}{2}\right), \\ \partial_X U^1\left(-\frac{1}{2}, y\right) = 0, \\ \partial_X U^1\left(\frac{1}{2}, y\right) = 0. \end{cases}$$

The solution to the above equation has the form $U^1(X, y) = \varphi_0^1(y)$. Then, we employ (1.11) and build the following problem for φ_0^1

$$\begin{cases} \frac{d^2}{dy^2}\varphi_0^1(y) = 0 & y \in (0, y_0), \\ \varphi_0^1(0) = 0, \\ \varphi_0^1(y_0) = 0. \end{cases}$$

We deduce that $\varphi_0^1(y) = 0$ and thus, $U^1(X, y) = 0$. Finally, employing (1.12) we

write the problem satisfied by u^1 outside the layer as two uncoupled problems

$$\begin{cases} \Delta u_{\text{int}}^1 = 0 & \text{in } \Omega_{\text{int}}^\varepsilon, \\ u_{\text{int}}^1 = 0 & \text{on } \partial\Omega_{\text{int}}^\varepsilon. \end{cases} \quad (1.14)$$

$$\begin{cases} \Delta u_{\text{ext}}^1 = 0 & \text{in } \Omega_{\text{ext}}^\varepsilon, \\ u_{\text{ext}}^1 = 0 & \text{on } \partial\Omega_{\text{ext}}^\varepsilon. \end{cases}$$

We deduce that $u^1 \equiv 0$.

Terms of order two

We consider Problem (1.10) for U^2

$$\begin{cases} \partial_X^2 U^2(X, y) = 0 & X \in \left(-\frac{1}{2}, \frac{1}{2}\right), \\ \partial_X U^2\left(-\frac{1}{2}, y\right) = 0, \\ \partial_X U^2\left(\frac{1}{2}, y\right) = 0. \end{cases}$$

The solution to this equation has the form $U^2(X, y) = \varphi_0^2(y)$. Then, we employ (1.11) and build the following problem for φ_0^2

$$\begin{cases} \frac{d^2}{dy^2} \varphi_0^2(y) = -\frac{1}{\widehat{\sigma}_0} [\sigma \partial_n u^0](y) & y \in (0, y_0), \\ \varphi_0^2(0) = 0, \\ \varphi_0^2(y_0) = 0. \end{cases}$$

We deduce that $\varphi_0^2(y)$ and thus, $U^2(X, y)$ have the following form.

$$\begin{aligned} U^2(X, y) &= \varphi_0^2(y) \\ &= -\frac{1}{\widehat{\sigma}_0} \int_0^y (y-t) [\sigma \partial_n u^0]_{\Gamma^\varepsilon}(t) dt + \frac{y}{\sigma_0 y_0} \int_0^{y_0} (y_0-t) [\sigma \partial_n u^0]_{\Gamma^\varepsilon}(t) dt. \end{aligned} \quad (1.15)$$

We assume the integrals in the expression of U^2 make sense and we make the same assumption for the rest of integrals that appear in this section. Finally, employing (1.12), we write the problem satisfied outside the layer by u^2 as two uncoupled

problems

$$\left\{ \begin{array}{ll} \Delta u_{\text{int}}^2 = 0 & \text{in } \Omega_{\text{int}}^\varepsilon, \\ u_{\text{int}}^2 \left(x_0 - \frac{\varepsilon}{2}, y \right) = \varphi_0^2(y) & y \in (0, y_0), \\ u_{\text{int}}^2 = 0 & \text{on } \partial\Omega \cap \partial\Omega_{\text{int}}^\varepsilon. \end{array} \right. \quad (1.16)$$

$$\left\{ \begin{array}{ll} \Delta u_{\text{ext}}^2 = 0 & \text{in } \Omega_{\text{ext}}^\varepsilon, \\ u_{\text{ext}}^2 \left(x_0 + \frac{\varepsilon}{2}, y \right) = \varphi_0^2(y) & y \in (0, y_0), \\ u_{\text{ext}}^2 = 0 & \text{on } \partial\Omega \cap \partial\Omega_{\text{ext}}^\varepsilon. \end{array} \right.$$

Terms of order three

We consider Problem (1.10) for U^3

$$\left\{ \begin{array}{l} \partial_X^2 U^3(X, y) = 0 \quad X \in \left(-\frac{1}{2}, \frac{1}{2} \right), \\ \partial_X U^3 \left(-\frac{1}{2}, y \right) = 0, \\ \partial_X U^3 \left(\frac{1}{2}, y \right) = 0. \end{array} \right.$$

The solution to this equation has the form $U^3(X, y) = \varphi_0^3(y)$. Then, we employ (1.11) and build the following problem for φ_0^3

$$\left\{ \begin{array}{l} \frac{d^2}{dy^2} \varphi_0^3(y) = 0 \quad y \in (0, y_0), \\ \varphi_0^3(0) = 0, \\ \varphi_0^3(y_0) = 0. \end{array} \right.$$

We deduce that $\varphi_0^3(y) = 0$ and thus, $U^3(X, y) = 0$. Finally, employing (1.12) we write the problem satisfied outside the layer by u^3 as two uncoupled problems

$$\left\{ \begin{array}{ll} \Delta u_{\text{int}}^3 = 0 & \text{in } \Omega_{\text{int}}^\varepsilon, \\ u_{\text{int}}^3 = 0 & \text{on } \partial\Omega_{\text{int}}^\varepsilon. \end{array} \right. \quad (1.17)$$

$$\left\{ \begin{array}{ll} \Delta u_{\text{ext}}^3 = 0 & \text{in } \Omega_{\text{ext}}^\varepsilon, \\ u_{\text{ext}}^3 = 0 & \text{on } \partial\Omega_{\text{ext}}^\varepsilon. \end{array} \right.$$

We deduce that $u^3 \equiv 0$.

Remark 1. *This algorithm could be employed to go up to any desired order, but the elemental problems satisfied by each term of the asymptotic expansion get more complex the further you go. In addition, this process generally decreases the regularity of these terms. Here we have stopped at the fourth term of the expansion, which provides a good balance between the order of accuracy and the complexity of the problem.*

Recapitulation of the asymptotic expansion

Proposition 1. *The asymptotic expansion (1.4), has the following form*

$$\begin{cases} u_{int}(x, y) = u_{int}^0(x, y) + \varepsilon^2 u_{int}^2(x, y) + O(\varepsilon^4) & \text{in } \Omega_{int}^\varepsilon, \\ u_{ext}(x, y) = u_{ext}^0(x, y) + \varepsilon^2 u_{ext}^2(x, y) + O(\varepsilon^4) & \text{in } \Omega_{ext}^\varepsilon, \\ U(X, y) = \varepsilon^2 \varphi_0^2(y) + O(\varepsilon^4) & \text{in } \left(-\frac{1}{2}, \frac{1}{2}\right) \times (0, y_0), \end{cases}$$

where functions φ_0^2 , u^0 , and u^2 are defined by Equations (1.15), (1.13), and (1.16), respectively. In addition, for $k \in \mathbb{N}$, the solution U^k to Equation (1.10) has the following form

$$U^k(X, y) = \begin{cases} 0 & \text{if } k = 0 \text{ or } k \text{ odd,} \\ \sum_{j=0}^{k-2} \varphi_j^k(y) X^j & \text{if } k \text{ even,} \end{cases}$$

and solution $u^k = (u_{int}^k, u_{ext}^k)$ to Problem (1.12) satisfies

$$u_{int}^k \equiv u_{ext}^k \equiv 0, \quad \text{if } k \text{ odd.}$$

Proof. We prove it by induction on k . For $k = 0, 1, 2, 3$, we have already calculated the expressions of u^k and U^k in the previous section. We distinguish two different cases for the proof: the case of an even number $k \geq 4$, and the case of an odd number $k \geq 4$. Let us thus prove the result for an even number k by assuming the result is true for all even numbers $i < k$. Thanks to the inductive assumptions, function U^i has the form

$$U^i(X, y) = \varphi_{i-2}^i(y) X^{i-2} + \varphi_{i-3}^i(y) X^{i-3} + \dots + \varphi_1^i(y) X + \varphi_0^i(y).$$

We begin by considering Problem (1.10) for the even number k . Solving this problem we obtain a solution of the form

$$U^k(X, y) = \varphi_{k-2}^k(y) X^{k-2} + \varphi_{k-3}^k(y) X^{k-3} + \dots + \varphi_1^k(y) X + \varphi_0^k(y),$$

and

$$\left\{ \begin{array}{l} \varphi_1^k(y) = \frac{1}{\widehat{\sigma}_0} \left\{ \sigma \partial_n u^{k-4} \right\}_{\Gamma^\varepsilon} (y), \\ \varphi_2^k(y) = \frac{1}{2\widehat{\sigma}_0} \left[\sigma \partial_n u^{k-4} \right]_{\Gamma^\varepsilon} (y), \\ \varphi_{k-j}^k(y) = \frac{-\frac{d^2}{dy^2} \varphi_{k-j-2}^{k-2}(y)}{(k-j)(k-j-1)} \quad j = 2, \dots, k-2. \end{array} \right.$$

In the above expression of U^k , we find function V^k , which reads as

$$V^k(X, y) = \varphi_{k-2}^k(y)X^{k-2} + \varphi_{k-3}^k(y)X^{k-3} + \dots + \varphi_1^k(y)X,$$

and has been defined at the first step of the algorithm. The only thing left to prove is that if k is an odd number, $U^k \equiv 0$ and $u_{\text{int}}^k \equiv u_{\text{ext}}^k \equiv 0$. We assume that for all odd number $j \in \mathbb{N}$, such that $j < k$, $U^j \equiv 0$ and $u_{\text{int}}^j \equiv u_{\text{ext}}^j \equiv 0$. Employing Equation (1.10), we have the following problem for U^k

$$\left\{ \begin{array}{l} \partial_X^2 U^k(X, y) = -\partial_y^2 U^{k-2}(X, y) \quad X \in \left(-\frac{1}{2}, \frac{1}{2}\right), \\ \widehat{\sigma}_0 \partial_X U^k\left(-\frac{1}{2}, y\right) = \sigma_{\text{int}} \partial_n u_{\text{int}}^{k-4}\left(x_0 - \frac{\varepsilon}{2}, y\right), \\ \widehat{\sigma}_0 \partial_X U^k\left(\frac{1}{2}, y\right) = \sigma_{\text{ext}} \partial_n u_{\text{ext}}^{k-4}\left(x_0 + \frac{\varepsilon}{2}, y\right). \end{array} \right.$$

Thanks to the inductive assumptions we know that $U^{k-2} \equiv 0$ and $u_{\text{int}}^{k-4} \equiv u_{\text{ext}}^{k-4} \equiv 0$. Thus, we conclude that U^k has the following form

$$U^k(X, y) = \varphi_0^k(y).$$

Now we employ Equation (1.11) to build the following problem

$$\left\{ \begin{array}{l} \frac{d^2}{dy^2} \varphi_0^k(y) = -\frac{1}{\widehat{\sigma}_0} \left[\sigma \partial_n u^{k-2} \right]_{\Gamma^\varepsilon} (y) \quad y \in (0, y_0), \\ \varphi_0^k(0) = 0, \\ \varphi_0^k(y_0) = 0. \end{array} \right.$$

Again, thanks to the inductive assumptions, we know that $u^{k-2} \equiv 0$. Thus, we conclude that $\varphi_0^k \equiv 0$ and consequently $U^k \equiv 0$. Now, employing (1.12), we

write the problems satisfied by u_{int}^k and u_{ext}^k as follows

$$\begin{cases} \Delta u_{\text{int}}^k = 0 & \text{in } \Omega_{\text{int}}^\varepsilon, \\ u_{\text{int}}^k = 0 & \text{on } \Gamma_{\text{int}}^\varepsilon, \\ u_{\text{int}}^k = 0 & \text{on } \partial\Omega \cap \partial\Omega_{\text{int}}^\varepsilon. \end{cases}$$

$$\begin{cases} \Delta u_{\text{ext}}^k = 0 & \text{in } \Omega_{\text{ext}}^\varepsilon, \\ u_{\text{ext}}^k = 0 & \text{on } \Gamma_{\text{ext}}^\varepsilon, \\ u_{\text{ext}}^k = 0 & \text{on } \partial\Omega \cap \partial\Omega_{\text{ext}}^\varepsilon. \end{cases}$$

We deduce that $u^k \equiv 0$. □

1.3.2 Equivalent models

Now that we know the expressions for the first four terms of the expansion, we truncate the series and we identify a simpler problem satisfied by

$$u^{(k)} = u^0 + \varepsilon u^1 + \dots + \varepsilon^k u^k \quad \text{in } \Omega_{\text{int}}^\varepsilon \cup \Omega_{\text{ext}}^\varepsilon$$

up to a residual term of order ε^{k+1} . We neglect the residual term of order ε^{k+1} to obtain an approximate model satisfied by function $u^{[k]}$. For the sake of simplicity we will employ the following notation for the domain.

Notation 1. We denote by Ω^ε the domain

$$\Omega^\varepsilon = \Omega_{\text{int}}^\varepsilon \cup \Omega_{\text{ext}}^\varepsilon,$$

where $\Omega_{\text{int}}^\varepsilon$ and $\Omega_{\text{ext}}^\varepsilon$ are the domains defined in Section 1.2.

We will also adopt the following notation for the different norms we employ in this document.

Notation 2. For any function $u \in L^2(\Omega)$, we denote the L^2 norm by

$$\|u\|_{0,\Omega} = \|u\|_{L^2(\Omega)}.$$

In the same way, for any function $u \in H^1(\Omega)$, we denote the norm in H^1 by

$$\|u\|_{1,\Omega} = \left(\|u\|_{0,\Omega}^2 + \|\nabla u\|_{0,\Omega}^2 \right)^{\frac{1}{2}}.$$

In the following, we define the order of convergence for an asymptotic model. Here, we formally derive two approximate models of order two and order four, respectively.

Definition 2. *Let $u^{[k]}$ be the solution to an asymptotic model, and let u be the solution to the reference problem. We say that the asymptotic model is of order $k + 1$, if there exists a constant C independent of ε , such that following relation is satisfied for a sufficiently small ε :*

$$\|u - u^{[k]}\|_{1, \Omega^\varepsilon} \leq C\varepsilon^{k+1}.$$

Second-order model

For deriving the second-order model, we truncate the series from the second term and we define $u^{(1)}$ as

$$u^{(1)} = u^0 + \varepsilon u^1 = u^0 \quad \text{in} \quad \Omega_{\text{int}}^\varepsilon \cup \Omega_{\text{ext}}^\varepsilon \quad (\text{see Proposition 1}).$$

From (1.13), we conclude that $u^{(1)}$ solves the following uncoupled problem

$$\begin{cases} \sigma_{\text{int}} \Delta u_{\text{int}}^{(1)} = f_{\text{int}} & \text{in} \quad \Omega_{\text{int}}^\varepsilon, \\ u_{\text{int}}^{(1)} = 0 & \text{on} \quad \partial\Omega_{\text{int}}^\varepsilon. \end{cases} \quad (1.18)$$

$$\begin{cases} \sigma_{\text{ext}} \Delta u_{\text{ext}}^{(1)} = f_{\text{ext}} & \text{in} \quad \Omega_{\text{ext}}^\varepsilon, \\ u_{\text{ext}}^{(1)} = 0 & \text{on} \quad \partial\Omega_{\text{ext}}^\varepsilon. \end{cases}$$

In this case, we have $u^{[1]} = u^{(1)}$ as $u^{(1)}$ does not depend on ε . We infer a second-order model satisfied by $u^{[1]}$ solution to Problem (1.18).

Fourth-order model

For deriving the model of order four, we truncate the series from the fourth term and we define $u^{(3)}$ as

$$u^{(3)} = u^0 + \varepsilon u^1 + \varepsilon^2 u^2 + \varepsilon^3 u^3 = u^0 + \varepsilon^2 u^2 \quad \text{in} \quad \Omega_{\text{int}}^\varepsilon \cup \Omega_{\text{ext}}^\varepsilon \quad (\text{see Proposition 1}).$$

From (1.13), (1.14), (1.16), and (1.17), we conclude that $u^{(3)}$ satisfies the following equations

$$\left\{ \begin{array}{ll} \sigma_{\text{int}} \Delta u_{\text{int}}^{(3)} = f_{\text{int}} & \text{in } \Omega_{\text{int}}^\varepsilon, \\ \sigma_{\text{ext}} \Delta u_{\text{ext}}^{(3)} = f_{\text{ext}} & \text{in } \Omega_{\text{ext}}^\varepsilon, \\ [u^{(3)}]_{\Gamma^\varepsilon} = 0, \\ \frac{d^2}{dy^2} \{u^{(3)}\}_{\Gamma^\varepsilon} = -\varepsilon^2 \frac{1}{\widehat{\sigma}_0} [\sigma \partial_n u^0]_{\Gamma^\varepsilon}, \\ u^{(3)} = 0 & \text{on } \partial\Omega \cap \partial\Omega^\varepsilon. \end{array} \right.$$

Then, we employ the expression $u^0 = u^{(3)} - \varepsilon^2 u^2$ to rewrite the right-hand side of the second transmission condition as:

$$-\varepsilon^2 \frac{1}{\widehat{\sigma}_0} [\sigma \partial_n u^0]_{\Gamma^\varepsilon} = -\varepsilon^2 \frac{1}{\widehat{\sigma}_0} [\sigma \partial_n u^{(3)}]_{\Gamma^\varepsilon} + \varepsilon^4 \frac{1}{\widehat{\sigma}_0} [\sigma \partial_n u^2]_{\Gamma^\varepsilon} = -\varepsilon^2 \frac{1}{\widehat{\sigma}_0} [\sigma \partial_n u^{(3)}]_{\Gamma^\varepsilon} + O(\varepsilon^4).$$

Thus $u^{(3)}$ satisfies the following equations

$$\left\{ \begin{array}{ll} \sigma_{\text{int}} \Delta u_{\text{int}}^{(3)} = f_{\text{int}} & \text{in } \Omega_{\text{int}}^\varepsilon, \\ \sigma_{\text{ext}} \Delta u_{\text{ext}}^{(3)} = f_{\text{ext}} & \text{in } \Omega_{\text{ext}}^\varepsilon, \\ [u^{(3)}]_{\Gamma^\varepsilon} = 0, \\ \frac{d^2}{dy^2} \{u^{(3)}\}_{\Gamma^\varepsilon} = -\varepsilon^2 \frac{1}{\widehat{\sigma}_0} [\sigma \partial_n u^{(3)}]_{\Gamma^\varepsilon} + O(\varepsilon^4), \\ u^{(3)} = 0 & \text{on } \partial\Omega \cap \partial\Omega^\varepsilon. \end{array} \right.$$

We define as $u^{[3]}$ the function we obtain when truncating the solution at the fourth term of the expansion and neglecting the terms of order four or higher in ε . Then, $u^{[3]}$ satisfies the following equations

$$\left\{ \begin{array}{ll} \sigma_{\text{int}} \Delta u_{\text{int}}^{[3]} = f_{\text{int}} & \text{in } \Omega_{\text{int}}^\varepsilon, \\ \sigma_{\text{ext}} \Delta u_{\text{ext}}^{[3]} = f_{\text{ext}} & \text{in } \Omega_{\text{ext}}^\varepsilon, \\ [u^{[3]}]_{\Gamma^\varepsilon} = 0, \\ [\sigma \partial_n u^{[3]}]_{\Gamma^\varepsilon} = -\frac{\widehat{\sigma}_0}{\varepsilon^2} \frac{d^2}{dy^2} \{u^{[3]}\}_{\Gamma^\varepsilon}, \\ u^{[3]} = 0 & \text{on } \partial\Omega \cap \partial\Omega^\varepsilon. \end{array} \right. \quad (1.19)$$

1.4 Static 2D configuration: second class of ITCs

1.4.1 Construction of a multiscale expansion

In this section, we perform an expansion of the solution in power series of ε , following the same steps as in Section 1.3.1. Then, by truncating this series and neglecting higher order terms in ε , we derive approximate models composed by equivalent transmission conditions in Section 1.4.2. The main difference with the first class of ITCs is that now we employ some formal Taylor series expansions to write the terms of the expansion across an artificial interface Γ situated in the middle of the thin layer. The resulting asymptotic models will be defined in the domain depicted at Figure 1.2b. We start by defining the jump and mean value of a function across interface Γ , in the same way we have done with the jump and the mean value across the thin layer in Definition 1.

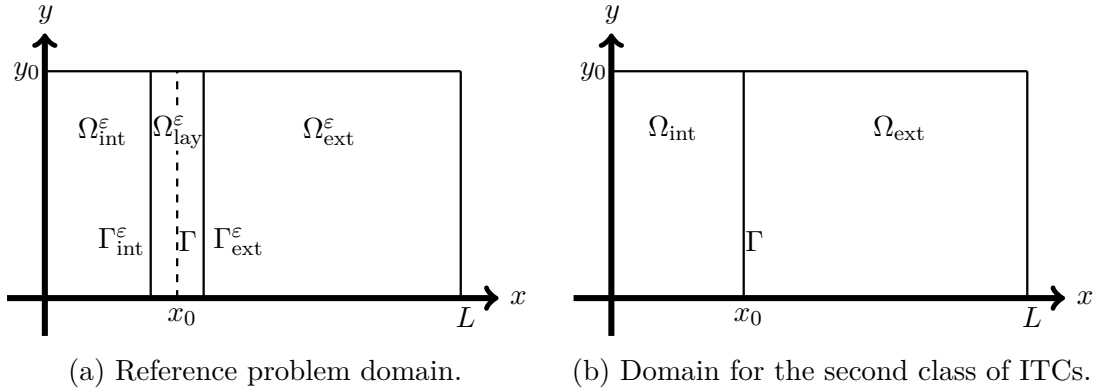


Figure 1.2: Domains for the reference model and for the second class of asymptotic models.

Definition 3. Let u be a function defined over Ω . We define its jump and mean value across interface Γ as

$$\begin{cases} [u]_{\Gamma} = u_{ext}|_{\Gamma} - u_{int}|_{\Gamma}, \\ \{u\}_{\Gamma} = \frac{1}{2} (u_{ext}|_{\Gamma} + u_{int}|_{\Gamma}). \end{cases}$$

Now we derive the asymptotic expansion. We start by performing an *Ansatz* in the form of power series of ε for the solution to Problem (1.3), that is, we look

for solutions

$$\begin{cases} u_{\text{int}}(x, y) \approx \sum_{k \geq 0} \varepsilon^k u_{\text{int}}^k(x, y) & \text{in } \Omega_{\text{int}}^\varepsilon, \\ u_{\text{ext}}(x, y) \approx \sum_{k \geq 0} \varepsilon^k u_{\text{ext}}^k(x, y) & \text{in } \Omega_{\text{ext}}^\varepsilon, \\ U(X, y) \approx \sum_{k \geq 0} \varepsilon^k U^k(X, y) & \text{in } \left(-\frac{1}{2}, \frac{1}{2}\right) \times (0, y_0). \end{cases} \quad (1.20)$$

where functions $(u_{\text{int}}^k)_{k \in \mathbb{N}}$ and $(u_{\text{ext}}^k)_{k \in \mathbb{N}}$ are now defined in ε -independent domains, contrary to the first approach. We emphasize that sequence $(u_{\text{int}}^k)_{k \in \mathbb{N}}$ (respectively $(u_{\text{ext}}^k)_{k \in \mathbb{N}}$) is defined in Ω_{int} (respectively Ω_{ext}) even if its associated series does not approach u in the thin layer. We assume that for $k \in \mathbb{N}$, the terms u_{int}^k and u_{ext}^k are as regular as necessary, see [19]. Then, we perform a formal Taylor series expansion of the terms $u_{\text{int}}^k|_{\Gamma_{\text{int}}^\varepsilon}$ and $u_{\text{ext}}^k|_{\Gamma_{\text{ext}}^\varepsilon}$ of the series, in order to write the transmission conditions across interface Γ . The formal Taylor series expansion writes as follows

$$\begin{cases} u_{\text{int}}^k \left(x_0 - \frac{\varepsilon}{2}, y\right) = \sum_{i \geq 0} \varepsilon^i \frac{(-1)^i}{2^i i!} \partial_n^i u_{\text{int}}^k(x_0, y), \\ u_{\text{ext}}^k \left(x_0 + \frac{\varepsilon}{2}, y\right) = \sum_{i \geq 0} \varepsilon^i \frac{1}{2^i i!} \partial_n^i u_{\text{ext}}^k(x_0, y). \end{cases}$$

We also perform a formal Taylor series expansion of the following form for the derivatives $\partial_n u_{\text{int}}^k|_{\Gamma_{\text{int}}^\varepsilon}$ and $\partial_n u_{\text{ext}}^k|_{\Gamma_{\text{ext}}^\varepsilon}$

$$\begin{cases} \partial_n u_{\text{int}}^k \left(x_0 - \frac{\varepsilon}{2}, y\right) = \sum_{i \geq 0} \frac{(-1)^i}{2^i i!} \partial_n^{i+1} u_{\text{int}}^k(x_0, y), \\ \partial_n u_{\text{ext}}^k \left(x_0 + \frac{\varepsilon}{2}, y\right) = \sum_{i \geq 0} \varepsilon^i \frac{1}{2^i i!} \partial_n^{i+1} u_{\text{ext}}^k(x_0, y). \end{cases}$$

Employing these formal Taylor series expansions and the *Ansatz* (1.20), we

expand the terms $u_{\text{int}}|_{\Gamma_{\text{int}}^\varepsilon}$ and $u_{\text{ext}}|_{\Gamma_{\text{ext}}^\varepsilon}$ in the following way

$$\begin{aligned} u_{\text{int}}|_{\Gamma_{\text{int}}^\varepsilon} &= u_{\text{int}}\left(x_0 - \frac{\varepsilon}{2}, y\right) = \sum_{k \geq 0} \varepsilon^k u_{\text{int}}^k\left(x_0 - \frac{\varepsilon}{2}, y\right) \\ &= \sum_{k \geq 0} \varepsilon^k \sum_{i \geq 0} \varepsilon^i \frac{(-1)^i}{2^i i!} \partial_n^i u_{\text{int}}^k(x_0, y) = \sum_{k \geq 0} \varepsilon^k \sum_{i=0}^k \frac{(-1)^i}{2^i i!} \partial_n^i u_{\text{int}}^{k-i}(x_0, y), \end{aligned} \quad (1.21)$$

$$\begin{aligned} u_{\text{ext}}|_{\Gamma_{\text{ext}}^\varepsilon} &= u_{\text{ext}}\left(x_0 + \frac{\varepsilon}{2}, y\right) = \sum_{k \geq 0} \varepsilon^k u_{\text{ext}}^k\left(x_0 + \frac{\varepsilon}{2}, y\right) \\ &= \sum_{k \geq 0} \varepsilon^k \sum_{i \geq 0} \varepsilon^i \frac{1}{2^i i!} \partial_n^i u_{\text{ext}}^k(x_0, y) = \sum_{k \geq 0} \varepsilon^k \sum_{i=0}^k \frac{1}{2^i i!} \partial_n^i u_{\text{ext}}^{k-i}(x_0, y). \end{aligned}$$

and the terms $\partial_n u_{\text{int}}^k|_{\Gamma_{\text{int}}^\varepsilon}$, $\partial_n u_{\text{ext}}^k|_{\Gamma_{\text{ext}}^\varepsilon}$ in the following way

$$\begin{aligned} \partial_n u_{\text{int}}|_{\Gamma_{\text{int}}^\varepsilon} &= \partial_n u_{\text{int}}\left(x_0 - \frac{\varepsilon}{2}, y\right) = \sum_{k \geq 0} \varepsilon^k \partial_n u_{\text{int}}^k\left(x_0 - \frac{\varepsilon}{2}, y\right) \\ &= \sum_{k \geq 0} \varepsilon^k \sum_{i \geq 0} \varepsilon^i \frac{(-1)^i}{2^i i!} \partial_n^{i+1} u_{\text{int}}^k(x_0, y) = \sum_{k \geq 0} \varepsilon^k \sum_{i=0}^k \frac{(-1)^i}{2^i i!} \partial_n^{i+1} u_{\text{int}}^{k-i}(x_0, y), \end{aligned} \quad (1.22)$$

$$\begin{aligned} \partial_n u_{\text{ext}}|_{\Gamma_{\text{ext}}^\varepsilon} &= \partial_n u_{\text{ext}}\left(x_0 + \frac{\varepsilon}{2}, y\right) = \sum_{k \geq 0} \varepsilon^k \partial_n u_{\text{ext}}^k\left(x_0 + \frac{\varepsilon}{2}, y\right) \\ &= \sum_{k \geq 0} \varepsilon^k \sum_{i \geq 0} \varepsilon^i \frac{1}{2^i i!} \partial_n^{i+1} u_{\text{ext}}^k(x_0, y) = \sum_{k \geq 0} \varepsilon^k \sum_{i=0}^k \frac{1}{2^i i!} \partial_n^{i+1} u_{\text{ext}}^{k-i}(x_0, y). \end{aligned}$$

Equations for the coefficients of the electric potential

Substituting the *Ansatz* (1.20) and the identities (1.21), (1.22) in the Equations (1.3) and collecting the terms with the same powers in ε , for every $k \in \mathbb{N}$ we obtain the following set of equations

$$\left\{ \begin{array}{ll} \sigma_{\text{int}} \Delta u_{\text{int}}^k(x, y) = f_{\text{int}}(x, y) \delta_0^k & \text{in } \Omega_{\text{int}}, & (1.23\text{a}) \\ \sigma_{\text{ext}} \Delta u_{\text{ext}}^k(x, y) = f_{\text{ext}}(x, y) \delta_0^k & \text{in } \Omega_{\text{ext}}, & (1.23\text{b}) \\ \partial_X^2 U^k(X, y) + \partial_y^2 U^{k-2}(X, y) = 0 & \text{in } \left(-\frac{1}{2}, \frac{1}{2}\right) \times (0, y_0), & (1.23\text{c}) \end{array} \right.$$

along with the following transmission conditions

$$\left\{ \begin{array}{ll} \sum_{i=0}^k \frac{(-1)^i}{2^i i!} \partial_n^i u_{\text{int}}^{k-i}(x_0, y) = U^k\left(\frac{-1}{2}, y\right) & y \in (0, y_0), & (1.24\text{a}) \\ \sum_{i=0}^k \frac{1}{2^i i!} \partial_n^i u_{\text{ext}}^{k-i}(x_0, y) = U^k\left(\frac{1}{2}, y\right) & y \in (0, y_0), & (1.24\text{b}) \\ \sigma_{\text{int}} \sum_{i=0}^{k-4} \frac{(-1)^i}{2^i i!} \partial_n^{i+1} u_{\text{int}}^{k-4-i}(x_0, y) = \hat{\sigma}_0 \partial_X U^k\left(\frac{-1}{2}, y\right) & y \in (0, y_0), & (1.24\text{c}) \\ \sigma_{\text{ext}} \sum_{i=0}^{k-4} \frac{1}{2^i i!} \partial_n^{i+1} u_{\text{ext}}^{k-4-i}(x_0, y) = \hat{\sigma}_0 \partial_X U^k\left(\frac{1}{2}, y\right) & y \in (0, y_0), & (1.24\text{d}) \end{array} \right.$$

and the following boundary conditions

$$\left\{ \begin{array}{ll} u^k(0, y) = u^k(L, y) = 0 & y \in (0, y_0), & (1.25\text{a}) \\ u^k(x, 0) = u^k(x, y_0) = 0 & x \in (0, x_0) \cup (x_0, L), & (1.25\text{b}) \\ U^k(X, 0) = U^k(X, y_0) = 0 & X \in \left(-\frac{1}{2}, \frac{1}{2}\right), & (1.25\text{c}) \end{array} \right.$$

where δ_0^k represents the Kronecker symbol. For determining the elemental problems satisfied by each of the terms of the expansion, we will also need a compatibility condition. To obtain it we apply the fundamental theorem of calculus for a smooth function U^k , along with Equations (1.23c), (1.24c), and (1.24d), and we obtain

$$\begin{aligned} & - \int_{-\frac{1}{2}}^{\frac{1}{2}} \partial_y^2 U^{k-2}(X, y) \, dX \\ & = \frac{1}{\hat{\sigma}_0} \sum_{i=0}^{k-4} \left(\frac{\sigma_{\text{ext}}}{2^i i!} \partial_n^{i+1} u_{\text{ext}}^{k-4-i}(x_0, y) + (-1)^{i+1} \frac{\sigma_{\text{int}}}{2^i i!} \partial_n^{i+1} u_{\text{int}}^{k-4-i}(x_0, y) \right). \end{aligned} \quad (1.26)$$

We adopt the convention that the terms with negative indices in Equation (1.23) - (1.26) are equal to 0. Employing Equations (1.23) - (1.26) we can determine the elementary problems satisfied outside and inside the layer for any $k \in \mathbb{N}$. For that purpose, we use the following algorithm composed of three steps.

Algorithm for the determination of the coefficients

We assume that the first terms of expansion (1.20) up to order ε^{k-1} have already been calculated and we calculate the equations for the k -th term. The first two steps consist in determining U^k and the third step consist in fixing u_{int}^k and u_{ext}^k . For every $k = 0, 1, 2, \dots$, we follow the next steps:

First step:

We select Equations (1.23c), (1.24c), and (1.24d), and we build the following differential problem in the variable X for U^k (the variable y plays the role of a parameter)

$$\left\{ \begin{array}{l} \partial_X^2 U^k(X, y) = -\partial_y^2 U^{k-2}(X, y) \quad X \in \left(-\frac{1}{2}, \frac{1}{2}\right), \\ \hat{\sigma}_0 \partial_X U^k\left(\frac{-1}{2}, y\right) = \sigma_{\text{int}} \sum_{i=0}^{k-4} \frac{(-1)^i}{2^i i!} \partial_n^{i+1} u_{\text{int}}^{k-4-i}(x_0, y), \\ \hat{\sigma}_0 \partial_X U^k\left(\frac{1}{2}, y\right) = \sigma_{\text{ext}} \sum_{i=0}^{k-4} \frac{1}{2^i i!} \partial_n^{i+1} u_{\text{ext}}^{k-4-i}(x_0, y). \end{array} \right. \quad (1.27)$$

There exists a solution U^k to (1.27) provided the compatibility condition (1.26) is satisfied. We deduce the expression of U^k up to a function in the variable y , denoted by $\psi_0^k(y)$. The function U^k has the following form

$$U^k(X, y) = V^k(X, y) + \psi_0^k(y),$$

where V^k represents the part of U^k that is determined at this step and has the form (see Proposition 2)

$$V^k(X, y) = \begin{cases} 0 & \text{if } k = 0, 1, 2, 3, \\ \psi_{k-2}^k(y)X^{k-2} + \psi_{k-3}^k(y)X^{k-3} + \dots + \psi_1^k(y)X & \text{if } k > 3. \end{cases}$$

Function ψ_0^k is determined at the second step.

Second step:

We involve the compatibility condition (1.26) for the $k + 2$ term, along with Equation (1.25c) to write the following differential problem in the variable y for function ψ_0^k , present in the expression of U^k .

$$\begin{cases} \frac{d^2}{dy^2} \psi_0^k(y) = h^k(y) & y \in (0, y_0), \\ \psi_0^k(0) = 0, \\ \psi_0^k(y_0) = 0, \end{cases} \quad (1.28)$$

where

$$\begin{aligned} h^k(y) = & -\frac{1}{\widehat{\sigma}_0} \sum_{i=0}^{k-2} \left(\frac{\sigma_{\text{ext}}}{2^i i!} \partial_n^{i+1} u_{\text{ext}}^{k-2-i}(x_0, y) + (-1)^{i+1} \frac{\sigma_{\text{int}}}{2^i i!} \partial_n^{i+1} u_{\text{int}}^{k-2-i}(x_0, y) \right) \\ & - \int_{-\frac{1}{2}}^{\frac{1}{2}} \partial_y^2 V^k(X, y) dX. \end{aligned}$$

Solving this differential equation we obtain function ψ_0^k and thus, the complete expression of U^k .

Third step:

We derive the equations outside the layer by employing Equations (1.23a), (1.23b), (1.24a), (1.24b), (1.25a), and (1.25b). We infer that u_{int}^k and u_{ext}^k are defined independently in the two subdomains Ω_{int} and Ω_{ext}

$$\begin{cases} \sigma_{\text{int}} \Delta u_{\text{int}}^k = f_{\text{int}} \delta_0^k & \text{in } \Omega_{\text{int}}, \\ u_{\text{int}}^k(x_0, y) = U^k\left(-\frac{1}{2}, y\right) - \sum_{i=1}^k \frac{(-1)^i}{2^i i!} \partial_n^i u_{\text{int}}^{k-i}(x_0, y), \\ u_{\text{int}}^k = 0 & \text{on } \partial\Omega \cap \partial\Omega_{\text{int}}. \end{cases} \quad (1.29)$$

$$\begin{cases} \sigma_{\text{ext}} \Delta u_{\text{ext}}^k = f_{\text{ext}} \delta_0^k & \text{in } \Omega_{\text{ext}}, \\ u_{\text{ext}}^k(x_0, y) = U^k\left(\frac{1}{2}, y\right) - \sum_{i=1}^k \frac{1}{2^i i!} \partial_n^i u_{\text{ext}}^{k-i}(x_0, y), \\ u_{\text{ext}}^k = 0 & \text{on } \partial\Omega \cap \partial\Omega_{\text{ext}}. \end{cases}$$

Now this algorithm is used to determine the first terms of the expansion.

First terms of the asymptotics

Terms of order zero

We consider Problem (1.27) for U^0

$$\left\{ \begin{array}{l} \partial_X^2 U^0(X, y) = 0 \quad X \in \left(\frac{-1}{2}, \frac{1}{2} \right), \\ \partial_X U^0 \left(-\frac{1}{2}, y \right) = 0, \\ \partial_X U^0 \left(\frac{1}{2}, y \right) = 0. \end{array} \right.$$

The solution to the above equation has the form $U^0(X, y) = \psi_0^0(y)$. Then, using (1.28) we build the following problem for ψ_0^0

$$\left\{ \begin{array}{l} \frac{d^2}{dy^2} \psi_0^0(y) = 0 \quad y \in (0, y_0), \\ \psi_0^0(0) = 0, \\ \psi_0^0(y_0) = 0. \end{array} \right.$$

We deduce that $\psi_0^0(y) = 0$ and thus, $U^0(X, y) = 0$. Finally, employing (1.29) we obtain that the limit solution u^0 satisfies homogeneous Dirichlet boundary conditions on Γ . Thus, the problem satisfied by u^0 reads as

$$\left\{ \begin{array}{ll} \Delta u_{\text{int}}^0 = f_{\text{int}} & \text{in } \Omega_{\text{int}}, \\ u_{\text{int}}^0 = 0 & \text{on } \partial\Omega_{\text{int}}. \end{array} \right. \quad (1.30)$$

$$\left\{ \begin{array}{ll} \Delta u_{\text{ext}}^0 = f_{\text{ext}} & \text{in } \Omega_{\text{ext}}, \\ u_{\text{ext}}^0 = 0 & \text{on } \partial\Omega_{\text{ext}}. \end{array} \right.$$

Terms of order one

We consider Problem (1.27) for U^1

$$\left\{ \begin{array}{l} \partial_X^2 U^1(X, y) = 0 \quad X \in \left(\frac{-1}{2}, \frac{1}{2} \right), \\ \partial_X U^1 \left(-\frac{1}{2}, y \right) = 0, \\ \partial_X U^1 \left(\frac{1}{2}, y \right) = 0. \end{array} \right.$$

The solution to this equation has the form $U^1(X, y) = \psi_0^1(y)$. Then, from (1.28) we deduce the following problem for ψ_0^1

$$\begin{cases} \frac{d^2}{dy^2} \psi_0^1(y) = 0 & y \in (0, y_0), \\ \psi_0^1(0) = 0, \\ \psi_0^1(y_0) = 0. \end{cases}$$

We thus have that $\psi_0^1(y) = 0$ and $U^1(X, y) = 0$. Finally, employing (1.29) we write the problem satisfied outside the layer by u^1 as two uncoupled problems

$$\begin{cases} \Delta u_{\text{int}}^1 = 0 & \text{in } \Omega_{\text{int}}, \\ u_{\text{int}}^1 = \frac{1}{2} \partial_n u_{\text{int}}^0 & \text{on } \Gamma, \\ u_{\text{int}}^1 = 0 & \text{on } \partial\Omega \cap \partial\Omega_{\text{int}}. \end{cases} \quad (1.31)$$

$$\begin{cases} \Delta u_{\text{ext}}^1 = 0 & \text{in } \Omega_{\text{ext}}, \\ u_{\text{ext}}^1 = -\frac{1}{2} \partial_n u_{\text{ext}}^0 & \text{on } \Gamma, \\ u_{\text{ext}}^1 = 0 & \text{on } \partial\Omega \cap \partial\Omega_{\text{ext}}. \end{cases}$$

Terms of order two

We consider Problem (1.27) for U^2

$$\begin{cases} \partial_X^2 U^2(X, y) = 0 & X \in \left(-\frac{1}{2}, \frac{1}{2}\right), \\ \partial_X U^2\left(-\frac{1}{2}, y\right) = 0, \\ \partial_X U^2\left(\frac{1}{2}, y\right) = 0. \end{cases}$$

The solution to this equation has the form $U^2(X, y) = \psi_0^2(y)$. Then, according to (1.28) we build the following problem for ψ_0^2

$$\begin{cases} \frac{d^2}{dy^2} \psi_0^2(y) = -\frac{1}{\bar{\sigma}_0} [\sigma_{\text{ext}} \partial_n u^0]_{\Gamma}(y) & y \in (0, y_0), \\ \psi_0^2(0) = 0, \\ \psi_0^2(y_0) = 0. \end{cases}$$

We deduce that ψ_0^2 has the following form

$$\psi_0^2(y) = \frac{-1}{\widehat{\sigma}_0} \int_0^y (y-t) [\sigma \partial_n u^0]_\Gamma(t) dt + \frac{y}{\widehat{\sigma}_0 y_0} \int_0^{y_0} (y_0-t) [\sigma \partial_n u^0]_\Gamma(t) dt. \quad (1.32)$$

Finally, (1.29) implies that the problem satisfied outside the layer by u^2 is composed of two uncoupled problems

$$\begin{cases} \Delta u_{\text{int}}^2 = 0 & \text{in } \Omega_{\text{int}}, \\ u_{\text{int}}^2(x_0, y) = \psi_0^2(y) & y \in (0, y_0), \\ u_{\text{int}}^2 = 0 & \text{on } \partial\Omega \cap \partial\Omega_{\text{int}}. \end{cases} \quad (1.33)$$

$$\begin{cases} \Delta u_{\text{ext}}^2 = 0 & \text{in } \Omega_{\text{ext}}, \\ u_{\text{ext}}^2(x_0, y) = \psi_0^2(y) & y \in (0, y_0), \\ u_{\text{ext}}^2 = 0 & \text{on } \partial\Omega \cap \partial\Omega_{\text{ext}}. \end{cases}$$

Terms of order three

We consider Problem (1.27) for U^3

$$\begin{cases} \partial_X^2 U^3(X, y) = 0 & X \in \left(-\frac{1}{2}, \frac{1}{2}\right), \\ \partial_X U^3\left(-\frac{1}{2}, y\right) = 0, \\ \partial_X U^3\left(\frac{1}{2}, y\right) = 0. \end{cases}$$

The solution to this equation has the form $U^3(X, y) = \psi_0^3(y)$. Then, we employ (1.28) and build the following problem for ψ_0^3

$$\begin{cases} \frac{d^2}{dy^2} \psi_0^3(y) = -\frac{1}{\widehat{\sigma}_0} [\sigma_{\text{ext}} \partial_n u^1]_\Gamma(y) - \frac{1}{\widehat{\sigma}_0} \{\sigma_{\text{ext}} \partial_n u^0\}_\Gamma(y) & y \in (0, y_0), \\ \psi_0^3(0) = 0, \\ \psi_0^3(y_0) = 0. \end{cases}$$

We deduce that ψ_0^3 has the following form

$$\begin{aligned} \psi_0^3(y) = & \frac{-1}{\widehat{\sigma}_0} \int_0^y (y-t) \left([\sigma \partial_n u^1]_\Gamma(t) + \{\sigma \partial_n u^0\}_\Gamma(t) \right) dt \\ & + \frac{y}{\widehat{\sigma}_0 y_0} \int_0^{y_0} (y_0-t) \left([\sigma \partial_n u^1]_\Gamma(t) + \{\sigma \partial_n u^0\}_\Gamma(t) \right) dt. \end{aligned} \quad (1.34)$$

Finally, employing (1.29) we write the problem satisfied outside the layer by u^3 as two uncoupled problems

$$\begin{cases} \Delta u_{\text{int}}^3 = 0 & \text{in } \Omega_{\text{int}}, \\ u_{\text{int}}^3(x_0, y) = \psi_0^3(y) & y \in (0, y_0), \\ u_{\text{int}}^3 = 0 & \text{on } \partial\Omega \cap \partial\Omega_{\text{int}}. \end{cases} \quad (1.35)$$

$$\begin{cases} \Delta u_{\text{ext}}^3 = 0 & \text{in } \Omega_{\text{ext}}, \\ u_{\text{ext}}^3(x_0, y) = \psi_0^3(y) & y \in (0, y_0), \\ u_{\text{ext}}^3 = 0 & \text{on } \partial\Omega \cap \partial\Omega_{\text{ext}}. \end{cases}$$

Recapitulation of the asymptotic expansion

Proposition 2. *The asymptotic expansion (1.20) has the following form outside the layer*

$$\begin{cases} u_{\text{int}}(x, y) = u_{\text{int}}^0(x, y) + \varepsilon u_{\text{int}}^1(x, y) + \varepsilon^2 u_{\text{int}}^2(x, y) + \varepsilon^3 u_{\text{int}}^3(x, y) + O(\varepsilon^4), \\ u_{\text{ext}}(x, y) = u_{\text{ext}}^0(x, y) + \varepsilon u_{\text{ext}}^1(x, y) + \varepsilon^2 u_{\text{ext}}^2(x, y) + \varepsilon^3 u_{\text{ext}}^3(x, y) + O(\varepsilon^4), \end{cases}$$

and the following form inside the layer, that is, for $(X, y) \in \left(-\frac{1}{2}, \frac{1}{2}\right) \times (0, y_0)$,

$$U(X, y) = \varepsilon^2 \psi_0^2(y) + \varepsilon^3 \psi_0^3(y) + O(\varepsilon^4),$$

where functions u^0 , u^1 , u^2 , and u^3 are defined by Equations (1.30), (1.31), (1.33), and (1.35), respectively, and functions ψ_0^2 and ψ_0^3 are defined by Equations (1.32) and (1.34), respectively. In addition, for $k \in \mathbb{N}$, the solution U^k to Equation (1.27) has the following form

$$U^k(X, y) = \begin{cases} 0 & k = 0, 1, \\ \sum_{j=0}^{k-2} \psi_j^k(y) X^j & k = 2l + 2, \quad l \in \mathbb{N}, \\ \sum_{j=0}^{k-3} \psi_j^k(y) X^j & k = 2l + 3, \quad l \in \mathbb{N}. \end{cases}$$

Proof. We prove it by induction on k . For $k = 0, 1, 2, 3$ we have already calculated the expressions of u^k and U^k in the previous section. We distinguish two different

cases for the proof: the case of an even number $k \geq 4$, and the case of an odd number $k \geq 4$. Let us thus prove the result for an even number k by assuming the result is true for all even numbers $i < k$. Thanks to the inductive assumption, function U^i has the form

$$U^i(X, y) = \psi_{i-2}^i(y)X^{i-2} + \psi_{i-3}^i(y)X^{i-3} + \dots + \psi_1^i(y)X + \psi_0^i(y).$$

We begin by considering Problem (1.27) for the even number k . Solving this problem we obtain a solution of the form

$$U^k(X, y) = \psi_{k-2}^k(y)X^{k-2} + \psi_{k-3}^k(y)X^{k-3} + \dots + \psi_1^k(y)X + \psi_0^k(y),$$

and

$$\left\{ \begin{array}{l} \psi_1^k(y) = \frac{1}{\widehat{\sigma}_0} \sum_{i=0}^{k-4} \left(\frac{\sigma_{\text{ext}}}{2^i i!} \partial_n^{i+1} u_{\text{ext}}^{k-4-i}(x_0, y) + (-1)^i \frac{\sigma_{\text{int}}}{2^i i!} \partial_n^{i+1} u_{\text{int}}^{k-4-i}(x_0, y) \right), \\ \psi_2^k(y) = \frac{1}{2\widehat{\sigma}_0} \left(\sum_{i=0}^{k-4} \left(\frac{\sigma_{\text{ext}}}{2^i i!} \partial_n^{i+1} u_{\text{ext}}^{k-4-i}(x_0, y) + (-1)^{i+1} \frac{\sigma_{\text{int}}}{2^i i!} \partial_n^{i+1} u_{\text{int}}^{k-4-i}(x_0, y) \right) \right), \\ \psi_{k-j}^k(y) = \frac{-\frac{d^2}{dy^2} \psi_{k-j-2}^k(y)}{(k-j)(k-j-1)} \quad j = 2, \dots, k-2. \end{array} \right.$$

In the above expression of U^k , we find function V^k which reads as

$$V^k(X, y) = \psi_{k-2}^k(y)X^{k-2} + \psi_{k-3}^k(y)X^{k-3} + \dots + \psi_1^k(y)X,$$

and has been defined at the first step of the algorithm. A similar argument can be involved when k is an odd number. □

1.4.2 Equivalent models

Now that we know the expressions for the first terms of the expansion, we truncate the series and we identify a simpler problem satisfied by

$$u^{(k)} = u^0 + \varepsilon u^1 + \dots + \varepsilon^k u^k \quad \text{in} \quad \Omega_{\text{int}} \cup \Omega_{\text{ext}}$$

up to a residual term of order ε^{k+1} . We neglect the residual term of order ε^{k+1} to obtain an approximate model satisfied by function $u^{[k]}$. Here, we formally derive two approximate models of order one and order two respectively.

First-order model

For deriving the first-order model, we truncate the series from the first term and we define $u^{(0)}$ as

$$u^{(0)} = u^0 \quad \text{in} \quad \Omega_{\text{int}} \cup \Omega_{\text{ext}} \quad (\text{see Proposition 2}).$$

From (1.30), we conclude that $u^{(0)}$ solves the problem

$$\begin{cases} \sigma_{\text{int}} \Delta u_{\text{int}}^{(0)} = f_{\text{int}} & \text{in} \quad \Omega_{\text{int}}, \\ u_{\text{int}}^{(0)} = 0 & \text{on} \quad \partial\Omega_{\text{int}}. \end{cases} \quad (1.36)$$

$$\begin{cases} \sigma_{\text{ext}} \Delta u_{\text{ext}}^{(0)} = f_{\text{ext}} & \text{in} \quad \Omega_{\text{ext}}, \\ u_{\text{ext}}^{(0)} = 0 & \text{on} \quad \partial\Omega_{\text{ext}}. \end{cases}$$

In this case, we have $u^{[0]} = u^{(0)}$ as $u^{(0)}$ does not depend on ε . We thus infer a first-order model satisfied by $u^{[0]}$ solution to Problem (1.36).

Second-order model

For deriving the second-order model, we truncate the series from the second term and we define $u^{(1)}$ as

$$u^{(1)} = u^0 + \varepsilon u^1 \quad \text{in} \quad \Omega_{\text{int}} \cup \Omega_{\text{ext}} \quad (\text{see Proposition 2}).$$

From (1.30) and (1.31) we conclude that $u^{(1)}$ satisfies the following equations

$$\begin{cases} \sigma_{\text{int}} \Delta u_{\text{int}}^{(1)} = f_{\text{int}} & \text{in} \quad \Omega_{\text{int}}, \\ u_{\text{int}}^{(1)} = \frac{\varepsilon}{2} \partial_n u_{\text{int}}^0 & \text{on} \quad \Gamma, \\ u_{\text{int}}^{(1)} = 0 & \text{on} \quad \partial\Omega \cap \partial\Omega_{\text{int}}. \end{cases} \quad (1.37)$$

$$\begin{cases} \sigma_{\text{ext}} \Delta u_{\text{ext}}^{(1)} = f_{\text{ext}} & \text{in} \quad \Omega_{\text{ext}}, \\ u_{\text{ext}}^{(1)} = -\frac{\varepsilon}{2} \partial_n u_{\text{ext}}^0 & \text{on} \quad \Gamma, \\ u_{\text{ext}}^{(1)} = 0 & \text{on} \quad \partial\Omega \cap \partial\Omega_{\text{ext}}. \end{cases}$$

Following the same procedure as in Section 1.3.2 we obtain the following second-order asymptotic model for $u^{[1]}$

$$\begin{cases} \sigma_{\text{int}} \Delta u_{\text{int}}^{[1]} = f_{\text{int}} & \text{in } \Omega_{\text{int}}, \\ u_{\text{int}}^{[1]} = \frac{\varepsilon}{2} \partial_n u_{\text{int}}^{[1]} & \text{on } \Gamma, \\ u_{\text{int}}^{[1]} = 0 & \text{on } \partial\Omega \cap \partial\Omega_{\text{int}}. \end{cases} \quad (1.38)$$

$$\begin{cases} \sigma_{\text{ext}} \Delta u_{\text{ext}}^{[1]} = f_{\text{ext}} & \text{in } \Omega_{\text{ext}}, \\ u_{\text{ext}}^{[1]} = -\frac{\varepsilon}{2} \partial_n u_{\text{ext}}^{[1]} & \text{on } \Gamma, \\ u_{\text{ext}}^{[1]} = 0 & \text{on } \partial\Omega \cap \partial\Omega_{\text{ext}}. \end{cases}$$

Third-order model

For deriving the third-order model, we truncate the series from the third term and we define $u^{(2)}$ as

$$u^{(2)} = u^0 + \varepsilon u^1 + \varepsilon^2 u^2 \quad \text{in } \Omega_{\text{int}} \cup \Omega_{\text{ext}} \quad (\text{see Proposition 2}).$$

From (1.30), (1.31), and (1.33) we conclude that $u^{(2)}$ satisfies the following equations

$$\begin{cases} \sigma_{\text{int}} \Delta u_{\text{int}}^{(2)} = f_{\text{int}} & \text{in } \Omega_{\text{int}}, \\ u_{\text{int}}^{(2)}(x_0, y) = g_1^2(y) & y \in (0, y_0), \\ u_{\text{int}}^{(2)} = 0 & \text{on } \partial\Omega \cap \partial\Omega_{\text{int}}. \end{cases} \quad (1.39)$$

$$\begin{cases} \sigma_{\text{ext}} \Delta u_{\text{ext}}^{(2)} = f_{\text{ext}} & \text{in } \Omega_{\text{ext}}, \\ u_{\text{ext}}^{(2)}(x_0, y) = g_2^2(y) & y \in (0, y_0), \\ u_{\text{ext}}^{(2)} = 0 & \text{on } \partial\Omega \cap \partial\Omega_{\text{ext}}. \end{cases}$$

where g_1^2 and g_2^2 are defined as follows

$$\left\{ \begin{array}{l} g_1^2(y) = \frac{\varepsilon}{2} \partial_n u_{\text{int}}^0(x_0, y) - \frac{\varepsilon^2}{\widehat{\sigma}_0} \int_0^y (y-t) [\sigma \partial_n u^0]_{\Gamma}(t) dt \\ \quad + \frac{\varepsilon^2 y}{\widehat{\sigma}_0 y_0} \int_0^{y_0} (y_0-t) [\sigma \partial_n u^0]_{\Gamma}(t) dt, \\ g_2^2(y) = -\frac{\varepsilon}{2} \partial_n u_{\text{ext}}^0(x_0, y) - \frac{\varepsilon^2}{\widehat{\sigma}_0} \int_0^y (y-t) [\sigma \partial_n u^0]_{\Gamma}(t) dt \\ \quad + \frac{\varepsilon^2 y}{\widehat{\sigma}_0 y_0} \int_0^{y_0} (y_0-t) [\sigma \partial_n u^0]_{\Gamma}(t) dt. \end{array} \right.$$

Following the same procedure as in Section 1.3.2 we obtain the following third-order asymptotic model for $u^{[2]}$

$$\left\{ \begin{array}{ll} \sigma_{\text{int}} \Delta u_{\text{int}}^{[2]} = f_{\text{int}} & \text{in } \Omega_{\text{int}}, \\ \sigma_{\text{ext}} \Delta u_{\text{ext}}^{[2]} = f_{\text{ext}} & \text{in } \Omega_{\text{ext}}, \\ T_1^2(u^{[2]}) = 0 & \text{on } \Gamma, \\ T_2^2(u^{[2]}) = 0 & \text{on } \Gamma, \\ u_{\text{ext}}^{[2]} = 0 & \text{on } \partial\Omega. \end{array} \right. \quad (1.40)$$

where T_1^2 and T_2^2 are defined as follows

$$\left\{ \begin{array}{l} T_1^2(u^{[2]}) = [u^{[2]}]_{\Gamma} + \varepsilon \{ \partial_n u^{[2]} \}_{\Gamma} + \frac{\varepsilon^2}{8} [\partial_n^2 u^{[2]}]_{\Gamma}, \\ T_2^2(u^{[2]}) = \frac{\varepsilon^2}{\widehat{\sigma}_0} [\sigma \partial_n u^{[2]}]_{\Gamma} + \frac{\varepsilon^2}{8} \frac{d^2}{dy^2} \{ \partial_n^2 u^{[2]} \}_{\Gamma} + \frac{\varepsilon}{4} \frac{d^2}{dy^2} [\partial_n u^{[2]}]_{\Gamma} + \frac{d^2}{dy^2} \{ u^{[2]} \}_{\Gamma}. \end{array} \right.$$

Fourth-order model

For deriving the fourth-order model, we truncate the series from the fourth term and we define $u^{(3)}$ as

$$u^{(3)} = u^0 + \varepsilon u^1 + \varepsilon^2 u^2 + \varepsilon^3 u^3 \quad \text{in } \Omega_{\text{int}} \cup \Omega_{\text{ext}} \quad (\text{see Proposition 2}).$$

From (1.30), (1.31), (1.33), and (1.35) we conclude that $u^{(3)}$ satisfies the following equations

$$\begin{cases} \sigma_{\text{int}} \Delta u_{\text{int}}^{(3)} = f_{\text{int}} & \text{in } \Omega_{\text{int}}, \\ u_{\text{int}}^{(3)}(x_0, y) = g_1^3(y) & y \in (0, y_0), \\ u_{\text{int}}^{(3)} = 0 & \text{on } \partial\Omega \cap \partial\Omega_{\text{int}}. \end{cases} \quad (1.41)$$

$$\begin{cases} \sigma_{\text{ext}} \Delta u_{\text{ext}}^{(3)} = f_{\text{ext}} & \text{in } \Omega_{\text{ext}}, \\ u_{\text{ext}}^{(3)}(x_0, y) = g_2^3(y) & y \in (0, y_0), \\ u_{\text{ext}}^{(3)} = 0 & \text{on } \partial\Omega \cap \partial\Omega_{\text{ext}}. \end{cases}$$

where g_1^3 and g_2^3 are defined as follows

$$\left\{ \begin{array}{l} g_1^3(y) = \frac{\varepsilon}{2} \partial_n u_{\text{int}}^0(x_0, y) - \frac{\varepsilon^2}{\widehat{\sigma}_0} \int_0^y (y-t) [\sigma \partial_n u^0]_{\Gamma}(t) dt \\ \quad + \frac{\varepsilon^3 y}{\widehat{\sigma}_0 y_0} \int_0^{y_0} (y_0-t) [\sigma \partial_n u^0]_{\Gamma}(t) dt \\ \quad - \frac{\varepsilon^3}{\widehat{\sigma}_0} \int_0^y (y-t) \left([\sigma \partial_n u^1]_{\Gamma}(t) + \{\sigma \partial_n u^0\}_{\Gamma}(t) \right) dt \\ \quad + \frac{\varepsilon^3 y}{\widehat{\sigma}_0 y_0} \int_0^{y_0} (y_0-t) \left([\sigma \partial_n u^1]_{\Gamma}(t) + \{\sigma \partial_n u^0\}_{\Gamma}(t) \right) dt, \\ \\ g_2^3(y) = -\frac{\varepsilon}{2} \partial_n u_{\text{ext}}^0(x_0, y) - \frac{\varepsilon^2}{\widehat{\sigma}_0} \int_0^y (y-t) [\sigma \partial_n u^0]_{\Gamma}(t) dt \\ \quad + \frac{\varepsilon^2 y}{\widehat{\sigma}_0 y_0} \int_0^{y_0} (y_0-t) [\sigma \partial_n u^0]_{\Gamma}(t) dt \\ \quad - \frac{\varepsilon^3}{\widehat{\sigma}_0} \int_0^y (y-t) \left([\sigma \partial_n u^1]_{\Gamma}(t) + \{\sigma \partial_n u^0\}_{\Gamma}(t) \right) dt \\ \quad + \frac{\varepsilon^3 y}{\widehat{\sigma}_0 y_0} \int_0^{y_0} (y_0-t) \left([\sigma \partial_n u^1]_{\Gamma}(t) + \{\sigma \partial_n u^0\}_{\Gamma}(t) \right) dt. \end{array} \right.$$

Following the same procedure as in Section 1.3.2 we obtain the following fourth-order asymptotic model for $u^{[3]}$

$$\begin{cases} \sigma_{\text{int}} \Delta u_{\text{int}}^{[3]} = f_{\text{int}} & \text{in } \Omega_{\text{int}}, \\ \sigma_{\text{ext}} \Delta u_{\text{ext}}^{[3]} = f_{\text{ext}} & \text{in } \Omega_{\text{ext}}, \\ T_1^3(u^{[3]}) = 0 & \text{on } \Gamma, \\ T_2^3(u^{[3]}) = 0 & \text{on } \Gamma, \\ u_{\text{ext}}^{[3]} = 0 & \text{on } \partial\Omega. \end{cases} \quad (1.42)$$

where T_1^3 and T_2^3 are defined as follows

$$\begin{cases} T_1^3(u^{[3]}) = [u^{[3]}]_{\Gamma} + \varepsilon \{\partial_n u^{[3]}\}_{\Gamma} + \frac{\varepsilon^2}{8} [\partial_n^2 u^{[3]}]_{\Gamma} + \frac{\varepsilon^3}{24} \{\partial_n^3 u^{[3]}\}_{\Gamma}, \\ T_2^3(u^{[3]}) = \frac{\varepsilon^2}{\hat{\sigma}_0} [\sigma \partial_n u^{[3]}]_{\Gamma} + \frac{\varepsilon^3}{\hat{\sigma}_0} \{\sigma \partial_n u^{[3]}\}_{\Gamma} + \frac{\varepsilon^3}{96} \frac{d^2}{dy^2} [\partial_n^3 u^{[3]}]_{\Gamma} \\ \quad + \frac{\varepsilon^2}{8} \frac{d^2}{dy^2} \{\partial_n^2 u^{[3]}\}_{\Gamma} + \frac{\varepsilon}{4} \frac{d^2}{dy^2} [\partial_n u^{[3]}]_{\Gamma} + \frac{d^2}{dy^2} \{u^{[3]}\}_{\Gamma}. \end{cases}$$

1.4.3 Artificial boundaries

When deriving the variational formulation of the second-order model (1.38), we notice that we cannot prove the coerciveness of the bilinear form, due to a negative term. This negative term could cause instabilities when solving the problem with the finite element method. However, to overcome this problem and restore stability we are going to use a technique based on introducing some new artificial boundaries, across of which we are going to rewrite the transmission conditions, see for example [15, 16]. We define these new artificial boundaries as follows

Definition 4. We define artificial boundaries $\Gamma_{\text{int}}^{\delta}$ and $\Gamma_{\text{ext}}^{\delta}$ as

$$\Gamma_{\text{int}}^{\delta} = \{(x_0 - \delta\varepsilon, y) : \delta > 0, y \in (0, y_0)\},$$

$$\Gamma_{\text{ext}}^{\delta} = \{(x_0 + \delta\varepsilon, y) : \delta > 0, y \in (0, y_0)\}.$$

We observe the new configuration defined by the artificial boundaries in Figure 1.3.

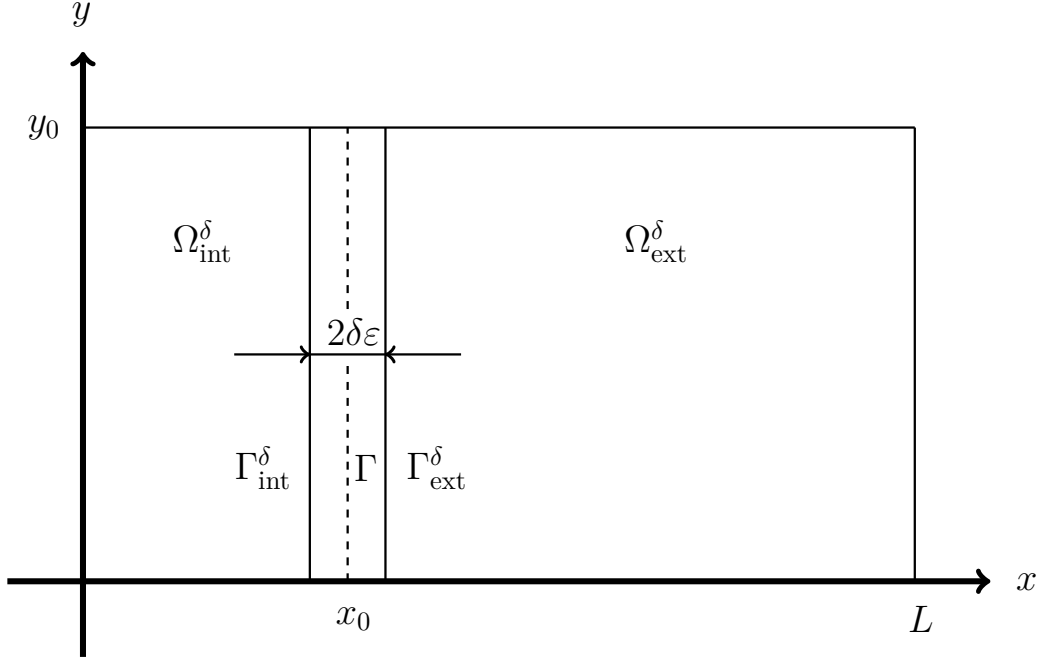


Figure 1.3: New configuration for the domain incorporating two artificial boundaries.

Remark 2. Domains Ω_{int}^δ and Ω_{ext}^δ and the boundaries Γ_{int}^δ and Γ_{ext}^δ depend on ε , but we do not include it in the notation for the sake of simplicity.

We apply a formal Taylor series expansion on the variable normal to the thin layer, x in this case, in order to write the boundary conditions over the artificial boundaries.

$$\left\{ \begin{array}{l} u_{\text{ext}}(x_0, y) = u_{\text{ext}}(x_0 + \delta\varepsilon, y) - \delta\varepsilon \partial_n u_{\text{ext}}(x_0 + \delta\varepsilon, y) + O(\varepsilon^2), \\ u_{\text{int}}(x_0, y) = u_{\text{int}}(x_0 - \delta\varepsilon, y) + \delta\varepsilon \partial_n u_{\text{int}}(x_0 - \delta\varepsilon, y) + O(\varepsilon^2), \\ \partial_n u_{\text{ext}}(x_0, y) = \partial_n u_{\text{ext}}(x_0 + \delta\varepsilon, y) - \delta\varepsilon \partial_n^2 u_{\text{ext}}(x_0 + \delta\varepsilon, y) + O(\varepsilon^2), \\ \partial_n u_{\text{int}}(x_0, y) = \partial_n u_{\text{int}}(x_0 - \delta\varepsilon, y) + \delta\varepsilon \partial_n^2 u_{\text{int}}(x_0 - \delta\varepsilon, y) + O(\varepsilon^2). \end{array} \right.$$

We substitute these expressions in the boundary conditions over Γ of Equation (1.38) and neglecting the terms of order two or higher in ε , we obtain the new boundary conditions defined over the new artificial boundaries. The resulting

asymptotic model reads as follows.

$$\begin{cases} \sigma_{\text{int}} \Delta u_{\delta, \text{int}}^{[1]} = f_{\text{int}} & \text{in } \Omega_{\text{int}}^{\delta}, \\ u_{\delta, \text{int}}^{[1]} = \frac{\varepsilon(1-2\delta)}{2} \partial_n u_{\delta, \text{int}}^{[1]} & \text{on } \Gamma_{\text{int}}^{\delta}, \\ u_{\delta, \text{int}}^{[1]} = 0 & \text{on } \partial\Omega \cap \partial\Omega_{\text{int}}^{\delta}. \end{cases} \quad (1.43)$$

$$\begin{cases} \sigma_{\text{ext}} \Delta u_{\delta, \text{ext}}^{[1]} = f_{\text{ext}} & \text{in } \Omega_{\text{ext}}^{\delta}, \\ u_{\delta, \text{ext}}^{[1]} = -\frac{\varepsilon(1-2\delta)}{2} \partial_n u_{\delta, \text{ext}}^{[1]} & \text{on } \Gamma_{\text{ext}}^{\delta}, \\ u_{\delta, \text{ext}}^{[1]} = 0 & \text{on } \partial\Omega \cap \partial\Omega_{\text{ext}}^{\delta}. \end{cases}$$

With this new formulation, if we select $\delta > \frac{1}{2}$, the negative term of the bilinear form in the variational formulation becomes positive and stability is restored. Henceforth, we will refer to this stabilized model as the stabilized δ -order two model.

Notation 3. We denote by Ω^{δ} the domain

$$\Omega^{\delta} = \Omega_{\text{int}}^{\delta} \cup \Omega_{\text{ext}}^{\delta},$$

where $\Omega_{\text{int}}^{\delta}$ and $\Omega_{\text{ext}}^{\delta}$ are the domains defined at Figure 1.3.

1.5 Time-harmonic problem in a 2D configuration

This section is dedicated to the derivation of asymptotic models when the frequency is non zero. The derivation of an asymptotic expansion and equivalent models is very similar to the one described in the previous sections. The main difference resides on the resulting asymptotic models. Thus, instead of deriving the entire process again, we will summarize it and we will concentrate on showing the obtained results using the two considered approaches, which have been detailed in the previous sections. We begin by presenting the model problem. Then, we derive a multiscale expansion, and finally we present the obtained approximate models.

1.5.1 Model problem

The problem we are interested in is the equation for the electric potential, which reads as follows

$$\operatorname{div} [(\sigma - i\epsilon_0\omega) \nabla u] = f. \quad (1.44)$$

Here, u represents the electric potential, σ stands for the conductivity, f denotes a current source, ω is the frequency, and ϵ_0 is the permittivity. We consider the same domain we had in Section 1.2, which is depicted at Figure 1.1. We consider the conductivity to be piecewise constant and to have a different value in each subdomain, being of the form $\sigma_{\text{lay}} = \hat{\sigma}_0 \varepsilon^{-3}$ inside the thin layer. Both the right-hand side f and the conductivity σ have the same form as the ones considered in Section 1.2. In this framework, the Problem (1.44) reads as follows

$$\left\{ \begin{array}{ll} (\sigma_{\text{int}} - i\epsilon_0\omega) \Delta u_{\text{int}} = f_{\text{int}} & \text{in } \Omega_{\text{int}}^\varepsilon, \\ (\sigma_{\text{ext}} - i\epsilon_0\omega) \Delta u_{\text{ext}} = f_{\text{ext}} & \text{in } \Omega_{\text{ext}}^\varepsilon, \\ (\hat{\sigma}_0 \varepsilon^{-3} - i\epsilon_0\omega) \Delta u_{\text{lay}} = 0 & \text{in } \Omega_{\text{lay}}^\varepsilon, \\ u_{\text{int}} = u_{\text{lay}} & \text{on } \Gamma_{\text{int}}^\varepsilon, \\ u_{\text{lay}} = u_{\text{ext}} & \text{on } \Gamma_{\text{ext}}^\varepsilon, \\ (\sigma_{\text{int}} - i\epsilon_0\omega) \partial_n u_{\text{int}} = (\hat{\sigma}_0 \varepsilon^{-3} - i\epsilon_0\omega) \partial_n u_{\text{lay}} & \text{on } \Gamma_{\text{int}}^\varepsilon, \\ (\hat{\sigma}_0 \varepsilon^{-3} - i\epsilon_0\omega) \partial_n u_{\text{lay}} = (\sigma_{\text{ext}} - i\epsilon_0\omega) \partial_n u_{\text{ext}} & \text{on } \Gamma_{\text{ext}}^\varepsilon, \\ u = 0 & \text{on } \partial\Omega, \end{array} \right. \quad (1.45)$$

where ∂_n represents the normal derivative in the direction of the normal vector, inwardly directed to $\Omega_{\text{ext}}^\varepsilon$ on $\Gamma_{\text{ext}}^\varepsilon$, and outwardly directed to $\Omega_{\text{int}}^\varepsilon$ on $\Gamma_{\text{int}}^\varepsilon$, see Figure 1.1.

1.5.2 First class of ITCs: construction of a multiscale expansion

To begin with, we perform a scaling inside the thin layer in the same way we have done in Section 1.3.1. Then, we perform an *Ansatz* in the form of power series of functions u_{int} , u_{ext} , and U , like the one performed in (1.4).

Substituting these expressions into the Equations (1.45) and collecting the terms

with the same powers in ε , for every $k \in \mathbb{N}$ we obtain the following set of equations

$$\left\{ \begin{array}{ll} (\sigma_{\text{int}} - i\varepsilon_0\omega) \Delta u_{\text{int}}^k(x, y) = f_{\text{int}}(x, y)\delta_0^k & \text{in } \Omega_{\text{ext}}^\varepsilon, \\ (\sigma_{\text{ext}} - i\varepsilon_0\omega) \Delta u_{\text{ext}}^k(x, y) = f_{\text{ext}}(x, y)\delta_0^k & \text{in } \Omega_{\text{ext}}^\varepsilon, \\ i\varepsilon_0\omega \partial_X^2 U^{k-3} - \hat{\sigma}_0 \partial_y^2 U^{k-2} + i\varepsilon_0\omega \partial_y^2 U^{k-5} = \hat{\sigma}_0 \partial_X^2 U^k & \text{in } \left(-\frac{1}{2}, \frac{1}{2}\right) \times (0, y_0), \end{array} \right. \quad (1.46)$$

along with the following transmission conditions

$$\left\{ \begin{array}{l} U^k\left(-\frac{1}{2}, y\right) = u_{\text{int}}^k\left(x_0 - \frac{\varepsilon}{2}, y\right), \\ U^k\left(\frac{1}{2}, y\right) = u_{\text{ext}}^k\left(x_0 + \frac{\varepsilon}{2}, y\right), \\ \hat{\sigma}_0 \partial_X U^k\left(-\frac{1}{2}, y\right) - i\varepsilon_0\omega \partial_X U^{k-3}\left(-\frac{1}{2}, y\right) = (\sigma_{\text{int}} - i\varepsilon_0\omega) \partial_n u_{\text{int}}^{k-4}\left(x_0 - \frac{\varepsilon}{2}, y\right), \\ \hat{\sigma}_0 \partial_X U^k\left(\frac{1}{2}, y\right) - i\varepsilon_0\omega \partial_X U^{k-3}\left(\frac{1}{2}, y\right) = (\sigma_{\text{ext}} - i\varepsilon_0\omega) \partial_n u_{\text{ext}}^{k-4}\left(x_0 + \frac{\varepsilon}{2}, y\right), \end{array} \right. \quad (1.47)$$

where $y \in (0, y_0)$, and the following boundary conditions

$$\left\{ \begin{array}{l} u^k(0, y) = u^k(L, y) = 0 \quad y \in (0, y_0), \\ u^k(x, 0) = u^k(x, y_0) = 0 \quad x \in \left(0, x_0 - \frac{\varepsilon}{2}\right) \cup \left(x_0 + \frac{\varepsilon}{2}, L\right), \\ U^k(X, 0) = U^k(X, y_0) = 0 \quad X \in \left(-\frac{\varepsilon}{2}, \frac{\varepsilon}{2}\right), \end{array} \right. \quad (1.48)$$

where δ_0^k still denotes the Kronecker symbol. Employing these equations we deduce the problem satisfied outside and inside the layer for any $k \in \mathbb{N}$. The process is similar to the one explained in Section 1.3.1. Then, we truncate the series and neglect the higher order terms in ε to derive new approximate models. We derive a second-order and a fourth-order model that we exhibit in the following section.

1.5.3 First class of ITCs: equivalent models

We employ Equations (1.46) - (1.48) to obtain the expressions for the first terms of the expansion. Then, we truncate the series and we identify a simpler problem satisfied by

$$u^{(k)} = u^0 + \varepsilon u^1 + \dots + \varepsilon^k u^k \quad \text{in } \Omega_{\text{int}}^\varepsilon \cup \Omega_{\text{ext}}^\varepsilon$$

up to a residual term of order ε^{k+1} . We neglect the residual term of order ε^{k+1} to obtain an approximate model satisfied by function $u^{[k]}$. Here, we formally derive two approximate models of order two and order four respectively.

Second-order model

$$\begin{cases} (\sigma_{\text{int}} - i\varepsilon_0\omega) \Delta u_{\text{int}}^{[1]} = f_{\text{int}} & \text{in } \Omega_{\text{int}}^\varepsilon, \\ u_{\text{int}}^{[1]} = 0 & \text{on } \partial\Omega_{\text{int}}^\varepsilon. \end{cases} \quad (1.49)$$

$$\begin{cases} (\sigma_{\text{ext}} - i\varepsilon_0\omega) \Delta u_{\text{ext}}^{[1]} = f_{\text{ext}} & \text{in } \Omega_{\text{ext}}^\varepsilon, \\ u_{\text{ext}}^{[1]} = 0 & \text{on } \partial\Omega_{\text{ext}}^\varepsilon. \end{cases}$$

Fourth-order model

$$\begin{cases} (\sigma_{\text{int}} - i\varepsilon_0\omega) \Delta u_{\text{int}}^{[3]} = f_{\text{int}} & \text{in } \Omega_{\text{int}}^\varepsilon, \\ (\sigma_{\text{ext}} - i\varepsilon_0\omega) \Delta u_{\text{ext}}^{[3]} = f_{\text{ext}} & \text{in } \Omega_{\text{ext}}^\varepsilon, \\ [u^{[3]}]_{\Gamma^\varepsilon} = 0, \\ [(\sigma - i\varepsilon_0\omega) \partial_n u^{[3]}]_{\Gamma^\varepsilon} = -\frac{\hat{\sigma}_0}{\varepsilon^2} \frac{d^2}{dy^2} \{u^{[3]}\}_{\Gamma^\varepsilon}, \\ u^{[3]} = 0 & \text{on } \partial\Omega \cap \partial\Omega^\varepsilon. \end{cases} \quad (1.50)$$

1.5.4 Second class of ITCs: construction of a multiscale expansion

To begin with, we perform a scaling inside the thin layer in the same way as in Section 1.3.1. Then, we perform an *Ansatz* in the form of power series of functions u_{int} , u_{ext} , and U , like the one performed in (1.4). Then, we employ some formal Taylor series expansions to rewrite the transmission conditions across interface Γ as formerly done in Section 1.4.1.

Substituting these expressions in the Equations (1.45) and collecting the terms

with the same powers in ε , for every $k \in \mathbb{N}$ we obtain the following set of equations

$$\left\{ \begin{array}{ll} (\sigma_{\text{int}} - i\varepsilon_0\omega) \Delta u_{\text{int}}^k(x, y) = f_{\text{int}}(x, y)\delta_0^k & \text{in } \Omega_{\text{ext}}, \\ (\sigma_{\text{ext}} - i\varepsilon_0\omega) \Delta u_{\text{ext}}^k(x, y) = f_{\text{ext}}(x, y)\delta_0^k & \text{in } \Omega_{\text{ext}}, \\ i\varepsilon_0\omega \partial_X^2 U^{k-3} - \hat{\sigma}_0 \partial_y^2 U^{k-2} + i\varepsilon_0\omega \partial_y^2 U^{k-5} = \hat{\sigma}_0 \partial_X^2 U^k & \text{in } \left(-\frac{1}{2}, \frac{1}{2}\right) \times (0, y_0), \end{array} \right. \quad (1.51)$$

along with the following transmission conditions

$$\left\{ \begin{array}{l} U^k\left(-\frac{1}{2}, y\right) = \sum_{i=0}^k \frac{(-1)^i}{2^i i!} \partial_n^i u_{\text{int}}^k(x_0, y), \\ U^k\left(\frac{1}{2}, y\right) = \sum_{i=0}^k \frac{1}{2^i i!} \partial_n^i u_{\text{ext}}^k(x_0, y), \\ \hat{\sigma}_0 \partial_X U^k\left(\frac{-1}{2}, y\right) - i\varepsilon_0\omega \partial_X U^{k-3}\left(\frac{-1}{2}, y\right) = (\sigma_{\text{int}} - i\varepsilon_0\omega) \sum_{i=0}^k \frac{(-1)^i}{2^i i!} \partial_n^{i+1} u_{\text{int}}^{k-4}(x_0, y), \\ \hat{\sigma}_0 \partial_X U^k\left(\frac{1}{2}, y\right) - i\varepsilon_0\omega \partial_X U^{k-3}\left(\frac{1}{2}, y\right) = (\sigma_{\text{ext}} - i\varepsilon_0\omega) \sum_{i=0}^k \frac{1}{2^i i!} \partial_n^{i+1} u_{\text{ext}}^{k-4}(x_0, y), \end{array} \right. \quad (1.52)$$

where $y \in (0, y_0)$, and the following boundary conditions

$$\left\{ \begin{array}{l} u^k(0, y) = u^k(L, y) = 0 \quad y \in (0, y_0), \\ u^k(x, 0) = u^k(x, y_0) = 0 \quad x \in \left(0, x_0 - \frac{\varepsilon}{2}\right) \cup \left(x_0 + \frac{\varepsilon}{2}, L\right) \\ U^k(X, 0) = U^k(X, y_0) = 0 \quad X \in \left(-\frac{\varepsilon}{2}, \frac{\varepsilon}{2}\right). \end{array} \right. \quad (1.53)$$

Employing these equations we deduce the problem satisfied outside and inside the layer for any $k \in \mathbb{N}$. The process is similar to the one explained in Section 1.4.1. Then, we truncate the series and neglect the higher order terms in ε to derive new approximate models. We derive a first-order model and a second-order model, as described in the following section.

1.5.5 Second class of ITCs: equivalent models

Equations (1.51) - (1.53) are used to obtain the expressions for the first terms of the expansion. Then, we truncate the series and we identify a simpler problem satisfied by

$$u^{(k)} = u^0 + \varepsilon u^1 + \dots + \varepsilon^k u^k \quad \text{in } \Omega_{\text{int}}^\varepsilon \cup \Omega_{\text{ext}}^\varepsilon$$

up to a residual term of order ε^{k+1} . We neglect the residual term of order ε^{k+1} to obtain an approximate model satisfied by function $u^{[k]}$. Here, we formally derive two approximate models of order one and order two respectively.

First-order model

$$\begin{cases} (\sigma_{\text{int}} - i\varepsilon_0\omega) \Delta u_{\text{int}}^{[0]} = f_{\text{int}} & \text{in } \Omega_{\text{int}}, \\ u_{\text{int}}^{[0]} = 0 & \text{on } \partial\Omega_{\text{int}}. \end{cases} \quad (1.54)$$

$$\begin{cases} (\sigma_{\text{ext}} - i\varepsilon_0\omega) \Delta u_{\text{ext}}^{[0]} = f_{\text{ext}} & \text{in } \Omega_{\text{ext}}, \\ u_{\text{ext}}^{[0]} = 0 & \text{on } \partial\Omega_{\text{ext}}. \end{cases}$$

Second-order model

$$\begin{cases} (\sigma_{\text{int}} - i\varepsilon_0\omega) \Delta u_{\text{int}}^{[1]} = f_{\text{int}} & \text{in } \Omega_{\text{int}}, \\ u_{\text{int}}^{[1]} = \frac{\varepsilon}{2} \partial_n u_{\text{int}}^{[1]} & \text{on } \Gamma, \\ u_{\text{int}}^{[1]} = 0 & \text{on } \partial\Omega \cap \partial\Omega_{\text{int}}. \end{cases} \quad (1.55)$$

$$\begin{cases} (\sigma_{\text{ext}} - i\varepsilon_0\omega) \Delta u_{\text{ext}}^{[1]} = f_{\text{ext}} & \text{in } \Omega_{\text{ext}}, \\ u_{\text{ext}}^{[1]} = -\frac{\varepsilon}{2} \partial_n u_{\text{ext}}^{[1]} & \text{on } \Gamma, \\ u_{\text{ext}}^{[1]} = 0 & \text{on } \partial\Omega \cap \partial\Omega_{\text{ext}}. \end{cases}$$

Remark 3. *The models obtained in this section are very similar to the ones obtained for the static case, (1.18) and (1.19) for the first class of ITCs and (1.36) and (1.38) for the second class of ITCs. In fact, it is possible to obtain the models we present in this section by simply substituting the conductivities σ_{int} and σ_{ext} by $\sigma_{\text{int}} - i\varepsilon_0\omega$ and $\sigma_{\text{ext}} - i\varepsilon_0\omega$ respectively.*

1.6 3D axisymmetric configuration

The main objective of this section is the derivation of approximate models in a 3D axisymmetric configuration. The plan of the section is the following. First we set the model problem we are interested in. Then, we develop a multiscale expansion in powers of ε for the solution to the model problem and we obtain the equations

for the first terms of the expansion adopting the first approach. Finally, we derive the desired approximate models. We then address the second class of problems, and for avoiding repetition with the previous sections only the main results are presented.

1.6.1 Model problem and scaling

Let $\tilde{\Omega} \subset \mathbb{R}^3$ be the domain of interest described at Figure 1.4. Domain $\tilde{\Omega}$ is a cylinder shaped domain and is decomposed into three subdomains: $\tilde{\Omega}_{\text{int}}^\varepsilon$, $\tilde{\Omega}_{\text{ext}}^\varepsilon$, and $\tilde{\Omega}_{\text{lay}}^\varepsilon$. Subdomain $\tilde{\Omega}_{\text{lay}}^\varepsilon$ is a thin layer of uniform thickness $\varepsilon > 0$. We denote by $\tilde{\Gamma}_{\text{int}}^\varepsilon$ the interface between $\tilde{\Omega}_{\text{int}}^\varepsilon$ and $\tilde{\Omega}_{\text{lay}}^\varepsilon$, and by $\tilde{\Gamma}_{\text{ext}}^\varepsilon$ the interface between $\tilde{\Omega}_{\text{lay}}^\varepsilon$ and $\tilde{\Omega}_{\text{ext}}^\varepsilon$. In this domain, we study the static electric potential equation, which read as follows

$$\operatorname{div}(\sigma \nabla \tilde{u}) = \tilde{f}. \quad (1.56)$$

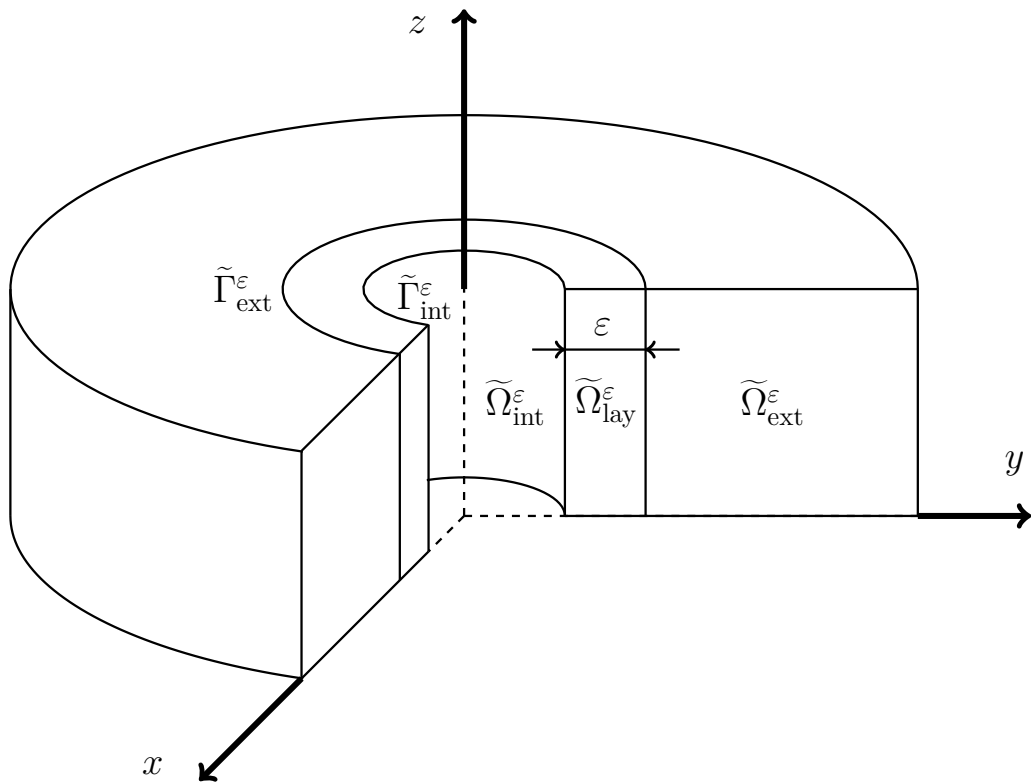
Here, \tilde{u} represents the electric potential, σ stands for the conductivity and \tilde{f} is the right-hand side, which corresponds to a current source. The conductivity is a piecewise constant function, with a different value in each subdomain. Specifically, the value of the conductivity inside the thin layer $\tilde{\Omega}_{\text{lay}}^\varepsilon$ is much larger than the one in the other subdomains and we assume that it depends on parameter ε . We consider a conductivity of the following form

$$\sigma = \begin{cases} \sigma_{\text{int}} & \text{in } \tilde{\Omega}_{\text{int}}^\varepsilon, \\ \sigma_{\text{lay}} = \hat{\sigma}_0 \varepsilon^{-3} & \text{in } \tilde{\Omega}_{\text{lay}}^\varepsilon, \\ \sigma_{\text{ext}} & \text{in } \tilde{\Omega}_{\text{ext}}^\varepsilon, \end{cases}$$

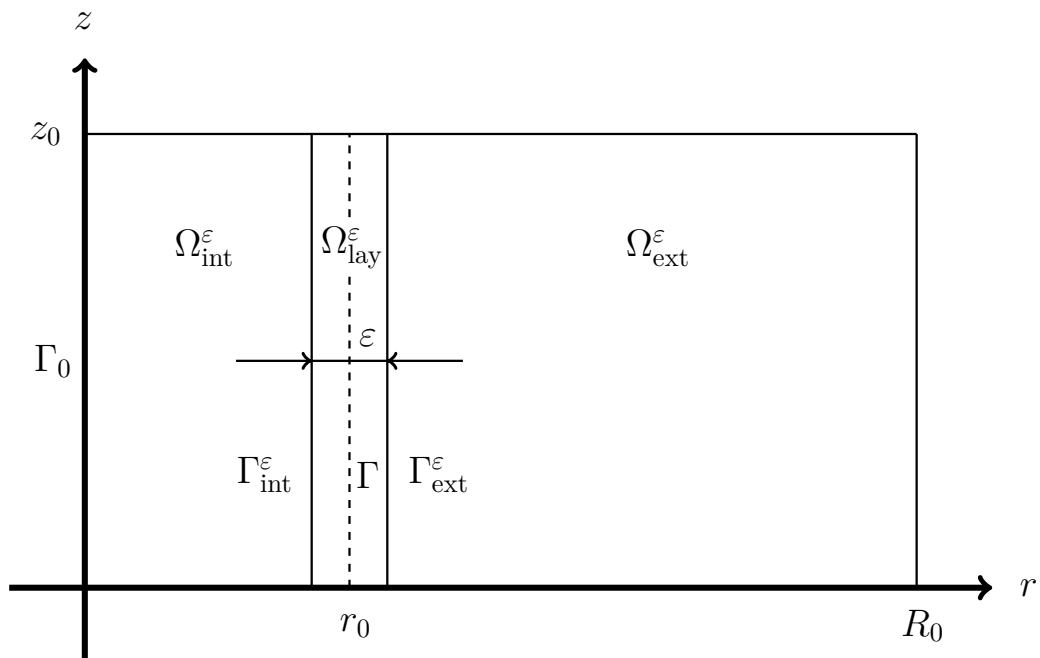
where $\hat{\sigma}_0 > 0$ is a given constant. We assume the right-hand side \tilde{f} is a piecewise smooth function that is independent of ε and vanishes inside the layer.

$$\tilde{f} = \begin{cases} \tilde{f}_{\text{int}} & \text{in } \tilde{\Omega}_{\text{int}}^\varepsilon, \\ \tilde{f}_{\text{lay}} = 0 & \text{in } \tilde{\Omega}_{\text{lay}}^\varepsilon, \\ \tilde{f}_{\text{ext}} & \text{in } \tilde{\Omega}_{\text{ext}}^\varepsilon. \end{cases}$$

We assume that we have a solution to (1.56) $\tilde{u} \in H^1(\tilde{\Omega})$. Then, denoting the



(a) Sectioned three dimensional domain.



(b) Meridian domain.

Figure 1.4: Domain of interest in three dimensions and meridian domain in terms of cylindrical coordinates

solution \tilde{u} by

$$\tilde{u} = \begin{cases} \tilde{u}_{\text{int}} & \text{in } \tilde{\Omega}_{\text{int}}^\varepsilon, \\ \tilde{u}_{\text{lay}} & \text{in } \tilde{\Omega}_{\text{lay}}^\varepsilon, \\ \tilde{u}_{\text{ext}} & \text{in } \tilde{\Omega}_{\text{ext}}^\varepsilon, \end{cases}$$

Problem (1.56) becomes

$$\left\{ \begin{array}{ll} \sigma_{\text{int}} \Delta \tilde{u}_{\text{int}} = \tilde{f}_{\text{int}} & \text{in } \tilde{\Omega}_{\text{int}}^\varepsilon, \\ \sigma_{\text{ext}} \Delta \tilde{u}_{\text{ext}} = \tilde{f}_{\text{ext}} & \text{in } \tilde{\Omega}_{\text{ext}}^\varepsilon, \\ \Delta \tilde{u}_{\text{lay}} = 0 & \text{in } \tilde{\Omega}_{\text{lay}}^\varepsilon, \\ \tilde{u}_{\text{int}} = \tilde{u}_{\text{lay}} & \text{on } \tilde{\Gamma}_{\text{int}}^\varepsilon, \\ \tilde{u}_{\text{lay}} = \tilde{u}_{\text{ext}} & \text{on } \tilde{\Gamma}_{\text{ext}}^\varepsilon, \\ \sigma_{\text{int}} \partial_n \tilde{u}_{\text{int}} = \hat{\sigma}_0 \varepsilon^{-3} \partial_n \tilde{u}_{\text{lay}} & \text{on } \tilde{\Gamma}_{\text{int}}^\varepsilon, \\ \hat{\sigma}_0 \varepsilon^{-3} \partial_n \tilde{u}_{\text{lay}} = \sigma_{\text{ext}} \partial_n \tilde{u}_{\text{ext}} & \text{on } \tilde{\Gamma}_{\text{ext}}^\varepsilon, \\ \tilde{u} = 0 & \text{on } \partial \tilde{\Omega}, \end{array} \right. \quad (1.57)$$

where ∂_n represents the normal derivative in the direction of the normal vector, which is interior to $\tilde{\Omega}_{\text{ext}}^\varepsilon$ on $\tilde{\Gamma}_{\text{ext}}^\varepsilon$, and exterior to $\tilde{\Omega}_{\text{int}}^\varepsilon$ on $\tilde{\Gamma}_{\text{int}}^\varepsilon$, as shown at Figure 1.4.

We introduce a system of cylindrical coordinates (r, θ, z) . We assume that the right-hand side \tilde{f} is an axisymmetric function and we know that the conductivity σ and the domain are also axisymmetric (a generalization of the results presented in this section can be found in Appendix A.2, where the source is no more assumed to be axisymmetric). As a consequence we eliminate one dimension because the solution is independent of the angular variable θ . We denote by u the function that meets

$$\tilde{u}(x, y, z) = \tilde{u}(r \cos(\theta), r \sin(\theta), z) = u(r, z),$$

and by f the function that satisfies

$$\tilde{f}(x, y, z) = \tilde{f}(r \cos(\theta), r \sin(\theta), z) = f(r, z).$$

If we write the Laplace operator in cylindrical coordinates we obtain the following expression

$$\Delta = \frac{1}{r} \frac{\partial}{\partial r} \left(r \frac{\partial}{\partial r} \right) + \frac{1}{r^2} \frac{\partial^2}{\partial \theta^2} + \frac{\partial^2}{\partial z^2}.$$

Taking into account that u does not depend on θ the equation of interest becomes

$$\sigma \Delta \tilde{u} = \tilde{f} \Rightarrow \sigma \frac{1}{r} \partial_r (r \partial_r u) + \sigma \partial_z^2 u = f.$$

Now the domain of interest is the meridian domain showed in Figure 1.4b and the problem of interest is the following

$$\left\{ \begin{array}{ll} \sigma_{\text{int}} \frac{1}{r} \partial_r (r \partial_r u_{\text{int}}) + \sigma_{\text{int}} \partial_z^2 u_{\text{int}} = f_{\text{int}} & \text{in } \Omega_{\text{int}}^\varepsilon, \\ \sigma_{\text{ext}} \frac{1}{r} \partial_r (r \partial_r u_{\text{ext}}) + \sigma_{\text{ext}} \partial_z^2 u_{\text{ext}} = f_{\text{ext}} & \text{in } \Omega_{\text{ext}}^\varepsilon, \\ \frac{1}{r} \partial_r (r \partial_r u_{\text{lay}}) + \partial_z^2 u_{\text{lay}} = 0 & \text{in } \Omega_{\text{lay}}^\varepsilon, \\ u_{\text{lay}} = u_{\text{int}} & \text{on } \Gamma_{\text{int}}^\varepsilon, \\ u_{\text{lay}} = u_{\text{ext}} & \text{on } \Gamma_{\text{ext}}^\varepsilon, \\ \hat{\sigma}_0 \varepsilon^{-3} \partial_r u_{\text{lay}} = \sigma_{\text{int}} \partial_n u_{\text{int}} & \text{on } \Gamma_{\text{int}}^\varepsilon, \\ \hat{\sigma}_0 \varepsilon^{-3} \partial_r u_{\text{lay}} = \sigma_{\text{ext}} \partial_n u_{\text{ext}} & \text{on } \Gamma_{\text{ext}}^\varepsilon, \\ u = 0 & \text{on } \partial\Omega - \Gamma_0, \\ \partial_r = 0 & \text{on } \Gamma_0. \end{array} \right. \quad (1.58)$$

In three dimensions there is no boundary condition on the axis z . When reducing the problem to two dimensions, a new boundary arises at the z axis, due to the symmetry of the solution, we adopt Neumann type conditions on this boundary. A key point for the derivation of a multiscale expansion for the solution to Problem (1.58) consists in performing a scaling along the direction normal to the thin layer. We begin by describing domain $\Omega_{\text{lay}}^\varepsilon$ in the following way

$$\Omega_{\text{lay}}^\varepsilon = \left\{ \gamma(z) + \varepsilon R n : \gamma(z) \in \Gamma, R \in \left(-\frac{1}{2}, \frac{1}{2} \right) \right\},$$

where γ is a parametrization of the curve Γ (see Figure 1.4), which is defined as

$$\gamma(z) = (r_0, z), \text{ for all } z \in (0, z_0),$$

and $n = (1, 0)$ is the normal vector to the curve Γ . This domain geometry induces the following scaling

$$r = r_0 + \varepsilon R \quad \Leftrightarrow \quad R = \varepsilon^{-1} (r - r_0)$$

As a consequence, we have

$$\partial_R^k = \varepsilon^k \partial_r^k, \quad k \in \mathbb{N}.$$

This scaling allows us to write the scalar operator $\frac{1}{r} \partial_r (r \partial_r) + \partial_z^2$ in the following way

$$\varepsilon^{-2} \partial_R^2 + \varepsilon^{-1} \frac{1}{r_0 + \varepsilon R} \partial_R + \partial_z^2.$$

Now we perform an expansion of the term $\frac{1}{r_0 + \varepsilon R}$ in powers of ε so that we obtain the following expression

$$\varepsilon^{-2} \partial_R^2 + \sum_{k=0}^{\infty} \varepsilon^{k-1} \frac{(-R)^k}{r_0^{k+1}} \partial_R + \partial_z^2.$$

We also notice that on the interfaces $\Gamma_{\text{int}}^\varepsilon$ and $\Gamma_{\text{ext}}^\varepsilon$ we rewrite the normal derivative in the following form $\partial_n = \partial_r = \varepsilon^{-1} \partial_R$. Finally we denote by U the function that satisfies

$$u_{\text{lay}}(r, z) = u_{\text{lay}}(r_0 + \varepsilon R, z) = U(R, z), \quad (R, z) \in \left(-\frac{1}{2}, \frac{1}{2}\right) \times (0, z_0).$$

We rewrite Equations (1.58) with the newly defined variables and functions and they satisfy the following equations

$$\left\{ \begin{array}{ll} \sigma_{\text{int}} \frac{1}{r} \partial_r (r \partial_r u_{\text{int}}) + \sigma_{\text{int}} \partial_z^2 u_{\text{int}} = f_{\text{int}} & \text{in } \Omega_{\text{int}}^\varepsilon, \\ \sigma_{\text{ext}} \frac{1}{r} \partial_r (r \partial_r u_{\text{ext}}) + \sigma_{\text{ext}} \partial_z^2 u_{\text{ext}} = f_{\text{ext}} & \text{in } \Omega_{\text{ext}}^\varepsilon, \\ \varepsilon^{-2} \partial_R^2 U + \sum_{k=0}^{\infty} \varepsilon^{k-1} \frac{(-R)^k}{r_0^{k+1}} \partial_R U + \partial_z^2 U = 0 & \text{in } \left(-\frac{1}{2}, \frac{1}{2}\right) \times (0, z_0), \end{array} \right. \quad (1.59)$$

along with the following transmission and boundary conditions

$$\left\{ \begin{array}{ll} u_{\text{int}}\left(r_0 - \frac{\varepsilon}{2}, z\right) = U\left(-\frac{1}{2}, z\right) & z \in (0, z_0), \\ u_{\text{ext}}\left(r_0 + \frac{\varepsilon}{2}, z\right) = U\left(\frac{1}{2}, z\right) & z \in (0, z_0), \\ \sigma_{\text{int}}\partial_r u_{\text{int}}\left(r_0 - \frac{\varepsilon}{2}, z\right) = \hat{\sigma}_0 \varepsilon^{-4} \partial_R U\left(-\frac{1}{2}, z\right) & z \in (0, z_0), \\ \sigma_{\text{ext}}\partial_r u_{\text{ext}}\left(r_0 + \frac{\varepsilon}{2}, z\right) = \hat{\sigma}_0 \varepsilon^{-4} \partial_R U\left(\frac{1}{2}, z\right) & z \in (0, z_0), \\ u = 0 & \text{on } \partial\Omega - \Gamma_0, \\ \partial_r u_{\text{int}} = 0 & \text{on } \Gamma_0, \end{array} \right. \quad (1.60)$$

1.6.2 First class of ITCs: construction of a multiscale expansion

We now derive the asymptotic expansion. To begin with, we perform an *Ansatz* in the form of power series of ε for the solution to Problems (1.59) and (1.60). We look for solutions

$$\left\{ \begin{array}{ll} u_{\text{int}}(r, z) \approx \sum_{k \geq 0} \varepsilon^k u_{\text{int}}^k(r, z) & \text{in } \Omega_{\text{int}}^\varepsilon, \\ u_{\text{ext}}(r, z) \approx \sum_{k \geq 0} \varepsilon^k u_{\text{ext}}^k(r, z) & \text{in } \Omega_{\text{ext}}^\varepsilon, \\ U(R, z) \approx \sum_{k \geq 0} \varepsilon^k U^k(R, z) & \text{in } \left(-\frac{1}{2}, \frac{1}{2}\right) \times (0, z_0). \end{array} \right. \quad (1.61)$$

Equations for the coefficients of the electric potential

Substituting the previous expressions into Equations (1.59) and (1.60) and collecting the terms with the same powers in ε , for every $k \in \mathbb{N}$ we obtain the following set of equations

$$\left\{ \begin{array}{l} \sigma_{\text{int}} \frac{1}{r} \partial_r (r \partial_r u_{\text{int}}^k) + \sigma_{\text{int}} \partial_z^2 u_{\text{int}}^k = f_{\text{int}} \delta_k^0 \quad \text{in } \Omega_{\text{int}}^\varepsilon, \\ \sigma_{\text{ext}} \frac{1}{r} \partial_r (r \partial_r u_{\text{ext}}^k) + \sigma_{\text{ext}} \partial_z^2 u_{\text{ext}}^k = f_{\text{ext}} \delta_k^0 \quad \text{in } \Omega_{\text{ext}}^\varepsilon, \\ \partial_R^2 U^k + \sum_{l=0}^{k-1} \frac{(-R)^{k-l-1}}{r_0^{k-l}} \partial_R U^l + \partial_z^2 U^{k-2} = 0 \quad \text{in } \left(-\frac{1}{2}, \frac{1}{2}\right) \times (0, z_0), \end{array} \right. \quad (1.62a)$$

$$(1.62b)$$

$$(1.62c)$$

along with the following transmission conditions

$$\left\{ \begin{array}{l} U^k \left(-\frac{1}{2}, z\right) = u_{\text{int}}^k \left(r_0 - \frac{\varepsilon}{2}, z\right) \quad z \in (0, z_0), \quad (1.63a) \\ U^k \left(\frac{1}{2}, z\right) = u_{\text{ext}}^k \left(r_0 + \frac{\varepsilon}{2}, z\right) \quad z \in (0, z_0), \quad (1.63b) \\ \hat{\sigma}_0 \partial_R U^k \left(-\frac{1}{2}, z\right) = \sigma_{\text{int}} \partial_r u_{\text{int}}^{k-4} \left(r_0 - \frac{\varepsilon}{2}, z\right) \quad z \in (0, z_0), \quad (1.63c) \\ \hat{\sigma}_0 \partial_R U^k \left(\frac{1}{2}, z\right) = \sigma_{\text{ext}} \partial_r u_{\text{ext}}^{k-4} \left(r_0 + \frac{\varepsilon}{2}, z\right) \quad z \in (0, z_0), \quad (1.63d) \end{array} \right.$$

and the following boundary conditions

$$\left\{ \begin{array}{l} \partial_r u_{\text{int}}^k(0, z) = u_{\text{ext}}^k(R_0, z) = 0 \quad z \in (0, z_0), \quad (1.64a) \\ u^k(r, 0) = u^k(r, z_0) = 0 \quad r \in \left(0, r_0 - \frac{\varepsilon}{2}\right) \cup \left(r_0 + \frac{\varepsilon}{2}, R_0\right), \quad (1.64b) \\ U^k(R, 0) = U^k(R, z_0) = 0 \quad R \in \left(-\frac{1}{2}, \frac{1}{2}\right). \quad (1.64c) \end{array} \right.$$

For determining the elemental problem satisfied by each of the terms of the expansion, we will also need the following equation obtained by applying the fundamental

theorem of calculus for a smooth function U^k ,

$$\int_{-\frac{1}{2}}^{\frac{1}{2}} \partial_R^2 U^k(R, z) dR = \partial_R U^k\left(\frac{1}{2}, z\right) - \partial_R U^k\left(-\frac{1}{2}, z\right).$$

If we substitute Equation (1.62c) to the left-hand side and Equations (1.63c) and (1.63d) to the right-hand side, we obtain the following compatibility condition

$$\int_{-\frac{1}{2}}^{\frac{1}{2}} \left(\partial_z^2 U^{k-2}(R, z) + \sum_{l=0}^{k-1} \frac{(-R)^{k-1-l}}{r_0^{k-l}} \partial_R U^l(R, z) \right) dR = \frac{-1}{\hat{\sigma}_0} \left[\sigma \partial_n u^{k-4} \right]_{\Gamma^\varepsilon}(z). \quad (1.65)$$

We adopt the convention that the terms with negative indices in Equations (1.62)-(1.65) are equal to 0. Employing Equations (1.62)-(1.65) we deduce the elementary problems satisfied outside and inside the layer for any $k \in \mathbb{N}$. For that purpose we employ the following algorithm composed of three steps.

Algorithm for the determination of the coefficients

Initialization of the algorithm:

Before showing the different steps to obtain function U^k and u^k for every k , we need to determine function U^0 up to a function in the variable z , denoted by φ_0^0 . For that purpose we consider Equations (1.62c), (1.63c), and (1.63d), and we build the following differential problem in the variable R for U^0 (the variable z plays the role of a parameter)

$$\begin{cases} \partial_R^2 U^0(R, z) = 0 & R \in \left(-\frac{1}{2}, \frac{1}{2}\right), \\ \hat{\sigma}_0 \partial_R U^0\left(-\frac{1}{2}, z\right) = 0, \\ \hat{\sigma}_0 \partial_R U^0\left(\frac{1}{2}, z\right) = 0. \end{cases}$$

From these equations we deduce that U^0 has the following form $U^0(R, z) = \varphi_0^0(z)$, where function φ_0^0 has yet to be determined and this will be done during the first step of the algorithm. After these preliminary steps, we move onto determining U^k and u^k for any k .

We assume that the first terms of the expansion (1.61) up to the order ε^{k-1} have already been calculated and we calculate the equations for the k -th term. We also assume that at rank k we know the form of U^k up to a function in the variable z , denoted by φ_0^k . We obtain the expression of U^k at rank $k-1$. The first

step consists in determining the expression of function U^{k+1} up to function φ_0^{k+1} . Then, at the second step we determine function φ_0^k involved in the expression of function U^k . Finally, we determine u_{int}^k and u_{ext}^k at the third step. For every $k = 0, 1, 2, \dots$, we perform the following steps:

First step:

We select Equations (1.62c), (1.63c), and (1.63d), and we build the following differential problem in the variable R for U^{k+1} (the variable z plays the role of a parameter)

$$\left\{ \begin{array}{l} \partial_R^2 U^{k+1}(R, z) = g^{k+1}(R, z) \quad R \in \left(-\frac{1}{2}, \frac{1}{2}\right), \\ \hat{\sigma}_0 \partial_R U^{k+1}\left(-\frac{1}{2}, z\right) = \sigma_{\text{int}} \partial_r u_{\text{int}}^{k-3}\left(r_0 - \frac{\varepsilon}{2}, z\right), \\ \hat{\sigma}_0 \partial_R U^{k+1}\left(\frac{1}{2}, z\right) = \sigma_{\text{ext}} \partial_r u_{\text{ext}}^{k-3}\left(r_0 + \frac{\varepsilon}{2}, z\right), \end{array} \right. \quad (1.66)$$

where

$$g^{k+1}(R, z) = - \sum_{l=0}^k \frac{(-R)^{k-l}}{r_0^{k-l+1}} \partial_R U^l(R, z) - \partial_z^2 U^{k-1}(R, z).$$

There exists a solution U^{k+1} to (1.66) provided the compatibility condition (1.65) is satisfied. We deduce the expression of U^{k+1} up to a function in the variable z , denoted by $\varphi_0^{k+1}(z)$. The function U^{k+1} has the following form

$$U^{k+1}(R, z) = V^{k+1}(R, z) + \varphi_0^{k+1}(z),$$

where V^{k+1} represents the part of U^{k+1} that is determined at this step and has the form (see Proposition 3)

$$V^k(R, z) = \begin{cases} 0 & \text{if } k = 0, 1, 2, 3 \\ \varphi_{k-2}^k(z)R^{k-2} + \varphi_{k-3}^k(z)R^{k-3} + \dots + \varphi_1^k(z)R & \text{if } k > 3. \end{cases}$$

Function φ_0^{k+1} represents the part of U^{k+1} that is determined at the following rank.

Second step:

We employ the compatibility condition (1.65) (at rank $k + 2$), along with Equation (1.64c) to write the following differential problem in the variable z for function φ_0^k , present in the expression of U^k .

$$\begin{cases} \frac{d^2}{dz^2} \varphi_0^k(z) = h^k(z) & z \in (0, z_0), \\ \varphi_0^k(0) = 0, \\ \varphi_0^k(z_0) = 0, \end{cases} \quad (1.67)$$

where

$$h^k(z) = - \int_{-\frac{1}{2}}^{\frac{1}{2}} \left(\partial_z^2 V^k(R, z) + \sum_{l=0}^{k+1} \frac{(-R)^{k+1-l}}{r_0^{k+2-l}} \partial_R U^l(R, z) \right) dR - \frac{1}{\widehat{\sigma}_0} \left[\sigma \partial_n u^{k-2} \right]_{\Gamma^\varepsilon}(z).$$

Solving this differential equation we obtain function φ_0^k and thus, the complete expression of U^k .

Third step:

We derive the equations outside the layer by employing Equations (1.62a), (1.62b), (1.63a), (1.63b), (1.64a), and (1.64b). We infer that u_{int}^k and u_{ext}^k are defined independently in the two subdomains $\Omega_{\text{int}}^\varepsilon$ and $\Omega_{\text{ext}}^\varepsilon$.

$$\begin{cases} \sigma_{\text{int}} \frac{1}{r} \partial_r (r \partial_r u_{\text{int}}^k) + \sigma_{\text{int}} \partial_z^2 u_{\text{int}}^k = 0 & \text{in } \Omega_{\text{int}}^\varepsilon, \\ u_{\text{int}}^k \left(r_0 - \frac{\varepsilon}{2}, z \right) = U^k \left(-\frac{1}{2}, z \right), \\ u_{\text{int}}^k = 0 & \text{on } \partial\Omega \cap \partial\Omega_{\text{int}}^\varepsilon - \Gamma_0, \\ \partial_r u_{\text{int}}^k = 0 & \text{on } \Gamma_0, \end{cases} \quad (1.68)$$

$$\begin{cases} \sigma_{\text{ext}} \frac{1}{r} \partial_r (r \partial_r u_{\text{ext}}^k) + \sigma_{\text{ext}} \partial_z^2 u_{\text{ext}}^k = 0 & \text{in } \Omega_{\text{ext}}^\varepsilon, \\ u_{\text{ext}}^k \left(r_0 + \frac{\varepsilon}{2}, z \right) = U^k \left(\frac{1}{2}, z \right), \\ u_{\text{ext}}^k = 0 & \text{on } \partial\Omega \cap \partial\Omega_{\text{ext}}^\varepsilon. \end{cases}$$

We will now employ this algorithm to obtain the equations for the first terms of the expansion.

First terms of the asymptotics

Terms of order zero

Thanks to the preliminary steps formerly performed during the initialization of the algorithm we already know that U^0 has the form $U^0(R, z) = \varphi_0^0(z)$. In the same way we consider Problem (1.66) for U^1

$$\left\{ \begin{array}{l} \partial_R^2 U^1(R, z) = 0 \quad R \in \left(-\frac{1}{2}, \frac{1}{2}\right), \\ \partial_R U^1\left(-\frac{1}{2}, z\right) = 0, \\ \partial_R U^1\left(\frac{1}{2}, z\right) = 0. \end{array} \right.$$

We deduce that the solution to this equation has the form $U^1(R, z) = \varphi_0^1(z)$. Then, we employ (1.67) and we build the following problem for φ_0^0

$$\left\{ \begin{array}{l} \frac{d^2}{dz^2} \varphi_0^0(z) = 0 \quad z \in (0, z_0), \\ \varphi_0^0(0) = 0, \\ \varphi_0^0(z_0) = 0. \end{array} \right.$$

We deduce that $\varphi_0^0(z) = 0$ and thus, $U^0(R, z) = 0$. Finally, employing (1.68), we obtain that the limit solution u^0 satisfies homogeneous Dirichlet boundary conditions on $\Gamma_{\text{int}}^\varepsilon$ and $\Gamma_{\text{ext}}^\varepsilon$. Thus, the problem satisfied by u^0 reads as

$$\left\{ \begin{array}{ll} \sigma_{\text{int}} \frac{1}{r} \partial_r (r \partial_r u_{\text{int}}^0) + \sigma_{\text{int}} \partial_z^2 u_{\text{int}}^0 = f_{\text{int}} & \text{in } \Omega_{\text{int}}^\varepsilon, \\ u_{\text{int}}^0 = 0 & \text{on } \partial\Omega_{\text{int}}^\varepsilon - \Gamma_0, \\ \partial_r u_{\text{int}}^0 = 0 & \text{on } \partial\Gamma_0, \end{array} \right. \quad (1.69)$$

$$\left\{ \begin{array}{ll} \sigma_{\text{ext}} \frac{1}{r} \partial_r (r \partial_r u_{\text{ext}}^0) + \sigma_{\text{ext}} \partial_z^2 u_{\text{ext}}^0 = f_{\text{ext}} & \text{in } \Omega_{\text{ext}}^\varepsilon, \\ u_{\text{ext}}^0 = 0 & \text{on } \partial\Omega_{\text{ext}}^\varepsilon. \end{array} \right.$$

Terms of order one

We consider Problem (1.66) for U^2

$$\begin{cases} \partial_R^2 U^2(R, z) = 0 & R \in \left(-\frac{1}{2}, \frac{1}{2}\right), \\ \partial_R U^2\left(-\frac{1}{2}, z\right) = 0, \\ \partial_R U^2\left(\frac{1}{2}, z\right) = 0. \end{cases}$$

We deduce that the solution to this equation has the form $U^2(R, z) = \varphi_0^2(z)$. Then, we employ (1.67) and we obtain the following problem for φ_0^1

$$\begin{cases} \frac{d^2}{dz^2} \varphi_0^1(z) = 0 & z \in (0, z_0), \\ \varphi_0^1(0) = 0, \\ \varphi_0^1(z_0) = 0. \end{cases}$$

We deduce that $\varphi_0^1(z) = 0$ and thus, $U^1(R, z) = 0$. Finally, employing (1.68) we write the problem satisfied outside the layer by u^1 as two uncoupled problems

$$\begin{cases} \frac{1}{r} \partial_r (r \partial_r u_{\text{int}}^1) + \partial_z^2 u_{\text{int}}^1 = 0 & \text{in } \Omega_{\text{int}}^\varepsilon, \\ u_{\text{int}}^1 = 0 & \text{on } \partial\Omega_{\text{int}}^\varepsilon - \Gamma_0, \\ \partial_r u_{\text{int}}^1 = 0 & \text{on } \Gamma_0, \end{cases} \quad (1.70)$$

$$\begin{cases} \frac{1}{r} \partial_r (r \partial_r u_{\text{ext}}^1) + \partial_z^2 u_{\text{ext}}^1 = 0 & \text{in } \Omega_{\text{ext}}^\varepsilon, \\ u_{\text{ext}}^1 = 0 & \text{on } \partial\Omega_{\text{ext}}^\varepsilon. \end{cases}$$

We deduce that $u^1 \equiv 0$.

Terms of order two

We consider Problem (1.66) for U^3

$$\begin{cases} \partial_R^2 U^3(R, z) = 0 & R \in \left(-\frac{1}{2}, \frac{1}{2}\right), \\ \partial_R U^3\left(-\frac{1}{2}, z\right) = 0, \\ \partial_R U^3\left(\frac{1}{2}, z\right) = 0. \end{cases}$$

We deduce that the solution to this equation has the form $U^3(R, z) = \varphi_0^3(z)$. Then, we employ (1.67) and φ_0^2 satisfies

$$\begin{cases} \frac{d^2}{dz^2} \varphi_0^2(z) = -\frac{1}{\widehat{\sigma}_0} [\sigma \partial_r u^0]_{\Gamma^\varepsilon}(z) & z \in (0, z_0), \\ \varphi_0^2(0) = 0, \\ \varphi_0^2(z_0) = 0. \end{cases}$$

We deduce that $\varphi_0^2(z)$ and thus, $U^2(R, z)$ have the following form

$$\begin{aligned} U^2(R, z) &= \varphi_0^2(z) \\ &= -\frac{1}{\widehat{\sigma}_0} \int_0^z (z-t) [\sigma \partial_r u^0]_{\Gamma^\varepsilon}(t) dt + \frac{z}{\widehat{\sigma}_0 z_0} \int_0^{z_0} (z_0-t) [\sigma \partial_r u^0]_{\Gamma^\varepsilon}(t) dt. \end{aligned} \quad (1.71)$$

Finally, employing (1.68) we write the problem satisfied by u^2 outside the layer as two uncoupled problems

$$\begin{cases} \frac{1}{r} \partial_r (r \partial_r u_{\text{int}}^2) + \partial_z^2 u_{\text{int}}^2 = 0 & \text{in } \Omega_{\text{int}}^\varepsilon, \\ u_{\text{int}}^2 \left(r_0 - \frac{\varepsilon}{2}, z \right) = \varphi_0^2(z), \\ u_{\text{int}}^2 = 0 & \text{on } \partial\Omega \cap \partial\Omega_{\text{int}}^\varepsilon - \Gamma_0, \\ \partial_r u_{\text{int}}^2 = 0 & \text{on } \partial\Omega \cap \Gamma_0, \end{cases} \quad (1.72)$$

$$\begin{cases} \frac{1}{r} \partial_r (r \partial_r u_{\text{ext}}^2) + \partial_z^2 u_{\text{ext}}^2 = 0 & \text{in } \Omega_{\text{ext}}^\varepsilon, \\ u_{\text{ext}}^2 \left(r_0 + \frac{\varepsilon}{2}, z \right) = \varphi_0^2(z), \\ u_{\text{ext}}^2 = 0 & \text{on } \partial\Omega \cap \partial\Omega_{\text{ext}}^\varepsilon. \end{cases}$$

Terms of order three

We consider Problem (1.66) for U^4

$$\begin{cases} \partial_R^2 U^4(R, z) = -\frac{d^2}{dz^2} \varphi_0^2(z) & R \in \left(\frac{-1}{2}, \frac{1}{2} \right), \\ \widehat{\sigma}_0 \partial_R U^4 \left(-\frac{1}{2}, z \right) = \sigma_{\text{int}} \partial_r u_{\text{int}}^0 \left(r_0 - \frac{\varepsilon}{2}, z \right), \\ \widehat{\sigma}_0 \partial_R U^4 \left(\frac{1}{2}, z \right) = \sigma_{\text{ext}} \partial_r u_{\text{ext}}^0 \left(r_0 + \frac{\varepsilon}{2}, z \right). \end{cases}$$

We deduce that the solution to this equation has the form

$$U^4(R, z) = \frac{1}{\widehat{\sigma}_0} [\sigma \partial_r u^0]_{\Gamma^\varepsilon}(z) \frac{R^2}{2} + \frac{1}{\widehat{\sigma}_0} \{ \sigma \partial_r u^0 \}_{\Gamma^\varepsilon}(z) R + \varphi_0^4(z).$$

Then, we employ (1.67) and we build the following problem for φ_0^3

$$\begin{cases} \frac{d^2}{dz^2} \varphi_0^3(z) = -\frac{1}{\widehat{\sigma}_0 r_0} \{ \sigma \partial_r u^0 \}_{\Gamma^\varepsilon}(z) & z \in (0, z_0), \\ \varphi_0^3(0) = 0, \\ \varphi_0^3(z_0) = 0. \end{cases}$$

We deduce that $\varphi_0^3(z)$ and thus, $U^3(R, z)$ have the following form

$$\begin{aligned} U^3(R, z) &= \varphi_0^3(z) \\ &= \frac{-1}{\widehat{\sigma}_0} \int_0^z \frac{(z-t)}{r_0} \{ \sigma \partial_r u^0 \}_{\Gamma^\varepsilon}(t) dt + \frac{z}{\widehat{\sigma}_0 z_0} \int_0^{z_0} \frac{(z_0-t)}{r_0} \{ \sigma \partial_r u^0 \}_{\Gamma^\varepsilon}(t) dt. \end{aligned} \quad (1.73)$$

Finally, employing (1.68) we write the problem satisfied outside the layer by u^3 as two uncoupled problems

$$\begin{cases} \frac{1}{r} \partial_r (r \partial_r u_{\text{int}}^3) + \sigma_{\text{int}} \partial_z^2 u_{\text{int}}^3 = 0 & \text{in } \Omega_{\text{int}}^\varepsilon, \\ u_{\text{int}}^3 \left(r_0 - \frac{\varepsilon}{2}, z \right) = U^3 \left(-\frac{1}{2}, z \right), \\ u_{\text{int}}^3 = 0 & \text{on } \partial\Omega \cap \partial\Omega_{\text{int}}^\varepsilon - \Gamma_0, \\ \partial_r u_{\text{int}}^3 = 0 & \text{on } \Gamma_0, \end{cases} \quad (1.74)$$

$$\begin{cases} \frac{1}{r} \partial_r (r \partial_r u_{\text{ext}}^3) + \sigma_{\text{ext}} \partial_z^2 u_{\text{ext}}^3 = 0 & \text{in } \Omega_{\text{ext}}^\varepsilon, \\ u_{\text{ext}}^3 \left(r_0 + \frac{\varepsilon}{2}, z \right) = U^3 \left(\frac{1}{2}, z \right), \\ u_{\text{ext}}^3 = 0 & \text{on } \partial\Omega \cap \partial\Omega_{\text{ext}}^\varepsilon. \end{cases}$$

Recapitulation of the asymptotic expansion

Proposition 3. *The asymptotic expansion (1.61), has the following form*

$$\begin{cases} u_{int}(r, z) = u_{int}^0(r, z) + \varepsilon^2 u_{int}^2(r, z) + \varepsilon^3 u_{int}^3(r, z) + O(\varepsilon^4) & \text{in } \Omega_{int}^\varepsilon, \\ u_{ext}(r, z) = u_{ext}^0(r, z) + \varepsilon^2 u_{ext}^2(r, z) + \varepsilon^3 u_{ext}^3(r, z) + O(\varepsilon^4) & \text{in } \Omega_{ext}^\varepsilon, \\ U(R, z) = \varepsilon^2 \varphi_0^2(z) + \varepsilon^3 \varphi_0^3(z) + O(\varepsilon^4) & \text{in } \left(-\frac{1}{2}, \frac{1}{2}\right) \times (0, z_0), \end{cases}$$

where functions u^0 , u^2 , u^3 , φ_0^2 , and φ_0^3 are defined by Equations (1.69), (1.72), (1.74), (1.71), and (1.73) respectively. For $k \in \mathbb{N}$, the solution U^k to Equation (1.66) has the following form

$$U^k(R, z) = \begin{cases} 0 & \text{if } k = 0, 1, \\ \varphi_0^k(z) & \text{if } k = 2, 3, \\ \sum_{j=0}^{k-2} \varphi_j^k(z) R^j & \text{if } k \geq 4, \end{cases}$$

Proof. We conduct the proof by induction on k . For $k = 0, 1, 2, 3$, we have already calculated the expressions of u^k and U^k in the previous section. Now let us assume that for any number $i \in \mathbb{N}$, such that $i < k$, function U^i has the form

$$U^i(R, z) = \varphi_{i-2}^i(z) R^{i-2} + \varphi_{i-3}^i(z) R^{i-3} + \dots + \varphi_1^i(z) R + \varphi_0^i(z),$$

We begin by considering Problem (1.66) for U^k . Solving this problem we obtain a solution of the form

$$U^k(R, z) = \varphi_{k-2}^k(z) R^{k-2} + \varphi_{k-3}^k(z) R^{k-3} + \dots + \varphi_1^k(z) R + \varphi_0^k(z),$$

In the above expression of U^k we find function V^k , defined as

$$V^k(R, z) = \varphi_{k-2}^k(z) R^{k-2} + \varphi_{k-3}^k(z) R^{k-3} + \dots + \varphi_1^k(z) R$$

at the first step of the algorithm.

□

1.6.3 First class of ITCs: equivalent models

Now that we know the expressions for the first terms of the expansion, we truncate the series and we identify a simpler problem satisfied by

$$u^{(k)} = u^0 + \varepsilon u^1 + \dots + \varepsilon^k u^k \quad \text{in} \quad \Omega_{\text{int}}^\varepsilon \cup \Omega_{\text{ext}}^\varepsilon$$

up to a residual term of order ε^{k+1} . We neglect the residual term of order ε^{k+1} to obtain an approximate model satisfied by function $u^{[k]}$. We formally derive three approximate models of second, third, and fourth order respectively.

Second-order model

For deriving the model of order two, we truncate the series from the second term and we define $u^{(1)}$ as

$$u^{(1)} = u^0 + \varepsilon u^1 = u^0 \quad \text{in} \quad \Omega_{\text{int}}^\varepsilon \cup \Omega_{\text{ext}}^\varepsilon \quad (\text{see Proposition 3}).$$

From (1.69), we deduce that $u^{(1)}$ solves the following uncoupled problem

$$\begin{cases} \sigma_{\text{int}} \frac{1}{r} \partial_r (r \partial_r u_{\text{int}}^{(1)}) + \sigma_{\text{int}} \partial_z^2 u_{\text{int}}^{(1)} = f_{\text{int}} & \text{in} \quad \Omega_{\text{int}}^\varepsilon, \\ u_{\text{int}}^{(1)} = 0 & \text{on} \quad \partial\Omega_{\text{int}}^\varepsilon - \Gamma_0, \\ \partial_r u_{\text{int}}^{(1)} = 0 & \text{on} \quad \Gamma_0, \end{cases} \quad (1.75)$$

$$\begin{cases} \sigma_{\text{ext}} \frac{1}{r} \partial_r (r \partial_r u_{\text{ext}}^{(1)}) + \sigma_{\text{ext}} \partial_z^2 u_{\text{ext}}^{(1)} = f_{\text{ext}} & \text{in} \quad \Omega_{\text{ext}}^\varepsilon, \\ u_{\text{ext}}^{(1)} = 0 & \text{on} \quad \partial\Omega_{\text{ext}}^\varepsilon. \end{cases}$$

In this case, we have $u^{[1]} = u^{(1)}$ as $u^{(1)}$ does not depend on ε . We infer a second-order model satisfied by $u^{[1]}$ solution to Problem (1.75).

Third-Order model

For deriving the model of order three, we truncate the series from the third term and we define $u^{(2)}$ as

$$u^{(2)} = u^0 + \varepsilon u^1 + \varepsilon^2 u^2 = u^0 + \varepsilon^2 u^2 \quad \text{in} \quad \Omega_{\text{int}}^\varepsilon \cup \Omega_{\text{ext}}^\varepsilon \quad (\text{see Proposition 3}).$$

From (1.69), (1.70), and (1.72) we deduce that $u^{(2)}$ satisfies the following equations

$$\left\{ \begin{array}{ll} \sigma_{\text{int}} \frac{1}{r} \partial_r (r \partial_r u_{\text{int}}^{(2)}) + \sigma_{\text{int}} \partial_z^2 u_{\text{int}}^{(2)} = f_{\text{int}} & \text{in } \Omega_{\text{int}}^\varepsilon, \\ \sigma_{\text{ext}} \frac{1}{r} \partial_r (r \partial_r u_{\text{ext}}^{(2)}) + \sigma_{\text{ext}} \partial_z^2 u_{\text{ext}}^{(2)} = f_{\text{ext}} & \text{in } \Omega_{\text{ext}}^\varepsilon, \\ [u^{(2)}]_{\Gamma^\varepsilon} = 0, \\ \frac{d^2}{dz^2} \{u^{(2)}\}_{\Gamma^\varepsilon} = -\varepsilon^2 \frac{1}{\widehat{\sigma}_0} [\sigma \partial_r u^0]_{\Gamma^\varepsilon} \\ u^{(2)} = 0 & \text{on } \partial\Omega \cap \partial\Omega^\varepsilon - \Gamma_0, \\ \partial_r u^{(2)} = 0 & \text{on } \Gamma_0. \end{array} \right.$$

Following the same procedure as in Section 1.3.2 we obtain the following third-order asymptotic model for $u^{[2]}$

$$\left\{ \begin{array}{ll} \sigma_{\text{int}} \frac{1}{r} \partial_r (r \partial_r u_{\text{int}}^{[2]}) + \sigma_{\text{int}} \partial_z^2 u_{\text{int}}^{[2]} = f_{\text{int}} & \text{in } \Omega_{\text{int}}^\varepsilon, \\ \sigma_{\text{ext}} \frac{1}{r} \partial_r (r \partial_r u_{\text{ext}}^{[2]}) + \sigma_{\text{ext}} \partial_z^2 u_{\text{ext}}^{[2]} = f_{\text{ext}} & \text{in } \Omega_{\text{ext}}^\varepsilon, \\ [u^{[2]}]_{\Gamma^\varepsilon} = 0, \\ \frac{d^2}{dz^2} \{u^{[2]}\}_{\Gamma^\varepsilon} + \varepsilon^2 \frac{1}{\widehat{\sigma}_0} [\sigma \partial_r u^{[2]}]_{\Gamma^\varepsilon} = 0, \\ u^{[2]} = 0 & \text{on } \partial\Omega \cap \partial\Omega^\varepsilon - \Gamma_0, \\ \partial_r u^{[2]} = 0 & \text{on } \Gamma_0. \end{array} \right. \quad (1.76)$$

Fourth-order model

For deriving the model of order four, we truncate the series from the fourth term and we define $u^{(3)}$ as

$$u^{(3)} = u^0 + \varepsilon u^1 + \varepsilon^2 u^2 + \varepsilon^3 u^3 = u^0 + \varepsilon^2 u^2 + \varepsilon^3 u^3 \quad \text{in } \Omega_{\text{int}}^\varepsilon \cup \Omega_{\text{ext}}^\varepsilon \quad (\text{see Proposition 3}).$$

From (1.69), (1.70), (1.72), and (1.74), we deduce that $u^{(3)}$ satisfies the following equations

$$\left\{ \begin{array}{ll} \sigma_{\text{int}} \frac{1}{r} \partial_r (r \partial_r u_{\text{int}}^{[3]}) + \sigma_{\text{int}} \partial_z^2 u_{\text{int}}^{[3]} = f_{\text{int}} & \text{in } \Omega_{\text{int}}^\varepsilon, \\ \sigma_{\text{ext}} \frac{1}{r} \partial_r (r \partial_r u_{\text{ext}}^{[3]}) + \sigma_{\text{ext}} \partial_z^2 u_{\text{ext}}^{[3]} = f_{\text{ext}} & \text{in } \Omega_{\text{ext}}^\varepsilon, \\ [u^{(3)}]_{\Gamma^\varepsilon} = 0, \\ \frac{d^2}{dz^2} \{u^{(3)}\}_{\Gamma^\varepsilon} = g, \\ u^{(3)} = 0 & \text{on } \partial\Omega \cap \partial\Omega^\varepsilon - \Gamma_0, \\ \partial_r u^{(3)} = 0 & \text{on } \Gamma_0, \end{array} \right.$$

where

$$g = -\varepsilon^2 \frac{1}{\widehat{\sigma}_0} [\sigma \partial_r u^0]_{\Gamma^\varepsilon} - \varepsilon^3 \frac{1}{\widehat{\sigma}_0} [\sigma \partial_r u^1]_{\Gamma^\varepsilon} - \varepsilon^3 \frac{1}{\widehat{\sigma}_0 r_0} \{\sigma \partial_r u^0\}_{\Gamma^\varepsilon}.$$

Following the same procedure as in Section 1.3.2 we obtain the following fourth-order asymptotic model for $u^{[3]}$

$$\left\{ \begin{array}{ll} \sigma_{\text{int}} \frac{1}{r} \partial_r (r \partial_r u_{\text{int}}^{[3]}) + \sigma_{\text{int}} \partial_z^2 u_{\text{int}}^{[3]} = f_{\text{int}} & \text{in } \Omega_{\text{int}}^\varepsilon, \\ \sigma_{\text{ext}} \frac{1}{r} \partial_r (r \partial_r u_{\text{ext}}^{[3]}) + \sigma_{\text{ext}} \partial_z^2 u_{\text{ext}}^{[3]} = f_{\text{ext}} & \text{in } \Omega_{\text{ext}}^\varepsilon, \\ [u^{[3]}]_{\Gamma^\varepsilon} = 0, \\ \varepsilon^2 \frac{1}{\widehat{\sigma}_0} [\sigma \partial_r u^{[3]}]_{\Gamma^\varepsilon} + \varepsilon^3 \frac{1}{\widehat{\sigma}_0 r_0} \{\sigma \partial_r u^{[3]}\}_{\Gamma^\varepsilon} = -\frac{d^2}{dz^2} \{u^{[3]}\}_{\Gamma^\varepsilon} \\ u^{[3]} = 0 & \text{on } \partial\Omega \cap \partial\Omega^\varepsilon - \Gamma_0, \\ \partial_r u^{[3]} = 0 & \text{on } \Gamma_0. \end{array} \right. \quad (1.77)$$

1.6.4 Second class of ITCs: construction of a multiscale expansion

In this section we expand the solution in power series of ε . Then, by truncating this series and neglecting higher order terms in ε , we derive approximate models

coupled with equivalent transmission conditions across interface Γ . Since we use the same procedure as in the previous sections, we will concentrate on presenting the obtained results, regarding the multiscale expansion and the derivation of the asymptotic models. The domain where the approximate models are defined is depicted at Figure 1.5. For deriving the equivalent models, we first use an *Ansatz* in the form of power series of ε for the solution to problems (1.59) and (1.60). We look for solutions

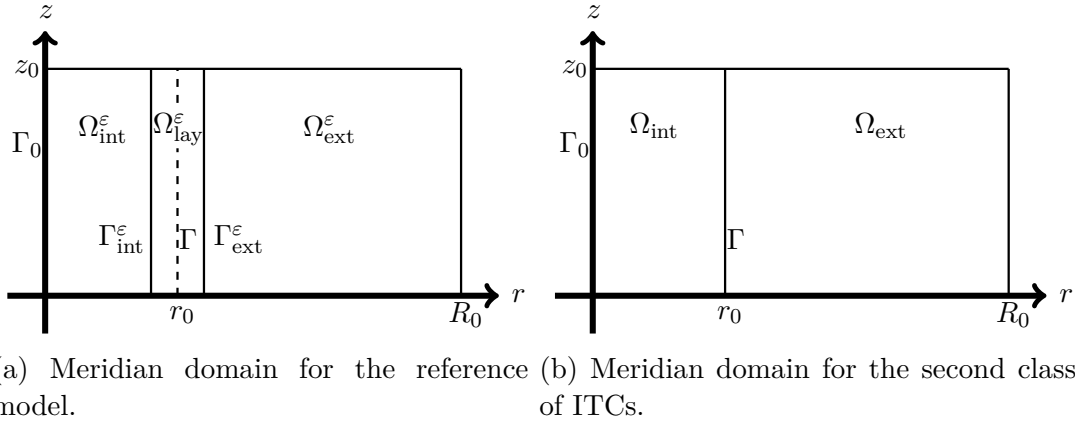


Figure 1.5: Meridian domains for the reference model and the second class of asymptotic models.

$$\begin{cases} u_{\text{int}}(r, z) \approx \sum_{k \geq 0} \varepsilon^k u_{\text{int}}^k(r, z) & \text{in } \Omega_{\text{int}}^\varepsilon, \\ u_{\text{ext}}(r, z) \approx \sum_{k \geq 0} \varepsilon^k u_{\text{ext}}^k(r, z) & \text{in } \Omega_{\text{ext}}^\varepsilon, \\ U(R, z) \approx \sum_{k \geq 0} \varepsilon^k U^k(R, z) & \text{in } \left(-\frac{1}{2}, \frac{1}{2}\right) \times (0, z_0). \end{cases} \quad (1.78)$$

where functions $(u_{\text{int}}^k)_{k \in \mathbb{N}}$ and $(u_{\text{ext}}^k)_{k \in \mathbb{N}}$ are now defined in ε -independent domains, contrary to the first approach. We emphasize that the sequence $(u_{\text{int}}^k)_{k \in \mathbb{N}}$ (respectively $(u_{\text{ext}}^k)_{k \in \mathbb{N}}$) is defined in Ω_{int} (respectively Ω_{ext}) even if its associated series does not approach u in the thin layer. We assume that for $k \in \mathbb{N}$, the terms u_{int}^k and u_{ext}^k are as regular as necessary, we refer to [19] which provides some regularity results. Then, we conduct a formal Taylor series expansion of the terms $u_{\text{int}}^k|_{\Gamma_{\text{int}}^\varepsilon}$ and $u_{\text{ext}}^k|_{\Gamma_{\text{ext}}^\varepsilon}$ of the series, in order to write the transmission conditions across interface Γ . We perform the formal Taylor series expansion in the same way as formerly done

in Section 1.4.1. Substituting this *Ansatz* and the formal Taylor series expansions into the Equations (1.59) and (1.60), and grouping the terms with the same powers in ε together, for every $k \in \mathbb{N}$ we obtain the following set of equations

$$\left\{ \begin{array}{ll} \sigma_{\text{int}} \frac{1}{r} \partial_r (r \partial_r u_{\text{int}}^k) + \sigma_{\text{int}} \partial_z^2 u_{\text{int}}^k = f_{\text{int}} \delta_k^0 & \text{in } \Omega_{\text{int}}, \\ \sigma_{\text{ext}} \frac{1}{r} \partial_r (r \partial_r u_{\text{ext}}^k) + \sigma_{\text{ext}} \partial_z^2 u_{\text{ext}}^k = f_{\text{ext}} \delta_k^0 & \text{in } \Omega_{\text{ext}}, \\ \partial_R^2 U^k + \sum_{i=0}^{k-1} \frac{(-R)^{k-i-1}}{r_0^{k-i}} \partial_R U^i + \partial_z^2 U^{k-2} = 0 & \text{in } \left(-\frac{1}{2}, \frac{1}{2}\right) \times (0, z_0), \end{array} \right. \quad (1.79)$$

along with the following transmission conditions

$$\left\{ \begin{array}{ll} \sum_{i=0}^k \frac{(-1)^i}{2^i i!} \partial_r^i u_{\text{int}}^{k-i}(r_0, z) = U^k \left(-\frac{1}{2}, z\right) & z \in (0, z_0), \\ \sum_{i=0}^k \frac{1}{2^i i!} \partial_r^i u_{\text{ext}}^{k-i}(r_0, z) = U^k \left(\frac{1}{2}, z\right) & z \in (0, z_0), \\ \sigma_{\text{int}} \sum_{i=0}^{k-4} \frac{(-1)^i}{2^i i!} \partial_r^{i+1} u_{\text{int}}^{k-i-4}(r_0, z) = \hat{\sigma}_0 \partial_R U^k \left(-\frac{1}{2}, z\right) & z \in (0, z_0), \\ \sigma_{\text{ext}} \sum_{i=0}^{k-4} \frac{1}{2^i i!} \partial_r^{i+1} u_{\text{ext}}^{k-i-4}(r_0, z) = \hat{\sigma}_0 \partial_R U^k \left(\frac{1}{2}, z\right) & z \in (0, z_0), \end{array} \right. \quad (1.80)$$

and the following boundary conditions

$$\left\{ \begin{array}{ll} \partial_r u_{\text{int}}^k(0, z) = u_{\text{ext}}^k(R_0, z) = 0 & z \in (0, z_0), \\ u^k(r, 0) = u^k(r, z_0) = 0 & r \in \left(0, r_0 - \frac{\varepsilon}{2}\right) \cup \left(r_0 + \frac{\varepsilon}{2}, R_0\right), \\ U^k(R, 0) = U^k(R, z_0) = 0 & R \in \left(-\frac{1}{2}, \frac{1}{2}\right). \end{array} \right. \quad (1.81)$$

Employing these equations ((1.79) - (1.81)), we determine the elementary problems satisfied outside and inside the layer for any $k \in \mathbb{N}$.

Proposition 4. *Following the same procedure as for the first class, we deduce that*

$U^0 \equiv U^1 \equiv 0$. Thus, the asymptotic expansion (1.78), has the following form

$$\begin{cases} u_{int}(r, z) = u_{int}^0(r, z) + \varepsilon u_{int}^1(r, z) + O(\varepsilon^2) & \text{in } \Omega_{int}^\varepsilon, \\ u_{ext}(r, z) = u_{int}^0(r, z) + \varepsilon u_{ext}^1(r, z) + O(\varepsilon^2) & \text{in } \Omega_{ext}^\varepsilon, \\ U(R, z) = O(\varepsilon^2) & \text{in } \left(-\frac{1}{2}, \frac{1}{2}\right) \times (0, z_0). \end{cases}$$

where the functions u^0 and u^1 satisfy the following problems

$$\begin{cases} \sigma_{int} \Delta u_{int}^0 = f_{int} & \text{in } \Omega_{int}, \\ u_{int}^0 = 0 & \text{on } \partial\Omega_{int} - \Gamma_0, \\ \partial_r u_{int}^0 = 0 & \text{on } \Gamma_0, \\ \sigma_{ext} \Delta u_{ext}^0 = f_{ext} & \text{in } \Omega_{ext}, \\ u_{ext}^0 = 0 & \text{on } \partial\Omega_{ext}, \end{cases} \quad (1.82)$$

and

$$\begin{cases} \sigma_{int} \Delta u_{int}^1 = f_{int} & \text{in } \Omega_{int}, \\ u_{int}^1 = \frac{1}{2} \partial_n u_{int}^1 & \text{on } \Gamma \\ u_{int}^1 = 0 & \text{on } \partial\Omega_{int} \cap \partial\Omega - \Gamma_0, \\ \partial_r u_{int}^1 = 0 & \text{on } \Gamma_0, \\ \sigma_{ext} \Delta u_{ext}^1 = f_{ext} & \text{in } \Omega_{ext}, \\ u_{ext}^1 = -\frac{1}{2} \partial_n u_{ext}^1 & \text{on } \Gamma \\ u_{ext}^1 = 0 & \text{on } \partial\Omega_{ext} \cap \partial\Omega. \end{cases} \quad (1.83)$$

1.6.5 Second class of ITCs: equivalent models

Once we know the expressions for the first terms of the expansion, we truncate the series and we identify a simpler problem satisfied by

$$u^{(k)} = u^0 + \varepsilon u^1 + \dots + \varepsilon^k u^k \quad \text{in } \Omega_{int} \cup \Omega_{ext}$$

up to a residual term of order ε^{k+1} . We neglect the residual term of order ε^{k+1} to obtain an approximate model satisfied by function $u^{[k]}$. Here, we formally derive two approximate models of order one and order two respectively.

First-order model

$$\left\{ \begin{array}{ll} \sigma_{\text{int}} \frac{1}{r} \partial_r (r \partial_r u_{\text{int}}^{[0]}) + \sigma_{\text{int}} \partial_z^2 u_{\text{int}}^{[0]} = f_{\text{int}} & \text{in } \Omega_{\text{int}}, \\ u_{\text{int}}^{[0]} = 0 & \text{on } \partial\Omega_{\text{int}} - \Gamma_0, \\ \partial_n u_{\text{int}}^{[0]} = 0 & \text{on } \Gamma_0, \end{array} \right. \quad (1.84)$$

$$\left\{ \begin{array}{ll} \sigma_{\text{ext}} \frac{1}{r} \partial_r (r \partial_r u_{\text{ext}}^{[0]}) + \sigma_{\text{ext}} \partial_z^2 u_{\text{ext}}^{[0]} = f_{\text{ext}} & \text{in } \Omega_{\text{ext}}, \\ u_{\text{ext}}^{[0]} = 0 & \text{on } \partial\Omega_{\text{ext}}. \end{array} \right.$$

Second-order model

$$\left\{ \begin{array}{ll} \sigma_{\text{int}} \frac{1}{r} \partial_r (r \partial_r u_{\text{int}}^{[1]}) + \sigma_{\text{int}} \partial_z^2 u_{\text{int}}^{[1]} = f_{\text{int}} & \text{in } \Omega_{\text{int}}, \\ u_{\text{int}}^{[1]} = \frac{\varepsilon}{2} \partial_r u_{\text{int}}^{[1]} & \text{on } \Gamma, \\ u_{\text{int}}^{[1]} = 0 & \text{on } \partial\Omega \cap \partial\Omega_{\text{int}} - \Gamma_0, \\ \partial_r u_{\text{int}}^{[1]} = 0 & \text{on } \Gamma_0, \end{array} \right. \quad (1.85)$$

$$\left\{ \begin{array}{ll} \sigma_{\text{ext}} \frac{1}{r} \partial_r (r \partial_r u_{\text{ext}}^{[1]}) + \sigma_{\text{ext}} \partial_z^2 u_{\text{ext}}^{[1]} = f_{\text{ext}} & \text{in } \Omega_{\text{ext}}, \\ u_{\text{ext}}^{[1]} = -\frac{\varepsilon}{2} \partial_r u_{\text{ext}}^{[1]} & \text{on } \Gamma, \\ u_{\text{ext}}^{[1]} = 0 & \text{on } \partial\Omega \cap \partial\Omega_{\text{ext}}. \end{array} \right.$$

DERIVATION OF ITCS WITH MIXED EXTERNAL BOUNDARY CONDITIONS

2.1 Introduction

This chapter is devoted to the derivation of asymptotic models in a configuration similar to the one considered in Chapter 1. The framework is the one that has been explained in Section 1.1. We consider the equations for the static electric potential (1.2) set in the domain described in Figure 1.1. The main difference with the previous chapter is that now we will consider mixed boundary conditions. We consider homogeneous Dirichlet boundary conditions in some parts of the boundary and homogeneous Neumann boundary conditions in the rest of the boundary. To clarify, the boundary conditions are set as follows

$$\begin{cases} u = 0 & \text{on } \Gamma_D, \\ \partial_n u = 0 & \text{on } \Gamma_N, \end{cases}$$

where the boundaries Γ_D and Γ_N are defined by

$$\begin{cases} \Gamma_D = \{(0, y) : y \in (0, y_0)\} \cup \{(L, y) : y \in (0, y_0)\}, \\ \Gamma_N = \{(x, 0) : x \in (0, L)\} \cup \{(x, y_0) : x \in (0, L)\}. \end{cases}$$

These boundary conditions are more realistic towards the application we will consider in the following chapters. The process of derivation of the asymptotic models differs from the previous one (Chapter 1) because of this change in the boundary conditions, and also do the resulting asymptotic models. The first steps of the process are very similar to the ones described in Chapter 1, so we refer the reader to sections 1.1 and 1.2 for more details concerning these steps and we will directly explain the remaining steps, which are original.

2.2 Static 2D configuration: first class of ITCs

2.2.1 Construction of a multiscale expansion

In order to derive an asymptotic expansion, we begin by performing an *Ansatz* in the form of power series of ε for functions u_{int} , u_{ext} , and U in the same way we have done in (1.4).

$$\left\{ \begin{array}{ll} u_{\text{int}}(x, y) \approx \sum_{k \geq 0} \varepsilon^k u_{\text{int}}^k(x, y) & \text{in } \Omega_{\text{int}}^\varepsilon, \end{array} \right. \quad (2.1a)$$

$$\left\{ \begin{array}{ll} u_{\text{ext}}(x, y) \approx \sum_{k \geq 0} \varepsilon^k u_{\text{ext}}^k(x, y) & \text{in } \Omega_{\text{ext}}^\varepsilon, \end{array} \right. \quad (2.1b)$$

$$\left\{ \begin{array}{ll} U(X, y) \approx \sum_{k \geq 0} \varepsilon^k U^k(X, y) & \text{in } \left(-\frac{1}{2}, \frac{1}{2}\right) \times (0, y_0). \end{array} \right. \quad (2.1c)$$

Equations for the coefficients of the electric potential

Substituting the expansions (2.1) into the Equations (1.3) and collecting the terms with the same powers in ε , for every $k \in \mathbb{N}$ we obtain the following set of equations

$$\left\{ \begin{array}{ll} \sigma_{\text{int}} \Delta u_{\text{int}}^k(x, y) = f_{\text{int}}(x, y) \delta_0^k & \text{in } \Omega_{\text{ext}}^\varepsilon, \end{array} \right. \quad (2.2a)$$

$$\left\{ \begin{array}{ll} \sigma_{\text{ext}} \Delta u_{\text{ext}}^k(x, y) = f_{\text{ext}}(x, y) \delta_0^k & \text{in } \Omega_{\text{ext}}^\varepsilon, \end{array} \right. \quad (2.2b)$$

$$\left\{ \begin{array}{ll} \partial_X^2 U^k(X, y) = -\partial_y^2 U^{k-2}(X, y) & \text{in } \left(-\frac{1}{2}, \frac{1}{2}\right) \times (0, y_0), \end{array} \right. \quad (2.2c)$$

along with the following transmission conditions

$$\left\{ \begin{array}{ll} U^k \left(-\frac{1}{2}, y \right) = u_{\text{int}}^k \left(x_0 - \frac{\varepsilon}{2}, y \right) & y \in (0, y_0), \quad (2.3a) \\ U^k \left(\frac{1}{2}, y \right) = u_{\text{ext}}^k \left(x_0 + \frac{\varepsilon}{2}, y \right) & y \in (0, y_0), \quad (2.3b) \\ \hat{\sigma}_0 \partial_X U^k \left(-\frac{1}{2}, y \right) = \sigma_{\text{int}} \partial_n u_{\text{int}}^{k-4} \left(x_0 - \frac{\varepsilon}{2}, y \right) & y \in (0, y_0), \quad (2.3c) \\ \hat{\sigma}_0 \partial_X U^k \left(\frac{1}{2}, y \right) = \sigma_{\text{ext}} \partial_n u_{\text{ext}}^{k-4} \left(x_0 + \frac{\varepsilon}{2}, y \right) & y \in (0, y_0), \quad (2.3d) \end{array} \right.$$

and the following boundary conditions

$$\left\{ \begin{array}{ll} u^k(0, y) = u^k(L, y) = 0 & y \in (0, y_0), \quad (2.4a) \\ \partial_n u^k(x, 0) = \partial_n u^k(x, y_0) = 0 & x \in \left(0, x_0 - \frac{\varepsilon}{2} \right) \cup \left(x_0 + \frac{\varepsilon}{2}, L \right), \quad (2.4b) \\ \partial_X U^k(X, 0) = \partial_X U^k(X, y_0) = 0 & X \in \left(-\frac{1}{2}, \frac{1}{2} \right), \quad (2.4c) \end{array} \right.$$

where δ_0^k still represents the Kronecker symbol. For determining the elemental problems satisfied by each of the terms of the expansion, we will also need a compatibility condition. To obtain it we apply the fundamental theorem of calculus for a smooth function U^k , along with the Equations (2.2c), (2.3c), and (2.3d), and we obtain

$$- \int_{-\frac{1}{2}}^{\frac{1}{2}} \partial_y^2 U^{k-2}(X, y) \, dX = \frac{1}{\hat{\sigma}_0} \left[\sigma \partial_n u^{k-4} \right]_{\Gamma^\varepsilon}(y). \quad (2.5)$$

We adopt the convention that the terms with negative indices in Equations (2.2) - (2.5) are equal to 0. Employing Equations (2.2) - (2.5) we deduce the elementary problems satisfied outside and inside the layer for any $k \in \mathbb{N}$. For that purpose, we employ the following algorithm composed of four steps.

Algorithm for the determination of the coefficients

Initialization of the algorithm:

Before showing the steps for the general algorithm for any k , we have to determine U^0 up to a constant λ_0 . For that purpose we consider Equations (2.2c),

(2.3c), and (2.3d), and we end up with the following differential problem in the variable X for U^0 , where the variable y plays the role of a parameter,

$$\left\{ \begin{array}{l} \partial_X^2 U^0(X, y) = 0 \quad X \in \left(\frac{-1}{2}, \frac{1}{2} \right), \\ \partial_X U^0 \left(-\frac{1}{2}, y \right) = 0, \\ \partial_X U^0 \left(\frac{1}{2}, y \right) = 0. \end{array} \right.$$

We deduce that the solution to this equation has the form $U^0(X, y) = \varphi_0^0(y)$. Then, we employ the compatibility condition (2.5) (at rank $k = 2$), along with Equation (2.4c) to obtain the following differential problem in the variable y for function φ_0^0 , related to U^0

$$\left\{ \begin{array}{l} \frac{d^2}{dy^2} \varphi_0^0(y) = 0 \quad y \in (0, y_0), \\ \frac{d}{dy} \varphi_0^0(0) = 0, \\ \frac{d}{dy} \varphi_0^0(y_0) = 0. \end{array} \right.$$

We deduce that φ_0^0 has the form $\varphi_0^0(y) = \lambda_0$ and thus, $U^0(X, y) = \lambda_0$, where constant λ_0 has yet to be determined and we will do it at the first step of the algorithm. After these preliminary steps, we can search to determine U^k and u^k for any even k .

We assume that the first terms of the expansion (2.1) up to the order ε^{k-1} have already been calculated, and we obtain the equations for the k -th term. In the same way as for the Dirichlet case, u^k and U^k will vanish for odd values of k , so we will only concentrate on determining them for even values of k .

The algorithm is divided in four steps. The first step consist in determining U^{k+2} at the rank $k + 2$ up to a function in the variable y , denoted by φ_0^{k+2} . The second step is plainly different from what we set for the Dirichlet case, it consists in determining a constant λ_k for fully determining the expression of U^k at the rank k . This constant was not involved in the Dirichlet case. The third step consists in determining u_{int}^k and u_{ext}^k , and finally the fourth step consists in determining the expression of U^{k+2} up to a constant λ_{k+2} , which will be calculated at the second step of the following rank. For every rank $k = 0, 1, 2, \dots$, we perform the following steps:

First step:

When the rank k of the algorithm begins, we already know function U^k has the following form

$$U^k(X, y) = V^k(X, y) + \widetilde{\varphi}_0^k(y) + \lambda_k,$$

where the only term we have not determined at this point is constant λ_k . We begin by selecting Equations (2.2c), (2.3c), and (2.3d), and we build the following differential problem in the variable X for U^{k+2} (the variable y plays the role of a parameter)

$$\left\{ \begin{array}{l} \partial_X^2 U^{k+2}(X, y) = -\partial_y^2 U^k(X, y) \quad X \in \left(-\frac{1}{2}, \frac{1}{2}\right), \\ \widehat{\sigma}_0 \partial_X U^{k+2} \left(-\frac{1}{2}, y\right) = \sigma_{\text{int}} \partial_n u_{\text{int}}^{k-2} \left(x_0 - \frac{\varepsilon}{2}, y\right), \\ \widehat{\sigma}_0 \partial_X U^{k+2} \left(\frac{1}{2}, y\right) = \sigma_{\text{ext}} \partial_n u_{\text{ext}}^{k-2} \left(x_0 + \frac{\varepsilon}{2}, y\right). \end{array} \right. \quad (2.6)$$

There exists a solution U^{k+2} of (2.6) provided the compatibility condition (2.5) is satisfied. We deduce the expression of U^{k+2} up to a function in the variable y , denoted by φ_0^{k+2} . The function U^{k+2} has the following form

$$U^{k+2}(X, y) = V^{k+2}(X, y) + \varphi_0^{k+2}(y),$$

where V^{k+2} represents the part of U^k that is determined at this step and has the form (see Proposition 5)

$$V^{k+2}(X, y) = \begin{cases} 0 & \text{if } k = 0, \\ \varphi_k^k(y)X^k + \varphi_{k-1}^k(y)X^{k-1} + \dots + \varphi_1^k(y)X & \text{if } k > 0. \end{cases}$$

Function φ_0^{k+2} represents the part of U^k that is determined at the following steps.

Second step:

We use the compatibility condition (2.5) (at rank $k+4$), along with Equation (2.4c) to write the following differential problem in the variable y for function φ_0^{k+2} , involved in the expression of U^{k+2} .

$$\left\{ \begin{array}{l} \frac{d^2}{dy^2} \varphi_0^{k+2}(y) = -\frac{1}{\widehat{\sigma}_0} [\sigma \partial_n u^k]_{\Gamma^\varepsilon}(y) - \int_{-\frac{1}{2}}^{\frac{1}{2}} \partial_y^2 V^{k+2}(X, y) dX \quad y \in (0, y_0), \\ \frac{d}{dy} \varphi_0^{k+2}(0) = 0, \\ \frac{d}{dy} \varphi_0^{k+2}(y_0) = 0. \end{array} \right. \quad (2.7)$$

Integrating the volumic Equation (2.7) from 0 to y_0 and applying the boundary conditions we obtain a compatibility condition for u^k of the following form

$$-\int_0^{y_0} \frac{1}{\widehat{\sigma}_0} [\sigma \partial_n u^k]_{\Gamma^\varepsilon}(y) dy = \int_0^{y_0} \int_{-\frac{1}{2}}^{\frac{1}{2}} \partial_y^2 V^{k+2}(X, y) dX dy. \quad (2.8)$$

For the sake of simplicity we introduce the following notation

$$C_k = \int_0^{y_0} \int_{-\frac{1}{2}}^{\frac{1}{2}} \partial_y^2 V^{k+2}(X, y) dX dy. \quad (2.9)$$

We employ Equations (2.3a) and (2.3b) for determining the values of u^k at $\Gamma_{\text{int}}^\varepsilon$ and $\Gamma_{\text{ext}}^\varepsilon$. We have

$$\begin{cases} u_{\text{int}}^k = U^k & \text{on } \Gamma_{\text{int}}^\varepsilon, \\ u_{\text{ext}}^k = U^k & \text{on } \Gamma_{\text{ext}}^\varepsilon, \end{cases} \quad (2.10)$$

where $U^k = V^k + \widetilde{\varphi}_0^k + \lambda_k$. We derive u^k by performing a decomposition into two different functions in the following way. We consider

$$u^k = \widetilde{u}^k + \lambda_k \bar{u}, \quad (2.11)$$

where \widetilde{u}^k satisfies the problem

$$\begin{cases} \sigma_{\text{int}} \Delta \widetilde{u}_{\text{int}}^k = f_{\text{int}} \delta_0^k & \text{in } \Omega_{\text{int}}^\varepsilon, \\ \widetilde{u}_{\text{int}}^k = V^k + \widetilde{\varphi}_0^k & \text{on } \Gamma_{\text{int}}^\varepsilon, \\ \widetilde{u}_{\text{int}}^k = 0 & \text{on } \partial \Omega_{\text{int}}^\varepsilon \cap \Gamma_D, \\ \partial_n \widetilde{u}_{\text{int}}^k = 0 & \text{on } \partial \Omega_{\text{int}}^\varepsilon \cap \Gamma_N, \\ \sigma_{\text{ext}} \Delta \widetilde{u}_{\text{ext}}^k = f_{\text{ext}} \delta_0^k & \text{in } \Omega_{\text{ext}}^\varepsilon, \\ \widetilde{u}_{\text{ext}}^k = V^k + \widetilde{\varphi}_0^k & \text{on } \Gamma_{\text{ext}}^\varepsilon, \\ \widetilde{u}_{\text{ext}}^k = 0 & \text{on } \partial \Omega_{\text{ext}}^\varepsilon \cap \Gamma_D, \\ \partial_n \widetilde{u}_{\text{ext}}^k = 0 & \text{on } \partial \Omega_{\text{ext}}^\varepsilon \cap \Gamma_N, \end{cases} \quad (2.12)$$

and \bar{u} satisfies the problem

$$\left\{ \begin{array}{ll} \Delta \bar{u}_{\text{int}} = 0 & \text{in } \Omega_{\text{int}}^\varepsilon, \\ \bar{u}_{\text{int}} = 1 & \text{on } \Gamma_{\text{int}}^\varepsilon, \\ \bar{u}_{\text{int}} = 0 & \text{on } \partial\Omega_{\text{int}}^\varepsilon \cap \Gamma_D, \\ \partial_n \bar{u}_{\text{int}} = 0 & \text{on } \partial\Omega_{\text{int}}^\varepsilon \cap \Gamma_N, \end{array} \right. \quad (2.13)$$

$$\left\{ \begin{array}{ll} \Delta \bar{u}_{\text{ext}} = 0 & \text{in } \Omega_{\text{ext}}^\varepsilon, \\ \bar{u}_{\text{ext}} = 1 & \text{on } \Gamma_{\text{ext}}^\varepsilon, \\ \bar{u}_{\text{ext}} = 0 & \text{on } \partial\Omega_{\text{ext}}^\varepsilon \cap \Gamma_D, \\ \partial_n \bar{u}_{\text{ext}} = 0 & \text{on } \partial\Omega_{\text{ext}}^\varepsilon \cap \Gamma_N, \end{array} \right.$$

Then, we choose constant λ_k such that the condition (2.8) is satisfied, which yields the following expression

$$\lambda_k = \frac{C_k - \int_0^{y_0} \frac{1}{\widehat{\sigma}_0} [\sigma \partial_n \tilde{u}^k]_{\Gamma^\varepsilon}(y) dy}{\int_0^{y_0} \frac{1}{\widehat{\sigma}_0} [\sigma \partial_n \bar{u}]_{\Gamma^\varepsilon}(y) dy}. \quad (2.14)$$

It is not difficult to derive an analytical solution for \bar{u} , which has the form

$$\bar{u}(x, y) = \begin{cases} \bar{u}_{\text{int}}(x, y) = \frac{x}{x_0 - \frac{\varepsilon}{2}} & (x, y) \in \left(0, x_0 - \frac{\varepsilon}{2}\right) \times (0, y_0), \\ \bar{u}_{\text{ext}}(x, y) = \frac{x - L}{x_0 + \frac{\varepsilon}{2} - L} & (x, y) \in \left(x_0 + \frac{\varepsilon}{2}, L\right) \times (0, y_0). \end{cases}$$

Thus, we deduce that

$$\int_0^{y_0} [\sigma \partial_n \bar{u}]_{\Gamma^\varepsilon}(y) dy \neq 0$$

and λ_k is well defined.

Third step:

We derive the equations outside the layer by employing Equations (2.2a), (2.2b), (2.3a), (2.3b), (2.4a), and (2.4b). We infer that u_{int}^k and u_{ext}^k are defined

independently in the two subdomains $\Omega_{\text{int}}^\varepsilon$ and $\Omega_{\text{ext}}^\varepsilon$.

$$\left\{ \begin{array}{ll} \sigma_{\text{int}} \Delta u_{\text{int}}^k = f_{\text{int}} \delta_0^k & \text{in } \Omega_{\text{int}}^\varepsilon, \\ u_{\text{int}}^k = U^k & \text{on } \Gamma_{\text{int}}^\varepsilon, \\ u_{\text{int}}^k = 0 & \text{on } \Gamma_D \cap \partial\Omega_{\text{int}}^\varepsilon, \\ \partial_n u_{\text{int}}^k = 0 & \text{on } \Gamma_N \cap \partial\Omega_{\text{int}}^\varepsilon, \end{array} \right. \quad (2.15)$$

$$\left\{ \begin{array}{ll} \sigma_{\text{ext}} \Delta u_{\text{ext}}^k = f_{\text{ext}} \delta_0^k & \text{in } \Omega_{\text{ext}}^\varepsilon, \\ u_{\text{ext}}^k = U^k & \text{on } \Gamma_{\text{ext}}^\varepsilon, \\ u_{\text{ext}}^k = 0 & \text{on } \Gamma_D \cap \partial\Omega_{\text{ext}}^\varepsilon, \\ \partial_n u_{\text{ext}}^k = 0 & \text{on } \Gamma_N \cap \partial\Omega_{\text{ext}}^\varepsilon. \end{array} \right.$$

Fourth step:

As we have already obtained the expression of function u^k and since condition (2.8) is satisfied, there exists a solution to (2.7), which is denoted by φ_0^{k+2} . The solution is unique up to the choice of a constant λ_{k+2} . Function φ_0^{k+2} has the form

$$\varphi_0^{k+2} = \widetilde{\varphi_0^{k+2}} + \lambda_{k+2},$$

where $\widetilde{\varphi_0^{k+2}}$ represents the part of φ_0^{k+2} that is determined at this step and constant λ_{k+2} will be calculated at the rank $k+2$ of the algorithm. Thus, we have the following expression of function U^{k+2}

$$U^{k+2}(X, y) = V^{k+2}(X, y) + \widetilde{\varphi_0^{k+2}}(y) + \lambda_{k+2},$$

which is the used in the first step of the following rank and where the only undetermined term at this point is constant λ_{k+2} .

First terms of the asymptotics

Terms of order zero

At this point we remark that thanks to the preliminary steps we performed in the initialization of the algorithm, we already know that U^0 has the following form $U^0(X, y) = \lambda_0$. We have $V^0 \equiv 0$ and $\widetilde{\varphi_0^0} \equiv 0$. At this rank, we will calculate

constant λ_0 and functions V^2 and φ_0^2 . We begin by considering Problem (2.6) for U^2

$$\begin{cases} \partial_X^2 U^2(X, y) = 0 & X \in \left(\frac{-1}{2}, \frac{1}{2}\right), \\ \partial_X U^2\left(-\frac{1}{2}, y\right) = 0, \\ \partial_X U^2\left(\frac{1}{2}, y\right) = 0. \end{cases}$$

We deduce that the solution to this equation has the form $U^2(X, y) = \varphi_0^2(y)$, and so $V^2 \equiv 0$. Then, thanks to (2.7) we get the following problem for φ_0^2

$$\begin{cases} \frac{d^2}{dy^2} \varphi_0^2(y) = -\frac{1}{\bar{\sigma}_0} [\sigma \partial_n u^0]_{\Gamma^\varepsilon} & y \in (0, y_0), \\ \frac{d}{dy} \varphi_0^2(0) = 0, \\ \frac{d}{dy} \varphi_0^2(y_0) = 0. \end{cases} \quad (2.16)$$

Integrating the first equation from 0 to y_0 and injecting the boundary conditions, we obtain condition (2.8) for u^0

$$\int_0^{y_0} [\sigma \partial_n u^0]_{\Gamma^\varepsilon}(t) dt = 0. \quad (2.17)$$

The constant (2.9) takes the value $C_0 = 0$. We employ this condition to calculate constant λ_0 , from Equation (2.10) we deduce that

$$\begin{cases} u_{\text{int}}^0 = \lambda_0 & \text{on } \Gamma_{\text{int}}^\varepsilon, \\ u_{\text{ext}}^0 = \lambda_0 & \text{on } \Gamma_{\text{ext}}^\varepsilon. \end{cases}$$

Thus, we derive u^0 by performing a decomposition (2.11) into two different functions in the following way

$$u^0 = \tilde{u}^0 + \lambda_0 \bar{u},$$

where \tilde{u}^0 satisfies the Problem (2.12)

$$\left\{ \begin{array}{ll} \sigma_{\text{int}} \Delta \tilde{u}_{\text{int}}^0 = f_{\text{int}} & \text{in } \Omega_{\text{int}}^\varepsilon, \\ \tilde{u}_{\text{int}}^0 = 0 & \text{on } \Gamma_{\text{int}}^\varepsilon, \\ \tilde{u}_{\text{int}}^0 = 0 & \text{on } \partial\Omega_{\text{int}}^\varepsilon \cap \Gamma_D, \\ \partial_n \tilde{u}_{\text{int}}^0 = 0 & \text{on } \partial\Omega_{\text{int}}^\varepsilon \cap \Gamma_N, \end{array} \right. \quad \left\{ \begin{array}{ll} \sigma_{\text{ext}} \Delta \tilde{u}_{\text{ext}}^0 = f_{\text{ext}} & \text{in } \Omega_{\text{ext}}^\varepsilon, \\ \tilde{u}_{\text{ext}}^0 = 0 & \text{on } \Gamma_{\text{ext}}^\varepsilon, \\ \tilde{u}_{\text{ext}}^0 = 0 & \text{on } \partial\Omega_{\text{ext}}^\varepsilon \cap \Gamma_D, \\ \partial_n \tilde{u}_{\text{ext}}^0 = 0 & \text{on } \partial\Omega_{\text{ext}}^\varepsilon \cap \Gamma_N, \end{array} \right.$$

and \bar{u} satisfies the Problem (2.13). Then, we choose constant λ_0 such that the condition (2.17) is satisfied, we obtain expression (2.14) for λ_0

$$\lambda_0 = - \frac{\int_0^{y_0} [\sigma \partial_n \tilde{u}^0]_{\Gamma^\varepsilon}(t) dt}{\int_0^{y_0} [\sigma \partial_n \bar{u}]_{\Gamma^\varepsilon}(t) dt}. \quad (2.18)$$

Employing (2.15), we obtain that the limit solution u^0 satisfies Dirichlet boundary conditions on $\Gamma_{\text{int}}^\varepsilon$ and $\Gamma_{\text{ext}}^\varepsilon$. The problems satisfied by u_{int}^0 and u_{ext}^0 are then

$$\left\{ \begin{array}{ll} \sigma_{\text{int}} \Delta u_{\text{int}}^0 = f_{\text{int}} & \text{in } \Omega_{\text{int}}^\varepsilon, \\ u_{\text{int}}^0 = \lambda_0 & \text{on } \Gamma_{\text{int}}^\varepsilon, \\ u_{\text{int}}^0 = 0 & \text{on } \Gamma_D \cap \partial\Omega_{\text{int}}^\varepsilon, \\ \partial_n u_{\text{int}}^0 = 0 & \text{on } \Gamma_N \cap \partial\Omega_{\text{int}}^\varepsilon, \end{array} \right. \quad \left\{ \begin{array}{ll} \sigma_{\text{ext}} \Delta u_{\text{ext}}^0 = f_{\text{ext}} & \text{in } \Omega_{\text{ext}}^\varepsilon, \\ u_{\text{ext}}^0 = \lambda_0 & \text{on } \Gamma_{\text{ext}}^\varepsilon, \\ u_{\text{ext}}^0 = 0 & \text{on } \Gamma_D \cap \partial\Omega_{\text{ext}}^\varepsilon, \\ \partial_n u_{\text{ext}}^0 = 0 & \text{on } \Gamma_N \cap \partial\Omega_{\text{ext}}^\varepsilon. \end{array} \right. \quad (2.19)$$

Finally, from Equation (2.16) we deduce that φ_0^2 has the following form

$$\varphi_0^2(y) = \tilde{\varphi}_0^2(y) + \lambda_2,$$

where $\widetilde{\varphi}_0^2$ is defined by

$$\widetilde{\varphi}_0^2(y) = - \int_0^y \int_0^s \frac{1}{\widehat{\sigma}_0} [\sigma \partial_n u^0]_{\Gamma^\varepsilon}(t) dt ds.$$

and λ_2 is a constant to be determined at the rank 2.

Terms of order two

At this point we already know that U^2 has the form

$$U^2(X, y) = \varphi_0^2(y) = \widetilde{\varphi}_0^2(y) + \lambda_2. \quad (2.20)$$

At this rank we will calculate constant λ_2 and functions V^4 and $\widetilde{\varphi}_0^4$. To begin with, we consider Problem (2.6) for U^4

$$\begin{cases} \partial_X^2 U^4(X, y) = \frac{1}{\widehat{\sigma}_0} [\sigma \partial_n u^0]_{\Gamma^\varepsilon}(y) & X \in \left(\frac{-1}{2}, \frac{1}{2}\right), \\ \partial_X U^4\left(-\frac{1}{2}, y\right) = \sigma_{\text{int}} \partial_n u_{\text{int}}^0\left(x_0 - \frac{\varepsilon}{2}, y\right), \\ \partial_X U^4\left(\frac{1}{2}, y\right) = \sigma_{\text{ext}} \partial_n u_{\text{ext}}^0\left(x_0 + \frac{\varepsilon}{2}, y\right). \end{cases}$$

We deduce that the solution to this equation has the form

$$U^4(X, y) = \frac{1}{2\widehat{\sigma}_0} [\sigma \partial_n u^0]_{\Gamma^\varepsilon}(y) X^2 + \frac{1}{\widehat{\sigma}_0} \{ \sigma \partial_n u^0 \}_{\Gamma^\varepsilon}(y) X + \varphi_0^4(y).$$

Thus, we have

$$V^4(X, y) = \frac{1}{2\widehat{\sigma}_0} [\sigma \partial_n u^0]_{\Gamma^\varepsilon}(y) X^2 + \frac{1}{\widehat{\sigma}_0} \{ \sigma \partial_n u^0 \}_{\Gamma^\varepsilon}(y) X.$$

Then, we employ (2.7) and we build the following problem for φ_0^4

$$\begin{cases} \frac{d^2}{dy^2} \varphi_0^4(y) = -\frac{1}{\widehat{\sigma}_0} [\sigma \partial_n u^2]_{\Gamma^\varepsilon}(y) - \frac{1}{24\widehat{\sigma}_0} \frac{d^2}{dy^2} [\sigma \partial_n u^0]_{\Gamma^\varepsilon}(y) & y \in (0, y_0), \\ \frac{d}{dy} \varphi_0^4(0) = 0, \\ \frac{d}{dy} \varphi_0^4(y_0) = 0. \end{cases}$$

Integrating the volumic equation from 0 to y_0 and employing the boundary conditions, we obtain condition (2.8) for u^2

$$\int_0^{y_0} [\sigma \partial_n u^2]_{\Gamma^\varepsilon}(t) dt = \frac{1}{24} \frac{d}{dy} [\sigma \partial_n u^0]_{\Gamma^\varepsilon}(y_0) - \frac{1}{24} \frac{d}{dy} [\sigma \partial_n u^0]_{\Gamma^\varepsilon}(0), \quad (2.21)$$

and we get that constant (2.9) takes the value

$$C_2 = \frac{1}{24} \frac{d}{dy} [\sigma \partial_n u^0]_{\Gamma^\varepsilon}(y_0) - \frac{1}{24} \frac{d}{dy} [\sigma \partial_n u^0]_{\Gamma^\varepsilon}(0).$$

We employ this condition along with equation (2.10) to calculate constant λ_2 , which gives rise to

$$\begin{cases} u_{\text{int}}^2 = \widetilde{\varphi}_0^2 + \lambda_2 & \text{on } \Gamma_{\text{int}}^\varepsilon, \\ u_{\text{ext}}^2 = \widetilde{\varphi}_0^2 + \lambda_2 & \text{on } \Gamma_{\text{ext}}^\varepsilon. \end{cases}$$

Thus, we derive u^2 by performing a decomposition (2.11) into two different functions in the following way

$$u^2 = \widetilde{u}^2 + \lambda_2 \bar{u},$$

where \widetilde{u}^2 satisfies the Problem (2.12)

$$\begin{cases} \sigma_{\text{int}} \Delta \widetilde{u}_{\text{int}}^2 = 0 & \text{in } \Omega_{\text{int}}^\varepsilon, \\ \widetilde{u}_{\text{int}}^2 = \widetilde{\varphi}_0^2 & \text{on } \Gamma_{\text{int}}^\varepsilon, \\ \widetilde{u}_{\text{int}}^2 = 0 & \text{on } \partial \Omega_{\text{int}}^\varepsilon \cap \Gamma_D, \\ \partial_n \widetilde{u}_{\text{int}}^2 = 0 & \text{on } \partial \Omega_{\text{int}}^\varepsilon \cap \Gamma_N, \\ \sigma_{\text{ext}} \Delta \widetilde{u}_{\text{ext}}^2 = 0 & \text{in } \Omega_{\text{ext}}^\varepsilon, \\ \widetilde{u}_{\text{ext}}^2 = \widetilde{\varphi}_0^2 & \text{on } \Gamma_{\text{ext}}^\varepsilon, \\ \widetilde{u}_{\text{ext}}^2 = 0 & \text{on } \partial \Omega_{\text{ext}}^\varepsilon \cap \Gamma_D, \\ \partial_n \widetilde{u}_{\text{ext}}^2 = 0 & \text{on } \partial \Omega_{\text{ext}}^\varepsilon \cap \Gamma_N, \end{cases}$$

and \bar{u} satisfies the Problem (2.13). Then, we choose constant λ_2 such that the condition (2.21) is satisfied, we find expression (2.14) for λ_2

$$\lambda_2 = \frac{C_2 - \int_0^{y_0} \frac{1}{\widehat{\sigma}_0} [\sigma \partial_n \widetilde{u}^2]_{\Gamma^\varepsilon} dy}{\int_0^{y_0} \frac{1}{\widehat{\sigma}_0} [\sigma \partial_n \bar{u}]_{\Gamma^\varepsilon} dy}.$$

Employing (2.15), we obtain the Dirichlet boundary conditions on $\Gamma_{\text{int}}^\varepsilon$ and $\Gamma_{\text{ext}}^\varepsilon$ for u^2 . Thus, we write the problems satisfied by u_{int}^2 and u_{ext}^2 as

$$\left\{ \begin{array}{ll} \sigma_{\text{int}} \Delta u_{\text{int}}^2 = 0 & \text{in } \Omega_{\text{int}}^\varepsilon, \\ u_{\text{int}}^2 = \widetilde{\varphi}_0^2 + \lambda_2 & \text{on } \Gamma_{\text{int}}^\varepsilon, \\ u_{\text{int}}^2 = 0 & \text{on } \Gamma_D \cap \partial\Omega_{\text{int}}^\varepsilon, \\ \partial_n u_{\text{int}}^2 = 0 & \text{on } \Gamma_N \cap \partial\Omega_{\text{int}}^\varepsilon, \end{array} \right. \quad (2.22)$$

$$\left\{ \begin{array}{ll} \sigma_{\text{ext}} \Delta u_{\text{ext}}^2 = 0 & \text{in } \Omega_{\text{ext}}^\varepsilon, \\ u_{\text{ext}}^2 = \widetilde{\varphi}_0^2 + \lambda_2 & \text{on } \Gamma_{\text{ext}}^\varepsilon, \\ u_{\text{ext}}^2 = 0 & \text{on } \Gamma_D \cap \partial\Omega_{\text{ext}}^\varepsilon, \\ \partial_n u_{\text{ext}}^2 = 0 & \text{on } \Gamma_N \cap \partial\Omega_{\text{ext}}^\varepsilon. \end{array} \right.$$

Finally, from Equation (2.16) we deduce that φ_0^4 has the following form

$$\varphi_0^4(y) = \widetilde{\varphi}_0^4(y) + \lambda_4,$$

where $\widetilde{\varphi}_0^4$ is defined as

$$\widetilde{\varphi}_0^4(y) = - \int_0^y \int_0^s \frac{1}{\widehat{\sigma}_0} [\sigma \partial_n u^2]_{\Gamma^\varepsilon}(t) dt ds - \int_0^y \int_0^s \frac{1}{24\widehat{\sigma}_0} \frac{d^2}{dy^2} [\sigma \partial_n u^0]_{\Gamma^\varepsilon}(t) dt ds.$$

and λ_4 is a constant to be determined at the rank 4.

Recapitulation of the asymptotic expansion

Proposition 5. *The asymptotic expansion (2.1), has the following form*

$$\left\{ \begin{array}{ll} u_{\text{int}}(x, y) = u_{\text{int}}^0(x, y) + \varepsilon^2 u_{\text{int}}^2(x, y) + O(\varepsilon^4) & \text{in } \Omega_{\text{int}}^\varepsilon, \\ u_{\text{ext}}(x, y) = u_{\text{ext}}^0(x, y) + \varepsilon^2 u_{\text{ext}}^2(x, y) + O(\varepsilon^4) & \text{in } \Omega_{\text{ext}}^\varepsilon, \\ U(X, y) = \lambda_0 + \varepsilon^2 \varphi_0^2(y) + O(\varepsilon^4) & \text{in } \left(-\frac{1}{2}, \frac{1}{2}\right) \times (0, y_0), \end{array} \right.$$

where constant λ_0 and functions φ_0^2 , u^0 , and u^2 are defined by Equations (2.18), (2.20), (2.19), and (2.22), respectively. For $k \in \mathbb{N}$, the solution U^k of Equation

(2.6) has the following form

$$U^k(X, y) = \begin{cases} 0 & \text{if } k \text{ odd,} \\ \sum_{j=1}^{k-2} \varphi_j^k(y) X^j + \widetilde{\varphi}_0^k(y) + \lambda_k & \text{if } k \text{ even,} \end{cases}$$

where $\widetilde{\varphi}_0^k$ is derived at the fourth step of the algorithm as a solution to (2.7) and solution $u^k = (u_{int}^k, u_{ext}^k)$ to Problem (1.12) satisfies

$$u_{int}^k \equiv u_{ext}^k \equiv 0, \quad \text{if } k \text{ odd.}$$

Proof. The proof is similar to the one performed for the Dirichlet case. In addition, once we have proved that for an even k function U^k has the form

$$U^k(X, y) = \varphi_{k-2}^k X^{k-2} + \varphi_{k-3}^k X^{k-3} + \dots + \varphi_1^k X + \varphi_0^k,$$

Equation (2.7) at the rank k allows us to deduce that φ_0^k has the form

$$\varphi_0^k(y) = \widetilde{\varphi}_0^k(y) + \lambda_k,$$

where function $\widetilde{\varphi}_0^k$ is obtained from Equation (2.7), and λ_k is obtained following the same arguments as the ones set at the second step of the algorithm. \square

2.2.2 Equivalent models

Now that we know the expressions for the first terms of the expansion, we truncate the series and we identify a simpler problem satisfied by

$$u^{(k)} = u^0 + \varepsilon u^1 + \dots + \varepsilon^k u^k \quad \text{in } \Omega_{int}^\varepsilon \cup \Omega_{ext}^\varepsilon$$

up to a residual term of order ε^{k+1} . We neglect the residual term of order ε^{k+1} to obtain an approximate model satisfied by function $u^{[k]}$. Here, we formally derive two approximate models of order two and order four respectively.

Second-order model

For deriving the second-order model, we truncate the series from the second term and we define $u^{(1)}$ as

$$u^{(1)} = u^0 + \varepsilon u^1 = u^0 \quad \text{in } \Omega_{int}^\varepsilon \cup \Omega_{ext}^\varepsilon \quad (\text{see Proposition 5}).$$

From (2.19), we conclude that $u^{(1)}$ solves the following uncoupled problems

$$\left\{ \begin{array}{ll} \sigma_{\text{int}} \Delta u_{\text{int}}^{(1)} = f_{\text{int}} & \text{in } \Omega_{\text{int}}^{\varepsilon}, \\ u_{\text{int}}^{(1)} = \lambda_0 & \text{on } \Gamma_{\text{int}}^{\varepsilon}, \\ u_{\text{int}}^{(1)} = 0 & \text{on } \partial\Omega_{\text{int}}^{\varepsilon} \cap \Gamma_D, \\ \partial_n u_{\text{int}}^{(1)} = 0 & \text{on } \partial\Omega_{\text{int}}^{\varepsilon} \cap \Gamma_N, \end{array} \right. \quad (2.23)$$

$$\left\{ \begin{array}{ll} \sigma_{\text{ext}} \Delta u_{\text{ext}}^{(1)} = f_{\text{ext}} & \text{in } \Omega_{\text{ext}}^{\varepsilon}, \\ u_{\text{ext}}^{(1)} = \lambda_0 & \text{on } \Gamma_{\text{ext}}^{\varepsilon}, \\ u_{\text{ext}}^{(1)} = 0 & \text{on } \partial\Omega_{\text{ext}}^{\varepsilon} \cap \Gamma_D, \\ \partial_n u_{\text{ext}}^{(1)} = 0 & \text{on } \partial\Omega_{\text{ext}}^{\varepsilon} \cap \Gamma_N. \end{array} \right.$$

In this case, we have $u^{[1]} = u^{(1)}$ as $u^{(1)}$ does not depend on ε . We infer a second-order model satisfied by $u^{[1]}$ solution to Problem (2.23).

Fourth-order model

For deriving the fourth-order model, we truncate the series from the fourth term and we define $u^{(3)}$ as

$$u^{(3)} = u^0 + \varepsilon u^1 + \varepsilon^2 u^2 + \varepsilon^3 u^3 = u^0 + \varepsilon^2 u^2 \quad \text{in } \Omega_{\text{int}}^{\varepsilon} \cup \Omega_{\text{ext}}^{\varepsilon} \quad (\text{see Proposition 5}).$$

From (2.19) and (2.22), and employing the same procedure we employed for the Dirichlet case in the Section (1.3.2), we deduce that $u^{(3)}$ satisfies the following transmission problem

$$\left\{ \begin{array}{ll} \sigma_{\text{int}} \Delta u_{\text{int}}^{(3)} = f_{\text{int}} & \text{in } \Omega_{\text{int}}^{\varepsilon}, \\ \sigma_{\text{ext}} \Delta u_{\text{ext}}^{(3)} = f_{\text{ext}} & \text{in } \Omega_{\text{ext}}^{\varepsilon}, \\ [u^{(3)}]_{\Gamma^{\varepsilon}} = 0, \\ \frac{d^2}{dy^2} \{u^{(3)}\}_{\Gamma^{\varepsilon}} = -\varepsilon^2 \frac{1}{\hat{\sigma}_0} [\sigma \partial_n u^{(3)}]_{\Gamma^{\varepsilon}} + O(\varepsilon^4), \\ \partial_n u^{(3)} = 0 & \text{on } \Omega^{\varepsilon} \cup \Gamma_N, \\ u^{(3)} = 0 & \text{on } \Omega^{\varepsilon} \cup \Gamma_D. \end{array} \right.$$

We define as $u^{[3]}$ the function we obtain when truncating the solution at the fourth element of the expansion and neglecting the terms of order four or higher in ε . Then, $u^{[3]}$ satisfies the following transmission problem

$$\left\{ \begin{array}{ll} \sigma_{\text{int}} \Delta u_{\text{int}}^{[3]} = f_{\text{int}} & \text{in } \Omega_{\text{int}}^{\varepsilon}, \\ \sigma_{\text{ext}} \Delta u_{\text{ext}}^{[3]} = f_{\text{ext}} & \text{in } \Omega_{\text{ext}}^{\varepsilon}, \\ [u^{[3]}]_{\Gamma^{\varepsilon}} = 0, & \\ [\sigma \partial_n u^{[3]}]_{\Gamma^{\varepsilon}} = -\frac{\hat{\sigma}_0}{\varepsilon^2} \frac{d^2}{dy^2} \{u^{[3]}\}_{\Gamma^{\varepsilon}}, & \\ \partial_n u^{[3]} = 0 & \text{on } \Omega^{\varepsilon} \cup \Gamma_N, \\ u^{[3]} = 0 & \text{on } \Omega^{\varepsilon} \cup \Gamma_D. \end{array} \right. \quad (2.24)$$

We remark that the obtained transmission conditions for the fourth-order model with mixed external boundary conditions coincide with the ones obtained for the fourth-order model (1.19) with Dirichlet external boundary conditions.

2.3 Static 2D configuration: second class of ITCs

2.3.1 Construction of a multiscale expansion

In this section we perform an expansion of the solution in power series of ε as we have done in Section 2.2.1. Then, by truncating this series and neglecting higher order terms in ε , we derive approximate models composed by equivalent conditions in Section 2.3.2. As in the previous chapter, the main difference with the first class of ITCs is that now we employ some formal Taylor series expansions to write the terms of the expansion across an artificial interface Γ situated in the middle of the thin layer. The resulting asymptotic models will be defined in the domain depicted at Figure 1.2b.

In order to avoid repetition, we will restrict ourselves to showing the obtained asymptotic models without showing the details regarding the calculi, due to them being similar to the ones performed in the previous sections and chapters.

We begin by performing an *Ansatz* in the form of power series of ε for functions u_{int} , u_{ext} , and U just as formerly done in (2.1) and we employ a formal Taylor series expansion of the terms u_{int}^k and u_{ext}^k to extend the domain up to interface Γ as in Section 1.4.1.

Equations for the coefficients of the electric potential

Substituting the expansions (1.20) into the Equations (1.3) and collecting the terms with the same powers in ε , for every $k \in \mathbb{N}$ we obtain the following set of equations

$$\left\{ \begin{array}{ll} \sigma_{\text{int}} \Delta u_{\text{int}}^k(x, y) = f_{\text{int}}(x, y) \delta_0^k & \text{in } \Omega_{\text{ext}}, \quad (2.25\text{a}) \\ \sigma_{\text{ext}} \Delta u_{\text{ext}}^k(x, y) = f_{\text{ext}}(x, y) \delta_0^k & \text{in } \Omega_{\text{ext}}, \quad (2.25\text{b}) \\ \partial_X^2 U^k(X, y) + \partial_y^2 U^{k-2}(X, y) = 0 & \text{in } \left(-\frac{1}{2}, \frac{1}{2}\right) \times (0, y_0), \quad (2.25\text{c}) \end{array} \right.$$

along with the following transmission conditions

$$\left\{ \begin{array}{ll} \sum_{i=0}^k \frac{(-1)^i}{2^i i!} \partial_n^i u_{\text{int}}^{k-i}(x_0, y) = U^k\left(\frac{-1}{2}, y\right) & y \in (0, y_0), \quad (2.26\text{a}) \\ \sum_{i=0}^k \frac{1}{2^i i!} \partial_n^i u_{\text{ext}}^{k-i}(x_0, y) = U^k\left(\frac{1}{2}, y\right) & y \in (0, y_0), \quad (2.26\text{b}) \\ \sigma_{\text{int}} \sum_{i=0}^{k-4} \frac{(-1)^i}{2^i i!} \partial_n^{i+1} u_{\text{int}}^{k-4-i}(x_0, y) = \hat{\sigma}_0 \partial_X U^k\left(\frac{-1}{2}, y\right) & y \in (0, y_0), \quad (2.26\text{c}) \\ \sigma_{\text{ext}} \sum_{i=0}^{k-4} \frac{1}{2^i i!} \partial_n^{i+1} u_{\text{ext}}^{k-4-i}(x_0, y) = \hat{\sigma}_0 \partial_X U^k\left(\frac{1}{2}, y\right) & y \in (0, y_0), \quad (2.26\text{d}) \end{array} \right.$$

and the following boundary conditions

$$\left\{ \begin{array}{ll} u^k(0, y) = u^k(L, y) = 0 & y \in (0, y_0), \quad (2.27\text{a}) \\ \partial_n u^k(x, 0) = \partial_n u^k(x, y_0) = 0 & x \in \left(0, x_0 - \frac{\varepsilon}{2}\right) \cup \left(x_0 + \frac{\varepsilon}{2}, L\right), \quad (2.27\text{b}) \\ \partial_X U^k(X, 0) = \partial_X U^k(X, y_0) = 0 & X \in \left(-\frac{1}{2}, \frac{1}{2}\right), \quad (2.27\text{c}) \end{array} \right.$$

For determining the elementary problems satisfied by each term of the expansion, we will also need the following compatibility condition

$$\begin{aligned}
& - \int_{-\frac{1}{2}}^{\frac{1}{2}} \partial_y^2 U^{k-2}(X, y) \, dX \\
& = \frac{1}{\hat{\sigma}_0} \sum_{i=0}^{k-4} \left(\frac{\sigma_{\text{ext}}}{2^i i!} \partial_n^{i+1} u_{\text{ext}}^{k-4-i}(x_0, y) + (-1)^{i+1} \frac{\sigma_{\text{int}}}{2^i i!} \partial_n^{i+1} u_{\text{int}}^{k-4-i}(x_0, y) \right).
\end{aligned} \tag{2.28}$$

We adopt the convention that the terms with negative indices in Equations (2.25) - (2.28) are equal to 0. Employing Equations ((2.25) - (2.28)) we deduce the elementary problems satisfied outside and inside the layer for every $k \in \mathbb{N}$.

First terms of the asymptotics

Terms of order zero

We consider Equations (2.25c), (2.26c), and (2.26d), and we end up with the following differential problem governing function U^0 in the variable X (the variable y has the role of a parameter)

$$\left\{ \begin{array}{l} \partial_X^2 U^0(X, y) = 0 \quad X \in \left(-\frac{1}{2}, \frac{1}{2} \right), \\ \partial_X U^0\left(-\frac{1}{2}, y\right) = 0, \\ \partial_X U^0\left(\frac{1}{2}, y\right) = 0. \end{array} \right.$$

The solution to this equation has the form $U^0(X, y) = \varphi_0^0(y)$. Then, we consider Equations (2.28) and (2.27b) and we build the following differential problem for function φ_0^0 in the variable y

$$\left\{ \begin{array}{l} \frac{d^2}{dy^2} \varphi_0^0(y) = 0 \quad y \in (0, y_0), \\ \frac{d}{dy} \varphi_0^0(0) = 0, \\ \frac{d}{dy} \varphi_0^0(y_0) = 0. \end{array} \right. \tag{2.29}$$

We deduce that the solution to this equation has the form $\varphi_0^0(y) = \lambda_0$. Again, we consider Equations (2.25c), (2.26c), and (2.26d) and we build the following

differential problem for function U^2 in the variable X (the variable y has the role of a parameter)

$$\begin{cases} \partial_X^2 U^2(X, y) = 0 & X \in \left(-\frac{1}{2}, \frac{1}{2}\right), \\ \partial_X U^2\left(-\frac{1}{2}, y\right) = 0, \\ \partial_X U^2\left(\frac{1}{2}, y\right) = 0. \end{cases}$$

We obtain that the solution to this equation has the form $U^2(X, y) = \varphi_0^2(y)$. Then, we consider Equations (2.28) and (2.27b), and we get the following differential problem for function φ_0^2 in the variable y

$$\begin{cases} \frac{d^2}{dy^2} \varphi_0^2(y) = -\frac{1}{\widehat{\sigma}_0} [\sigma \partial_n u^0]_{\Gamma^\varepsilon} & y \in (0, y_0), \\ \frac{d}{dy} \varphi_0^2(0) = 0, \\ \frac{d}{dy} \varphi_0^2(y_0) = 0. \end{cases}$$

Integrating the volumic equation from 0 to y_0 and employing the boundary conditions, we obtain condition

$$\int_0^{y_0} [\sigma \partial_n u^0]_{\Gamma^\varepsilon}(t) dt = 0. \quad (2.30)$$

We employ this condition with Equations of (2.26a) and (2.26b) to calculate constant λ_0 . We get

$$\begin{cases} u_{\text{int}}^0 = \lambda_0 & \text{on } \Gamma_{\text{int}}^\varepsilon, \\ u_{\text{ext}}^0 = \lambda_0 & \text{on } \Gamma_{\text{ext}}^\varepsilon. \end{cases}$$

Thus, we construct u^0 by performing a decomposition into two different functions in the following way

$$u^0 = \tilde{u}^0 + \lambda_0 \bar{u},$$

where \tilde{u}^0 satisfies the problem

$$\begin{cases} \sigma_{\text{int}} \Delta \tilde{u}_{\text{int}}^0 = f_{\text{int}} & \text{in } \Omega_{\text{int}}^\varepsilon, \\ \tilde{u}_{\text{int}}^0 = 0 & \text{on } \Gamma_{\text{int}}^\varepsilon, \\ \tilde{u}_{\text{int}}^0 = 0 & \text{on } \partial\Omega_{\text{int}}^\varepsilon \cap \Gamma_D, \\ \partial_n \tilde{u}_{\text{int}}^0 = 0 & \text{on } \partial\Omega_{\text{int}}^\varepsilon \cap \Gamma_N, \end{cases}$$

$$\begin{cases} \sigma_{\text{ext}} \Delta \tilde{u}_{\text{ext}}^0 = f_{\text{ext}} & \text{in } \Omega_{\text{ext}}^\varepsilon, \\ \tilde{u}_{\text{ext}}^0 = 0 & \text{on } \Gamma_{\text{ext}}^\varepsilon, \\ \tilde{u}_{\text{ext}}^0 = 0 & \text{on } \partial\Omega_{\text{ext}}^\varepsilon \cap \Gamma_D, \\ \partial_n \tilde{u}_{\text{ext}}^0 = 0 & \text{on } \partial\Omega_{\text{ext}}^\varepsilon \cap \Gamma_N, \end{cases}$$

and \bar{u} satisfies the problem

$$\begin{cases} \Delta \bar{u}_{\text{int}} = 0 & \text{in } \Omega_{\text{int}}^\varepsilon, \\ \bar{u}_{\text{int}} = 1 & \text{on } \Gamma, \\ \bar{u}_{\text{int}} = 0 & \text{on } \partial\Omega_{\text{int}}^\varepsilon \cap \Gamma_D, \\ \partial_n \bar{u}_{\text{int}} = 0 & \text{on } \partial\Omega_{\text{int}}^\varepsilon \cap \Gamma_N, \end{cases} \quad (2.31)$$

$$\begin{cases} \Delta \bar{u}_{\text{ext}} = 0 & \text{in } \Omega_{\text{ext}}^\varepsilon, \\ \bar{u}_{\text{ext}} = 1 & \text{on } \Gamma, \\ \bar{u}_{\text{ext}} = 0 & \text{on } \partial\Omega_{\text{ext}}^\varepsilon \cap \Gamma_D, \\ \partial_n \bar{u}_{\text{ext}} = 0 & \text{on } \partial\Omega_{\text{ext}}^\varepsilon \cap \Gamma_N. \end{cases}$$

Then, we choose constant λ_0 such that the condition (2.17) is satisfied. It has the expression

$$\lambda_0 = - \frac{\int_0^{y_0} [\sigma \partial_n \tilde{u}^0]_\Gamma(t) dt}{\int_0^{y_0} [\sigma \partial_n \bar{u}]_\Gamma(t) dt}. \quad (2.32)$$

In the same way we did in Section 2.2.1 it is possible to prove that $\int_0^{y_0} [\sigma \partial_n \bar{u}]_\Gamma(t) dt \neq 0$ and thus, λ_0 is well defined. Finally, employing Equations (2.25a), (2.25b), (2.26a), (2.26b), (2.27a), and (2.27b), we obtain that the limit

solution u^0 satisfies Dirichlet boundary conditions on $\Gamma_{\text{int}}^\varepsilon$ and $\Gamma_{\text{ext}}^\varepsilon$. The problems satisfied by u_{int}^0 and u_{ext}^0 are thus

$$\left\{ \begin{array}{ll} \sigma_{\text{int}} \Delta u_{\text{int}}^0 = f_{\text{int}} & \text{in } \Omega_{\text{int}}^\varepsilon, \\ u_{\text{int}}^0 = \lambda_0 & \text{on } \Gamma_{\text{int}}^\varepsilon, \\ u_{\text{int}}^0 = 0 & \text{on } \Gamma_D \cap \partial\Omega_{\text{int}}^\varepsilon, \\ \partial_n u_{\text{int}}^0 = 0 & \text{on } \Gamma_N \cap \partial\Omega_{\text{int}}^\varepsilon, \end{array} \right. \quad (2.33)$$

$$\left\{ \begin{array}{ll} \sigma_{\text{ext}} \Delta u_{\text{ext}}^0 = f_{\text{ext}} & \text{in } \Omega_{\text{ext}}^\varepsilon, \\ u_{\text{ext}}^0 = \lambda_0 & \text{on } \Gamma_{\text{ext}}^\varepsilon, \\ u_{\text{ext}}^0 = 0 & \text{on } \Gamma_D \cap \partial\Omega_{\text{ext}}^\varepsilon, \\ \partial_n u_{\text{ext}}^0 = 0 & \text{on } \Gamma_N \cap \partial\Omega_{\text{ext}}^\varepsilon. \end{array} \right.$$

Terms of order one

We consider Equations (2.25c), (2.26c), and (2.26d), and we build the following differential problem for function U^1 in the variable X (the variable y has the role of a parameter)

$$\left\{ \begin{array}{l} \partial_X^2 U^1(X, y) = 0 \quad X \in \left(-\frac{1}{2}, \frac{1}{2} \right), \\ \partial_X U^1 \left(-\frac{1}{2}, y \right) = 0, \\ \partial_X U^1 \left(\frac{1}{2}, y \right) = 0. \end{array} \right.$$

The solution to this equation has the form $U^1(X, y) = \varphi_0^1(y)$. Then, we consider Equations (2.28) and (2.27b), and we build the following differential problem for function φ_0^1 in the variable y

$$\left\{ \begin{array}{l} \frac{d^2}{dy^2} \varphi_0^1(y) = 0 \quad y \in (0, y_0), \\ \frac{d}{dy} \varphi_0^1(0) = 0, \\ \frac{d}{dy} \varphi_0^1(y_0) = 0. \end{array} \right.$$

We deduce that the solution to this equation has the form $\varphi_0^1(y) = \lambda_1$. Again, we consider Equations (2.25c), (2.26c), and (2.26d), and we build the following

differential problem for function U^3 in the variable X (the variable y has the role of a parameter)

$$\begin{cases} \partial_X^2 U^3(X, y) = 0 & X \in \left(\frac{-1}{2}, \frac{1}{2}\right), \\ \partial_X U^3\left(-\frac{1}{2}, y\right) = 0, \\ \partial_X U^3\left(\frac{1}{2}, y\right) = 0. \end{cases}$$

We obtain that the solution to this equation has the form $U^3(X, y) = \varphi_0^3(y)$. Then, we consider Equations (2.28) and (2.27b), and we build the following differential problem for function φ_0^3 in the variable y

$$\begin{cases} \frac{d^2}{dy^2} \varphi_0^3(y) = -\frac{1}{\hat{\sigma}_0} [\sigma \partial_n u^1]_\Gamma - \frac{1}{\hat{\sigma}_0} \{\sigma \partial_n u^0\}_\Gamma & y \in (0, y_0), \\ \frac{d}{dy} \varphi_0^3(0) = 0, \\ \frac{d}{dy} \varphi_0^3(y_0) = 0. \end{cases}$$

Integrating the first equation from 0 to y_0 and employing the boundary conditions, we obtain

$$\int_0^{y_0} [\sigma \partial_n u^1]_\Gamma(t) dt = - \int_0^{y_0} \{\sigma \partial_n u^0\}_\Gamma(t) dt. \quad (2.34)$$

We employ (2.34) to calculate constant λ_1 with the help of Equations (2.26a) and (2.26b). We have

$$\begin{cases} u_{\text{int}}^1 = \lambda_1 + \frac{1}{2} \partial_n u_{\text{int}}^0 & \text{on } \Gamma_{\text{int}}^\varepsilon, \\ u_{\text{ext}}^1 = \lambda_1 - \frac{1}{2} \partial_n u_{\text{ext}}^0 & \text{on } \Gamma_{\text{ext}}^\varepsilon. \end{cases}$$

Thus, we derive u^1 by performing a decomposition into two different functions in the following way

$$u^1 = \tilde{u}^1 + \lambda_0 \bar{u},$$

where \tilde{u}^1 satisfies the problem

$$\left\{ \begin{array}{ll} \sigma_{\text{int}} \Delta \tilde{u}_{\text{int}}^1 = 0 & \text{in } \Omega_{\text{int}}^\varepsilon, \\ \tilde{u}_{\text{int}}^1 = \frac{1}{2} \partial_n u_{\text{int}}^0 & \text{on } \Gamma_{\text{int}}^\varepsilon, \\ \tilde{u}_{\text{int}}^1 = 0 & \text{on } \partial \Omega_{\text{int}}^\varepsilon \cap \Gamma_D, \\ \partial_n \tilde{u}_{\text{int}}^1 = 0 & \text{on } \partial \Omega_{\text{int}}^\varepsilon \cap \Gamma_N, \end{array} \right.$$

$$\left\{ \begin{array}{ll} \sigma_{\text{ext}} \Delta \tilde{u}_{\text{ext}}^1 = 0 & \text{in } \Omega_{\text{ext}}^\varepsilon, \\ \tilde{u}_{\text{ext}}^1 = -\frac{1}{2} \partial_n u_{\text{ext}}^0 & \text{on } \Gamma_{\text{ext}}^\varepsilon, \\ \tilde{u}_{\text{ext}}^1 = 0 & \text{on } \partial \Omega_{\text{ext}}^\varepsilon \cap \Gamma_D, \\ \partial_n \tilde{u}_{\text{ext}}^1 = 0 & \text{on } \partial \Omega_{\text{ext}}^\varepsilon \cap \Gamma_N, \end{array} \right.$$

and \bar{u} satisfies the Problem (2.31). Then, we choose constant λ_1 such that the condition (2.34) is satisfied, we obtain

$$\lambda_1 = - \frac{- \int_0^{y_0} \{ \sigma \partial_n u^0 \}_\Gamma (t) dt - \int_0^{y_0} [\sigma \partial_n \tilde{u}^1]_\Gamma (t) dt}{\int_0^{y_0} [\sigma \partial_n \bar{u}]_\Gamma (t) dt}. \quad (2.35)$$

We remark $\int_0^{y_0} [\sigma \partial_n \bar{u}]_\Gamma (t) dt \neq 0$ and thus, λ_1 is well defined. Finally, employing Equations (2.25a), (2.25b), (2.26a), (2.26b), (2.27a), and (2.27b), we obtain the problems satisfied by u_{int}^0 and u_{ext}^0

$$\left\{ \begin{array}{ll} \sigma_{\text{int}} \Delta u_{\text{int}}^1 = f_{\text{int}} & \text{in } \Omega_{\text{int}}^\varepsilon, \\ u_{\text{int}}^1 = \lambda_1 + \frac{1}{2} \partial_n u_{\text{int}}^0 & \text{on } \Gamma_{\text{int}}^\varepsilon, \\ u_{\text{int}}^1 = 0 & \text{on } \Gamma_D \cap \partial \Omega_{\text{int}}^\varepsilon, \\ \partial_n u_{\text{int}}^1 = 0 & \text{on } \Gamma_N \cap \partial \Omega_{\text{int}}^\varepsilon, \end{array} \right. \quad (2.36)$$

$$\left\{ \begin{array}{ll} \sigma_{\text{ext}} \Delta u_{\text{ext}}^1 = f_{\text{ext}} & \text{in } \Omega_{\text{ext}}^\varepsilon, \\ u_{\text{ext}}^1 = \lambda_1 - \frac{1}{2} \partial_n u_{\text{ext}}^0 & \text{on } \Gamma_{\text{ext}}^\varepsilon, \\ u_{\text{ext}}^1 = 0 & \text{on } \Gamma_D \cap \partial \Omega_{\text{ext}}^\varepsilon, \\ \partial_n u_{\text{ext}}^1 = 0 & \text{on } \Gamma_N \cap \partial \Omega_{\text{ext}}^\varepsilon. \end{array} \right.$$

Recapitulation of the asymptotic expansion

Proposition 6. *The asymptotic expansion (1.4) has the following form*

$$\begin{cases} u_{int}(x, y) = u_{int}^0(x, y) + \varepsilon u_{int}^1(x, y) + O(\varepsilon^2) & \text{in } \Omega_{int}, \\ u_{ext}(x, y) = u_{ext}^0(x, y) + \varepsilon u_{ext}^1(x, y) + O(\varepsilon^2) & \text{in } \Omega_{ext}, \\ U(X, y) = \lambda_0 + \varepsilon \lambda_1 + O(\varepsilon^2) & \text{in } \left(-\frac{1}{2}, \frac{1}{2}\right) \times (0, y_0), \end{cases}$$

where functions u_0 and u_1 are defined by Equations (2.33) and (2.36), respectively. Constants λ_0 and λ_1 are defined by Equations (2.32) and (2.35).

2.3.2 Equivalent models

From Equations (2.25) - (2.28) we deduce the expressions for the first terms of the expansion. Then, we truncate the series and we identify a simpler problem satisfied by

$$u^{(k)} = u^0 + \varepsilon u^1 + \dots + \varepsilon^k u^k \quad \text{in } \Omega_{int} \cup \Omega_{ext}$$

up to a residual term of order ε^{k+1} . We neglect the residual term of order ε^{k+1} to obtain an approximate model satisfied by function $u^{[k]}$. Here, we formally derive two approximate models of order one and order two respectively.

First-order model

$$\begin{cases} \sigma_{int} \Delta u_{int}^{[0]} = f_{int} & \text{in } \Omega_{int}^\varepsilon, \\ u_{int}^{[0]} = \lambda_0 & \text{on } \Gamma_{int}^\varepsilon, \\ u_{int}^{[0]} = 0 & \text{on } \partial\Omega_{int}^\varepsilon \cap \Gamma_D, \\ \partial_n u_{int}^{[0]} = 0 & \text{on } \partial\Omega_{int}^\varepsilon \cap \Gamma_N, \end{cases} \quad (2.37)$$

$$\begin{cases} \sigma_{ext} \Delta u_{ext}^{[0]} = f_{ext} & \text{in } \Omega_{ext}^\varepsilon, \\ u_{ext}^{[0]} = \lambda_0 & \text{on } \Gamma_{ext}^\varepsilon, \\ u_{ext}^{[0]} = 0 & \text{on } \partial\Omega_{ext}^\varepsilon \cap \Gamma_D, \\ \partial_n u_{ext}^{[0]} = 0 & \text{on } \partial\Omega_{ext}^\varepsilon \cap \Gamma_N. \end{cases}$$

Second-order model

$$\left\{ \begin{array}{ll} \sigma_{\text{int}} \Delta u_{\text{int}}^{[1]} = f_{\text{int}} & \text{in } \Omega_{\text{int}}^{\varepsilon}, \\ u_{\text{int}}^{[1]} = \lambda_1 + \frac{\varepsilon}{2} \partial_n u_{\text{int}}^{[1]} & \text{on } \Gamma_{\text{int}}^{\varepsilon}, \\ u_{\text{int}}^{[1]} = 0 & \text{on } \partial\Omega_{\text{int}}^{\varepsilon} \cap \Gamma_D, \\ \partial_n u_{\text{int}}^{[1]} = 0 & \text{on } \partial\Omega_{\text{int}}^{\varepsilon} \cap \Gamma_N, \end{array} \right. \quad (2.38)$$

$$\left\{ \begin{array}{ll} \sigma_{\text{ext}} \Delta u_{\text{ext}}^{[1]} = f_{\text{ext}} & \text{in } \Omega_{\text{ext}}^{\varepsilon}, \\ u_{\text{ext}}^{[1]} = \lambda_1 - \frac{\varepsilon}{2} \partial_n u_{\text{int}}^{[1]} & \text{on } \Gamma_{\text{ext}}^{\varepsilon}, \\ u_{\text{ext}}^{[1]} = 0 & \text{on } \partial\Omega_{\text{ext}}^{\varepsilon} \cap \Gamma_D, \\ \partial_n u_{\text{ext}}^{[1]} = 0 & \text{on } \partial\Omega_{\text{ext}}^{\varepsilon} \cap \Gamma_N. \end{array} \right.$$

ANALYSIS OF THE ITCS

3.1 Introduction

This chapter is devoted to the validation of the multiscale expansion we have derived in Chapter 1 and the convergence results. We perform proofs of existence, uniqueness, and uniform estimates for the reference model problem we have studied and then, we prove the convergence of the asymptotic models towards the solution to the reference model.

This chapter is structured as follows. Section 3.2 is devoted to the study of reference model (1.2), regarding the well-posedness of the model and the derivation of uniform estimates. Then, in Section 3.3, we study the convergence of the asymptotic expansion for the reference model and we give estimates for the expansion of the reference model. Sections 3.4 and 3.5 are dedicated to the study of the asymptotic models we have derived employing the first and second approach respectively. In these sections we derive the variational formulations for the asymptotic models and we prove stability and convergence results.

3.2 The reference model: well-posedness and uniform estimates

In this section we will prove that there exists a solution to Problem (1.2) and that this solution is unique. Instead of considering directly Problem (1.2), we will consider a similar one. This problem is defined employing the same configuration we have defined in Section 1.2. We remark that constants σ_{int} , σ_{ext} , and $\hat{\sigma}_0$ are strictly positive, and this fact will play an important role in the following proofs. We remark Figure 1.1 shows the configuration of the domain we are working with.

In this framework we consider the following problem

$$\left\{ \begin{array}{ll} \sigma_{\text{int}} \Delta u_{\text{int}} = f_{\text{int}} & \text{in } \Omega_{\text{int}}^\varepsilon, \\ \sigma_{\text{ext}} \Delta u_{\text{ext}} = f_{\text{ext}} & \text{in } \Omega_{\text{ext}}^\varepsilon, \\ \widehat{\sigma}_0 \varepsilon^{-3} \Delta u_{\text{lay}} = f_{\text{lay}} & \text{in } \Omega_{\text{lay}}^\varepsilon, \\ u_{\text{int}} = u_{\text{lay}} & \text{on } \Gamma_{\text{int}}^\varepsilon, \\ u_{\text{lay}} = u_{\text{ext}} & \text{on } \Gamma_{\text{ext}}^\varepsilon, \\ \widehat{\sigma}_0 \varepsilon^{-3} \partial_n u_{\text{lay}} - \sigma_{\text{int}} \partial_n u_{\text{int}} = g_{\text{int}} & \text{on } \Gamma_{\text{int}}^\varepsilon, \\ \widehat{\sigma}_0 \varepsilon^{-3} \partial_n u_{\text{lay}} - \sigma_{\text{ext}} \partial_n u_{\text{ext}} = g_{\text{ext}} & \text{on } \Gamma_{\text{ext}}^\varepsilon, \\ u = 0 & \text{on } \partial\Omega. \end{array} \right. \quad (3.1)$$

This problem is similar to Problem (1.2) and it generalizes it because the right-hand side f_{lay} does not vanish inside the layer any more and because it includes the right-hand side functions g_{int} and g_{ext} . The results obtained for this problem will be useful in later sections, where we prove the convergence of the asymptotic models.

We write the variational formulation of Problem (3.1). Assuming $f \in L^2(\Omega)$, $g_{\text{int}} \in L^2(\Gamma_{\text{int}}^\varepsilon)$, and $g_{\text{ext}} \in L^2(\Gamma_{\text{ext}}^\varepsilon)$, a weak solution to (3.1) is a function $u \in H_0^1(\Omega)$ that for all $w \in H_0^1(\Omega)$ verifies

$$a(u, w) = l(w) \quad (3.2)$$

where

$$\begin{aligned} a(u, w) &= \sigma_{\text{int}} \int_{\Omega_{\text{int}}^\varepsilon} \nabla u \cdot \nabla w \, dx + \sigma_{\text{ext}} \int_{\Omega_{\text{ext}}^\varepsilon} \nabla u \cdot \nabla w \, dx + \widehat{\sigma}_0 \varepsilon^{-3} \int_{\Omega_{\text{lay}}^\varepsilon} \nabla u \cdot \nabla w \, dx, \\ l(w) &= - \int_{\Omega_{\text{int}}^\varepsilon} f_{\text{int}} w \, dx - \int_{\Omega_{\text{ext}}^\varepsilon} f_{\text{ext}} w \, dx - \int_{\Omega_{\text{lay}}^\varepsilon} f_{\text{lay}} w \, dx + \int_{\Gamma_{\text{int}}^\varepsilon} g_{\text{int}} w \, ds \\ &\quad + \int_{\Gamma_{\text{ext}}^\varepsilon} g_{\text{ext}} w \, ds. \end{aligned}$$

We will see that a strong solution to (3.1) is also a weak solution. We denote as $C_c^1(\Omega)$ the space of functions which are continuously differentiable and with compact support. We select $w \in C_c^1(\Omega)$, we multiply the equations in (3.1) with

w and we integrate over the domain in order to obtain:

$$\begin{aligned} & \sigma_{\text{int}} \int_{\Omega_{\text{int}}^\varepsilon} \Delta u w \, dx + \sigma_{\text{ext}} \int_{\Omega_{\text{ext}}^\varepsilon} \Delta u w \, dx + \hat{\sigma}_0 \varepsilon^{-3} \int_{\Omega_{\text{lay}}^\varepsilon} \Delta u w \, dx \\ &= \int_{\Omega_{\text{int}}^\varepsilon} f_{\text{int}} w \, dx + \int_{\Omega_{\text{ext}}^\varepsilon} f_{\text{ext}} w \, dx + \int_{\Omega_{\text{lay}}^\varepsilon} f_{\text{lay}} w \, dx. \end{aligned}$$

We integrate by parts and we have

$$\begin{aligned} & \sigma_{\text{int}} \int_{\Omega_{\text{int}}^\varepsilon} \nabla u \cdot \nabla w + \sigma_{\text{ext}} \int_{\Omega_{\text{ext}}^\varepsilon} \nabla u \cdot \nabla w \, dx + \hat{\sigma}_0 \varepsilon^{-3} \int_{\Omega_{\text{lay}}^\varepsilon} \nabla u \cdot \nabla w \, dx \\ &= - \int_{\Omega_{\text{int}}^\varepsilon} f_{\text{int}} w \, dx - \int_{\Omega_{\text{ext}}^\varepsilon} f_{\text{ext}} w \, dx - \int_{\Omega_{\text{lay}}^\varepsilon} f_{\text{lay}} w \, dx + \int_{\Gamma_{\text{int}}^\varepsilon} g_{\text{int}} w \, ds + \int_{\Gamma_{\text{ext}}^\varepsilon} g_{\text{ext}} w \, ds. \end{aligned}$$

We say that a function $u \in C^1(\Omega)$ satisfying the above variational equation is a weak solution to (3.1). As $C_c^1(\Omega)$ is dense in $H_0^1(\Omega)$, this identity is also true for $w \in H_0^1(\Omega)$. We check that a weak solution is also a strong solution. If we assume $u \in C^2(\bar{\Omega})$, $u = 0$ in $\partial\Omega$ and it satisfies (3.2), (i.e. u is a classical solution of (3.1)) integrating by parts we obtain

$$\begin{aligned} & \sigma_{\text{int}} \int_{\Omega_{\text{int}}^\varepsilon} (\Delta u - f_{\text{int}}) w \, dx + \sigma_{\text{ext}} \int_{\Omega_{\text{ext}}^\varepsilon} (\Delta u - f_{\text{ext}}) w \, dx \\ & \quad + \hat{\sigma}_0 \varepsilon^{-3} \int_{\Omega_{\text{lay}}^\varepsilon} (\Delta u - f_{\text{lay}}) w \, dx = 0. \end{aligned}$$

As $C_c^1(\Omega)$ is dense in $L^2(\Omega)$, we deduce that u satisfies (3.1) almost everywhere, and in fact everywhere because $u \in C^2(\bar{\Omega})$. If u is not a classical solution, it is still possible to prove this result using the green formula in $H^1(\Delta) = \{u : u \in H^1(\Omega^\varepsilon) \text{ and } \Delta u \in L^2(\Omega^\varepsilon)\}$. Now we give the theorem and proof that guarantees the existence and uniqueness of a solution to this problem and present some uniform estimates for this solution.

Theorem 1. *For all $\varepsilon > 0$ there exists a unique $u \in H_0^1(\Omega)$, solution to Problem (3.2) with data $f \in L^2(\Omega)$, $g_{\text{int}} \in L^2(\Gamma_{\text{int}}^\varepsilon)$, $g_{\text{ext}} \in L^2(\Gamma_{\text{ext}}^\varepsilon)$. Moreover, there exists $\varepsilon_0 > 0$ and a constant $C > 0$, such that for all $\varepsilon \in (0, \varepsilon_0)$,*

$$\|u\|_{1,\Omega} \leq C \left(\|f\|_{0,\Omega} + \|g_{\text{int}}\|_{0,\Gamma_{\text{int}}^\varepsilon} + \|g_{\text{ext}}\|_{0,\Gamma_{\text{ext}}^\varepsilon} \right).$$

Proof. We would like to employ the Lax-Milgram Lemma. For that purpose, we have to first prove that the bilinear form a is coercive and continuous in $H_0^1(\Omega)$, and that the linear form l is continuous in $H_0^1(\Omega)$. We start by proving coerciveness of

a in $H_0^1(\Omega)$. For that purpose, applying Poincaré inequality, there exist a constant k_1 such that for all $w \in H_0^1(\Omega)$

$$\int_{\Omega} |w|^2 dx \leq k_1 \int_{\Omega} |\nabla w|^2 dx \Rightarrow \|w\|_{1,\Omega}^2 \leq k_2 \|\nabla w\|_{0,\Omega}^2, \quad (3.3)$$

where $k_2 = k_1 + 1$. Substituting $u = w$ in the definition of a and applying (3.3) we obtain

$$\begin{aligned} a(w, w) &= \sigma_{\text{int}} \int_{\Omega_{\text{int}}^{\varepsilon}} |\nabla w|^2 dx + \sigma_{\text{ext}} \int_{\Omega_{\text{ext}}^{\varepsilon}} |\nabla w|^2 dx + \widehat{\sigma}_0 \varepsilon^{-3} \int_{\Omega_{\text{lay}}^{\varepsilon}} |\nabla w|^2 dx \\ &\geq \min(\sigma_{\text{int}}, \sigma_{\text{ext}}, \widehat{\sigma}_0 \varepsilon^{-3}) \|\nabla w\|_{0,\Omega}^2 \\ &\geq k_3 \|w\|_{1,\Omega}^2, \end{aligned} \quad (3.4)$$

where $k_3 = \frac{1}{k_2} \min(\sigma_{\text{int}}, \sigma_{\text{ext}}, \widehat{\sigma}_0 \varepsilon^{-3})$. With this, the coerciveness of a in $H_0^1(\Omega)$ gets proved. Now we would like to prove the continuity of l in $H_0^1(\Omega)$. For that purpose, let us first define the Dirichlet trace operator. Let Σ be the boundary of O , where $O \in \{\Omega_{\text{int}}^{\varepsilon}, \Omega_{\text{ext}}^{\varepsilon}\}$, the Dirichlet trace operator is defined as

$$\begin{aligned} \gamma_{\Sigma} : H^1(O) &\longrightarrow H^{\frac{1}{2}}(\Sigma) \\ w &\longmapsto w_{\Sigma} := w|_{\Sigma}. \end{aligned} \quad (3.5)$$

Let $k_4 > 0$ be the continuity constant of the Dirichlet trace operator γ_{Σ} . Then, for all $w \in H^1(O)$ we obtain

$$\|\gamma_{\Sigma}(w)\|_{\frac{1}{2},\Sigma} = \|w_{\Sigma}\|_{\frac{1}{2},\Sigma} \leq k_4 \|w\|_{1,O}.$$

For the sake of simplicity, we write w instead of $w_{\Gamma_{\text{int}}^{\varepsilon}}$ and $w_{\Gamma_{\text{ext}}^{\varepsilon}}$. Applying this result and the Cauchy-Schwarz inequality to the definition of l , we obtain

$$\begin{aligned} |l(w)| &\leq \|f_{\text{int}}\|_{0,\Omega_{\text{int}}^{\varepsilon}} \|w\|_{0,\Omega_{\text{int}}^{\varepsilon}} + \|f_{\text{ext}}\|_{0,\Omega_{\text{ext}}^{\varepsilon}} \|w\|_{0,\Omega_{\text{ext}}^{\varepsilon}} + \|f_{\text{lay}}\|_{0,\Omega_{\text{lay}}^{\varepsilon}} \|w\|_{0,\Omega_{\text{lay}}^{\varepsilon}} \\ &\quad + \|g_{\text{int}}\|_{0,\Gamma_{\text{int}}^{\varepsilon}} \|w\|_{0,\Gamma_{\text{int}}^{\varepsilon}} + \|g_{\text{ext}}\|_{0,\Gamma_{\text{ext}}^{\varepsilon}} \|w\|_{0,\Gamma_{\text{ext}}^{\varepsilon}} \\ &\leq k_5 \|w\|_{1,\Omega} \left(\|f_{\text{int}}\|_{0,\Omega_{\text{int}}^{\varepsilon}} + \|f_{\text{ext}}\|_{0,\Omega_{\text{ext}}^{\varepsilon}} + \|f_{\text{lay}}\|_{0,\Omega_{\text{lay}}^{\varepsilon}} \right. \\ &\quad \left. + \|g_{\text{int}}\|_{0,\Gamma_{\text{int}}^{\varepsilon}} + \|g_{\text{ext}}\|_{0,\Gamma_{\text{ext}}^{\varepsilon}} \right), \end{aligned} \quad (3.6)$$

where $k_5 = \max(1, k_4)$. This proves the continuity of l in space $H_0^1(\Omega)$. Finally, we prove the continuity of a in $H_0^1(\Omega)$, applying the Cauchy-Schwarz inequality to the definition of a , for $u \in H_0^1(\Omega)$, we deduce

$$\begin{aligned}
|a(u, w)| &\leq \sigma_{\text{int}} \|\nabla u\|_{0, \Omega_{\text{int}}^\varepsilon} \|\nabla w\|_{0, \Omega_{\text{int}}^\varepsilon} + \sigma_{\text{ext}} \|\nabla u\|_{0, \Omega_{\text{ext}}^\varepsilon} \|\nabla w\|_{0, \Omega_{\text{ext}}^\varepsilon} \\
&\quad + \widehat{\sigma}_0 \varepsilon^{-3} \|\nabla u\|_{0, \Omega_{\text{lay}}^\varepsilon} \|\nabla w\|_{0, \Omega_{\text{lay}}^\varepsilon} \\
&\leq \left(\sigma_{\text{int}} + \sigma_{\text{ext}} + \widehat{\sigma}_0 \varepsilon^{-3} \right) \|\nabla u\|_{0, \Omega} \|\nabla w\|_{0, \Omega} \\
&\leq k_6 \|u\|_{1, \Omega} \|w\|_{1, \Omega},
\end{aligned} \tag{3.7}$$

where $k_6 = \sigma_{\text{int}} + \sigma_{\text{ext}} + \widehat{\sigma}_0 \varepsilon^{-3}$. The identity (3.4) proves that a is coercive in $H_0^1(\Omega)$, the identity (3.7) assures that a is continuous in $H_0^1(\Omega)$, and the identity (3.6) demonstrates that l is continuous in $H_0^1(\Omega)$. We now apply the Lax-Milgram Lemma to conclude that there exists a unique $u \in H_0^1(\Omega)$ such that for all $w \in H_0^1(\Omega)$,

$$a(u, w) = l(w).$$

To prove the second part of the theorem, dealing with uniform estimates, we select

$$\varepsilon_0 = \sqrt[3]{\frac{\widehat{\sigma}_0}{\min(\sigma_{\text{int}}, \sigma_{\text{ext}})}}.$$

Then, for any $\varepsilon \in (0, \varepsilon_0)$ and taking $w = u$ in (3.4), we obtain

$$|a(u, u)| \geq k_7 \|u\|_{1, \Omega}^2, \tag{3.8}$$

where $k_7 = \frac{1}{k_2} \min(\sigma_{\text{int}}, \sigma_{\text{ext}})$. On the other hand, we take $w = u$ in (3.6), and we obtain

$$\begin{aligned}
|l(u)| &\leq k_5 \|u\|_{1, \Omega} \left(\|f_{\text{int}}\|_{0, \Omega_{\text{int}}^\varepsilon} + \|f_{\text{ext}}\|_{0, \Omega_{\text{ext}}^\varepsilon} + \|f_{\text{lay}}\|_{0, \Omega_{\text{lay}}^\varepsilon} \right. \\
&\quad \left. + \|g_{\text{int}}\|_{0, \Gamma_{\text{int}}^\varepsilon} + \|g_{\text{ext}}\|_{0, \Gamma_{\text{ext}}^\varepsilon} \right).
\end{aligned} \tag{3.9}$$

Finally, taking $w = u$ in the variational formulation

$$|a(u, u)| = |l(u)|$$

and applying (3.8) in the left-hand side and (3.9) in the right-hand side, we obtain

$$k_7 \|u\|_{1,\Omega}^2 \leq k_5 \|u\|_{1,\Omega} \left(\|f_{\text{int}}\|_{0,\Omega_{\text{int}}^\varepsilon} + \|f_{\text{ext}}\|_{0,\Omega_{\text{ext}}^\varepsilon} + \|f_{\text{lay}}\|_{0,\Omega_{\text{lay}}^\varepsilon} + \|g_{\text{int}}\|_{0,\Gamma_{\text{int}}^\varepsilon} + \|g_{\text{ext}}\|_{0,\Gamma_{\text{ext}}^\varepsilon} \right).$$

Denoting $C = \frac{k_5}{k_7}$ we derive the desired result

$$\|u\|_{1,\Omega} \leq C \left(\|f_{\text{int}}\|_{0,\Omega_{\text{int}}^\varepsilon} + \|f_{\text{ext}}\|_{0,\Omega_{\text{ext}}^\varepsilon} + \|f_{\text{lay}}\|_{0,\Omega_{\text{lay}}^\varepsilon} + \|g_{\text{int}}\|_{0,\Gamma_{\text{int}}^\varepsilon} + \|g_{\text{ext}}\|_{0,\Gamma_{\text{ext}}^\varepsilon} \right).$$

□

3.3 Convergence of the asymptotic expansion for the reference model

We start by defining the residue for the reference Problem (1.2). We use domain Ω defined in Figure 1.1. The residue of order N of the asymptotic expansion (1.4) is defined by removing the first N terms to the solution u of the reference Problem (1.2).

Definition 5. *Let u be the solution to Problem (1.2). Given the expansion in power series (1.4) and a specific order $N \in \mathbb{N}$, we define the residue r^N as*

$$\begin{cases} r_{\text{int}}^N(x, y) = u_{\text{int}}(x, y) - \sum_{k=0}^N \varepsilon^k u_{\text{int}}^k(x, y) & \text{in } \Omega_{\text{int}}^\varepsilon, \\ r_{\text{ext}}^N(x, y) = u_{\text{ext}}(x, y) - \sum_{k=0}^N \varepsilon^k u_{\text{ext}}^k(x, y) & \text{in } \Omega_{\text{ext}}^\varepsilon, \\ r_{\text{lay}}^N(x, y) = u_{\text{lay}}(x, y) - \sum_{k=0}^N \varepsilon^k U^k \left(\frac{x - x_0}{\varepsilon}, y \right) & \text{in } \Omega_{\text{lay}}^\varepsilon. \end{cases}$$

Proposition 7. *Let $N \in \mathbb{N}$. The residue r^N defined in Definition 5 satisfies the*

following equations

$$\left\{ \begin{array}{ll} \sigma_{int} \Delta r_{int}^N = 0 & \text{in } \Omega_{int}^\varepsilon, \\ \sigma_{ext} \Delta r_{ext}^N = 0 & \text{in } \Omega_{ext}^\varepsilon, \\ \widehat{\sigma}_0 \varepsilon^{-3} \Delta r_{lay}^N = f_{lay}^N & \text{in } \Omega_{lay}^\varepsilon, \\ r_{int}^N = r_{lay}^N & \text{on } \Gamma_{int}^\varepsilon, \\ r_{lay}^N = r_{ext}^N & \text{on } \Gamma_{ext}^\varepsilon, \\ \widehat{\sigma}_0 \varepsilon^{-3} \partial_n r_{lay}^N - \sigma_{int} \partial_n r_{int}^N = g_{int}^N & \text{on } \Gamma_{int}^\varepsilon, \\ \widehat{\sigma}_0 \varepsilon^{-3} \partial_n r_{lay}^N - \sigma_{ext} \partial_n r_{ext}^N = g_{ext}^N & \text{on } \Gamma_{ext}^\varepsilon, \\ r^N = 0 & \text{on } \partial\Omega, \end{array} \right.$$

where

$$\begin{aligned} f_{lay}^N &= \varepsilon^{N-4} \left(-\widehat{\sigma}_0 \partial_y^2 u_{lay}^{N-1} - \varepsilon \widehat{\sigma}_0 \partial_y^2 u_{lay}^N \right), \\ g_{int}^N &= \varepsilon^{N-3} \left(\sigma_{int} \partial_n u_{int}^{N-3} + \dots + \varepsilon^3 \sigma_{int} \partial_n u_{int}^N \right), \\ g_{ext}^N &= \varepsilon^{N-4} \left(\sigma_{ext} \partial_n u_{ext}^{N-3} + \dots + \varepsilon^3 \sigma_{ext} \partial_n u_{ext}^N \right). \end{aligned} \quad (3.10)$$

Proof. We deduce this result by applying Equations (1.5), (1.6), (1.7), and (3.1) to the definition of the residue.

Equation in Ω_{int}^ε :

$$\begin{aligned} \sigma_{int} \Delta r_{int}^N(x, y) &= \sigma_{int} \Delta u_{int} - \sum_{k=0}^N \varepsilon^k \sigma_{int} \Delta u_{int}^k(x, y) \\ &= f_{int}(x, y) - \sigma_{int} \Delta u_{int}^0(x, y) - \sum_{k=1}^N \varepsilon^k \sigma_{int} \Delta u_{int}^k(x, y) = 0. \end{aligned}$$

Equation in Ω_{ext}^ε :

$$\begin{aligned} \sigma_{ext} \Delta r_{ext}^N(x, y) &= \sigma_{ext} \Delta u_{ext} - \sum_{k=0}^N \varepsilon^k \sigma_{ext} \Delta u_{ext}^k(x, y) \\ &= f_{ext}(x, y) - \sigma_{ext} \Delta u_{ext}^0(x, y) - \sum_{k=1}^N \varepsilon^k \sigma_{ext} \Delta u_{ext}^k(x, y) = 0. \end{aligned}$$

Equation in $\Omega_{\text{lay}}^\varepsilon$: We remark that we have defined the variable X as $X = \frac{x - x_0}{\varepsilon}$. Then, we have

$$\begin{aligned}
\hat{\sigma}_0 \varepsilon^{-3} \Delta r_{\text{lay}}^N(x, y) &= \hat{\sigma}_0 \varepsilon^{-3} \Delta u_{\text{lay}}(x, y) - \sum_{k=0}^N \varepsilon^{k-3} \hat{\sigma}_0 \Delta U^k(X, y) \\
&= \sum_{k=0}^N \varepsilon^{k-5} \hat{\sigma}_0 \partial_X^2 U^k(X, y) + \sum_{k=0}^N \varepsilon^{k-3} \hat{\sigma}_0 \partial_y^2 U^k(X, y) \\
&= \varepsilon^{-5} \hat{\sigma}_0 \partial_X^2 U^0(X, y) + \varepsilon^{-4} \hat{\sigma}_0 \partial_X^2 U^1(X, y) \\
&\quad + \varepsilon^{N-4} \hat{\sigma}_0 \partial_X^2 U^{N+1}(X, y) + \varepsilon^{N-3} \hat{\sigma}_0 \partial_X^2 U^{N+2}(X, y) \\
&\quad + \sum_{k=0}^{N-2} \varepsilon^{k-3} \hat{\sigma}_0 \left(\partial_X^2 U^{k+2}(X, y) - \partial_y^2 U^k(X, y) \right) \\
&= \varepsilon^{N-4} \hat{\sigma}_0 \left(-\partial_y^2 U^{N-1}(X, y) - \varepsilon \partial_y^2 U^N(X, y) \right), \\
&= \varepsilon^{N-4} \hat{\sigma}_0 \left(-\partial_y^2 u_{\text{lay}}^{N-1}(x, y) - \varepsilon \partial_y^2 u_{\text{lay}}^N(x, y) \right).
\end{aligned}$$

Equation on $\Gamma_{\text{int}}^\varepsilon$:

$$\begin{aligned}
r_{\text{lay}}^N \left(x_0 - \frac{\varepsilon}{2}, y \right) &= u_{\text{lay}} \left(x_0 - \frac{\varepsilon}{2}, y \right) - \sum_{k=0}^N \varepsilon^k U^k \left(-\frac{1}{2}, y \right) \\
&= u_{\text{int}} \left(x_0 - \frac{\varepsilon}{2}, y \right) - \sum_{k=0}^N \varepsilon^k u_{\text{int}}^k \left(x_0 - \frac{\varepsilon}{2}, y \right) = r_{\text{int}}^N \left(x_0 - \frac{\varepsilon}{2}, y \right).
\end{aligned}$$

Equation on $\Gamma_{\text{ext}}^\varepsilon$:

$$\begin{aligned}
r_{\text{lay}}^N \left(x_0 + \frac{\varepsilon}{2}, y \right) &= u_{\text{lay}} \left(x_0 + \frac{\varepsilon}{2}, y \right) - \sum_{k=0}^N \varepsilon^k U^k \left(\frac{1}{2}, y \right) \\
&= u_{\text{ext}} \left(x_0 + \frac{\varepsilon}{2}, y \right) - \sum_{k=0}^N \varepsilon^k u_{\text{ext}}^k \left(x_0 + \frac{\varepsilon}{2}, y \right) = r_{\text{ext}}^N \left(x_0 + \frac{\varepsilon}{2}, y \right).
\end{aligned}$$

Equation on $\Gamma_{\text{int}}^\varepsilon$:

$$\begin{aligned}
& \widehat{\sigma}_0 \varepsilon^{-3} \partial_n r_{\text{lay}}^N \left(x_0 - \frac{\varepsilon}{2}, y \right) = \widehat{\sigma}_0 \varepsilon^{-3} \partial_n u_{\text{lay}} \left(x_0 - \frac{\varepsilon}{2}, y \right) - \widehat{\sigma}_0 \sum_{k=0}^N \varepsilon^{k-4} \partial_X U^k \left(-\frac{1}{2}, y \right) \\
& = \sigma_{\text{int}} \partial_n u_{\text{int}} \left(x_0 - \frac{\varepsilon}{2}, y \right) - \sigma_{\text{int}} \sum_{k=0}^N \varepsilon^{k-4} \partial_n u_{\text{int}}^{k-4} \left(x_0 - \frac{\varepsilon}{2}, y \right) \\
& = \sigma_{\text{int}} \partial_n u_{\text{int}} \left(x_0 - \frac{\varepsilon}{2}, y \right) - \sigma_{\text{int}} \sum_{k=0}^N \varepsilon^k \partial_n u_{\text{int}}^k \left(x_0 - \frac{\varepsilon}{2}, y \right) \\
& \quad + \varepsilon^{N-3} \left(\sigma_{\text{int}} \partial_n u_{\text{int}}^{N-3} \left(x_0 - \frac{\varepsilon}{2}, y \right) + \dots + \varepsilon^3 \sigma_{\text{int}} \partial_n u_{\text{int}}^N \left(x_0 - \frac{\varepsilon}{2}, y \right) \right) \\
& = \sigma_{\text{int}} \partial_n r_{\text{int}}^N \left(x_0 - \frac{\varepsilon}{2}, y \right) \\
& \quad + \varepsilon^{N-3} \left(\sigma_{\text{int}} \partial_n u_{\text{int}}^{N-3} \left(x_0 - \frac{\varepsilon}{2}, y \right) + \dots + \varepsilon^3 \sigma_{\text{int}} \partial_n u_{\text{int}}^N \left(x_0 - \frac{\varepsilon}{2}, y \right) \right).
\end{aligned}$$

Equation on $\Gamma_{\text{ext}}^\varepsilon$:

$$\begin{aligned}
& \widehat{\sigma}_0 \varepsilon^{-3} \partial_n r_{\text{lay}}^N \left(x_0 + \frac{\varepsilon}{2}, y \right) = \widehat{\sigma}_0 \varepsilon^{-3} \partial_n u_{\text{lay}} \left(x_0 + \frac{\varepsilon}{2}, y \right) - \widehat{\sigma}_0 \sum_{k=0}^N \varepsilon^{k-4} \partial_X U^k \left(\frac{1}{2}, y \right) \\
& = \sigma_{\text{ext}} \partial_n u_{\text{ext}} \left(x_0 + \frac{\varepsilon}{2}, y \right) - \sigma_{\text{ext}} \sum_{k=0}^N \varepsilon^{k-4} \partial_n u_{\text{ext}}^{k-4} \left(x_0 + \frac{\varepsilon}{2}, y \right) \\
& = \sigma_{\text{ext}} \partial_n u_{\text{ext}} \left(x_0 + \frac{\varepsilon}{2}, y \right) - \sigma_{\text{ext}} \sum_{k=0}^N \varepsilon^k \partial_n u_{\text{ext}}^k \left(x_0 + \frac{\varepsilon}{2}, y \right) \\
& \quad + \varepsilon^{N-3} \left(\sigma_{\text{ext}} \partial_n u_{\text{ext}}^{N-3} \left(x_0 + \frac{\varepsilon}{2}, y \right) + \dots + \varepsilon^3 \sigma_{\text{ext}} \partial_n u_{\text{ext}}^N \left(x_0 + \frac{\varepsilon}{2}, y \right) \right) \\
& = \sigma_{\text{ext}} \partial_n r_{\text{ext}}^N \left(x_0 + \frac{\varepsilon}{2}, y \right) \\
& \quad + \varepsilon^{N-3} \left(\sigma_{\text{ext}} \partial_n u_{\text{ext}}^{N-3} \left(x_0 + \frac{\varepsilon}{2}, y \right) + \dots + \varepsilon^3 \sigma_{\text{ext}} \partial_n u_{\text{ext}}^N \left(x_0 + \frac{\varepsilon}{2}, y \right) \right).
\end{aligned}$$

□

Theorem 2. *Let $N \in \mathbb{N}$. For $\varepsilon \in (0, \varepsilon_0)$ and under the assumptions $f_{\text{lay}}^N \in L^2(\Omega_{\text{lay}}^\varepsilon)$, $g_{\text{int}}^N \in L^2(\Gamma_{\text{int}}^\varepsilon)$, $g_{\text{ext}}^N \in L^2(\Gamma_{\text{ext}}^\varepsilon)$, $f_{\text{lay}}^{N+5} \in L^2(\Omega_{\text{lay}}^\varepsilon)$, $g_{\text{int}}^{N+5} \in L^2(\Gamma_{\text{int}}^\varepsilon)$, $g_{\text{ext}}^{N+5} \in L^2(\Gamma_{\text{ext}}^\varepsilon)$, and $u^k \in H^1(\Omega^\varepsilon)$ for $k \leq N+5$, the following estimate holds for*

the residue defined in Definition 5,

$$\|r_{ext}^N\|_{1,\Omega_{ext}^\varepsilon} + \|r_{int}^N\|_{1,\Omega_{int}^\varepsilon} + \sqrt{\varepsilon} \|r_{lay}^N\|_{1,\Omega_{lay}^\varepsilon} \leq C\varepsilon^{N+1},$$

for a positive constant $C > 0$ independent of ε .

Proof. Applying Theorem 1 and Proposition 7, for $\varepsilon \in (0, \varepsilon_0)$, we deduce that there exists a unique $r^N \in H_0^1(\Omega)$ and it satisfies the following estimate

$$\begin{aligned} \|r^N\|_{1,\Omega} \leq & C \left(\varepsilon^{N-4} \widehat{\sigma}_0 \left\| \partial_y^2 u_{lay}^{N-1} \right\|_{0,\Omega_{lay}^\varepsilon} + \varepsilon^{N-5} \widehat{\sigma}_0 \left\| \partial_y^2 u_{lay}^N \right\|_{0,\Omega_{lay}^\varepsilon} \right. \\ & + \varepsilon^{N-3} \sigma_{int} \left\| \partial_n u_{int}^{N-3} \right\|_{0,\Gamma_{int}^\varepsilon} + \dots + \varepsilon^N \sigma_{int} \left\| \partial_n u_{int}^N \right\|_{0,\Gamma_{int}^\varepsilon} \\ & \left. + \varepsilon^{N-3} \sigma_{ext} \left\| \partial_n u_{ext}^{N-3} \right\|_{0,\Gamma_{ext}^\varepsilon} + \dots + \varepsilon^N \sigma_{ext} \left\| \partial_n u_{ext}^N \right\|_{0,\Gamma_{ext}^\varepsilon} \right). \end{aligned}$$

We deduce that $\|r^N\|_{1,\Omega} = O(\varepsilon^{N-4})$. We concentrate now on the part of the domain which is outside the thin layer. In Ω_{int}^ε we have

$$\begin{aligned} \|r_{int}^N\|_{1,\Omega_{int}^\varepsilon} \leq & \|r_{int}^{N+5}\|_{1,\Omega_{int}^\varepsilon} + \varepsilon^{N+1} \|u_{int}^{N+1}\|_{1,\Omega_{int}^\varepsilon} + \varepsilon^{N+2} \|u_{int}^{N+2}\|_{1,\Omega_{int}^\varepsilon} \\ & + \varepsilon^{N+3} \|u_{int}^{N+3}\|_{1,\Omega_{int}^\varepsilon} + \varepsilon^{N+4} \|u_{int}^{N+4}\|_{1,\Omega_{int}^\varepsilon} + \varepsilon^{N+5} \|u_{int}^{N+5}\|_{1,\Omega_{int}^\varepsilon}. \end{aligned}$$

We deduce that $\|r_{int}^N\|_{1,\Omega_{int}^\varepsilon} = O(\varepsilon^{N+1})$. In Ω_{ext}^ε we have

$$\begin{aligned} \|r_{ext}^N\|_{1,\Omega_{ext}^\varepsilon} \leq & \|r_{ext}^{N+5}\|_{1,\Omega_{ext}^\varepsilon} + \varepsilon^{N+1} \|u_{ext}^{N+1}\|_{1,\Omega_{ext}^\varepsilon} + \varepsilon^{N+2} \|u_{ext}^{N+2}\|_{1,\Omega_{ext}^\varepsilon} \\ & + \varepsilon^{N+3} \|u_{ext}^{N+3}\|_{1,\Omega_{ext}^\varepsilon} + \varepsilon^{N+4} \|u_{ext}^{N+4}\|_{1,\Omega_{ext}^\varepsilon} + \varepsilon^{N+5} \|u_{ext}^{N+5}\|_{1,\Omega_{ext}^\varepsilon}. \end{aligned}$$

We conclude that $\|r_{ext}^N\|_{1,\Omega_{ext}^\varepsilon} = O(\varepsilon^{N+1})$. Now we focus on the part corresponding

to the layer. Here we have

$$\begin{aligned}
\|u_{\text{lay}}^k\|_{1,\Omega_{\text{lay}}^\varepsilon} &= \left(\int_{\Omega_{\text{lay}}^\varepsilon} |u_{\text{lay}}^k|^2 dx + \int_{\Omega_{\text{lay}}^\varepsilon} |\nabla u_{\text{lay}}^k|^2 dx \right)^{\frac{1}{2}} \\
&= \left(\int_0^{y_0} \int_{-\frac{\varepsilon}{2}}^{\frac{\varepsilon}{2}} \left| U^k \left(\frac{x-x_0}{\varepsilon}, y \right) \right|^2 dx dy + \int_0^{y_0} \int_{-\frac{\varepsilon}{2}}^{\frac{\varepsilon}{2}} \left| \partial_x U^k \left(\frac{x-x_0}{\varepsilon}, y \right) \right|^2 dx dy \right. \\
&\quad \left. + \int_0^{y_0} \int_{-\frac{\varepsilon}{2}}^{\frac{\varepsilon}{2}} \left| \partial_y U^k \left(\frac{x-x_0}{\varepsilon}, y \right) \right|^2 dx dy \right)^{\frac{1}{2}} \\
&= \left(\int_0^{y_0} \int_{-\frac{1}{2}}^{\frac{1}{2}} |U^k(X, y)|^2 \varepsilon dX dy + \int_0^{y_0} \int_{-\frac{1}{2}}^{\frac{1}{2}} |\varepsilon^{-1} \partial_x U^k(X, y)|^2 \varepsilon dX dy \right. \\
&\quad \left. + \int_0^{y_0} \int_{-\frac{1}{2}}^{\frac{1}{2}} |\partial_y U^k(X, y)|^2 \varepsilon dX dy \right)^{\frac{1}{2}}.
\end{aligned}$$

We conclude that $\|u_{\text{lay}}^k\|_{1,\Omega_{\text{lay}}^\varepsilon} = O(\varepsilon^{-\frac{1}{2}})$. Thus, taking this into account, we obtain

$$\begin{aligned}
\|r_{\text{lay}}^N\|_{1,\Omega_{\text{lay}}^\varepsilon} &\leq \|r_{\text{lay}}^{N+5}\|_{1,\Omega_{\text{lay}}^\varepsilon} + \varepsilon^{N+1} \|u_{\text{lay}}^{N+1}\|_{1,\Omega_{\text{lay}}^\varepsilon} + \varepsilon^{N+2} \|u_{\text{lay}}^{N+2}\|_{1,\Omega_{\text{lay}}^\varepsilon} \\
&\quad + \varepsilon^{N+3} \|u_{\text{lay}}^{N+3}\|_{1,\Omega_{\text{lay}}^\varepsilon} + \varepsilon^{N+4} \|u_{\text{lay}}^{N+4}\|_{1,\Omega_{\text{lay}}^\varepsilon} + \varepsilon^{N+5} \|u_{\text{lay}}^{N+6}\|_{1,\Omega_{\text{lay}}^\varepsilon}.
\end{aligned}$$

We deduce that $\|r_{\text{lay}}^N\|_{1,\Omega_{\text{lay}}^\varepsilon} = O(\varepsilon^{N+\frac{1}{2}})$. Now we deduce the desired result

$$\|r_{\text{ext}}^N\|_{1,\Omega_{\text{ext}}^\varepsilon} + \|r_{\text{int}}^N\|_{1,\Omega_{\text{int}}^\varepsilon} + \sqrt{\varepsilon} \|r_{\text{lay}}^N\|_{1,\Omega_{\text{lay}}^\varepsilon} \leq C\varepsilon^{N+1}.$$

□

Remark 4. We remark that the assumptions of Theorem 2 are rather strong assumptions because in general the expansion consumes regularity at each order and the first term of the expansion u^0 , solution to (1.13), belongs only to $H^3(\Omega^\varepsilon)$.

3.4 Validation of the equivalent conditions: first class of ITCs

3.4.1 Second-order model: variational formulation

This section is devoted to the derivation of a variational formulation for the second-order asymptotic model we have derived in Section 1.3.2. This is required to develop a performance assessment by applying a finite element method and it will also be necessary for the convergence proofs presented in the following sections.

Problem (1.18) is uncoupled into two independent problems. Therefore we write two variational formulations, one for each problem. We introduce functional spaces $H_0^1(\Omega_{\text{int}}^\varepsilon)$ and $H_0^1(\Omega_{\text{ext}}^\varepsilon)$ as the functional framework.

We multiply the equations of Problem (1.18) defined over $\Omega_{\text{int}}^\varepsilon$ and $\Omega_{\text{ext}}^\varepsilon$ by test functions $w_{\text{int}} \in H_0^1(\Omega_{\text{int}}^\varepsilon)$ and $w_{\text{ext}} \in H_0^1(\Omega_{\text{ext}}^\varepsilon)$. Then, we integrate over the domains and we obtain

$$\begin{aligned} \int_{\Omega_{\text{int}}^\varepsilon} f_{\text{int}} w_{\text{int}} \, dx &= \int_{\Omega_{\text{int}}^\varepsilon} \sigma_{\text{int}} \Delta u_{\text{int}} w_{\text{int}} \, dx, \\ \int_{\Omega_{\text{ext}}^\varepsilon} f_{\text{ext}} w_{\text{ext}} \, dx &= \int_{\Omega_{\text{ext}}^\varepsilon} \sigma_{\text{ext}} \Delta u_{\text{ext}} w_{\text{ext}} \, dx. \end{aligned}$$

Integrating by parts, we obtain

$$\begin{aligned} - \int_{\Omega_{\text{int}}^\varepsilon} f_{\text{int}} w_{\text{int}} \, dx &= \int_{\Omega_{\text{int}}^\varepsilon} \sigma_{\text{int}} \nabla u_{\text{int}} \cdot \nabla w_{\text{int}} \, dx - \int_{\partial\Omega_{\text{int}}^\varepsilon} \sigma_{\text{int}} \partial_n u_{\text{int}} w_{\text{int}} \, ds, \\ - \int_{\Omega_{\text{ext}}^\varepsilon} f_{\text{ext}} w_{\text{ext}} \, dx &= \int_{\Omega_{\text{ext}}^\varepsilon} \sigma_{\text{ext}} \nabla u_{\text{ext}} \cdot \nabla w_{\text{ext}} \, dx - \int_{\partial\Omega_{\text{ext}}^\varepsilon} \sigma_{\text{ext}} \partial_n u_{\text{ext}} w_{\text{ext}} \, ds. \end{aligned}$$

If we take into account the properties of the test functions, we directly deduce the variational formulations for both uncoupled problems (1.18). Assuming $f_{\text{int}} \in L^2(\Omega_{\text{int}}^\varepsilon)$ and $f_{\text{ext}} \in L^2(\Omega_{\text{ext}}^\varepsilon)$, the problem reduces to finding $u_{\text{int}} \in H_0^1(\Omega_{\text{int}}^\varepsilon)$ such that for all $w_{\text{int}} \in H_0^1(\Omega_{\text{int}}^\varepsilon)$

$$- \int_{\Omega_{\text{int}}^\varepsilon} f_{\text{int}} w_{\text{int}} \, dx = \int_{\Omega_{\text{int}}^\varepsilon} \sigma_{\text{int}} \nabla u_{\text{int}} \cdot \nabla w_{\text{int}} \, dx, \quad (3.11)$$

and finding $u_{\text{ext}} \in H_0^1(\Omega_{\text{ext}}^\varepsilon)$ such that for all $w_{\text{ext}} \in H_0^1(\Omega_{\text{ext}}^\varepsilon)$

$$- \int_{\Omega_{\text{ext}}^\varepsilon} f_{\text{ext}} w_{\text{ext}} \, dx = \int_{\Omega_{\text{ext}}^\varepsilon} \sigma_{\text{ext}} \nabla u_{\text{ext}} \cdot \nabla w_{\text{ext}} \, dx. \quad (3.12)$$

3.4.2 Fourth-order model: variational formulation

In this section we derive a variational formulation for the fourth-order asymptotic model we have derived in Section 1.3.2. This is required to perform a performance assessment by applying a finite element method and it will also be necessary for the convergence proofs performed in the following sections. Instead of considering Problem (1.19) directly, we will consider the following problem

$$\left\{ \begin{array}{ll} \sigma_{\text{int}} \Delta u_{\text{int}} = f_{\text{int}} & \text{in } \Omega_{\text{int}}^\varepsilon, \\ \sigma_{\text{ext}} \Delta u_{\text{ext}} = f_{\text{ext}} & \text{in } \Omega_{\text{ext}}^\varepsilon, \\ [u]_{\Gamma^\varepsilon} = 0, \\ \varepsilon^{-2} \widehat{\sigma}_0 \frac{d^2}{dy^2} \{u\}_{\Gamma^\varepsilon} + [\sigma \partial_n u]_{\Gamma^\varepsilon} = g, \\ u = 0 & \text{on } \partial\Omega \cap \partial\Omega^\varepsilon. \end{array} \right. \quad (3.13)$$

This problem is similar to Problem (1.19) and it generalizes it by including the right-hand side function g . Thus, the results obtained for this problem can also be applied to Problem (1.19) by simply setting $g \equiv 0$. We begin by selecting the functional space, denoted by V_4 and defined as follows.

Definition 6. *Functional space V_4 is given by*

$$V_4 = \left\{ w : w_{\text{int}} \in H^1(\Omega_{\text{int}}^\varepsilon), w_{\text{ext}} \in H^1(\Omega_{\text{ext}}^\varepsilon), \nabla_{\Gamma^\varepsilon} \{w\} \in L^2(\Gamma^\varepsilon), \right. \\ \left. w|_{\Gamma_{\text{int}}^\varepsilon} = w|_{\Gamma_{\text{ext}}^\varepsilon}, w|_{\partial\Omega \cap \partial\Omega_{\text{int}}^\varepsilon} = 0, w|_{\partial\Omega \cap \partial\Omega_{\text{ext}}^\varepsilon} = 0 \right\}$$

Remark 5. *Mean values and jumps are defined over the interfaces $\Gamma_{\text{int}}^\varepsilon$ and $\Gamma_{\text{ext}}^\varepsilon$. As jump and mean values only depend on the variable y , when we write Γ^ε we are referring to the interval $y \in (0, y_0)$.*

Proposition 8. *Functional space V_4 , characterized in Definition 6, equipped with the norm*

$$\|w\|_{V_4} = \left(\|w\|_{1, \Omega^\varepsilon}^2 + \|\nabla_{\Gamma^\varepsilon} \{w\}\|_{0, \Gamma^\varepsilon}^2 \right)^{\frac{1}{2}},$$

is a Hilbert space.

Proof. As $H^1(\Omega^\varepsilon)$ is a Hilbert space and V_4 is a subspace of $H^1(\Omega^\varepsilon)$, if we prove that V_4 is closed, then, we deduce that V_4 is a Hilbert space. Let us prove that V_4

is closed. Let $\langle w_n \rangle_{n \in \mathbb{N}} \in V_4$ be a convergent sequence in V_4 and let w be its limit. We have to prove that $w \in V_4$.

Since $\langle w_n \rangle_{n \in \mathbb{N}} \in (H^1(\Omega^\varepsilon))_{n \in \mathbb{N}}$, we deduce that $w \in H^1(\Omega^\varepsilon)$. It is enough to verify that $w|_{\Gamma_{\text{int}}^\varepsilon} = w|_{\Gamma_{\text{ext}}^\varepsilon}$ and that $\nabla_{\Gamma^\varepsilon} \{w\} \in L^2(\Gamma^\varepsilon)$. For the first step, let γ_{int} be the Dirichlet trace operator of boundary $\Gamma_{\text{int}}^\varepsilon$ and γ_{ext} be the Dirichlet trace operator of boundary $\Gamma_{\text{ext}}^\varepsilon$, defined in the same as in (3.5). For any $n \in \mathbb{N}$, $w_n \in V_4$, we know that

$$w_{\text{int},n}|_{\Gamma_{\text{int}}^\varepsilon} = w_{\text{ext},n}|_{\Gamma_{\text{ext}}^\varepsilon}. \quad (3.14)$$

Then, since $\langle w_n \rangle_{n \in \mathbb{N}}$ is convergent in $H^1(\Omega^\varepsilon)$, we obtain

$$\begin{cases} w_{\text{int},n} \xrightarrow{n \rightarrow \infty} w_{\text{int}}, \\ w_{\text{ext},n} \xrightarrow{n \rightarrow \infty} w_{\text{ext}}. \end{cases}$$

Finally, as the Dirichlet trace operator is continuous, we deduce that

$$\begin{cases} \gamma_{\text{int}}(w_{\text{int},n}) \xrightarrow{n \rightarrow \infty} \gamma_{\text{int}}(w_{\text{int}}), \\ \gamma_{\text{ext}}(w_{\text{ext},n}) \xrightarrow{n \rightarrow \infty} \gamma_{\text{ext}}(w_{\text{ext}}), \end{cases} \Rightarrow \begin{cases} w_{\text{int},n}|_{\Gamma_{\text{int}}^\varepsilon} \xrightarrow{n \rightarrow \infty} w_{\text{int}}|_{\Gamma_{\text{int}}^\varepsilon}, \\ w_{\text{ext},n}|_{\Gamma_{\text{ext}}^\varepsilon} \xrightarrow{n \rightarrow \infty} w_{\text{ext}}|_{\Gamma_{\text{ext}}^\varepsilon}, \end{cases}$$

and thus, by employing (3.14) we obtain

$$w_{\text{int}}|_{\Gamma_{\text{int}}^\varepsilon} = w_{\text{ext}}|_{\Gamma_{\text{ext}}^\varepsilon}.$$

For the second step, it is only necessary to verify that $\nabla_{\Gamma^\varepsilon} w \in L^2(\Gamma^\varepsilon)$. We know that for any $n \in \mathbb{N}$, $\nabla_{\Gamma^\varepsilon} w_n \in L^2(\Gamma^\varepsilon)$. Then, as $L^2(\Gamma^\varepsilon)$ is a closed space, we deduce that $\nabla_{\Gamma^\varepsilon} w \in L^2(\Gamma^\varepsilon)$. □

We now derive the variational formulation. For that purpose, we select a test function $w \in V_4$ and we multiply the equations in $\Omega_{\text{int}}^\varepsilon$ and $\Omega_{\text{ext}}^\varepsilon$ of Problem (3.13) with this test function

$$\int_{\Omega_{\text{int}}^\varepsilon} f_{\text{int}} w \, dx + \int_{\Omega_{\text{ext}}^\varepsilon} f_{\text{ext}} w \, dx = \int_{\Omega_{\text{int}}^\varepsilon} \sigma_{\text{int}} \Delta u_{\text{int}} w \, dx + \int_{\Omega_{\text{ext}}^\varepsilon} \sigma_{\text{ext}} \Delta u_{\text{ext}} w \, dx.$$

Integrating by parts we obtain

$$\begin{aligned}
& - \int_{\Omega_{\text{int}}^\varepsilon} f_{\text{int}} w \, dx - \int_{\Omega_{\text{ext}}^\varepsilon} f_{\text{ext}} w \, dx = \int_{\Omega_{\text{int}}^\varepsilon} \sigma_{\text{int}} \nabla u_{\text{int}} \cdot \nabla w \, dx + \int_{\Omega_{\text{ext}}^\varepsilon} \sigma_{\text{ext}} \nabla u_{\text{ext}} \cdot \nabla w \, dx \\
& - \int_{\partial\Omega \cap \partial\Omega_{\text{int}}^\varepsilon} \sigma_{\text{int}} \partial_n u_{\text{int}} w \, ds - \int_{\partial\Omega \cap \partial\Omega_{\text{ext}}^\varepsilon} \sigma_{\text{ext}} \partial_n u_{\text{ext}} w \, ds - \int_{\Gamma_{\text{int}}^\varepsilon} \sigma_{\text{int}} \partial_n u_{\text{int}} w \, ds \\
& - \int_{\Gamma_{\text{ext}}^\varepsilon} \sigma_{\text{ext}} \partial_n u_{\text{ext}} w \, ds.
\end{aligned}$$

We rewrite the traces of functions u_{int} and u_{ext} using the jump and mean value expressions, whose definitions have been presented in Definition 1. We proceed in the following way

$$\begin{cases} \sigma_{\text{int}} \partial_n u_{\text{int}} \left(x_0 - \frac{\varepsilon}{2}, y \right) = \{\sigma \partial_n u\}_{\Gamma^\varepsilon}(y) - \frac{1}{2} [\sigma \partial_n u]_{\Gamma^\varepsilon}(y), \\ \sigma_{\text{ext}} \partial_n u_{\text{ext}} \left(x_0 + \frac{\varepsilon}{2}, y \right) = \{\sigma \partial_n u\}_{\Gamma^\varepsilon}(y) + \frac{1}{2} [\sigma \partial_n u]_{\Gamma^\varepsilon}(y). \end{cases}$$

Substituting these expressions in the previous equation, we derive an identity in the form of a Green formula for the configuration we are working with

$$\begin{aligned}
& - \int_{\Omega_{\text{int}}^\varepsilon} f_{\text{int}} w \, dx - \int_{\Omega_{\text{ext}}^\varepsilon} f_{\text{ext}} w \, dx = \int_{\Omega_{\text{int}}^\varepsilon} \sigma_{\text{int}} \nabla u_{\text{int}} \cdot \nabla w \, dx \\
& + \int_{\Omega_{\text{ext}}^\varepsilon} \sigma_{\text{ext}} \nabla u_{\text{ext}} \cdot \nabla w \, dx + \int_{\Gamma^\varepsilon} \{\sigma \partial_n u\}_{\Gamma^\varepsilon} [w]_{\Gamma^\varepsilon} \, ds \\
& + \int_{\Gamma^\varepsilon} [\sigma \partial_n u]_{\Gamma^\varepsilon} \{w\}_{\Gamma^\varepsilon} \, ds - \int_{\partial\Omega \cap \partial\Omega_{\text{int}}^\varepsilon} \sigma_{\text{int}} \partial_n u_{\text{int}} w \, ds \\
& - \int_{\partial\Omega \cap \partial\Omega_{\text{ext}}^\varepsilon} \sigma_{\text{ext}} \partial_n u_{\text{ext}} w \, ds.
\end{aligned} \tag{3.15}$$

Taking into account the properties of the test functions, we directly deduce the variational formulation in V_4 for Problem (1.19) from Equation (3.15). Assuming $f_{\text{int}} \in L^2(\Omega_{\text{int}}^\varepsilon)$ and $f_{\text{ext}} \in L^2(\Omega_{\text{ext}}^\varepsilon)$ the variational problem reduces to finding $u \in V_4$, such that for all $w \in V_4$,

$$a(u, w) = l(w), \tag{3.16}$$

where

$$\begin{aligned}
a(u, w) &= \sigma_{\text{int}} \int_{\Omega_{\text{int}}^\varepsilon} \nabla u \cdot \nabla w \, dx + \sigma_{\text{ext}} \int_{\Omega_{\text{ext}}^\varepsilon} \nabla u \cdot \nabla w \, dx \\
&\quad + \widehat{\sigma}_0 \varepsilon^{-2} \int_{\Gamma^\varepsilon} \nabla_{\Gamma^\varepsilon} \{u\}_{\Gamma^\varepsilon} \nabla_{\Gamma^\varepsilon} \{w\}_{\Gamma^\varepsilon} \, ds, \\
l(w) &= - \int_{\Omega_{\text{int}}^\varepsilon} f_{\text{int}} w \, dx - \int_{\Omega_{\text{ext}}^\varepsilon} f_{\text{ext}} w \, dx - \int_{\Gamma^\varepsilon} g \{w\}_{\Gamma^\varepsilon} \, ds.
\end{aligned}$$

3.4.3 Stability results

We will develop an expansion in power series of ε for the Problem (1.19) in the form

$$\begin{cases} u_{\text{ext}}^{[3]} \approx \sum_{k \geq 0} \varepsilon^k \hat{u}_{\text{ext}}^k & \text{in } \Omega_{\text{int}}^\varepsilon, \\ u_{\text{int}}^{[3]} \approx \sum_{k \geq 0} \varepsilon^k \hat{u}_{\text{int}}^k & \text{in } \Omega_{\text{ext}}^\varepsilon. \end{cases} \quad (3.17)$$

We substitute these series in Equations (1.19) and we collect the terms with the same power in ε . For every $k \in \mathbb{N}$ we obtain the following set of equations

$$\begin{cases} \sigma_{\text{int}} \Delta \hat{u}_{\text{int}}^k = f_{\text{int}} \delta_k^0 & \text{in } \Omega_{\text{int}}^\varepsilon, \\ \sigma_{\text{ext}} \Delta \hat{u}_{\text{ext}}^k = f_{\text{ext}} \delta_k^0 & \text{in } \Omega_{\text{ext}}^\varepsilon, \\ [\hat{u}^k]_{\Gamma^\varepsilon} = 0, \\ -\hat{\sigma}_0 \frac{d^2}{dy^2} \{\hat{u}^k\}_{\Gamma^\varepsilon} = [\sigma \partial_n \hat{u}^{k-2}]_{\Gamma^\varepsilon}, \\ \hat{u}^k = 0 & \text{on } \partial\Omega \cap \partial\Omega^\varepsilon. \end{cases} \quad (3.18)$$

Definition 7. Given the expansion in power series (3.17) and $N \in \mathbb{N}$, we define the residue \hat{r}^N as

$$\begin{cases} \hat{r}_{\text{int}}^N(x, y) = u_{\text{int}}^{[3]}(x, y) - \sum_{k=0}^N \varepsilon^k \hat{u}_{\text{int}}^k(x, y) & \text{in } \Omega_{\text{int}}^\varepsilon, \\ \hat{r}_{\text{ext}}^N(x, y) = u_{\text{ext}}^{[3]}(x, y) - \sum_{k=0}^N \varepsilon^k \hat{u}_{\text{ext}}^k(x, y) & \text{in } \Omega_{\text{ext}}^\varepsilon. \end{cases}$$

In order to prove the existence, uniqueness, and uniform estimates of Problem (3.16), we will write a Poincaré inequality for the configuration we are working on.

Theorem 3. There exists a constant $C > 0$ such that for all $u \in V_4$,

$$\int_{\Omega^\varepsilon} |u|^2 dx \leq C \int_{\Omega^\varepsilon} |\nabla u|^2 dx.$$

Proof. We follow a similar reasoning to the one presented in [4] (Proposition 8.13 and corollary 9.19). For all $u \in V_4$, u is continuous across the interfaces $\Gamma_{\text{int}}^\varepsilon$ and $\Gamma_{\text{ext}}^\varepsilon$, and it vanishes in the rest of the boundary. We take $(x, y) \in \Omega^\varepsilon$ and we

distinguish two possible cases. Case I: if $(x, y) \in \Omega_{\text{ext}}^\varepsilon$, we obtain

$$|u(x, y)| = |u(L, y) - u(x, y)| = \left| \int_x^L \partial_t u(t, y) dt \right| \leq \int_I |\partial_t u(t, y)| dt,$$

where we have defined $I = \left(0, x_0 - \frac{\varepsilon}{2}\right) \cup \left(x_0 + \frac{\varepsilon}{2}, L\right)$. Case II: if $(x, y) \in \Omega_{\text{int}}^\varepsilon$, we obtain

$$\begin{aligned} |u(x, y)| &= |u(L, y) - u(x, y)| = \left| \int_x^{x_0 - \frac{\varepsilon}{2}} \partial_t u(t, y) dt + \int_{x_0 + \frac{\varepsilon}{2}}^L \partial_t u(t, y) dt \right| \\ &\leq \int_I |\partial_t u(t, y)| dt. \end{aligned}$$

Thus, we deduce that for all $(x, y) \in \Omega^\varepsilon$

$$|u(x, y)| \leq \int_I |\partial_t u(t, y)| dt.$$

We now apply Cauchy-Schwartz inequality to obtain

$$|u(x, y)|^2 \leq L \int_I |\partial_t u(t, y)|^2 dt.$$

We continue by integrating in the x variable and we obtain

$$\int_I |u(x, y)|^2 dx \leq L(L - \varepsilon) \int_I |\partial_t u(t, y)|^2 dt \leq L^2 \int_I |\partial_t u(t, y)|^2 dt.$$

Finally, we integrate in the y variable to deduce the desired result

$$\int_{\Omega^\varepsilon} |u|^2 dx \leq L^2 \int_{\Omega^\varepsilon} |\partial_x u|^2 dx \leq L^2 \int_{\Omega^\varepsilon} |\nabla u|^2 dx.$$

□

Theorem 4. *For all $\varepsilon > 0$ there exists a unique $u \in V_4$ solution to Problem (3.16) with data $f_{\text{int}} \in L^2(\Omega_{\text{int}}^\varepsilon)$, $f_{\text{ext}} \in L^2(\Omega_{\text{ext}}^\varepsilon)$, and $g \in L^2(\Gamma^\varepsilon)$. Moreover, there exists $\varepsilon_0 > 0$ and a constant $C > 0$, such that for all $\varepsilon \in (0, \varepsilon_0)$,*

$$\|u\|_{V_4} \leq C \left(\|f_{\text{int}}\|_{0, \Omega_{\text{int}}^\varepsilon} + \|f_{\text{ext}}\|_{0, \Omega_{\text{ext}}^\varepsilon} + \|g\|_{0, \Gamma^\varepsilon} \right).$$

Proof. We first employ the Lax-Milgram Lemma. To do so, we have to prove first that the bilinear form a is coercive and continuous in V_4 , and that the linear form l is continuous in V_4 . We begin by proving the coerciveness of a . Using Theorem 3, we know that there exists a constant k_1 such that for all $w \in V_4$

$$\int_{\Omega^\varepsilon} |w|^2 dx \leq k_1 \int_{\Omega^\varepsilon} |\nabla w|^2 dx \Rightarrow \|w\|_{1, \Omega^\varepsilon}^2 \leq k_2 \|\nabla w\|_{0, \Omega^\varepsilon}^2, \quad (3.19)$$

where $k_2 = k_1 + 1$. Then, applying this result to the definition of a , we obtain

$$\begin{aligned}
a(w, w) &= \sigma_{\text{int}} \int_{\Omega_{\text{int}}^\varepsilon} |\nabla w|^2 dx + \sigma_{\text{ext}} \int_{\Omega_{\text{ext}}^\varepsilon} |\nabla w|^2 dx + \hat{\sigma}_0 \varepsilon^{-2} \int_{\Gamma^\varepsilon} |\nabla_{\Gamma^\varepsilon} \{w\}|^2 ds \\
&\geq \min(\sigma_{\text{int}}, \sigma_{\text{ext}}) \int_{\Omega^\varepsilon} |\nabla w|^2 dx + \hat{\sigma}_0 \varepsilon^{-2} \int_{\Gamma^\varepsilon} |\nabla_{\Gamma^\varepsilon} \{w\}|^2 ds \\
&\geq k_3 \|w\|_{V_4}^2,
\end{aligned} \tag{3.20}$$

where $k_3 = \frac{1}{k_2} \min(\sigma_{\text{int}}, \sigma_{\text{ext}}, \hat{\sigma}_0 \varepsilon^{-2})$. The above result shows the coerciveness of a in V_4 . We now prove the continuity of l in V_4 . For that purpose, we employ the Dirichlet trace operator γ_Σ as in Equation (3.5). Let $k_4 > 0$ be the continuity constant of the Dirichlet trace operator. Then, for all $w \in V_4$, we obtain

$$\|\gamma_\Sigma(w)\|_{\frac{1}{2}, \Sigma} = \|w_\Sigma\|_{\frac{1}{2}, \Sigma} \leq k_4 \|w\|_{1, \Omega}.$$

For the sake of simplicity in the notations, we shall write w instead of $w_{\Gamma_{\text{int}}^\varepsilon}$ and $w_{\Gamma_{\text{ext}}^\varepsilon}$. Applying this result and the Cauchy-Schwarz inequality to the definition of l we obtain

$$\begin{aligned}
|l(w)| &\leq \|f_{\text{int}}\|_{0, \Omega_{\text{int}}^\varepsilon} \|w\|_{0, \Omega_{\text{int}}^\varepsilon} + \|f_{\text{ext}}\|_{0, \Omega_{\text{ext}}^\varepsilon} \|w\|_{0, \Omega_{\text{ext}}^\varepsilon} + \|g\|_{0, \Gamma^\varepsilon} \|\{w\}\|_{0, \Gamma^\varepsilon} \\
&\leq k_5 \|w\|_{1, \Omega^\varepsilon} \left(\|f_{\text{int}}\|_{0, \Omega_{\text{int}}^\varepsilon} + \|f_{\text{ext}}\|_{0, \Omega_{\text{ext}}^\varepsilon} + \|g\|_{0, \Gamma^\varepsilon} \right) \\
&\leq k_5 \|w\|_{V_4} \left(\|f_{\text{int}}\|_{0, \Omega_{\text{int}}^\varepsilon} + \|f_{\text{ext}}\|_{0, \Omega_{\text{ext}}^\varepsilon} + \|g\|_{0, \Gamma^\varepsilon} \right).
\end{aligned} \tag{3.21}$$

where $k_5 = \max(1, k_4)$. This proves the continuity of l in V_4 . Finally, we prove the continuity of a in V_4 , applying the Cauchy-Schwarz inequality to the definition of a , for $u \in V_4$, we deduce

$$\begin{aligned}
|a(u, w)| &\leq \sigma_{\text{int}} \|\nabla u\|_{0, \Omega_{\text{int}}^\varepsilon} \|\nabla w\|_{0, \Omega_{\text{int}}^\varepsilon} + \sigma_{\text{ext}} \|\nabla u\|_{0, \Omega_{\text{ext}}^\varepsilon} \|\nabla w\|_{0, \Omega_{\text{ext}}^\varepsilon} \\
&\quad + \hat{\sigma}_0 \varepsilon^{-2} \|\nabla_{\Gamma^\varepsilon} \{u\}\|_{0, \Gamma^\varepsilon} \|\nabla_{\Gamma^\varepsilon} \{w\}\|_{0, \Gamma^\varepsilon} \\
&\leq (\sigma_{\text{int}} + \sigma_{\text{ext}}) \|u\|_{1, \Omega^\varepsilon} \|w\|_{1, \Omega^\varepsilon} \\
&\quad + \hat{\sigma}_0 \varepsilon^{-2} \|\nabla_{\Gamma^\varepsilon} \{u\}\|_{0, \Gamma^\varepsilon} \|\nabla_{\Gamma^\varepsilon} \{w\}\|_{0, \Gamma^\varepsilon} \\
&\leq k_6 \|u\|_{V_4} \|w\|_{V_4},
\end{aligned} \tag{3.22}$$

where $k_6 = (\sigma_{\text{int}} + \sigma_{\text{ext}} + \hat{\sigma}_0 \varepsilon^{-2})$. Identity (3.20) proves that a is coercive in V_4 , identity (3.22) shows that a is continuous in V_4 , and identity (3.21) demonstrates that l is continuous in V_4 . We now apply the Lax-Milgram Lemma to deduce that there exists a unique $u \in V_4$ such that for all $w \in V_4$,

$$a(u, w) = l(w).$$

Now only the uniform estimates remain to prove. For that purpose, we consider ε_0 as

$$\varepsilon_0 = \sqrt{\frac{\hat{\sigma}_0}{\min(\sigma_{\text{int}}, \sigma_{\text{ext}})}}.$$

Then, for any $\varepsilon \in (0, \varepsilon_0)$, taking $w = u$ in Equation (3.20), we deduce that

$$a(u, u) \geq k_7 \|u\|_{V_4}^2, \quad (3.23)$$

where $k_7 = \frac{1}{k_2} \min(\sigma_{\text{int}}, \sigma_{\text{ext}})$. On the other hand, we take $w = u$ in (3.21)

$$|l(u)| \leq k_5 \|u\|_{V_4} \left(\|f_{\text{int}}\|_{0, \Omega_{\text{int}}^\varepsilon} + \|f_{\text{ext}}\|_{0, \Omega_{\text{ext}}^\varepsilon} + \|g\|_{0, \Gamma^\varepsilon} \right). \quad (3.24)$$

Finally, taking $w = u$ in the variational formulation

$$|a(u, u)| = |l(u)|$$

and applying (3.23) in the left-hand side and (3.24) in the right-hand side we obtain

$$k_7 \|u\|_{V_4}^2 \leq k_5 \|u\|_{V_4} \left(\|f_{\text{int}}\|_{0, \Omega_{\text{int}}^\varepsilon} + \|f_{\text{ext}}\|_{0, \Omega_{\text{ext}}^\varepsilon} + \|g\|_{0, \Gamma^\varepsilon} \right).$$

Introducing $C = \frac{k_5}{k_7}$, we obtain the desired result

$$\|u\|_{V_4} \leq C \left(\|f_{\text{int}}\|_{0, \Omega_{\text{int}}^\varepsilon} + \|f_{\text{ext}}\|_{0, \Omega_{\text{ext}}^\varepsilon} + \|g\|_{0, \Gamma^\varepsilon} \right)$$

□

Proposition 9. *Let $N \in \mathbb{N}$, the residue \hat{r}^N defined in Definition 7 satisfies the following equations*

$$\left\{ \begin{array}{ll} \sigma_{\text{int}} \Delta \hat{r}_{\text{int}}^N = 0 & \text{in } \Omega_{\text{int}}^\varepsilon, \\ \sigma_{\text{ext}} \Delta \hat{r}_{\text{ext}}^N = 0 & \text{in } \Omega_{\text{ext}}^\varepsilon, \\ [\hat{r}^N]_{\Gamma^\varepsilon} = 0, \\ \varepsilon^{-2} \hat{\sigma}_0 \frac{d^2}{dy^2} \{ \hat{r}^N \}_{\Gamma^\varepsilon} + [\sigma \partial_n \hat{r}^N]_{\Gamma^\varepsilon} = g^N, \\ \hat{r}^N = 0 & \text{on } \partial\Omega \cap \partial\Omega^\varepsilon, \end{array} \right.$$

where

$$g^N = \varepsilon^{N+1} \left(- \left[\sigma \partial_n \hat{u}^{N+1} \right]_{\Gamma^\varepsilon} - \varepsilon \left[\sigma \partial_n \hat{u}^{N+2} \right]_{\Gamma^\varepsilon} \right).$$

Proof. We deduce this result by applying Equations (3.18) and (1.19) to the definition of the residue.

Equation in $\Omega_{\text{int}}^\varepsilon$:

$$\sigma_{\text{int}} \Delta \hat{r}_{\text{int}}^N = \sigma_{\text{int}} \Delta u_{\text{int}}^{[3]} - \sum_{k=0}^N \varepsilon^k \sigma_{\text{int}} \Delta \hat{u}_{\text{int}}^k = f_{\text{int}} - \sigma_{\text{int}} \Delta \hat{u}_{\text{int}}^0 - \sum_{k=1}^N \varepsilon^k \sigma_{\text{int}} \Delta \hat{u}_{\text{int}}^k = 0.$$

Equation in $\Omega_{\text{ext}}^\varepsilon$:

$$\sigma_{\text{ext}} \Delta \hat{r}_{\text{ext}}^N = \sigma_{\text{ext}} \Delta u_{\text{ext}}^{[3]} - \sum_{k=0}^N \varepsilon^k \sigma_{\text{ext}} \Delta \hat{u}_{\text{ext}}^k = f_{\text{ext}} - \sigma_{\text{int}} \Delta \hat{u}_{\text{ext}}^0 - \sum_{k=1}^N \varepsilon^k \sigma_{\text{ext}} \Delta \hat{u}_{\text{ext}}^k = 0.$$

First transmission condition:

$$\left[\hat{r}^N \right]_{\Gamma^\varepsilon} = \left[u^{[3]} \right]_{\Gamma^\varepsilon} - \sum_{k=0}^N \varepsilon^k \left[\hat{u}^k \right]_{\Gamma^\varepsilon} = 0.$$

Second transmission condition:

$$\begin{aligned} -\hat{\sigma}_0 \frac{d^2}{dy^2} \left\{ \hat{r}^N \right\}_{\Gamma^\varepsilon} &= -\hat{\sigma}_0 \frac{d^2}{dy^2} \left\{ u^{[3]} \right\}_{\Gamma^\varepsilon} - \hat{\sigma}_0 \sum_{k=0}^N \varepsilon^k \frac{d^2}{dy^2} \left\{ \hat{u}^k \right\}_{\Gamma^\varepsilon} \\ &= \varepsilon^2 \left[\sigma \partial_n u^{[3]} \right]_{\Gamma^\varepsilon} - \sum_{k=0}^N \varepsilon^k \left[\sigma \partial_n \hat{u}^{k-2} \right]_{\Gamma^\varepsilon} \\ &= \varepsilon^2 \left[\sigma \partial_n u^{[3]} \right]_{\Gamma^\varepsilon} - \varepsilon^2 \sum_{k=0}^N \varepsilon^k \left[\sigma \partial_n \hat{u}^k \right]_{\Gamma^\varepsilon} \\ &\quad + \varepsilon^{N+3} \left[\sigma \partial_n \hat{u}^{N+1} \right]_{\Gamma^\varepsilon} + \varepsilon^{N+4} \left[\sigma \partial_n \hat{u}^{N+2} \right]_{\Gamma^\varepsilon} \\ &= \varepsilon^2 \left[\sigma \partial_n \hat{r}^N \right]_{\Gamma^\varepsilon} + \varepsilon^{N+3} \left[\sigma \partial_n \hat{u}^{N+1} \right]_{\Gamma^\varepsilon} + \varepsilon^{N+4} \left[\sigma \partial_n \hat{u}^{N+2} \right]_{\Gamma^\varepsilon}. \end{aligned}$$

□

Theorem 5. Let $N \in \mathbb{N}$. For $\varepsilon \in (0, \varepsilon_0)$ and under the assumption $g^N \in L^2(\Gamma^\varepsilon)$, the following estimate holds for the residue \hat{r}^N defined in Definition 7, for a constant $C > 0$ independent of ε

$$\left\| \hat{r}_{\text{ext}}^N \right\|_{1, \Omega_{\text{ext}}^\varepsilon} + \left\| \hat{r}_{\text{int}}^N \right\|_{1, \Omega_{\text{int}}^\varepsilon} \leq C \varepsilon^{N+1}.$$

Proof. We deduce this result directly from Theorem 4 and Proposition 9

$$\left\| \widehat{r}_{\text{ext}}^N \right\|_{1, \Omega_{\text{ext}}^\varepsilon} + \left\| \widehat{r}_{\text{int}}^N \right\|_{1, \Omega_{\text{int}}^\varepsilon} \leq C \varepsilon^{N+1} \left(\left\| \left[\sigma \partial_n \widehat{u}^{N+1} \right]_{\Gamma^\varepsilon} \right\|_{0, \Gamma^\varepsilon} + \varepsilon \left\| \left[\sigma \partial_n \widehat{u}^{N+2} \right]_{\Gamma^\varepsilon} \right\|_{0, \Gamma^\varepsilon} \right)$$

We deduce that

$$\left\| \widehat{r}_{\text{ext}}^N \right\|_{1, \Omega_{\text{ext}}^\varepsilon} + \left\| \widehat{r}_{\text{int}}^N \right\|_{1, \Omega_{\text{int}}^\varepsilon} = O(\varepsilon^{N+1}).$$

□

3.4.4 Convergence results

Theorem 6. *Let u be the solution to the reference Problem (1.2) and let $u^{[1]}$ be the solution to the second-order asymptotic model (1.18), which writes as*

$$\begin{cases} \sigma_{\text{int}} \Delta u_{\text{int}}^{[1]} = f_{\text{int}} & \text{in } \Omega_{\text{int}}^\varepsilon, \\ u_{\text{int}}^{[1]} = 0 & \text{on } \partial \Omega_{\text{int}}^\varepsilon. \end{cases}$$

$$\begin{cases} \sigma_{\text{ext}} \Delta u_{\text{ext}}^{[1]} = f_{\text{ext}} & \text{in } \Omega_{\text{ext}}^\varepsilon, \\ u_{\text{ext}}^{[1]} = 0 & \text{on } \partial \Omega_{\text{ext}}^\varepsilon. \end{cases}$$

Under the assumptions of Theorem 2 for $N = 1$, $\varepsilon \in (0, \varepsilon_0)$ and with data $f_{\text{int}} \in L^2(\Omega_{\text{int}}^\varepsilon)$ and $f_{\text{ext}} \in L^2(\Omega_{\text{ext}}^\varepsilon)$. The following estimate holds: there exists a constant $C > 0$ independent of ε , such that

$$\left\| u_{\text{int}} - u_{\text{int}}^{[1]} \right\|_{1, \Omega_{\text{int}}^\varepsilon} + \left\| u_{\text{ext}} - u_{\text{ext}}^{[1]} \right\|_{1, \Omega_{\text{ext}}^\varepsilon} \leq C \varepsilon^2.$$

Proof. We deduce this result directly from Theorem 2. For the second-order model, we have that the truncated series $u^{(1)}$ satisfies Problem (1.18). Thus, we have $u^{[1]} = u^{(1)}$ and we deduce the desired result

$$\begin{aligned} \left\| u_{\text{int}} - u_{\text{int}}^{[1]} \right\|_{1, \Omega_{\text{int}}^\varepsilon} + \left\| u_{\text{ext}} - u_{\text{ext}}^{[1]} \right\|_{1, \Omega_{\text{ext}}^\varepsilon} &= \left\| u_{\text{int}} - u_{\text{int}}^{(1)} \right\|_{1, \Omega_{\text{int}}^\varepsilon} + \left\| u_{\text{ext}} - u_{\text{ext}}^{(1)} \right\|_{1, \Omega_{\text{ext}}^\varepsilon} \\ &= \left\| r_{\text{int}}^1 \right\|_{1, \Omega_{\text{int}}^\varepsilon} + \left\| r_{\text{ext}}^1 \right\|_{1, \Omega_{\text{ext}}^\varepsilon} \leq C \varepsilon^2. \end{aligned}$$

□

Theorem 7. *Let u be the solution to the reference Problem (1.2) and let $u^{[3]}$ be the solution to the fourth-order asymptotic model (1.19), which writes as*

$$\left\{ \begin{array}{ll} \sigma_{int} \Delta u_{int}^{[3]} = f_{int} & \text{in } \Omega_{int}^\varepsilon, \\ \sigma_{ext} \Delta u_{ext}^{[3]} = f_{ext} & \text{in } \Omega_{ext}^\varepsilon, \\ [u^{[3]}]_{\Gamma^\varepsilon} = 0, \\ [\sigma \partial_n u^{[3]}]_{\Gamma^\varepsilon} = -\frac{\hat{\sigma}_0}{\varepsilon^2} \frac{d^2}{dy^2} \{u^{[3]}\}_{\Gamma^\varepsilon}, \\ u^{[3]} = 0 & \text{on } \partial\Omega \cap \partial\Omega^\varepsilon. \end{array} \right.$$

Under the assumptions of Theorem 2 and Theorem 5 for $N = 3$, $\varepsilon \in (0, \varepsilon_0)$ and with a data $f_{int} \in L^2(\Omega_{int}^\varepsilon)$ and $f_{ext} \in L^2(\Omega_{ext}^\varepsilon)$. The following estimate holds: there exists a constant $C > 0$ independent of ε , such that

$$\|u_{int} - u_{int}^{[3]}\|_{1, \Omega_{int}^\varepsilon} + \|u_{ext} - u_{ext}^{[3]}\|_{1, \Omega_{ext}^\varepsilon} \leq C\varepsilon^4.$$

Proof. To begin with, we consider the expansion (3.17) of $u^{[3]}$ that we have described above. More specifically, we consider Equations (3.18). We deduce that for $k = 0, 1, 2, 3$, we obtain the following expressions for \hat{u}^k

k=0:

$$\left\{ \begin{array}{ll} \sigma_{int} \Delta \hat{u}_{int}^0 = f_{int} & \text{in } \Omega_{int}^\varepsilon, \\ \hat{u}_{int}^0 = 0 & \text{on } \partial\Omega_{int}^\varepsilon. \end{array} \right.$$

$$\left\{ \begin{array}{ll} \sigma_{ext} \Delta \hat{u}_{ext}^0 = f_{ext} & \text{in } \Omega_{ext}^\varepsilon, \\ \hat{u}_{ext}^0 = 0 & \text{on } \partial\Omega_{ext}^\varepsilon. \end{array} \right.$$

k=1:

We deduce that $\hat{u}^1 \equiv 0$.

k=2:

$$\left\{ \begin{array}{ll} \sigma_{\text{int}} \Delta \hat{u}_{\text{int}}^2 = 0 & \text{in } \Omega_{\text{int}}^\varepsilon, \\ \sigma_{\text{ext}} \Delta \hat{u}_{\text{ext}}^2 = 0 & \text{in } \Omega_{\text{ext}}^\varepsilon, \\ [\hat{u}^2]_{\Gamma^\varepsilon} = 0, \\ [\sigma \partial_n \hat{u}^2]_{\Gamma^\varepsilon} = -\hat{\sigma}_0 \frac{d^2}{dy^2} \{ \hat{u}^0 \}_{\Gamma^\varepsilon}, \\ \hat{u}^2 = 0 & \text{on } \partial\Omega \cap \partial\Omega^\varepsilon. \end{array} \right.$$

k=3:

We deduce that $\hat{u}^3 \equiv 0$.

If we compare the above expressions with the ones in Section 1.3.2, we deduce that

$$\hat{u}^k \equiv u^k \quad k = 0, 1, 2, 3.$$

Thus, using Theorem 2 and Theorem 5 we deduce the desired result

$$\begin{aligned} & \left\| u_{\text{int}} - u_{\text{int}}^{[3]} \right\|_{1, \Omega_{\text{int}}^\varepsilon} + \left\| u_{\text{ext}} - u_{\text{ext}}^{[3]} \right\|_{1, \Omega_{\text{ext}}^\varepsilon} \\ & \leq \left\| u_{\text{int}} - u_{\text{int}}^{(3)} \right\|_{1, \Omega_{\text{int}}^\varepsilon} + \left\| u_{\text{int}}^{[3]} - u_{\text{int}}^{(3)} \right\|_{1, \Omega_{\text{int}}^\varepsilon} + \left\| u_{\text{ext}} - u_{\text{ext}}^{(3)} \right\|_{1, \Omega_{\text{ext}}^\varepsilon} + \left\| u_{\text{ext}}^{[3]} - u_{\text{ext}}^{(3)} \right\|_{1, \Omega_{\text{ext}}^\varepsilon} \\ & = \left\| u_{\text{int}} - u_{\text{int}}^{(3)} \right\|_{1, \Omega_{\text{int}}^\varepsilon} + \left\| u_{\text{int}}^{[3]} - \hat{u}_{\text{int}}^{(3)} \right\|_{1, \Omega_{\text{int}}^\varepsilon} + \left\| u_{\text{ext}} - u_{\text{ext}}^{(3)} \right\|_{1, \Omega_{\text{ext}}^\varepsilon} + \left\| u_{\text{ext}}^{[3]} - \hat{u}_{\text{ext}}^{(3)} \right\|_{1, \Omega_{\text{ext}}^\varepsilon} \\ & = \left\| r_{\text{int}}^3 \right\|_{1, \Omega_{\text{int}}^\varepsilon} + \left\| \hat{r}_{\text{int}}^3 \right\|_{1, \Omega_{\text{int}}^\varepsilon} + \left\| r_{\text{ext}}^3 \right\|_{1, \Omega_{\text{ext}}^\varepsilon} + \left\| \hat{r}_{\text{ext}}^3 \right\|_{1, \Omega_{\text{ext}}^\varepsilon} \leq C\varepsilon^4. \end{aligned}$$

□

3.5 Validation of the equivalent conditions: second class of ITCs

3.5.1 First-order model: variational formulation

This section is devoted to the derivation of a variational formulation for the first-order and second-order asymptotic models we have derived in Section 1.4.2. This is required to develop a performance assessment by applying a finite element method and it will also be necessary for the convergence and stability proofs performed in the following sections.

We remark that the domain and configuration for these models have been presented in Section 1.4.1 and Figure 1.2. Problem (1.36) is uncoupled into two independent problems. Therefore we write two variational formulations, one for each problem. We first introduce functional spaces $H_0^1(\Omega_{\text{int}})$ and $H_0^1(\Omega_{\text{ext}})$ as the functional framework.

We select as test functions $w_{\text{int}} \in H_0^1(\Omega_{\text{int}})$ and $w_{\text{ext}} \in H_0^1(\Omega_{\text{ext}})$, and we multiply the equations in Ω_{int} and Ω_{ext} of Problem (1.36) with these test functions. Then, we integrate over the domains and we obtain

$$\begin{aligned} \int_{\Omega_{\text{int}}} f_{\text{int}} w_{\text{int}} \, dx &= \int_{\Omega_{\text{int}}} \sigma_{\text{int}} \Delta u_{\text{int}} w_{\text{int}} \, dx \\ \int_{\Omega_{\text{ext}}} f_{\text{ext}} w_{\text{ext}} \, dx &= \int_{\Omega_{\text{ext}}} \sigma_{\text{ext}} \Delta u_{\text{ext}} w_{\text{ext}} \, dx. \end{aligned}$$

Integrating by parts, we obtain

$$\begin{aligned} - \int_{\Omega_{\text{int}}} f_{\text{int}} w_{\text{int}} \, dx &= \int_{\Omega_{\text{int}}^\varepsilon} \sigma_{\text{int}} \nabla u_{\text{int}} \cdot \nabla w_{\text{int}} \, dx - \int_{\partial\Omega_{\text{int}}} \sigma_{\text{int}} \partial_n u_{\text{int}} w_{\text{int}} \, ds, \\ - \int_{\Omega_{\text{ext}}} f_{\text{ext}} w_{\text{ext}} \, dx &= \int_{\Omega_{\text{ext}}} \sigma_{\text{ext}} \nabla u_{\text{ext}} \cdot \nabla w_{\text{ext}} \, dx - \int_{\partial\Omega_{\text{ext}}} \sigma_{\text{ext}} \partial_n u_{\text{ext}} w_{\text{ext}} \, ds. \end{aligned}$$

If we take into account the properties of the test functions, we directly deduce the variational formulation for both the uncoupled problems (1.36). Assuming $f_{\text{int}} \in L^2(\Omega_{\text{int}})$ and $f_{\text{ext}} \in L^2(\Omega_{\text{ext}})$, the variational formulations reduce to finding $u_{\text{int}} \in H_0^1(\Omega_{\text{int}})$ such that for all $w_{\text{int}} \in H_0^1(\Omega_{\text{int}})$

$$- \int_{\Omega_{\text{int}}} f_{\text{int}} w_{\text{int}} \, dx = \int_{\Omega_{\text{int}}} \sigma_{\text{int}} \nabla u_{\text{int}} \cdot \nabla w_{\text{int}} \, dx, \quad (3.25)$$

and finding $u_{\text{ext}} \in H_0^1(\Omega_{\text{ext}})$ such that for all $w_{\text{ext}} \in H_0^1(\Omega_{\text{ext}})$

$$- \int_{\Omega_{\text{ext}}} f_{\text{ext}} w_{\text{ext}} \, dx = \int_{\Omega_{\text{ext}}} \sigma_{\text{ext}} \nabla u_{\text{ext}} \cdot \nabla w_{\text{ext}} \, dx. \quad (3.26)$$

3.5.2 Second-order model: variational formulation

In this section, we derive a variational formulation for the second-order asymptotic model (1.38) we have derived in Section 1.4.2. We introduce functional spaces V_{int} and V_{ext} as the functional framework, which are defined as follows

$$\begin{aligned} V_{\text{int}} &= \left\{ w \in H^1(\Omega_{\text{int}}) : w|_{\partial\Omega \cap \partial\Omega_{\text{int}}} = 0 \right\}, \\ V_{\text{ext}} &= \left\{ w \in H^1(\Omega_{\text{ext}}) : w|_{\partial\Omega \cap \partial\Omega_{\text{ext}}} = 0 \right\}. \end{aligned} \quad (3.27)$$

We select as test functions $w_{\text{int}} \in V_{\text{int}}$ and $w_{\text{ext}} \in V_{\text{ext}}$, and we multiply the equations in Ω_{int} and Ω_{ext} of Problem (1.38) with these test functions. Then, we integrate over the domain and integrating by parts we obtain

$$\begin{aligned} - \int_{\Omega_{\text{int}}} f_{\text{int}} w_{\text{int}} \, dx &= \int_{\Omega_{\text{int}}} \sigma_{\text{int}} \nabla u_{\text{int}} \cdot \nabla w_{\text{int}} \, dx - \int_{\partial\Omega_{\text{int}}} \sigma_{\text{int}} \partial_n u_{\text{int}} w_{\text{int}} \, ds, \\ - \int_{\Omega_{\text{ext}}} f_{\text{ext}} w_{\text{ext}} \, dx &= \int_{\Omega_{\text{ext}}} \sigma_{\text{ext}} \nabla u_{\text{ext}} \cdot \nabla w_{\text{ext}} \, dx - \int_{\partial\Omega_{\text{ext}}} \sigma_{\text{ext}} \partial_n u_{\text{ext}} w_{\text{ext}} \, ds. \end{aligned}$$

Taking into account the properties of the test functions and the boundary conditions in Γ , we deduce the variational formulation for both the uncoupled problems (1.38). Assuming $f_{\text{int}} \in L^2(\Omega_{\text{int}})$ and $f_{\text{ext}} \in L^2(\Omega_{\text{ext}})$, the variational formulations consist in finding $u_{\text{int}} \in V_{\text{int}}$, such that for all $w_{\text{int}} \in V_{\text{int}}$

$$- \int_{\Omega_{\text{int}}} f_{\text{int}} w_{\text{int}} \, dx = \int_{\Omega_{\text{int}}} \sigma_{\text{int}} \nabla u_{\text{int}} \cdot \nabla w_{\text{int}} \, dx - \int_{\Gamma} \frac{2\sigma_{\text{int}}}{\varepsilon} u_{\text{int}} w_{\text{int}} \, ds,$$

and finding $u_{\text{ext}} \in V_{\text{ext}}$, such that for all $w_{\text{ext}} \in V_{\text{ext}}$

$$- \int_{\Omega_{\text{ext}}} f_{\text{ext}} w_{\text{ext}} \, dx = \int_{\Omega_{\text{ext}}} \sigma_{\text{ext}} \nabla u_{\text{ext}} \cdot \nabla w_{\text{ext}} \, dx - \int_{\Gamma} \frac{2\sigma_{\text{ext}}}{\varepsilon} u_{\text{ext}} w_{\text{ext}} \, ds.$$

Observing these variational formulations, we notice that we cannot prove the co-erciveness of the bilinear form due to the terms

$$- \int_{\Gamma} \frac{2\sigma_{\text{int}}}{\varepsilon} u_{\text{int}} w_{\text{int}} \, ds \quad \text{and} \quad - \int_{\Gamma} \frac{2\sigma_{\text{ext}}}{\varepsilon} u_{\text{ext}} w_{\text{ext}} \, ds$$

being negative. These negative terms could cause instabilities when numerically solving the problem with the finite element method. However, to overcome this problem and recover stability, we have derived new models across some artificial boundaries in Section 1.4.3. With these models, we will no longer have instability problems, as we will prove in the following section.

3.5.3 Stabilized δ -order two model: variational formulation

In this section, we derive a variational formulation for the stabilized δ -order two model (1.43) we have derived in Section 1.4.3. Instead of directly considering Problem (1.43), we will consider the following problem

$$\begin{cases} \sigma_{\text{int}} \Delta u_{\text{int}} = f_{\text{int}} & \text{in } \Omega_{\text{int}}^{\delta}, \\ u_{\text{int}} - \frac{\varepsilon(1-2\delta)}{2} \partial_n u_{\text{int}} = g_{\text{int}} & \text{on } \Gamma_{\text{int}}^{\delta}, \\ u_{\text{int}} = 0 & \text{on } \partial\Omega \cap \partial\Omega_{\text{int}}^{\delta}, \end{cases}$$

$$\begin{cases} \sigma_{\text{ext}} \Delta u_{\text{ext}} = f_{\text{ext}} & \text{in } \Omega_{\text{ext}}^{\delta}, \\ u_{\text{ext}} + \frac{\varepsilon(1-2\delta)}{2} \partial_n u_{\text{ext}} = g_{\text{ext}} & \text{on } \Gamma_{\text{ext}}^{\delta}, \\ u_{\text{ext}} = 0 & \text{on } \partial\Omega \cap \partial\Omega_{\text{ext}}^{\delta}. \end{cases}$$

This problem is similar to Problem (1.43) and it generalizes it by including the right-hand side functions g_1 and g_2 . Thus, the results obtained for this problem can also be applied to Problem (1.43) by simply applying $g_1 \equiv 0$ and $g_2 \equiv 0$. We begin by selecting the functional framework. We introduce functional spaces V_{int}^{δ} and V_{ext}^{δ} , which are defined as follows

$$V_{\text{int}}^{\delta} = \left\{ w \in H^1(\Omega_{\text{int}}^{\delta}) : w|_{\partial\Omega \cap \partial\Omega_{\text{int}}^{\delta}} = 0 \right\},$$

$$V_{\text{ext}}^{\delta} = \left\{ w \in H^1(\Omega_{\text{ext}}^{\delta}) : w|_{\partial\Omega \cap \partial\Omega_{\text{ext}}^{\delta}} = 0 \right\}.$$

Proceeding in the same way as in the previous section, we derive the following variational formulation. Assuming $f_{\text{int}} \in L^2(\Omega_{\text{int}}^{\delta})$ and $f_{\text{ext}} \in L^2(\Omega_{\text{ext}}^{\delta})$, the variational formulations reduce to finding $u_{\text{int}} \in V_{\text{int}}^{\delta}$, such that for all $w_{\text{int}} \in V_{\text{int}}^{\delta}$

$$a_{\text{int}}(u_{\text{int}}, w_{\text{int}}) = l_{\text{int}}(w_{\text{int}}), \quad (3.28)$$

and finding $u_{\text{ext}} \in V_{\text{ext}}^{\delta}$, such that for all $w_{\text{ext}} \in V_{\text{ext}}^{\delta}$

$$a_{\text{ext}}(u_{\text{ext}}, w_{\text{ext}}) = l_{\text{ext}}(w_{\text{ext}}), \quad (3.29)$$

where

$$a_{\text{int}}(u_{\text{int}}, w_{\text{int}}) = \int_{\Omega_{\text{int}}^\delta} \sigma_{\text{int}} \nabla u_{\text{int}} \cdot \nabla w_{\text{int}} \, dx - \int_{\Gamma_{\text{int}}^\delta} \frac{2\sigma_{\text{int}}}{\varepsilon(1-2\delta)} u_{\text{int}} w_{\text{int}} \, ds,$$

$$a_{\text{ext}}(u_{\text{ext}}, w_{\text{ext}}) = \int_{\Omega_{\text{ext}}^\delta} \sigma_{\text{ext}} \nabla u_{\text{ext}} \cdot \nabla w_{\text{ext}} \, dx - \int_{\Gamma_{\text{ext}}^\delta} \frac{2\sigma_{\text{ext}}}{\varepsilon(1-2\delta)} u_{\text{ext}} w_{\text{ext}} \, ds,$$

and

$$l_{\text{int}}(w_{\text{int}}) = - \int_{\Omega_{\text{int}}^\delta} f_{\text{int}} w_{\text{int}} \, dx - \int_{\Gamma_{\text{int}}^\delta} \frac{2\sigma_{\text{int}}}{\varepsilon(1-2\delta)} g_{\text{int}} w_{\text{int}} \, ds,$$

$$l_{\text{ext}}(w_{\text{ext}}) = - \int_{\Omega_{\text{ext}}^\delta} f_{\text{ext}} w_{\text{ext}} \, dx - \int_{\Gamma_{\text{ext}}^\delta} \frac{2\sigma_{\text{ext}}}{\varepsilon(1-2\delta)} g_{\text{ext}} w_{\text{ext}} \, ds,$$

Now, with these variational formulations, we observe that if we select $\delta > \frac{1}{2}$, the last term of the bilinear form is positive, which enforces the coerciveness of the corresponding bilinear form.

3.5.4 Stability results

We first develop an expansion in power series of ε for the Problem (1.43) in the form

$$\begin{cases} u_{\delta,\text{ext}}^{[1]} \approx \sum_{k \geq 0} \varepsilon^k \hat{u}_{\delta,\text{ext}}^k & \text{in } \Omega_{\text{int}}^\delta, \\ u_{\delta,\text{int}}^{[1]} \approx \sum_{k \geq 0} \varepsilon^k \hat{u}_{\delta,\text{int}}^k & \text{in } \Omega_{\text{ext}}^\delta. \end{cases} \quad (3.30)$$

We substitute these series into the Equations (1.43) and we collect the terms with the same powers in ε . For every $k \in \mathbb{N}$ we obtain the following set of equations

$$\begin{cases} \sigma_{\text{int}} \Delta \hat{u}_{\delta,\text{int}}^k = f_{\text{int}} \delta_k^0 & \text{in } \Omega_{\text{int}}^\delta, \\ \hat{u}_{\delta,\text{int}}^k = \frac{\varepsilon(1-2\delta)}{2} \partial_n \hat{u}_{\delta,\text{int}}^{k-1} & \text{in } \Gamma_{\text{int}}^\delta, \\ \hat{u}_{\delta,\text{int}}^k = 0 & \text{on } \partial\Omega \cap \partial\Omega_{\text{int}}^\delta. \end{cases} \quad (3.31)$$

$$\begin{cases} \sigma_{\text{ext}} \Delta \hat{u}_{\delta,\text{ext}}^k = f_{\text{ext}} \delta_k^0 & \text{in } \Omega_{\text{ext}}^\delta, \\ \hat{u}_{\delta,\text{ext}}^k = -\frac{\varepsilon(1-2\delta)}{2} \partial_n \hat{u}_{\delta,\text{ext}}^{k-1} & \text{in } \Gamma_{\text{ext}}^\delta, \\ \hat{u}_{\delta,\text{ext}}^k = 0 & \text{on } \partial\Omega \cap \partial\Omega_{\text{ext}}^\delta. \end{cases}$$

Definition 8. Given the expansion in power series (3.30) and $N \in \mathbb{N}$, we define the residue \widehat{r}_δ^N as

$$\begin{cases} \widehat{r}_{\delta,int}^N(x, y) = u_{\delta,int}^{[3]}(x, y) - \sum_{k=0}^N \varepsilon^k \widehat{u}_{\delta,int}^k(x, y), \\ \widehat{r}_{\delta,ext}^N(x, y) = u_{\delta,ext}^{[3]}(x, y) - \sum_{k=0}^N \varepsilon^k \widehat{u}_{\delta,ext}^k(x, y), \end{cases}$$

We now prove the existence, uniqueness, and uniform estimates of the solution to problems (3.28) and (3.29).

Theorem 8. For all $\varepsilon > 0$ and $\delta > \frac{1}{2}$ there exists a unique $u = (u_{int}, u_{ext})$ where $u_{int} \in V_{int}^\delta$ and $u_{ext} \in V_{ext}^\delta$ are solutions to (3.28) and (3.29) respectively with data $f_{int} \in L^2(\Omega_{int}^\delta)$, $f_{ext} \in L^2(\Omega_{ext}^\delta)$, $g_{int} \in L^2(\Gamma_{int}^\delta)$, $g_{ext} \in L^2(\Gamma_{ext}^\delta)$. Moreover there exists ε_0 and a constant $C > 0$ such that for all $\varepsilon \in (0, \varepsilon_0)$

$$\|u\|_{1,\Omega^\delta} \leq \varepsilon^{-1} C \left(\|f_{int}\|_{0,\Omega_{int}^\delta} + \|f_{ext}\|_{0,\Omega_{ext}^\delta} + \|g_{int}\|_{0,\Gamma_{int}^\delta} + \|g_{ext}\|_{0,\Gamma_{ext}^\delta} \right). \quad (3.32)$$

Proof. We focus on the problem over domain Ω_{int}^δ and the same reasoning can be applied for the problem over domain Ω_{ext}^δ . For proving the existence and uniqueness result, we employ the Lax-Milgram Lemma. To do so, we have to prove that the bilinear form a_{int} is coercive and continuous in V_{int}^δ , and that the linear form l_{int} is continuous in V_{int}^δ . We start by proving coerciveness of a in V_{int}^δ . Applying Poincaré inequality, there exists a constant k_1 , such that for all $w \in V_{int}^\delta$

$$\int_{\Omega_{int}^\delta} |w|^2 dx \leq k_1 \int_{\Omega_{int}^\delta} |\nabla w|^2 dx \Rightarrow \|w\|_{1,\Omega_{int}^\delta}^2 \leq k_2 \|\nabla w\|_{0,\Omega_{int}^\delta}^2 \quad (3.33)$$

where $k_2 = k_1 + 1$. Substituting $u_{int} = w$ into the definition of a_{int} and applying (3.33) to this expression, we obtain

$$\begin{aligned} a_{int}(w, w) &= \sigma_{int} \int_{\Omega_{int}^\delta} |\nabla w|^2 dx + \frac{2}{\varepsilon(2\delta - 1)} \int_{\Gamma_{int}^\delta} g_{int} w ds \geq \sigma_{int} \|\nabla w\|_{0,\Omega_{int}^\delta}^2 \\ &\geq k_3 \|w\|_{1,\Omega_{int}^\delta}^2, \end{aligned} \quad (3.34)$$

where $k_3 = \frac{\sigma_{int}}{k_2}$. The above result shows the coerciveness of a_{int} in V_{int}^δ . We now prove the continuity of l_{int} in V_{int}^δ . For that purpose, we define the Dirichlet trace operator for the subdomain Ω_{int}^δ as in (3.5). Let $k_4 > 0$ be the continuity constant of the Dirichlet trace operator $\gamma_{\Gamma_{int}^\delta}$. Then, for all $w \in H^1(\Omega_{int}^\delta)$ we obtain

$$\|\gamma_{\Gamma_{int}^\delta}(w)\|_{\frac{1}{2},\Gamma_{int}^\delta} = \|w_{\Gamma_{int}^\delta}\|_{\frac{1}{2},\Gamma_{int}^\delta} \leq k_4 \|w\|_{1,\Omega_{int}^\delta}.$$

For the sake of simplicity in the notations, we shall write w instead of $w_{\Gamma_{\text{int}}^\delta}$. Applying this result and the Cauchy-Schwarz inequality to the definition of l_{int} we obtain

$$\begin{aligned} |l_{\text{int}}(w)| &\leq \|f_{\text{int}}\|_{0,\Omega_{\text{int}}^\delta} \|w\|_{0,\Omega_{\text{int}}^\delta} + \frac{2\sigma_{\text{int}}}{\varepsilon(2\delta-1)} \|g_{\text{int}}\|_{0,\Gamma_{\text{int}}^\delta} \|w\|_{0,\Gamma_{\text{int}}^\delta} \\ &\leq k_5 \|w\|_{1,\Omega_{\text{int}}^\delta} \left(\|f_{\text{int}}\|_{0,\Omega_{\text{int}}^\delta} + \|g_{\text{int}}\|_{0,\Gamma_{\text{int}}^\delta} \right). \end{aligned} \quad (3.35)$$

where $k_5 = \max\left(1, \frac{2k_4\sigma_{\text{int}}}{\varepsilon(2\delta-1)}\right)$. This proves the continuity of l_{int} in V_{int}^δ . Finally, we have the continuity of a_{int} in V_{int}^δ : applying the Cauchy-Schwarz inequality to the definition of a_{int} , for all $u, w \in V_{\text{int}}^\delta$, we deduce

$$\begin{aligned} |a_{\text{int}}(u, w)| &\leq \sigma_{\text{int}} \|\nabla u\|_{0,\Omega_{\text{int}}^\delta} \|\nabla w\|_{0,\Omega_{\text{int}}^\delta} + \frac{2\sigma_{\text{int}}}{\varepsilon(2\delta-1)} \|u\|_{0,\Gamma_{\text{int}}^\delta} \|w\|_{0,\Gamma_{\text{int}}^\delta} \\ &\leq k_6 \|u\|_{1,\Omega^\delta} \|w\|_{1,\Omega^\delta} \end{aligned} \quad (3.36)$$

where $k_6 = \sigma_{\text{int}} + \frac{2\sigma_{\text{int}}k_4}{\varepsilon(2\delta-1)} + \sigma_{\text{ext}}$. The identity (3.34) proves that a_{int} is coercive in V_{int}^δ , the identity (3.36) assures that a_{int} is continuous in V_{int}^δ , and the identity (3.35) demonstrates that l_{int} is continuous in V_{int}^δ . As a conclusion we apply the Lax-Milgram Lemma to deduce that there exists a unique $u_{\text{int}} \in V_{\text{int}}^\delta$, such that for all $w \in V_{\text{int}}^\delta$,

$$a_{\text{int}}(u_{\text{int}}, w) = l_{\text{int}}(w).$$

To prove the second part of the theorem regarding the uniform estimates, we select ε_0 as

$$\varepsilon_0 = \frac{2k_4\sigma_{\text{int}}}{2\delta-1}.$$

Then, for any $\varepsilon \in (0, \varepsilon_0)$ and taking $w = u_{\text{int}}$ in (3.35)

$$|l_{\text{int}}(u_{\text{int}})| \leq \varepsilon^{-1} k_7 \|u_{\text{int}}\|_{1,\Omega_{\text{int}}^\delta} \left(\|f_{\text{int}}\|_{0,\Omega_{\text{int}}^\delta} + \|g_{\text{int}}\|_{0,\Gamma_{\text{int}}^\delta} \right), \quad (3.37)$$

where $k_7 = \frac{2k_4\sigma_{\text{int}}}{2\delta-1}$. On the other hand, taking $w = u_{\text{int}}$ in (3.34), we obtain

$$|a_{\text{int}}(u_{\text{int}}, u_{\text{int}})| \geq k_3 \|u_{\text{int}}\|_{1,\Omega_{\text{int}}^\delta}^2. \quad (3.38)$$

Finally, taking $w = u_{\text{int}}$ in the variational formulation

$$|a_{\text{int}}(u_{\text{int}}, u_{\text{int}})| = |l_{\text{int}}(u_{\text{int}})|$$

and applying (3.38) in the left-hand side and (3.37) in the right-hand side we obtain

$$k_3 \|u_{\text{int}}\|_{1,\Omega_{\text{int}}^\delta}^2 \leq \varepsilon^{-1} k_7 \|u\|_{1,\Omega_{\text{int}}^\delta} \left(\|f_{\text{int}}\|_{0,\Omega_{\text{int}}^\delta} + \|g_{\text{int}}\|_{0,\Gamma_{\text{int}}^\delta} \right).$$

We introduce $C_{\text{int}} = \frac{k_7}{k_3}$. Employing the same process as for the variational formulation over domain $\Omega_{\text{ext}}^\delta$ we obtain a similar estimate involving a constant C_{ext} . Defining $C = \max(C_{\text{int}}, C_{\text{ext}})$ we obtain the desired result

$$\|u\|_{1,\Omega^\delta} \leq \varepsilon^{-1} C \left(\|f_{\text{int}}\|_{0,\Omega_{\text{int}}^\delta} + \|f_{\text{ext}}\|_{0,\Omega_{\text{ext}}^\delta} + \|g_{\text{int}}\|_{0,\Gamma_{\text{int}}^\delta} + \|g_{\text{ext}}\|_{0,\Gamma_{\text{ext}}^\delta} \right).$$

□

Proposition 10. *Let $N \in \mathbb{N}$. The residue \widehat{r}_δ^N defined in Definition 8 satisfies the following equations*

$$\left\{ \begin{array}{ll} \sigma_{\text{int}} \Delta \widehat{r}_{\delta,\text{int}}^N = 0 & \text{in } \Omega_{\text{int}}^\delta, \\ \widehat{r}_{\delta,\text{int}}^N - \frac{\varepsilon(1-2\delta)}{2} \widehat{r}_{\delta,\text{int}}^N = g_{\text{int}}^N & \text{on } \Gamma_{\text{int}}^\delta, \\ \widehat{r}_{\delta,\text{int}}^N = 0 & \text{on } \partial\Omega \cap \partial\Omega_{\text{int}}^\delta. \end{array} \right.$$

$$\left\{ \begin{array}{ll} \sigma_{\text{int}} \Delta \widehat{r}_{\delta,\text{ext}}^N = 0 & \text{in } \Omega_{\text{ext}}^\delta, \\ \widehat{r}_{\delta,\text{ext}}^N + \frac{\varepsilon(1-2\delta)}{2} \widehat{r}_{\delta,\text{ext}}^N = g_{\text{ext}}^N & \text{on } \Gamma_{\text{ext}}^\delta, \\ \widehat{r}_{\delta,\text{ext}}^N = 0 & \text{on } \partial\Omega \cap \partial\Omega_{\text{ext}}^\delta, \end{array} \right.$$

where

$$g_{\text{int}}^N = \varepsilon^{N+1} \frac{1-2\delta}{2} \partial_n u_{\text{int}}^N,$$

$$g_{\text{ext}}^N = \varepsilon^{N+1} \frac{1-2\delta}{2} \partial_n u_{\text{ext}}^N.$$

Proof. We deduce this result by applying Equations (3.31) and (1.43) to the definition of the residue.

Equation in $\Omega_{\text{int}}^\delta$:

$$\sigma_{\text{int}} \Delta \widehat{r}_{\delta,\text{int}}^N = \sigma_{\text{int}} \Delta u_{\delta,\text{int}}^{[1]} - \sum_{k=0}^N \varepsilon^k \sigma_{\text{int}} \Delta \widehat{u}_{\delta,\text{int}}^k = f_{\text{int}} - \sigma_{\text{int}} \Delta \widehat{u}_{\delta,\text{int}}^0 - \sum_{k=1}^N \varepsilon^k \sigma_{\text{int}} \Delta \widehat{u}_{\delta,\text{int}}^k = 0.$$

Equation in $\Omega_{\text{ext}}^\delta$:

$$\sigma_{\text{ext}} \Delta \widehat{r}_{\delta, \text{ext}}^N = \sigma_{\text{ext}} \Delta u_{\delta, \text{ext}}^{[1]} - \sum_{k=0}^N \varepsilon^k \sigma_{\text{ext}} \Delta \widehat{u}_{\delta, \text{ext}}^k = f_{\text{ext}} - \sigma_{\text{ext}} \Delta \widehat{u}_{\delta, \text{ext}}^0 - \sum_{k=1}^N \varepsilon^k \sigma_{\text{ext}} \Delta \widehat{u}_{\delta, \text{ext}}^k = 0.$$

Equation in $\Gamma_{\text{int}}^\delta$:

$$\begin{aligned} & \widehat{r}_{\delta, \text{int}}^N - \frac{\varepsilon(1-2\delta)}{2} \partial_n \widehat{r}_{\delta, \text{int}}^N \\ &= u_{\delta, \text{int}}^{[1]} - \sum_{k=0}^N \varepsilon^k \widehat{u}_{\delta, \text{int}}^k - \frac{\varepsilon(1-2\delta)}{2} \partial_n u_{\delta, \text{int}}^{[1]} + \sum_{k=0}^N \varepsilon^{k+1} \frac{\varepsilon(1-2\delta)}{2} \partial_n \widehat{u}_{\delta, \text{int}}^k \\ &= - \sum_{k=0}^N \varepsilon^k \left(\widehat{u}_{\delta, \text{int}}^k - \frac{\varepsilon(1-2\delta)}{2} \partial_n \widehat{u}_{\delta, \text{int}}^{k-1} \right) + \varepsilon^{N+1} \frac{1-2\delta}{2} \partial_n \widehat{u}_{\delta, \text{int}}^N \\ &= \varepsilon^{N+1} \frac{1-2\delta}{2} \partial_n \widehat{u}_{\delta, \text{int}}^N \end{aligned}$$

Following the same procedure we prove the equations for $\widehat{r}_{\delta, \text{ext}}^N$.

□

Theorem 9. *Let $N \in \mathbb{N}$. For $\varepsilon \in (0, \varepsilon_0)$ and under the assumptions $g_{\text{int}}^N \in L^2(\Gamma_{\text{int}}^\delta)$, $g_{\text{ext}}^N \in L^2(\Gamma_{\text{ext}}^\delta)$, $g_{\text{int}}^{N+1} \in L^2(\Gamma_{\text{int}}^\delta)$, $g_{\text{ext}}^{N+1} \in L^2(\Gamma_{\text{ext}}^\delta)$, and $u^k \in H^1(\Omega^\varepsilon)$ for $k \leq N+1$, there exists a constant $C > 0$, independent of ε , for which the following estimate holds for the residue \widehat{r}_δ^N defined in Definition 8,*

$$\left\| \widehat{r}_{\delta, \text{ext}}^N \right\|_{1, \Omega_{\text{ext}}^\delta} + \left\| \widehat{r}_{\delta, \text{int}}^N \right\|_{1, \Omega_{\text{int}}^\delta} \leq C \varepsilon^{N+1}.$$

Proof. We deduce this result directly from Theorem 8 and Proposition 10

$$\begin{aligned} \left\| \widehat{r}_{\delta, \text{ext}}^N \right\|_{1, \Omega_{\text{ext}}^\delta} + \left\| \widehat{r}_{\delta, \text{int}}^N \right\|_{1, \Omega_{\text{int}}^\delta} &\leq C \varepsilon^{-1} \left(\varepsilon^{N+1} \frac{1-2\delta}{2} \left\| \partial_n \widehat{u}_{\delta, \text{int}}^N \right\|_{0, \Gamma_{\text{int}}^\delta} \right. \\ &\quad \left. + \varepsilon^{N+1} \frac{1-2\delta}{2} \left\| \partial_n \widehat{u}_{\delta, \text{ext}}^N \right\|_{0, \Gamma_{\text{ext}}^\delta} \right) \end{aligned}$$

We deduce that

$$\left\| \widehat{r}_{\delta, \text{ext}}^N \right\|_{1, \Omega_{\text{ext}}^\delta} + \left\| \widehat{r}_{\delta, \text{int}}^N \right\|_{1, \Omega_{\text{int}}^\delta} = O(\varepsilon^N).$$

Finally, writing

$$\begin{cases} \widehat{r}_{\delta, \text{int}}^N = \widehat{r}_{\delta, \text{int}}^{N+1} + \varepsilon^{N+1} \widehat{u}_{\delta, \text{int}}^{N+1}, \\ \widehat{r}_{\delta, \text{ext}}^N = \widehat{r}_{\delta, \text{ext}}^{N+1} + \varepsilon^{N+1} \widehat{u}_{\delta, \text{ext}}^{N+1}, \end{cases}$$

we deduce the desired result

$$\left\| \widehat{r}_{\delta, \text{ext}}^N \right\|_{1, \Omega_{\text{ext}}^\delta} + \left\| \widehat{r}_{\delta, \text{int}}^N \right\|_{1, \Omega_{\text{int}}^\delta} = O(\varepsilon^{N+1}).$$

□

3.5.5 Convergence results

Theorem 10. *Let u be the solution to reference Problem (1.2) and let $u^{[0]}$ the solution to the first-order asymptotic model (1.36), which writes as*

$$\begin{cases} \sigma_{\text{int}} \Delta u_{\text{int}}^{[0]} = f_{\text{int}} & \text{in } \Omega_{\text{int}}, \\ u_{\text{int}}^{[0]} = 0 & \text{on } \partial\Omega_{\text{int}}, \end{cases}$$

$$\begin{cases} \sigma_{\text{ext}} \Delta u_{\text{ext}}^{[0]} = f_{\text{ext}} & \text{in } \Omega_{\text{ext}}, \\ u_{\text{ext}}^{[0]} = 0 & \text{on } \partial\Omega_{\text{ext}}. \end{cases}$$

Under the assumptions of Theorem 2 for $N = 0$ and $\varepsilon \in (0, \varepsilon_0)$, with the data $f_{\text{int}} \in L^2(\Omega_{\text{int}})$ and $f_{\text{ext}} \in L^2(\Omega_{\text{ext}})$. The following estimate holds: there exists a constant $C > 0$ independent of ε , such that

$$\left\| u_{\text{int}} - u_{\text{int}}^{[0]} \right\|_{1, \Omega_{\text{int}}^\varepsilon} + \left\| u_{\text{ext}} - u_{\text{ext}}^{[0]} \right\|_{1, \Omega_{\text{ext}}^\varepsilon} \leq C\varepsilon.$$

Proof. We deduce this result directly from Theorem 2. For the first-order model, we have that the truncated series $u^{(0)}$ satisfies Problem (1.36). Thus, we have $u^{[0]} = u^{(0)}$ and we deduce the desired result

$$\begin{aligned} \left\| u_{\text{int}} - u_{\text{int}}^{[0]} \right\|_{1, \Omega_{\text{int}}^\varepsilon} + \left\| u_{\text{ext}} - u_{\text{ext}}^{[0]} \right\|_{1, \Omega_{\text{ext}}^\varepsilon} &= \left\| u_{\text{int}} - u_{\text{int}}^{(0)} \right\|_{1, \Omega_{\text{int}}^\varepsilon} + \left\| u_{\text{ext}} - u_{\text{ext}}^{(0)} \right\|_{1, \Omega_{\text{ext}}^\varepsilon} \\ &= \left\| r_{\text{int}}^0 \right\|_{1, \Omega_{\text{int}}^\varepsilon} + \left\| r_{\text{ext}}^0 \right\|_{1, \Omega_{\text{ext}}^\varepsilon} \leq C\varepsilon. \end{aligned}$$

□

Theorem 11. *Let u be the solution to reference Problem (1.2) and let $u_\delta^{[1]}$ be the*

solution to the stabilized δ -order two model (1.43), which writes as

$$\begin{cases} \sigma_{int} \Delta u_{\delta,int}^{[1]} = f_{int} & \text{in } \Omega_{int}^{\delta}, \\ u_{\delta,int}^{[1]} = \frac{\varepsilon(1-2\delta)}{2} \partial_n u_{\delta,int}^{[1]} & \text{on } \Gamma_{int}^{\delta}, \\ u_{\delta,int}^{[1]} = 0 & \text{on } \partial\Omega \cap \partial\Omega_{int}^{\delta}. \end{cases}$$

$$\begin{cases} \sigma_{ext} \Delta u_{\delta,ext}^{[1]} = f_{ext} & \text{in } \Omega_{ext}^{\delta}, \\ u_{\delta,ext}^{[1]} = -\frac{\varepsilon(1-2\delta)}{2} \partial_n u_{\delta,ext}^{[1]} & \text{on } \Gamma_{ext}^{\delta}, \\ u_{\delta,ext}^{[1]} = 0 & \text{on } \partial\Omega \cap \partial\Omega_{ext}^{\delta}. \end{cases}$$

Under the assumptions of Theorem 2 and Theorem 9 for $N = 1$ and $\varepsilon \in (0, \varepsilon_0)$, with the data $f_{int} \in L^2(\Omega_{int})$ and $f_{ext} \in L^2(\Omega_{ext})$. The following estimate holds: there exists a constant $C > 0$ independent from ε , such that

$$\|u_{int} - u_{\delta,int}^{[1]}\|_{1,\Omega_{int}^{\delta}} + \|u_{ext} - u_{\delta,ext}^{[1]}\|_{1,\Omega_{ext}^{\delta}} \leq C\varepsilon^2.$$

Proof. To begin with, we consider the expansion (3.30) of $u_{\delta}^{[1]}$ that we have described above. More specifically, we consider Equations (3.31). We deduce that for $k = 0, 1$, we have the following expressions for \hat{u}_{δ}^k

$k = 0$:

$$\begin{cases} \sigma_{int} \Delta \hat{u}_{\delta,int}^0 = f_{int} & \text{in } \Omega_{int}^{\delta}, \\ \hat{u}_{\delta,int}^0 = 0 & \text{on } \partial\Omega_{int}^{\delta}. \end{cases}$$

$$\begin{cases} \sigma_{ext} \Delta \hat{u}_{\delta,ext}^0 = f_{ext} & \text{in } \Omega_{ext}^{\delta}, \\ \hat{u}_{\delta,ext}^0 = 0 & \text{on } \partial\Omega_{ext}^{\delta}. \end{cases}$$

$k = 1$:

$$\left\{ \begin{array}{ll} \sigma_{\text{int}} \Delta \hat{u}_{\delta, \text{int}}^1 = 0 & \text{in } \Omega_{\text{int}}^\delta, \\ \hat{u}_{\delta, \text{int}}^1 = \frac{1-2\delta}{2} \partial_n \hat{u}_{\delta, \text{int}}^0 & \text{on } \Gamma_{\text{int}}^\delta, \\ \hat{u}_{\delta, \text{int}}^1 = 0 & \text{on } \partial\Omega \cap \partial\Omega_{\text{int}}^\delta. \end{array} \right.$$

$$\left\{ \begin{array}{ll} \sigma_{\text{ext}} \Delta \hat{u}_{\delta, \text{ext}}^1 = 0 & \text{in } \Omega_{\text{ext}}^\delta, \\ \hat{u}_{\delta, \text{ext}}^1 = -\frac{1-2\delta}{2} \partial_n \hat{u}_{\delta, \text{ext}}^0 & \text{on } \Gamma_{\text{ext}}^\delta, \\ \hat{u}_{\delta, \text{ext}}^1 = 0 & \text{on } \partial\Omega \cap \partial\Omega_{\text{ext}}^\delta. \end{array} \right.$$

If we truncate the series from the second term and we consider the truncated series $\hat{u}_\delta^{(1)} = \hat{u}_\delta^0 + \varepsilon \hat{u}_\delta^1$, we obtain the following equations

$$\left\{ \begin{array}{ll} \sigma_{\text{int}} \Delta \hat{u}_{\delta, \text{int}}^{(1)} = 0 & \text{in } \Omega_{\text{int}}^\delta, \\ \hat{u}_{\delta, \text{int}}^{(1)} - \frac{1-2\delta}{2} \partial_n \hat{u}_{\delta, \text{int}}^{(1)} = O(\varepsilon^2) & \text{on } \Gamma_{\text{int}}^\delta, \\ \hat{u}_{\delta, \text{int}}^{(1)} = 0 & \text{on } \partial\Omega \cap \partial\Omega_{\text{int}}^\delta. \end{array} \right. \quad (3.39)$$

$$\left\{ \begin{array}{ll} \sigma_{\text{ext}} \Delta \hat{u}_{\delta, \text{ext}}^{(1)} = 0 & \text{in } \Omega_{\text{ext}}^\delta, \\ \hat{u}_{\delta, \text{ext}}^{(1)} + \frac{1-2\delta}{2} \partial_n \hat{u}_{\delta, \text{ext}}^{(1)} = O(\varepsilon^2) & \text{on } \Gamma_{\text{ext}}^\delta, \\ \hat{u}_{\delta, \text{ext}}^{(1)} = 0 & \text{on } \partial\Omega \cap \partial\Omega_{\text{ext}}^\delta. \end{array} \right.$$

Now we rewrite the equations of Problem (1.37) to derive transmission conditions across the artificial boundaries $\Gamma_{\text{int}}^\delta$ and $\Gamma_{\text{ext}}^\delta$. Following the same procedure we have employed in Section 1.4.3, we use a formal Taylor series expansion of function $u^{(1)}$, solution to Problem (1.38) and we derive the following expressions for the

jump and mean value

$$\left\{ \begin{array}{l} [u]_{\Gamma} = [u]_{\Gamma^{\delta}} - 2\delta\varepsilon \{ \partial_n u \}_{\Gamma^{\delta}}, \\ \{u\}_{\Gamma} = \{u\}_{\Gamma^{\delta}} - \frac{1}{2}\delta\varepsilon [\partial_n u]_{\Gamma^{\delta}}, \\ [\partial_n u]_{\Gamma} = [\partial_n u]_{\Gamma^{\delta}} - 2\delta\varepsilon \{ \partial_n^2 u \}_{\Gamma^{\delta}}, \\ \{ \partial_n u \}_{\Gamma} = \{ \partial_n u \}_{\Gamma^{\delta}} - \frac{1}{2}\delta\varepsilon [\partial_n^2 u]_{\Gamma^{\delta}}. \end{array} \right.$$

Applying these expressions, we obtain the equations for the new function $u_{\delta}^{(1)}$

$$\left\{ \begin{array}{ll} \sigma_{\text{int}} \Delta u_{\delta, \text{int}}^{(1)} = 0 & \text{in } \Omega_{\text{int}}^{\delta}, \\ u_{\delta, \text{int}}^{(1)} - \frac{1-2\delta}{2} \partial_n u_{\delta, \text{int}}^{(1)} = O(\varepsilon^2) & \text{on } \Gamma_{\text{int}}^{\delta}, \\ u_{\delta, \text{int}}^{(1)} = 0 & \text{on } \partial\Omega \cap \partial\Omega_{\text{int}}^{\delta}. \end{array} \right. \quad (3.40)$$

$$\left\{ \begin{array}{ll} \sigma_{\text{ext}} \Delta u_{\delta, \text{ext}}^{(1)} = 0 & \text{in } \Omega_{\text{ext}}^{\delta}, \\ u_{\delta, \text{ext}}^{(1)} + \frac{1-2\delta}{2} \partial_n u_{\delta, \text{ext}}^{(1)} = O(\varepsilon^2) & \text{on } \Gamma_{\text{ext}}^{\delta}, \\ u_{\delta, \text{ext}}^{(1)} = 0 & \text{on } \partial\Omega \cap \partial\Omega_{\text{ext}}^{\delta}. \end{array} \right.$$

Now we define $v := \widehat{u}_{\delta}^{(1)} - u_{\delta}^{(1)}$. From Equations (3.40) and (3.39) we deduce that v satisfies the following equations

$$\left\{ \begin{array}{ll} \sigma_{\text{int}} \Delta v_{\text{int}} = 0 & \text{in } \Omega_{\text{int}}^{\delta}, \\ v_{\text{int}} - \frac{1-2\delta}{2} \partial_n v_{\text{int}} = O(\varepsilon^2) & \text{on } \Gamma_{\text{int}}^{\delta}, \\ v_{\text{int}} = 0 & \text{on } \partial\Omega \cap \partial\Omega_{\text{int}}^{\delta}. \end{array} \right. \quad (3.41)$$

$$\left\{ \begin{array}{ll} \sigma_{\text{ext}} \Delta v_{\text{ext}} = 0 & \text{in } \Omega_{\text{ext}}^{\delta}, \\ v_{\text{ext}} + \frac{1-2\delta}{2} \partial_n v_{\text{ext}} = O(\varepsilon^2) & \text{on } \Gamma_{\text{ext}}^{\delta}, \\ v_{\text{ext}} = 0 & \text{on } \partial\Omega \cap \partial\Omega_{\text{ext}}^{\delta}. \end{array} \right.$$

Thus, if we apply Theorem 8, we deduce

$$\|v\|_{1,\Omega^\delta} = \|\widehat{u}_\delta^{(1)} - u_\delta^{(1)}\|_{1,\Omega^\delta} \leq C\varepsilon^2.$$

Now we finally derive the desired convergence result. Applying Theorem 2 and Theorem 9 we deduce the desired result

$$\begin{aligned} & \left\| u_{\text{int}} - u_{\delta,\text{int}}^{[1]} \right\|_{1,\Omega_{\text{int}}^\delta} + \left\| u_{\text{ext}} - u_{\delta,\text{ext}}^{[1]} \right\|_{1,\Omega_{\text{ext}}^\delta} \\ & \leq \left\| u_{\text{int}} - u_{\text{int}}^{(1)} \right\|_{1,\Omega_{\text{int}}^\delta} + \left\| u_{\delta,\text{int}}^{[1]} - u_{\text{int}}^{(1)} \right\|_{1,\Omega_{\text{int}}^\delta} \\ & \quad + \left\| u_{\text{ext}} - u_{\text{ext}}^{(1)} \right\|_{1,\Omega_{\text{ext}}^\delta} + \left\| u_{\delta,\text{ext}}^{[1]} - u_{\text{ext}}^{(1)} \right\|_{1,\Omega_{\text{ext}}^\delta} \\ & \leq \left\| u_{\text{int}} - u_{\text{int}}^{(1)} \right\|_{1,\Omega_{\text{int}}^\delta} + \left\| u_{\delta,\text{int}}^{[1]} - \widehat{u}_{\delta,\text{int}}^{(1)} \right\|_{1,\Omega_{\text{int}}^\delta} + \left\| u_{\text{int}}^{(1)} - \widehat{u}_{\delta,\text{int}}^{(1)} \right\|_{1,\Omega_{\text{int}}^\delta} \\ & \quad + \left\| u_{\text{ext}} - u_{\text{ext}}^{(1)} \right\|_{1,\Omega_{\text{ext}}^\delta} + \left\| u_{\delta,\text{ext}}^{[1]} - \widehat{u}_{\delta,\text{ext}}^{(1)} \right\|_{1,\Omega_{\text{ext}}^\delta} + \left\| u_{\text{ext}}^{(1)} - \widehat{u}_{\delta,\text{ext}}^{(1)} \right\|_{1,\Omega_{\text{ext}}^\delta} \\ & \leq \left\| u_{\text{int}} - u_{\text{int}}^{(1)} \right\|_{1,\Omega_{\text{int}}^\delta} + \left\| u_{\delta,\text{int}}^{[1]} - \widehat{u}_{\delta,\text{int}}^{(1)} \right\|_{1,\Omega_{\text{int}}^\delta} + \left\| u_{\text{int}}^{(1)} - \widehat{u}_{\delta,\text{int}}^{(1)} \right\|_{1,\Omega_{\text{int}}^\delta} \\ & \quad + \left\| \widehat{u}_{\delta,\text{int}}^{(1)} - u_{\delta,\text{int}}^{(1)} \right\|_{1,\Omega_{\text{int}}^\delta} + \left\| u_{\text{ext}} - u_{\text{ext}}^{(1)} \right\|_{1,\Omega_{\text{ext}}^\delta} + \left\| u_{\delta,\text{ext}}^{[1]} - \widehat{u}_{\delta,\text{ext}}^{(1)} \right\|_{1,\Omega_{\text{ext}}^\delta} \\ & \quad + \left\| u_{\text{ext}}^{(1)} - \widehat{u}_{\delta,\text{ext}}^{(1)} \right\|_{1,\Omega_{\text{ext}}^\delta} + \left\| \widehat{u}_{\delta,\text{ext}}^{(1)} - u_{\delta,\text{ext}}^{(1)} \right\|_{1,\Omega_{\text{ext}}^\delta} \\ & \leq C\varepsilon^2. \end{aligned}$$

□

NUMERICAL RESULTS

4.1 Introduction

This chapter is devoted to numerical tests regarding the approximate problems we have derived. For this purpose, we have implemented a finite element code that we employ to discretize the variational formulations derived in Chapter 3 in order to obtain approximate solutions of the models. The code is capable of solving the 2D Laplace equation and the 3D axisymmetric Laplace equation in the meridian domain. For a deeper explanation about the finite element method and the developed code, we refer the reader to Appendix B.

4.2 2D configuration

4.2.1 Dirichlet conditions

First class of ITCs

We first compare the solutions obtained with the reference model against our derived asymptotic models. In this section, we consider non-realistic model problems useful for analyzing the convergence behaviour. More physically meaningful results will be depicted on section 4.5.

We first show some figures of the reference model so that we can qualitatively understand the solution we are trying to approximate. For these experiments, the considered domain is a $2 \text{ m} \times 1 \text{ m}$ rectangle domain formed by a thin layer with

thickness equal to 0.25 m. We also consider a conductivity of the following form

$$\sigma = \begin{cases} \sigma_{\text{int}} = 5 \text{ S/m} & \text{in } \Omega_{\text{int}}^\varepsilon, \\ \sigma_{\text{lay}} = 64 \text{ S/m} & \text{in } \Omega_{\text{lay}}^\varepsilon, \\ \sigma_{\text{ext}} = 3 \text{ S/m} & \text{in } \Omega_{\text{ext}}^\varepsilon, \end{cases} \quad (4.1)$$

and the following right-hand side

$$f = \begin{cases} f_{\text{int}} = 1 \text{ C} & \text{in } \Omega_{\text{int}}^\varepsilon, \\ f_{\text{lay}} = 0 \text{ C} & \text{in } \Omega_{\text{lay}}^\varepsilon, \\ f_{\text{ext}} = 1 \text{ C} & \text{in } \Omega_{\text{ext}}^\varepsilon, \end{cases}$$

where the units S/m and C correspond to Siemens per meter and Coulomb. We solve the reference Problem (1.2) by employing the Finite Element Method. For discretizing the domain, we use 384 triangular shaped elements and Lagrange interpolating Polynomials of second degree. In Figure 4.1, we observe the solution we obtain for the reference Problem (1.2) in this case.

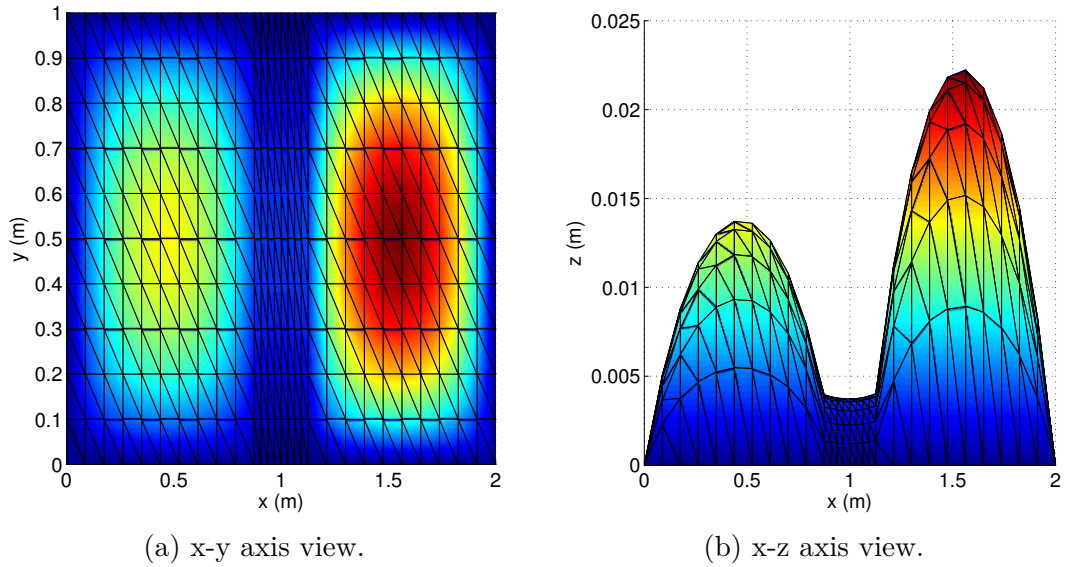


Figure 4.1: Solution to the reference Problem (1.2) .

Now, we perform a qualitative comparison between the solution to the reference model we have shown and the approximate models (1.18) and (1.19). Using the same parameters and configuration, we solve these approximate models. Figure 4.2 shows the solution we obtain for the asymptotic models of order two, (1.18),

and order four, (1.19). We notice that the fourth-order model is more accurate and approximates better the effect of the highly conductive thin layer than the second-order model. In order to better observe this behaviour, in the following lines we show a quantitative comparison of these models.

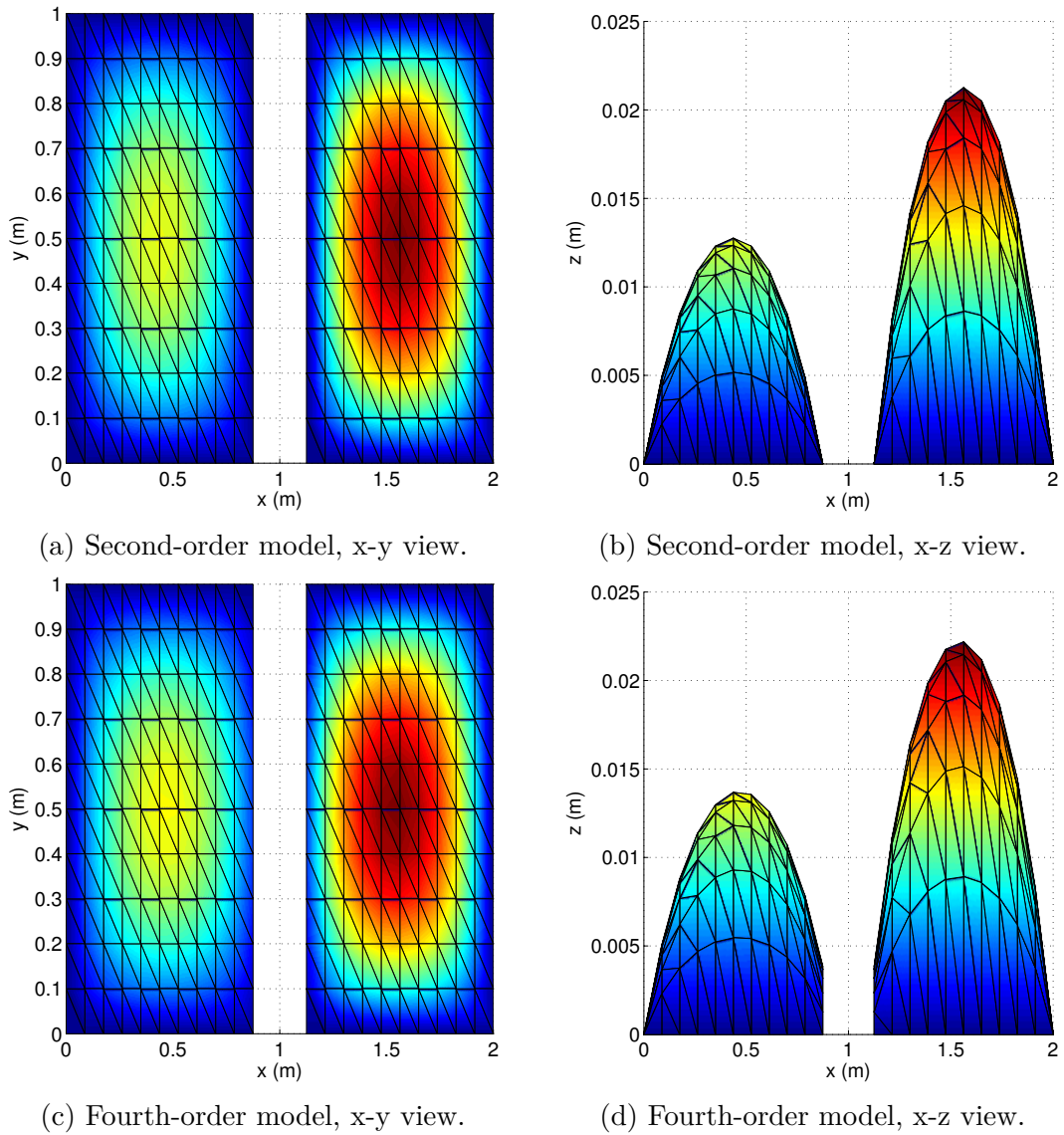


Figure 4.2: Solution to the second-order model (1.18) and the fourth-order model (1.19) of the first class.

To do so, we calculate the H^1 error between the reference solution and the approximate models for different thicknesses of the thin layer. In Figure 4.3 we observe the obtained convergence rates for the H^1 relative error and Table 4.1

shows the slopes of the curves corresponding to this figure. From these results we observe that the numerical convergence rates we have obtained coincide with the theoretical convergence rates proved in Chapter 3. As expected, the fourth-order model performs better than the second-order model.

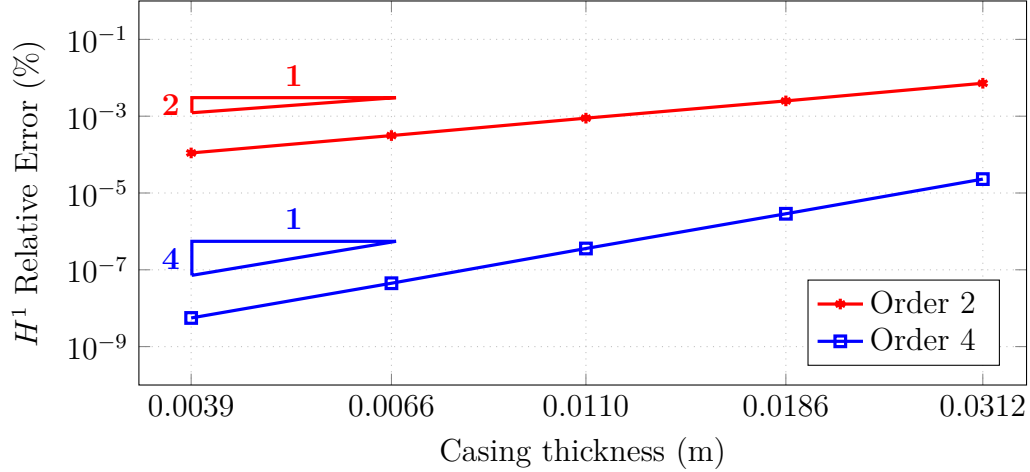


Figure 4.3: H^1 error of the second-order model (1.18) and fourth-order model (1.19) of the first class for different values of ε .

Casing thickness (ε)	0.0052	0.0088	0.0985	0.1086	Expected ($\varepsilon \rightarrow 0$)
Order 2 H^1 slopes	2.0103	2.0152	2.0082	1.9275	2
Order 4 H^1 slopes	4.0066	4.0003	3.9506	3.7250	4

Table 4.1: Slopes corresponding to the curves of Figure 4.3.

Second class of ITCs

We first compare the solution to the reference model and the asymptotic models of the second class. We employ the same physical parameters as explained in the previous section for these new tests. In Figure 4.4, we observe the solution we obtain for the reference Problem (1.2) and in Figure 4.5, we observe the solution we obtain for the asymptotic models of order one (1.36), and order two (1.38).

As we stated in the previous sections, the stability of the second-order model cannot be guaranteed. As a result, large variations in the solution occur when we slightly change the material parameters. We illustrate this fact in Figure 4.6, where we show the solution for the second-order model for different values of ε . We

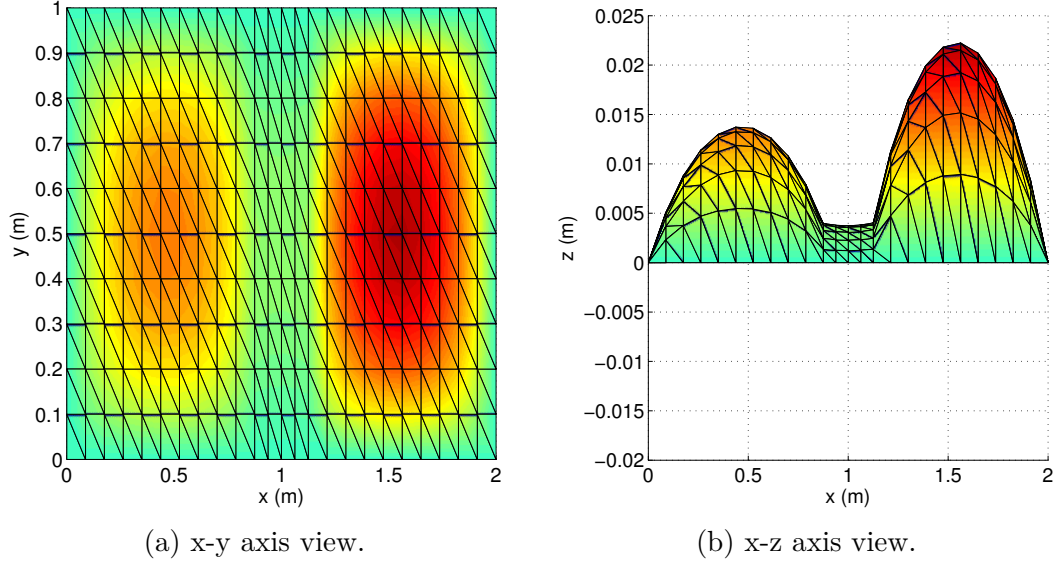


Figure 4.4: Solution to the reference Problem (1.2) .

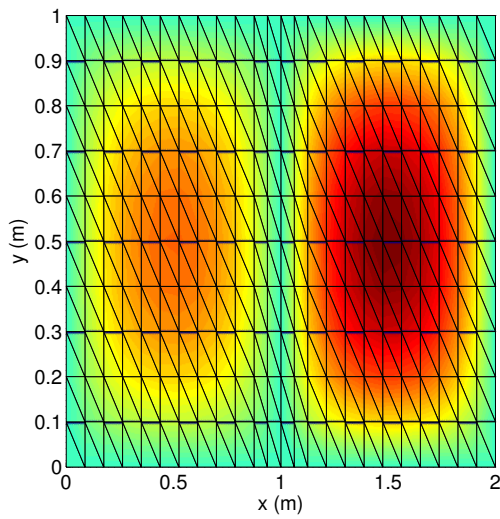
observe that the solution drastically changes around the transmission conditions for every small variation in the value of ε .

To deliver a more quantitative comparison of the models we have derived, we calculate the L^2 and H^1 errors between the reference solution and the approximate models for different thicknesses of the thin layer. In Figure 4.7, we observe the obtained convergence rates for the L^2 relative error and in Figure 4.8 the convergence rates for the H^1 relative error.

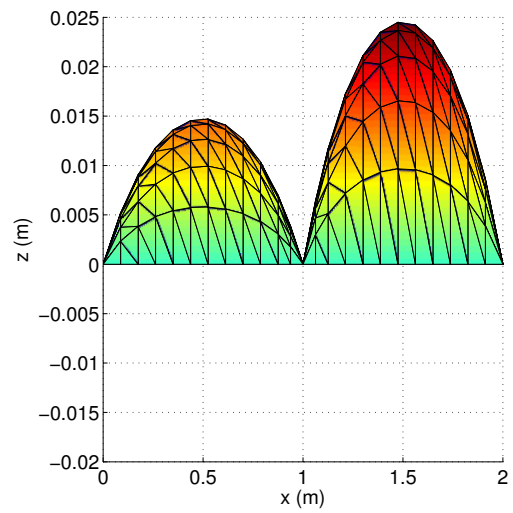
Casing thickness (ε)	0.0052	0.0088	0.0985	0.1086	Expected ($\varepsilon \rightarrow 0$)
Order 1 L^2 slopes	0.9833	0.9713	0.9500	0.9103	1
Order 1 H^1 slopes	0.9888	0.9810	0.9673	0.9421	1
Order 2 L^2 slopes	1.9968	2.0420	2.0059	2.0460	2
Order 2 H^1 slopes	1.3788	1.9847	1.2003	1.6763	2
δ -Order 2 L^2 slopes	2.0035	2.0054	2.0084	2.0076	2
δ -Order 2 H^1 slopes	2.0002	2.0038	2.0074	2.0078	2

Table 4.2: Slopes corresponding to the curves of Figures 4.7 and 4.8.

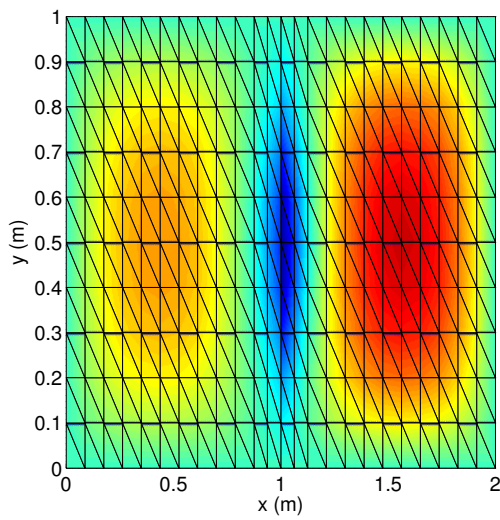
We observe that the numerical convergence rates we have obtained coincide with the theoretical convergence rates proved in Section 3.5 for the first-order



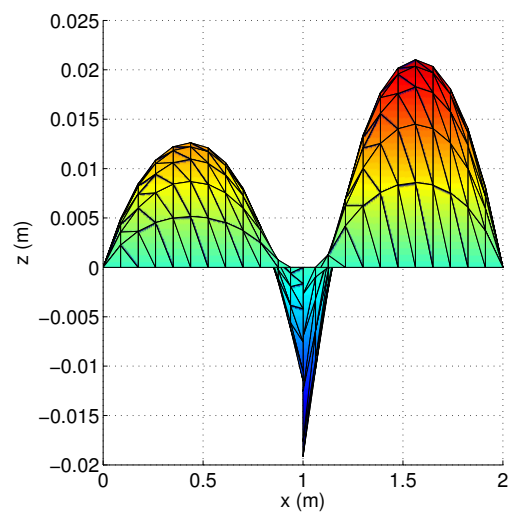
(a) First-order model, x-y view.



(b) First-order model, x-z view.



(c) Second-order model, x-y view.



(d) Second-order model, x-z view.

Figure 4.5: Solution to the first-order model (1.36) and the second-order model (1.38) of the second class.

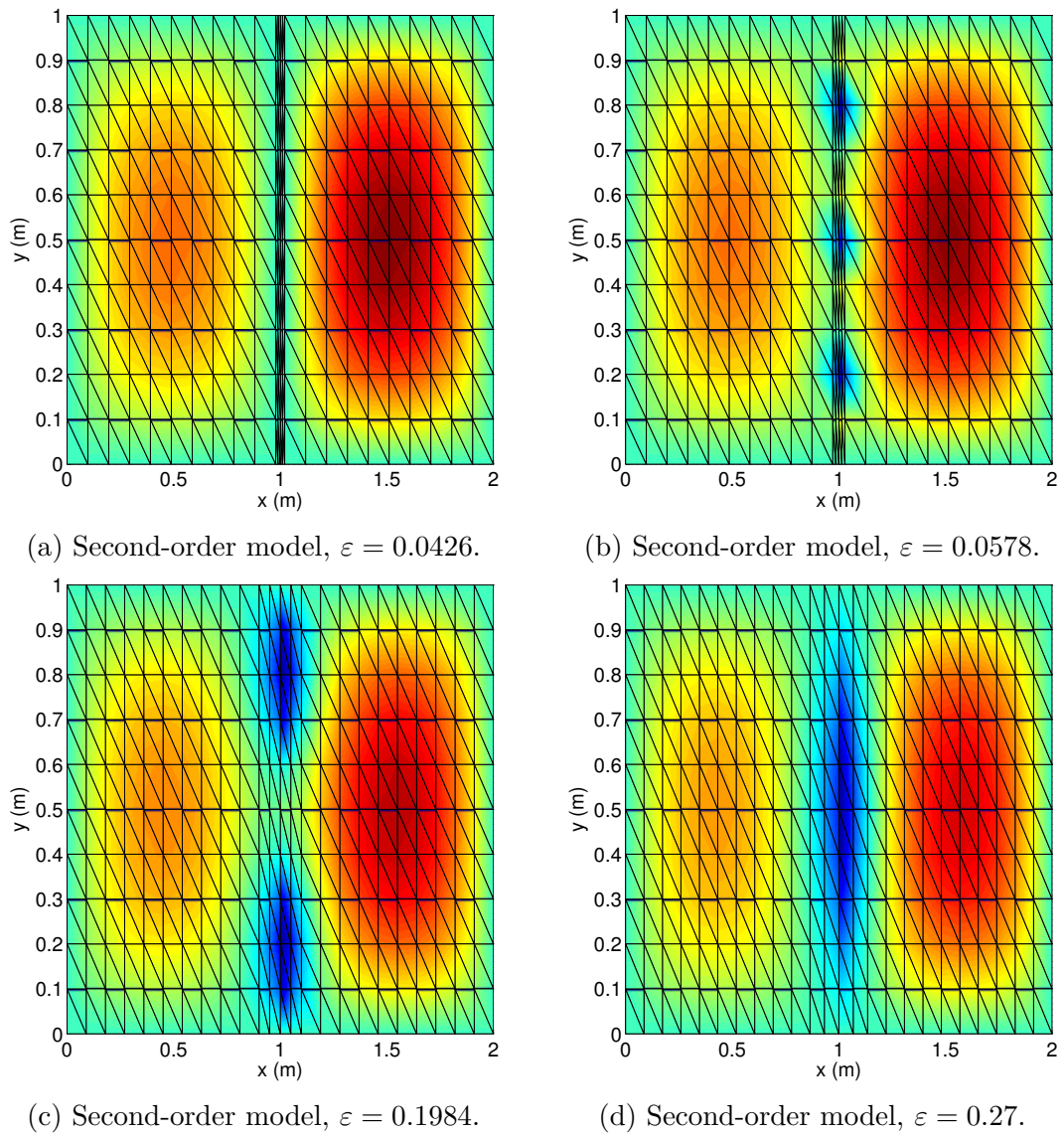


Figure 4.6: Instabilities of the solutions to the second-order model (1.38) for different values of ε .

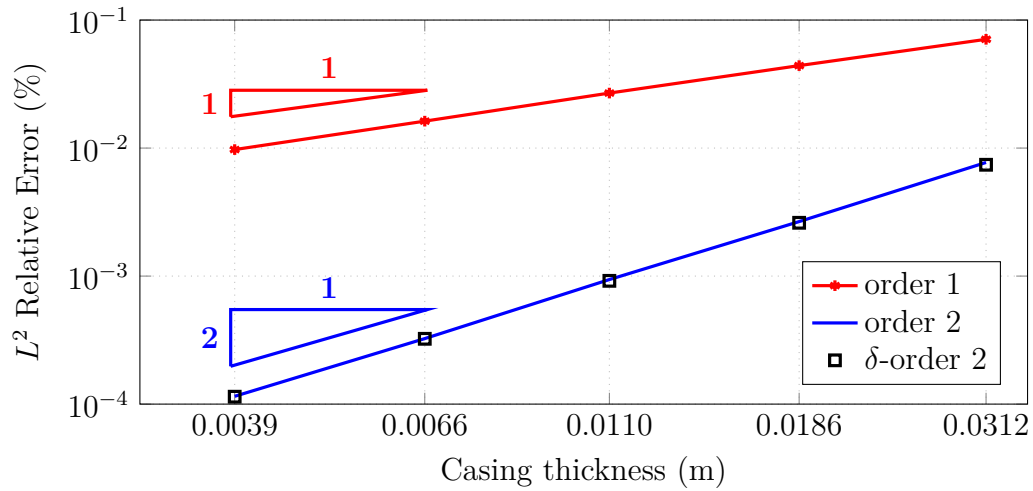


Figure 4.7: L^2 error of the first-order model (1.36), second-order model (1.38), and stabilized δ -order two model (1.43) of the second class for different values of ε .

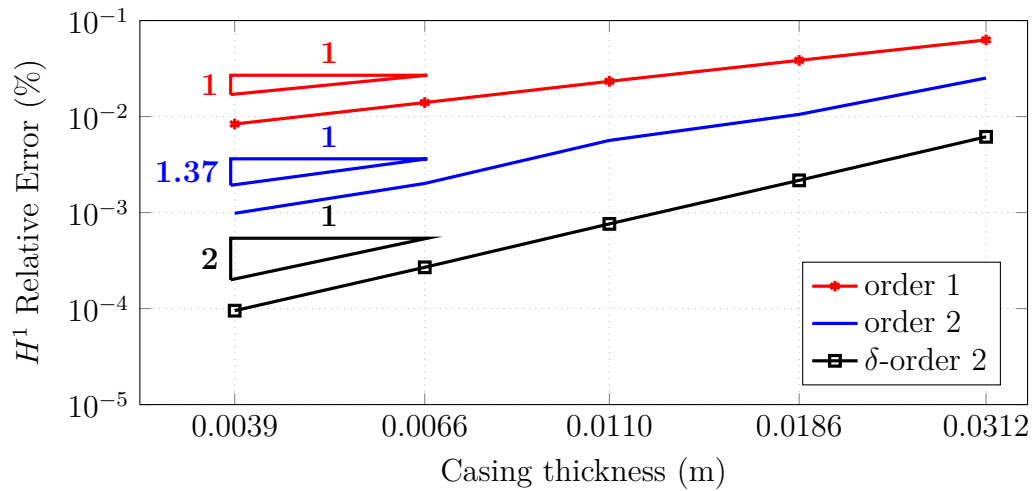


Figure 4.8: H^1 error of the first-order model (1.36), second-order model (1.38), and stabilized δ -order two model (1.43) of the second class for different values of ε .

model. On the other hand, for the second-order model, even though we still recover the expected theoretical order of convergence for the L^2 relative error, due to the instabilities, it does not perform as well for the H^1 relative error. Even so, it still outperforms the first-order model.

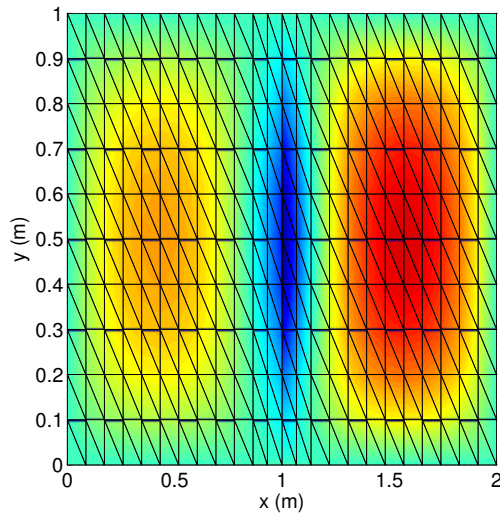
To overcome these instabilities, in Section 1.4.3, we have derived a new second-order model by defining some artificial boundaries and moving the transmission conditions to these new boundaries. To derive this new model (1.43) we employ a parameter δ that controls the distance between the artificial boundaries. In Chapter 3 we prove that for $\delta > 0.5$ this approach solves the problem of instabilities. Figure 4.9 shows a problem with instabilities and how they can be eliminated when applying a δ parameter greater than 0.5. However, the instabilities are not completely removed if this δ parameter is not greater than 0.5. To illustrate this fact, the example of Figure 4.9 shows that for $\delta=0.1$ the instabilities are still present, whereas when $\delta = 0.51$ is applied, the instabilities disappear.

Figure 4.7 compares the obtained convergence rates for the L^2 relative error. Figure 4.8 shows the convergence rates for the H^1 relative error for the unstable second-order model and for the stabilized δ -order two model. We observe that for the L^2 error both models behave similarly. For the H^1 error, the second-order model does not converge properly, whereas the stabilized δ -order two model delivers the correct convergence rates. In Table 4.2 we display the slopes of the curves corresponding to those figures which show the expected theoretical convergence rates.

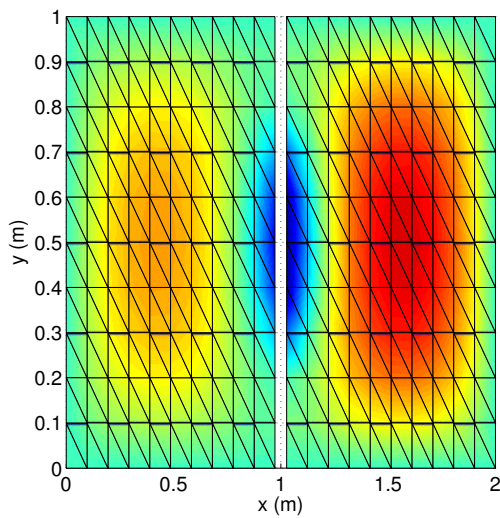
We observe that if we apply the artificial boundary technique with a δ greater than 0.5, instability problems disappear, and the numerical convergence rates coincide with the theoretical convergence rates proved in Section 3.5, for both the L^2 and the H^1 errors.

Comparison

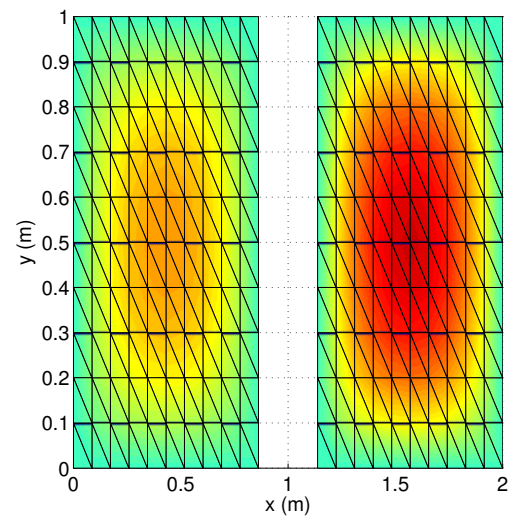
In this section, we will do a brief comparison between the different derived asymptotic models. We mention the strong and weak points of each class of ITCs. For the first class of ITCs, the model with highest order reaches a convergence of order four, whereas for the second class of ITCs, the model with highest order only reaches a convergence of order two. We observe these convergence rates in L^2 norm for the four models we have derived in Figure 4.10 and in H^1 norm in Figure 4.11. We see that all the models converge with the expected order of accuracy in L^2 norm. On the other hand, in H^1 norm, all models converge with the expected order of accuracy except the second-order model of the second class due to the instabilities.



(a) Second-order model with instabilities.



(b) stabilized δ -order two model for $\delta = 0.1$.



(c) stabilized δ -order two model for $\delta = 0.51$.

Figure 4.9: Removing the instabilities of the second-order model (1.38) with the artificial boundaries.

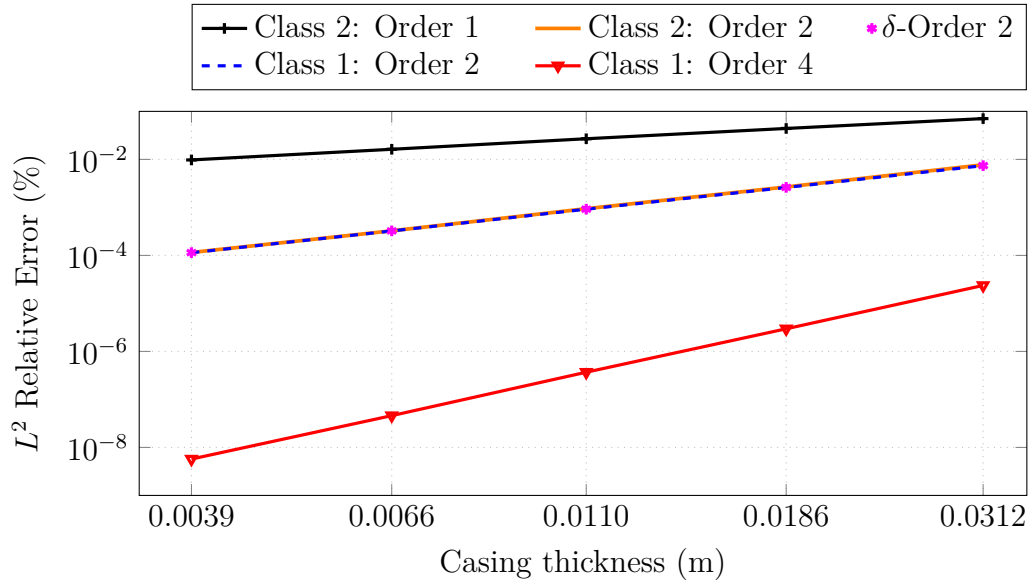


Figure 4.10: L^2 relative error of the different asymptotic models for different values of ε

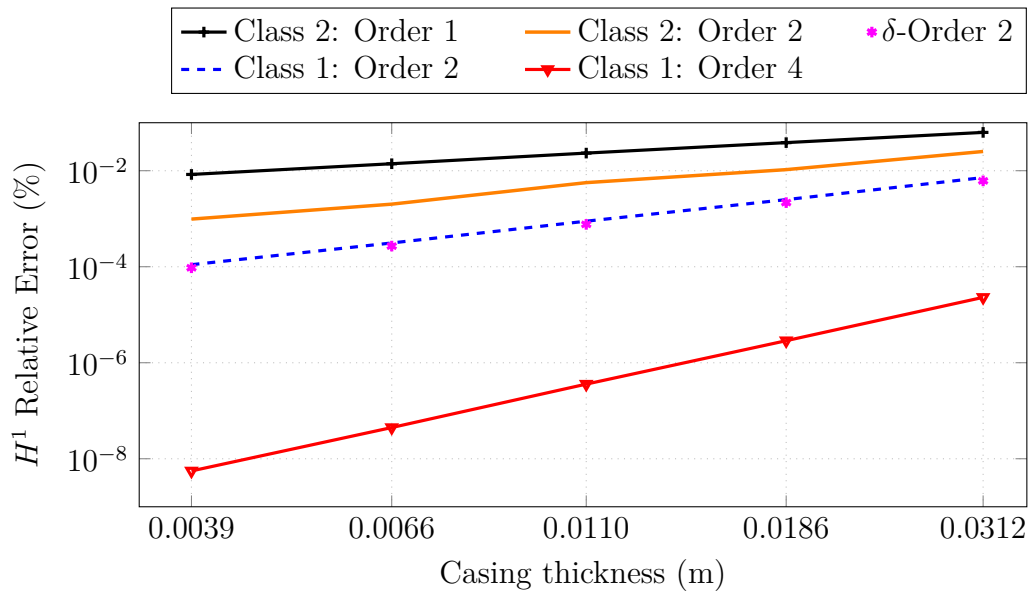


Figure 4.11: H^1 relative error of the different asymptotic models for different values of ε

Another drawback of the second class of ITCs is that the model of order two presents instabilities whereas the models derived with the first approach are both stable.

Regarding the domain, a strong point of the second class of ITCs is that the domain does not depend on ε , while the domain for the first class ITCs depends on ε . Even though this point is not very relevant for our configuration, due to the thin layer having a straight shape, it could be very interesting when considering more complex configurations, in which the shape of the thin layer is curved. In such a case, the fact of having a single interface between the two subdomains instead of having a gap greatly reduces the complexity of implementation of the model. All these features are summarized in Table 4.3.

Model	Numerical order	Stability	ε -independent domain
Class 1: Order 2	2	✓	✗
Class 1: Order 4	4	✓	✗
Class 2: Order 1	1	✓	✓
Class 2: Order 2	1-2	✗	✓
δ -Order 2	2	✓	✗

Table 4.3: Comparison of the different derived models.

4.2.2 Mixed boundary conditions

Second class of ITCs

Here we consider the case of approximate problems with mixed conditions. We follow the same plan we have considered for the Dirichlet case. We use the material properties of Equation (4.1) and the following source:

$$f(x, y) = \begin{cases} f_{\text{int}}(x, y) = y^2 C & \text{in } \Omega_{\text{int}}^\varepsilon, \\ f_{\text{lay}}(x, y) = 0 C & \text{in } \Omega_{\text{lay}}^\varepsilon, \\ f_{\text{ext}}(x, y) = y^2 C & \text{in } \Omega_{\text{ext}}^\varepsilon. \end{cases}$$

We begin with a qualitative comparison between the solution to the reference model and the asymptotic models. We show some figures of the reference model,

as an illustration of the solution we intend to approximate and then, we show some figures of the approximate models to visualize how they approximate the reference solution. Figure 4.12 depicts the solution we obtain for the reference model.

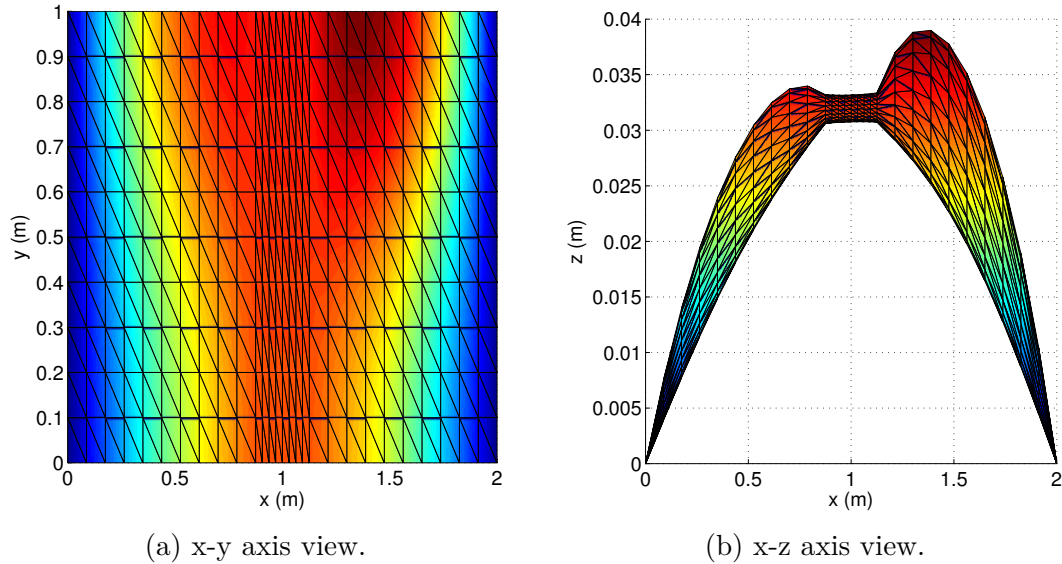


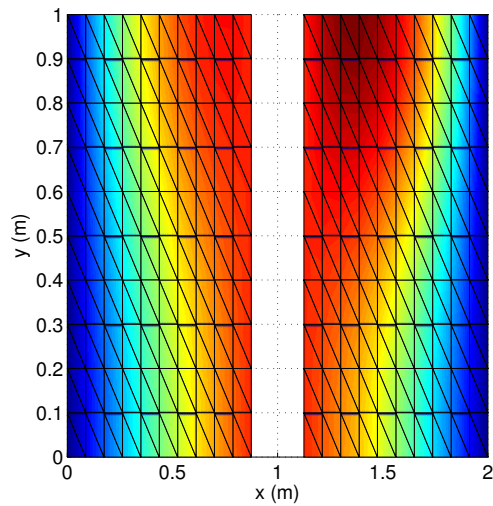
Figure 4.12: Solution to the reference problem with mixed boundary conditions.

Now, we provide a qualitative comparison between the solution to the reference model we have shown and the approximate models (2.23) and (2.24). Figure 4.13 shows the solution we obtain for the asymptotic models of order two, (2.23), and order four, (2.24). As expected, we notice that the fourth-order model is more accurate and approximates better the effect of the high conductive thin layer than the second-order model.

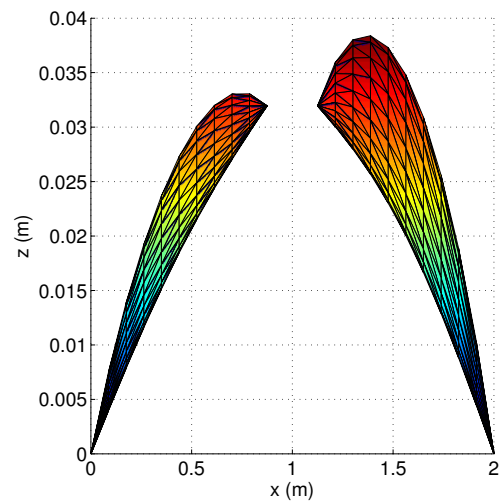
As in the previous section, we have calculated the H^1 error between the reference solution and the approximate models for different thicknesses of the thin layer. Figure 4.14 displays the obtained convergence rates for the H^1 relative error. Table 4.4 shows the slopes of the curves corresponding to this figures. From these results we conclude that the numerical rates of converge are the expected ones.

Casing thickness (ε)	0.0117	0.0234	0.0469	0.0938	Expected ($\varepsilon \rightarrow 0$)
Order 2 H^1 slopes	1.9864	2.0529	2.0817	2.0984	2
Order 4 H^1 slopes	4.0221	4.032	4.0454	4.0523	4

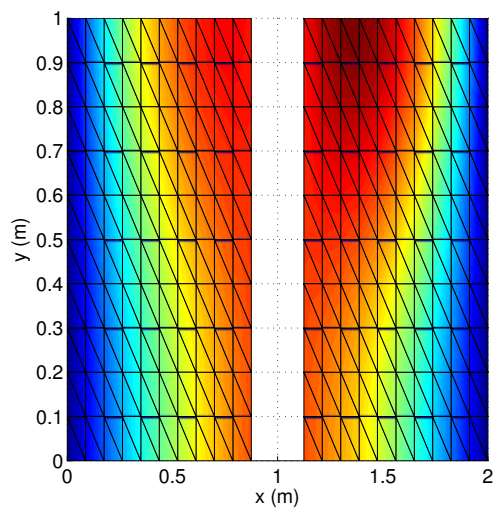
Table 4.4: Slopes corresponding to the curves of Figure 4.14.



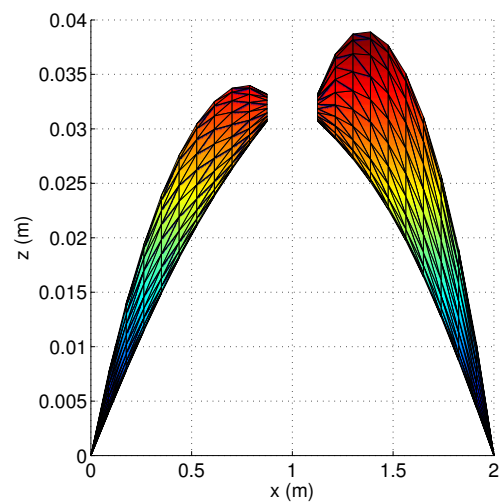
(a) Second-order model, x-y view.



(b) Second-order model, x-z view.



(c) Fourth-order model, x-y view.



(d) Fourth-order model, x-z view.

Figure 4.13: Solution to the second-order model (2.23) and the fourth-order model (2.24) of the first class with mixed conditions.

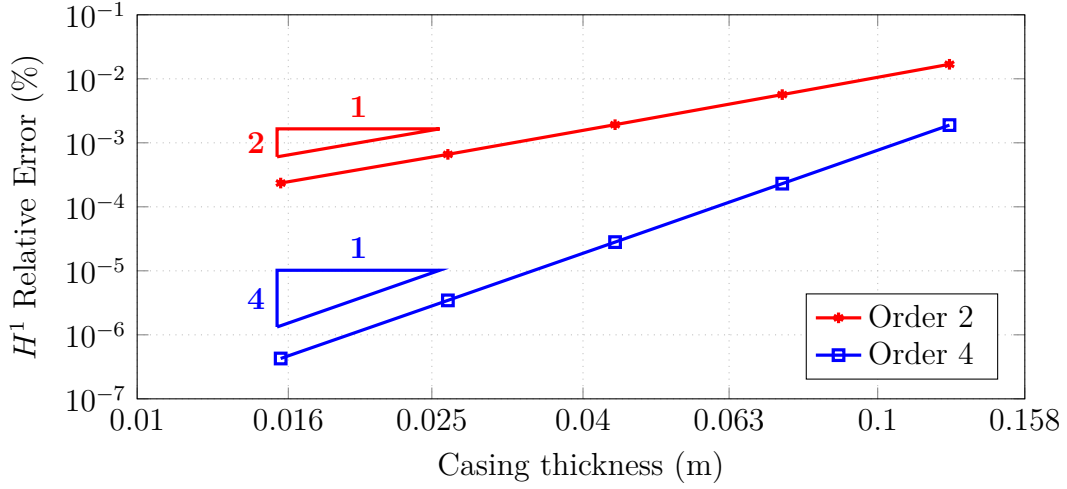


Figure 4.14: H^1 error of the second-order model (2.23) and fourth-order model (2.24) of the first class with mixed conditions for different values of ε .

4.3 2D time-harmonic configuration

This section is devoted to numerical tests regarding the approximate problems we have derived when the frequency is not zero any more. For this purpose, we employ the finite element method along with the variational formulations derived in Appendix A.3. We employ the same physical parameters previously introduced in Section 4.2.1, but now we have to also consider the permittivity ϵ_0 and the frequency ω . We select these two parameters as follows

$$\begin{cases} \epsilon_0 = 3 \text{ F m}^{-1}, \\ \omega = 8 \text{ Hz}. \end{cases}$$

Figure 4.15 depicts the solution we obtain for the reference Problem (1.45). In the same way, Figure 4.16 shows solution we obtain for the asymptotic models of order two (1.49), and order four (1.50). We observe that the fourth-order model is more accurate and approximates better the effect of the high conductive thin layer than the second-order model.

Again, we calculate the H^1 error between the reference solution and the approximate models for different thicknesses of the thin layer. Figure 4.17 displays the convergence rates for the H^1 relative error. Table 4.5 shows the slopes of the curves corresponding to this figure. From these results we deduce that the numerical rates of converge are the expected ones

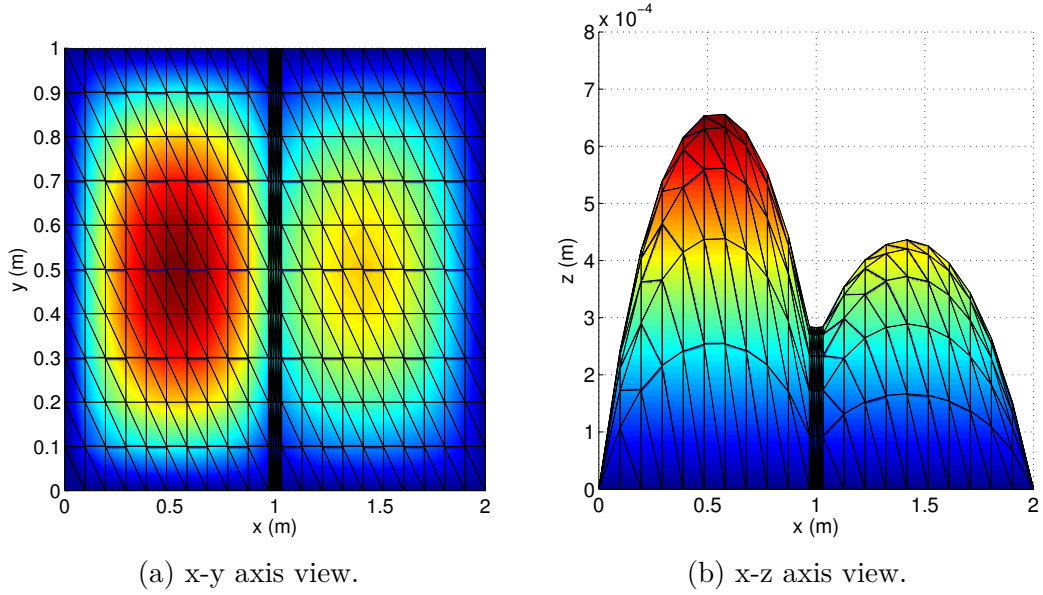


Figure 4.15: Real part of the solution to the frequency dependent model Problem (1.45).

Casing thickness (ε)	0.0052	0.0088	0.0148	0.0249	Expected ($\varepsilon \rightarrow 0$)
Order 2 H^1 slopes	1.9980	1.9871	1.9491	1.8227	2
Order 4 H^1 slopes	4.0437	4.0541	4.0234	3.7893	4

Table 4.5: Slopes corresponding to the curves of Figure 4.17.

4.4 3D Axisymmetric configuration

In this section we consider the case of an axisymmetric cylinder shaped domain. For this purpose, we employ the finite element method along with the variational formulations derived in Appendix A.4. We use the physical parameters defined in Section 4.2.1.

Figure 4.18 displays the solution to the reference Problem (1.58). Figure 4.19 shows the solution to the asymptotic models of order two (1.75), and order four (1.77). As in the 2D case, we notice that the fourth-order model is more accurate and approximates better the effect of the high conductive thin layer than the second-order model.

We calculate the H^1 error between the reference solution and the approximate

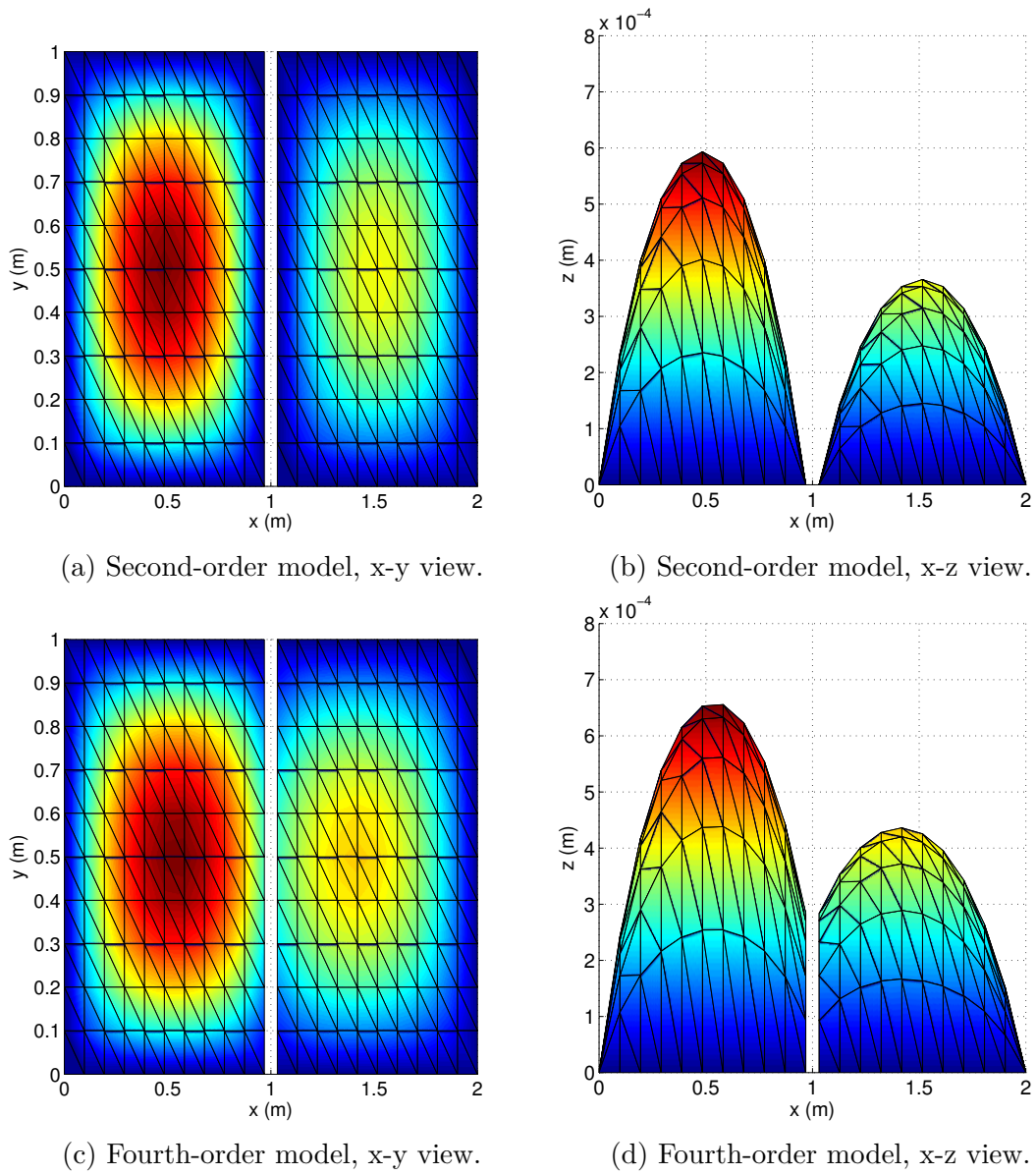


Figure 4.16: Real part of the solution to the second-order model (1.49) and the fourth-order model (1.50) for the frequency dependent configuration.

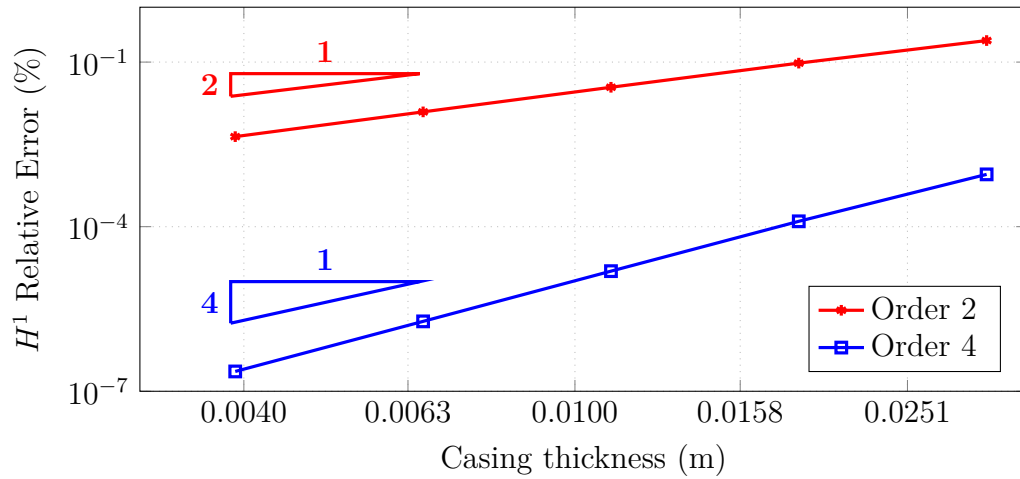


Figure 4.17: H^1 relative error of the second-order model and fourth-order model for different values of ε for the frequency dependent configuration.

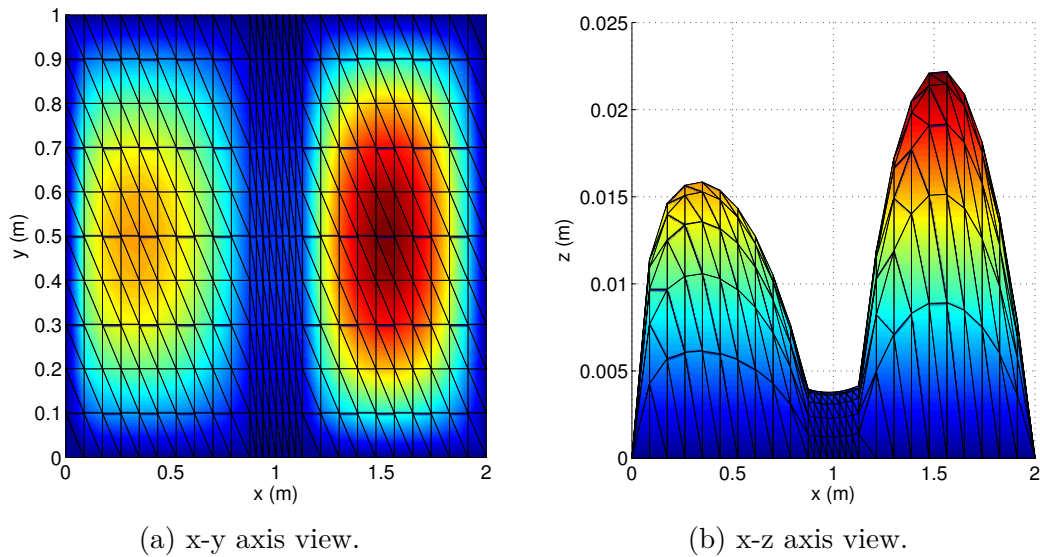


Figure 4.18: Solution to the 3D axisymmetric reference Problem (1.58) .

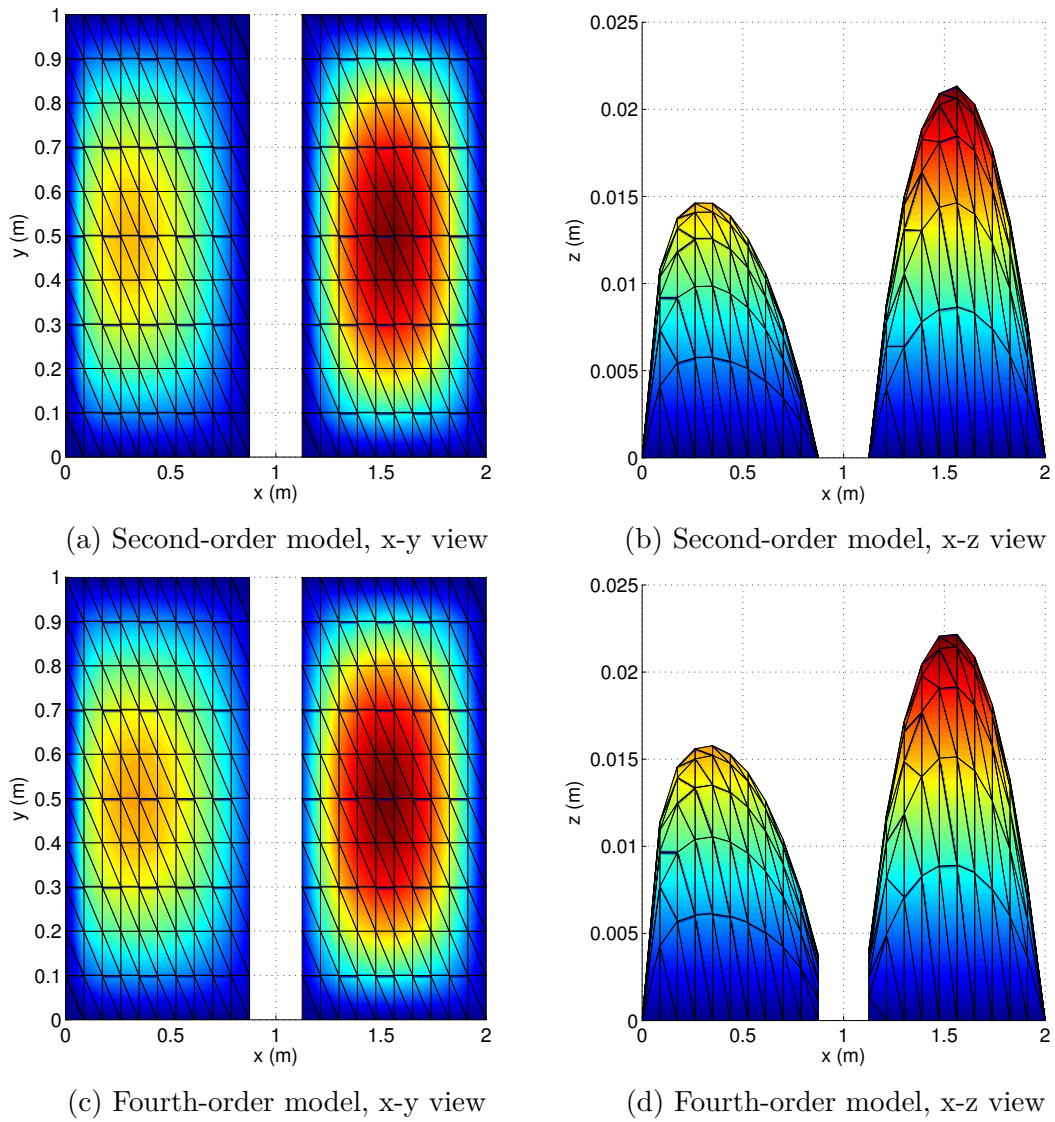


Figure 4.19: Solution to the second-order model (1.75) and the fourth-order model (1.77) for the 3D axisymmetric configuration.

models for different thicknesses of the thin layer. Figure 4.20 depicts the convergence rates for the H^1 relative error. Table 4.6 shows the slopes of the curves corresponding to this figure. From these results we deduce that the numerical rates of converge are the expected ones

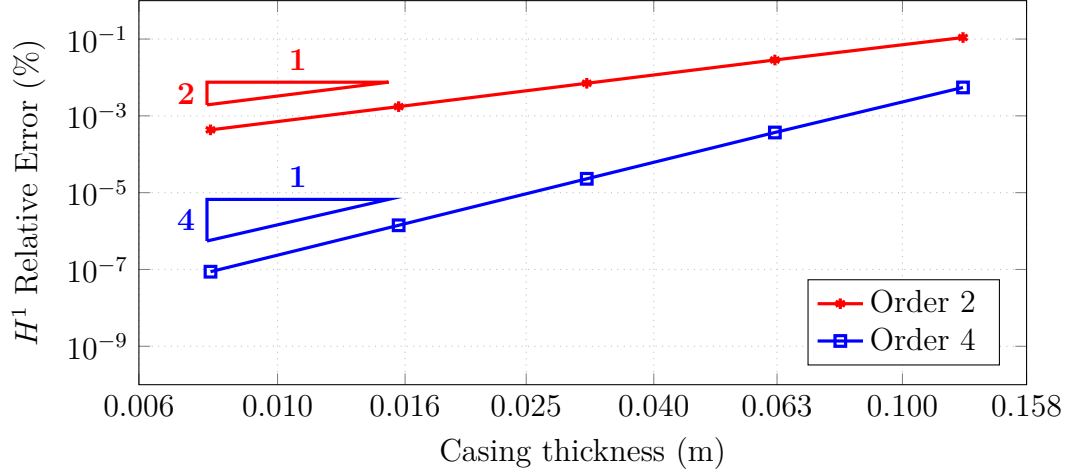


Figure 4.20: H^1 error of the second-order model (1.75) and fourth-order model (1.77) for different values of ε for the 3D axisymmetric configuration.

Casing thickness (ε)	0.0117	0.0234	0.0469	0.0938	Expected ($\varepsilon \rightarrow 0$)
Order 2 H^1 slopes	2.0117	2.0182	2.0150	1.9425	2
Order 4 H^1 slopes	4.0150	4.0206	4.0060	3.8967	4

Table 4.6: Slopes corresponding to the curves of Figure 4.20.

4.5 Application

According to [28], the second derivative of the electric potential in the vertical axis direction can be employed to determine the resistivity of the rock formations. This second derivative of the potential in the axis direction can be approximated by a second difference formula, which we explicit later in this section.

The configuration is similar to the one employed in Section 1.6. We begin with a three dimensional cased borehole where we consider the equations for the electric potential

$$\operatorname{div}(\sigma \Delta u) = f.$$

Since all the elements composing the configuration are axisymmetric, we employ cylindrical coordinates to eliminate one dimension due to the solution not being dependent of the angular variable. We place a transmitter inside the borehole, in the part of the domain denoted as $\Omega_{\text{int}}^\varepsilon$, touching the casing from the inside. Then, we place three equidistant receivers several meters above the transmitter, in the same way we have done with the receiver, touching the casing from the inside. This configuration is depicted at figure 4.21. We consider the following right-hand side

$$f = \begin{cases} 1 & \text{at the transmitter,} \\ 0 & \text{in the rest of the domain,} \end{cases}$$

and a conductivity of the following form

$$\sigma = \begin{cases} \sigma_{\text{int}} & \text{in } \Omega_{\text{int}}^\varepsilon, \\ \sigma_{\text{lay}} & \text{in } \Omega_{\text{lay}}^\varepsilon, \\ \sigma_{\text{ext}} & \text{in } \Omega_{\text{ext}}^\varepsilon, \end{cases}$$

where σ_{lay} is several magnitudes greater than σ_{int} and σ_{ext} . The electric potential should tend to 0 when far away from the transmitter. Thus, we consider homogeneous Dirichlet boundary conditions, $u = 0$, on the exterior face of the cylinder. On both bases of the cylinder, we consider homogeneous Neumann boundary conditions, $\partial_n u = 0$.

The receivers are 1.85 m above the transmitter and there is a 0.15 m separation between them. The three receivers and the transmitter form what we call the instrument. Even if we move the instrument, this distance between transmitter and receivers remains fixed. The inside of the borehole has a radius of 0.16 m and the thickness of the casing is 0.01 m. The whole domain, is 10 m in the horizontal direction and several km in the vertical direction.

According to [28], the electric field, when in the presence of a casing, can be divided into a near zone, an intermediate zone and a far zone. In the intermediate zone, the second derivative of the potential in the axis direction can be applied to determine the resistivity of the formation. For approximating the second derivative of the potential, we employ the second difference of potential measured at the receivers. Let (r_1, z_1) , (r_1, z_2) , and (r_1, z_3) be the positions of the first, second, and third receivers respectively and let h denote the distance between the receivers. We perform the following formal Taylor series expansion on the z variable around the

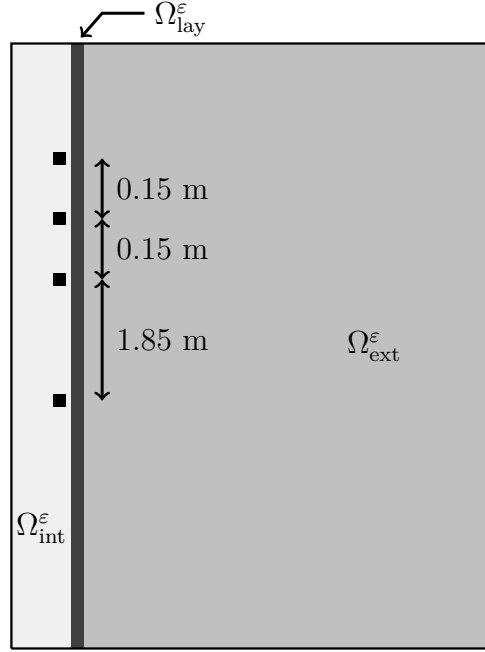


Figure 4.21: 2D domain considered for the application.

point (r_1, z_2)

$$\begin{cases} u(r_1, z_2 + h) = u(r_1, z_2) + \partial_z u(r_1, z_2) h + \partial_z^2 u(r_1, z_2) \frac{h^2}{2} + O(h^3), \\ u(r_1, z_2 - h) = u(r_1, z_2) - \partial_z u(r_1, z_2) h + \partial_z^2 u(r_1, z_2) \frac{h^2}{2} + O(h^3). \end{cases}$$

Adding both expressions and taking into account $z_1 = z_2 - h$ and $z_3 = z_2 + h$ we obtain the following second difference formula for the second derivative of the potential

$$\partial_z^2 u(r_1, z_2) = \frac{u(r_1, z_3) - 2u(r_1, z_2) + u(r_1, z_1)}{h^2} + O(h).$$

According to [28], if we measure this values at the receivers, we can recover the values of the resistivity in the rock formations, more precisely, the second derivative of the potential should be proportional to the square root of the rock conductivity:

$$\partial_z^2 u(r_1, z_2) \approx C \cdot \sigma_{\text{ext}}^{\frac{1}{2}}, \quad C > 0.$$

4.5.1 One rock layer with varying conductivity

For the first experiment we consider $\sigma_{\text{int}} = 1 \text{ S/m}$ and $\sigma_{\text{lay}} = 10^6 \text{ S/m}$. We will perform several simulations employing different conductivities in the rock formations to check if our method can recover these conductivities. In these simulations, the resistivity in the rock formation, $\rho_{\text{ext}} = \sigma_{\text{ext}}^{-1}$, will vary between $1 \text{ } \Omega \cdot m$ and $10000 \text{ } \Omega \cdot m$, where Ω corresponds to ohm. In Figure 4.22 we observe the results of measuring the second difference of potential at the receivers for different configurations in which the resistivity of the rock formation is varying from one another. The graphic is plotted in logarithmic scale and the curve has a slope of -0.5 , which means we are properly recovering the values of resistivity in the rock formations. What is more, we observe that when we perform this procedure applying the fourth-order asymptotic model derived in Section 1.6.3, we also recover perfectly the values of the resistivity in the rock formations and we produce a negligible error with respect to the reference model.

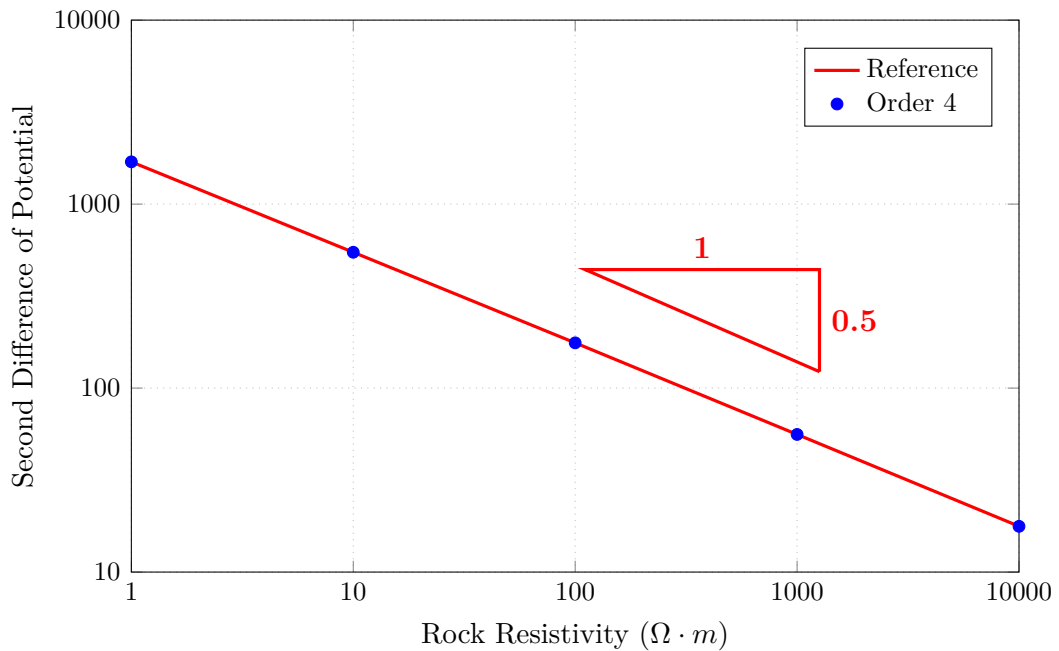


Figure 4.22: Second difference of potential for different rock resistivities.

4.5.2 Two rock layers with fixed conductivity

Now we perform a second experiment. In this case, we consider two rock formations with different conductivity values. Then, we try to recover the conductivity of both

rock formations applying the same method we have explained above. For that purpose we calculate the second difference of potential for different positions of the instrument along the z axis. The expected outcome is that when we place the instrument horizontally aligned with the first rock formation we should measure the conductivity of that rock formation and when we horizontally align it with the second rock formation we should measure the conductivity of the second rock formation. The interface is located between the two rock formations at $z = 0$. We consider the resistivity of the top rock formation to be $10 \Omega \cdot m$ and the conductivity of the down rock formation to be $1000 \Omega \cdot m$. We observe this configuration in Figure 4.23a.

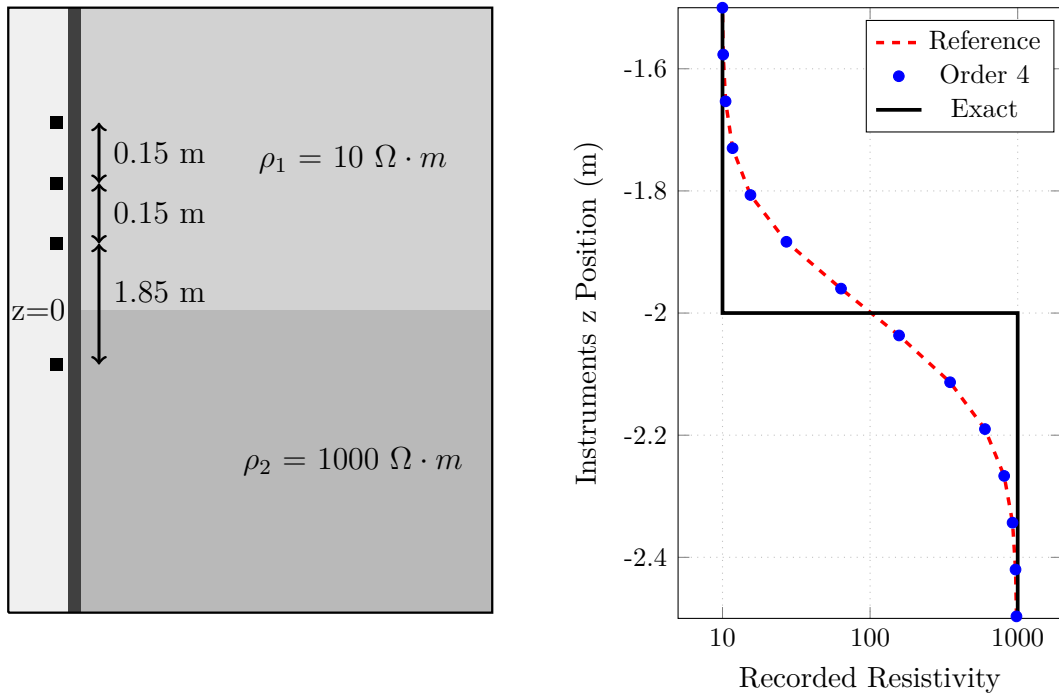


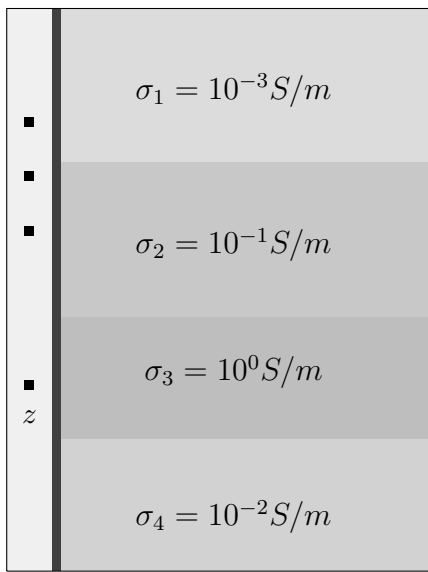
Figure 4.23: Borehole surrounded by a two layered formation and second difference of potential measured at the receivers for the reference model and the approximate model of order four.

Figure 4.23b shows the second difference of potential for different positions of the instrument along the vertical direction. The y axis shows the position of the transmitter along the vertical direction. We observe that when the transmitter is located at $z = -2$, when the second receiver is located at $z = 0$, the instru-

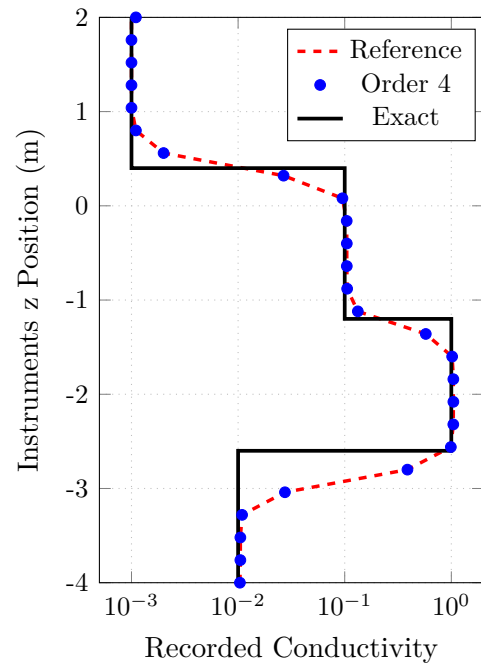
ments measures a change in the conductivity, it goes from measuring $10 \Omega \cdot m$ to measuring $1000 \Omega \cdot m$, which indeed are the values of the conductivity in the two rock formations we have considered. Moreover, we observe that when we apply this procedure to the fourth-order asymptotic model derived in Section 1.6.3, we also recover perfectly the values of the resistivity in both rock formations and we produce a negligible error with respect to the reference model.

4.5.3 Several rock layers with fixed conductivity

Finally Figure 4.24a shows a more complex configuration where several rock layers with different conductivities are present. We perform a similar experiment by moving the instrument along the z axis while we record the second difference of potential in each position. Figure 4.24b shows the results of such recordings. We observe that again we perfectly recover the values of the conductivity in the rock formations with both models, the reference model and the fourth-order asymptotic model, once again the error being negligible.



(a) Domain with a four layered rock formation.



(b) Second difference of potential for different positions of the instrument in a four layered formation.

Figure 4.24: Borehole surrounded by a four layered formation and second difference of potential measured at the receivers for the reference model and the approximate model of order four.

SEMI-ANALYTICAL SOLUTIONS

5.1 Introduction

In this chapter we follow the methodology presented in [30] to derive semi-analytical solutions for several asymptotic models in a 3D cylindrical configuration. Similar results regarding the derivation of semi-analytical solutions can be found in [39]. The main advantage of this approach is that from the computational point of view, once they are derived, the evaluation of these solutions is much more efficient than to compute purely numerical solutions. By providing semi-analytical solutions of the problems, we are able to reduce the computational cost for computing the solutions of the asymptotic models. The more complex the considered geometry of the problem is, the more complex the construction of these solutions is. The main results of these chapters are Propositions 11, 12, and 13, where we characterize a decomposition in Fourier series for the solutions to asymptotic models of orders one, two, and four.

5.2 Framework

In this chapter we consider the following model problem

$$\operatorname{div}(\sigma \nabla u) = f \quad \text{in } \Omega.$$

We assume that the domain Ω is a cylinder which is infinite and homogeneous in the z direction, and axisymmetric around the z axis

$$\Omega = \left\{ (r, \theta, z) \in \mathbb{R}^3 : 0 \leq r < R_0, 0 \leq \theta < 2\pi, -\infty < z < \infty \right\}$$

This domain is decomposed into three subdomains described as follows

$$\begin{aligned}\Omega_{\text{int}}^\varepsilon &= \left\{ (r, \theta, z) \in \mathbb{R}^3 : 0 \leq r < r_0 - \frac{\varepsilon}{2}, 0 \leq \theta < 2\pi, -\infty < z < \infty \right\}, \\ \Omega_{\text{lay}}^\varepsilon &= \left\{ (r, \theta, z) \in \mathbb{R}^3 : r_0 - \frac{\varepsilon}{2} < r < r_0 + \frac{\varepsilon}{2}, 0 \leq \theta < 2\pi, -\infty < z < \infty \right\}, \\ \Omega_{\text{ext}}^\varepsilon &= \left\{ (r, \theta, z) \in \mathbb{R}^3 : r_0 + \frac{\varepsilon}{2} < r < R_0, 0 \leq \theta < 2\pi, -\infty < z < \infty \right\}.\end{aligned}\quad (5.1)$$

Figure 1.4a, shows a similar configuration to the one considered here. The first step for deriving semi-analytical solutions consists in employing a Fourier transform along the variables z and θ as follows

$$\widehat{u}_k(r, \xi) = \frac{1}{2\pi} \int_{(-\pi, \pi) \times \mathbb{R}} u(r, \theta, z) \cos(k\theta) e^{i\xi z} d\theta dz. \quad (5.2)$$

Using the Fourier modes \widehat{u}_k , we can use the following inverse Fourier transform to obtain the expression of u

$$u(r, \theta, z) = \sum_{k=0}^{\infty} \frac{\zeta_k}{2\pi} \int_{\mathbb{R}} \widehat{u}_k(r, \xi) e^{-i\xi z} d\xi \cos(k\theta), \quad (5.3)$$

where

$$\zeta_k = \begin{cases} 1 & k = 0, \\ 2 & k > 0. \end{cases}$$

5.3 Dirichlet conditions

This section is devoted to the derivation of semi-analytical solutions for a problem with homogeneous Dirichlet boundary conditions. We cite the work [18] related to this topic, where the method of separation of variables is employed to derive analytical solutions for the Poisson equation in a cylinder. We adopt the second approach developed in Chapter 1 to derive approximate models of the second class in a 3D cylindrical domain Ω . Doing so, we obtain the following first-order asymptotic model

$$\begin{cases} \sigma_{\text{int}} \Delta u_{\text{int}} = f_{\text{int}} & \text{in } \Omega_{\text{int}}, \\ u_{\text{int}} = 0 & \text{on } \partial\Omega_{\text{int}}, \\ \sigma_{\text{ext}} \Delta u_{\text{ext}} = f_{\text{ext}} & \text{in } \Omega_{\text{ext}}, \\ u_{\text{ext}} = 0 & \text{on } \partial\Omega_{\text{ext}}. \end{cases}$$

In this chapter, the Laplace operator is considered to be written in cylindrical coordinates. It gets the following form

$$\Delta = \frac{1}{r} \partial_r (r \partial_r) + \frac{1}{r^2} \partial_\theta^2 + \partial_z^2.$$

This model can be seen as a generalization to a 3D cylindrical domain of Problem (1.84) we have derived in Section 1.6.5. We remark that domain Ω_{int} is the cylinder

$$\{(r, \theta, z) \in \mathbb{R}^3 : 0 \leq r < r_0, 0 \leq \theta < 2\pi, -\infty < z < \infty\}$$

and domain Ω_{ext} is defined as

$$\{(r, \theta, z) \in \mathbb{R}^3 : r_0 < r < R_0, 0 \leq \theta < 2\pi, -\infty < z < \infty\}.$$

The right-hand side is a punctual source situated inside the borehole. Thus, we will consider a right-hand side of the following form

$$\tilde{f}(x, y, z) = \begin{cases} \tilde{f}_{\text{int}}(x, y, z) = A\delta(x - x_t)\delta(y)\delta(z) & \text{in } \Omega_{\text{int}}, \\ \tilde{f}_{\text{ext}}(x, y, z) = 0 & \text{in } \Omega_{\text{ext}}, \end{cases} \quad (5.4)$$

where δ represents the Dirac distribution, $(x_t, 0, 0)$ represents the position of the punctual source and $A \in \mathbb{C}$ is a given complex constant. A detailed definition of the Dirac distribution can be found in [18]. We see it as a distribution that meets the property

$$\int_{-\infty}^{\infty} \delta(x - x_t) f(x) dx = f(x_t),$$

for a smooth enough function f . Since equations (1.84) are written in cylindrical coordinates, we explicit the right-hand side with cylindrical coordinates as follows

$$f(r, \theta, z) = \begin{cases} f_{\text{int}}(r, \theta, z) = \frac{A}{r} \delta(r - r_t) \delta(\theta) \delta(z) & \text{in } \Omega_{\text{int}}, \\ f_{\text{ext}}(r, \theta, z) = 0 & \text{in } \Omega_{\text{ext}}. \end{cases} \quad (5.5)$$

With this right-hand side, we deduce that the solution vanishes inside Ω_{ext} . Thus, taking this into account and the fact that the domain we consider is infinite along the z direction, we have the following volumic equation

$$\sigma_{\text{int}} \Delta u(r, \theta, z) = \frac{A}{r} \delta(r - r_t) \delta(\theta) \delta(z) \quad (5.6)$$

where

$$(r, \theta, z) \in (0, r_0) \times [0, 2\pi) \times (-\infty, \infty),$$

with the following boundary condition

$$u(r_0, \theta, z) = 0, \quad (\theta, z) \in [0, 2\pi) \times (-\infty, \infty). \quad (5.7)$$

Definition 9. Following [1], for $k \in \mathbb{Z}$, the Bessel functions of first kind J_k and second kind Y_k are defined as two independent solutions to the Bessel equation

$$x^2 \frac{d^2 y}{dx^2} + x \frac{dy}{dx} + (x^2 - k^2)y = 0.$$

According to the Frobenius method, it is possible to obtain the following series expression for function J_k

$$J_k(x) = \sum_{j=0}^{\infty} \frac{(-1)^j}{j! \Gamma(j+k+1)} \left(\frac{x}{2}\right)^{2j+k},$$

where Γ represents the Gamma function. Function J_k can then be used to define Y_k :

$$Y_k(x) = \lim_{l \rightarrow k} \frac{J_l(x) \cos(l\pi) - J_{-l}(x)}{\sin(l\pi)}.$$

Definition 10. Following [1], for $k \in \mathbb{Z}$, the modified Bessel functions of first kind I_k and second kind K_k are defined as two independent solutions to the modified Bessel equation

$$x^2 \frac{d^2 y}{dx^2} + x \frac{dy}{dx} - (x^2 + k^2)y = 0.$$

We can obtain the expression of these functions from the Bessel functions given in Definition 9

$$I_k(x) = \lim_{l \rightarrow k} i^{-l} J_l(ix),$$

$$K_k(x) = \lim_{l \rightarrow k} \frac{\pi I_{-l}(x) - I_l(x)}{2 \sin(l\pi)}.$$

Notation 4. For the sake of shortness we introduce the following notation

$$\Delta_k(\xi) = 2\pi r_t \left(K_k(|\xi|r_t) I'_k(|\xi|r_t) - K'_k(|\xi|r_t) I_k(|\xi|r_t) \right).$$

The main result of this section is the following proposition:

Proposition 11. The differential problem composed of Equation (5.6), together with boundary condition (5.7), admits a decomposition in Fourier series of the form (5.3), where the Fourier modes \hat{u}_k are bounded around the z axis and have the following form

$$\begin{cases} \hat{u}_k(r, \xi) = C_1^k(|\xi|) I_k(|\xi|r), & r \in (0, r_t), \xi \in \mathbb{R}, \\ \hat{u}_k(r, \xi) = C_3^k(|\xi|) I_k(|\xi|r) + C_4^k(|\xi|) K_k(|\xi|r), & r \in (r_t, r_0), \xi \in \mathbb{R}. \end{cases}$$

The coefficients C_1^k , C_3^k , C_4^k are defined as

$$\begin{cases} C_1^k(|\xi|) = \frac{A(-K_k(|\xi|r_t)I_k(|\xi|r_0) + K_k(|\xi|r_0)I_k(|\xi|r_t))}{I_k(|\xi|r_0)\sigma_{int}|\xi|\Delta_k(\xi)}, \\ C_3^k(|\xi|) = \frac{AK_k(|\xi|r_0)I_k(|\xi|r_t)}{I_k(|\xi|r_0)\sigma_{int}|\xi|\Delta_k(\xi)}, \\ C_4^k(|\xi|) = \frac{-AI_k(|\xi|r_t)}{\sigma_{int}|\xi|\Delta_k(\xi)}. \end{cases}$$

Proof. In the following we will describe the steps to prove the result of Proposition 11. We proceed as in [30], we begin by applying the Fourier transform (5.2) to Equations (5.6) and (5.7) so that we obtain the following equation

$$\partial_r^2 \hat{u}_k + \frac{1}{r} \partial_r \hat{u}_k - \left(\xi^2 + \frac{k^2}{r^2} \right) \hat{u}_k = \frac{A}{2\pi\sigma_{int}r} \delta(r - r_t), \quad (5.8)$$

for

$$(r, \xi) \in (0, r_0) \times (-\infty, \infty),$$

along with the boundary condition

$$\hat{u}_k(r_0, \xi) = 0, \quad \xi \in (-\infty, \infty).$$

These equations define an ordinary differential equation (ODE) in the variable r whose right-hand side is a Dirac distribution. For the sake of shortness we will forget about the variable ξ for the moment, as it plays the role of a parameter inside the ODE. For dealing with this kind of right-hand side, as it has no support outside the punctual source, we consider a homogeneous ODE outside the punctual source

$$\partial_r^2 \hat{u}_k + \frac{1}{r} \partial_r \hat{u}_k - \left(\xi^2 + \frac{k^2}{r^2} \right) \hat{u}_k = 0 \quad \text{in} \quad (0, r_t) \cup (r_t, r_0).$$

Regarding the behaviour at the punctual source, we begin by imposing the following transmission condition at the point r_t to ensure the continuity of \hat{u}_k at this point

$$\hat{u}_k(r_t^-) = \hat{u}_k(r_t^+). \quad (5.9)$$

Then, we integrate Equation 5.8 in a neighbourhood of r_t . For $\delta > 0$, we integrate

in the interval $(r_t - \delta, r_t + \delta)$ and then, we will make δ tend to zero.

$$\begin{aligned} & \overbrace{\int_{r_t-\delta}^{r_t+\delta} \partial_r^2 \hat{u}_k \, dr}^{I_1} + \overbrace{\int_{r_t-\delta}^{r_t+\delta} \frac{1}{r} \partial_r \hat{u}_k \, dr}^{I_2} - \overbrace{\int_{r_t-\delta}^{r_t+\delta} \left(\xi^2 + \frac{k^2}{r^2} \right) \hat{u}_k \, dr}^{I_3} \\ & \qquad \qquad \qquad = \underbrace{\int_{r_t-\delta}^{r_t+\delta} \frac{A}{2\pi\sigma_{\text{int}} r} \delta(r - r_t) \, dr}_{I_4}. \end{aligned}$$

This equation involves four integrals, denoted as I_1 , I_2 , I_3 , and I_4 , to be determined. From the definition of the Dirac distribution, we deduce the integral for the right-hand side I_4 gets the value $\frac{A}{2\pi\sigma_{\text{int}} r_t}$. For the first integral on the left-hand side I_1 , we obtain the following value

$$\int_{r_t-\delta}^{r_t+\delta} \partial_r^2 \hat{u}_k \, dr = \partial_r \hat{u}_k(r_t + \delta) - \partial_r \hat{u}_k(r_t - \delta).$$

Making δ tend to zero, as $\partial_r \hat{u}_k$ is not necessarily continuous at r_t , we obtain the value $\partial_r \hat{u}_k(r_t^+) - \partial_r \hat{u}_k(r_t^-)$. Then, integrating by parts the integral I_2 we obtain

$$\int_{r_t-\delta}^{r_t+\delta} \frac{1}{r} \partial_r \hat{u}_k \, dr = \left[\frac{1}{r} \hat{u}_k \right]_{r_t-\delta}^{r_t+\delta} + \int_{r_t-\delta}^{r_t+\delta} \frac{1}{r^2} \hat{u}_k \, dr.$$

As we are seeking for a continuous function \hat{u}_k and since functions $\frac{1}{r}$ and $\frac{1}{r^2}$ are continuous, making δ tend to zero we deduce that this integral vanishes. Finally, regarding the integral I_3 , once again as we are seeking a continuous function \hat{u}_k , and $-\xi^2 - \frac{k^2}{r^2}$ is also continuous in a neighbourhood of r_t , making δ tend to zero we deduce that this integral also vanishes. Thus, from this integration we obtain the following transmission condition at the point r_t

$$\partial_r \hat{u}_k(r_t^+) - \partial_r \hat{u}_k(r_t^-) = \frac{A}{2\pi\sigma_{\text{int}} r_t}. \quad (5.10)$$

Taking these transmission conditions into account, we consider the following ODE

$$\left\{ \begin{array}{ll} \partial_r^2 \hat{u}_k(r) + \frac{1}{r} \partial_r \hat{u}_k(r) - \left(\xi^2 + \frac{k^2}{r^2} \right) \hat{u}_k(r) = 0 & \text{in } (0, r_t), \\ \partial_r^2 \hat{u}_k(r) + \frac{1}{r} \partial_r \hat{u}_k(r) - \left(\xi^2 + \frac{k^2}{r^2} \right) \hat{u}_k(r) = 0 & \text{in } (r_t, r_0), \\ \hat{u}_k(r_t^-) = \hat{u}_k(r_t^+), \\ \partial_r \hat{u}_k(r_t^+) - \partial_r \hat{u}_k(r_t^-) = \frac{A}{2\pi\sigma_{\text{int}} r_t}, \\ \hat{u}_k(r_0) = 0. \end{array} \right.$$

These volumic equations are homogeneous linear differential equations and we can analytically solve them. For that purpose we begin by doing the following change of variables

$$x = |\xi|r.$$

We define function v as

$$v(x) = v(|\xi|r) = \hat{u}_k(r) = \hat{u}_k\left(\frac{x}{|\xi|}\right).$$

Applying this change of variables and multiplying both sides of the equation by x^2 , we obtain the following equation for v

$$x^2v''(x) + xv'(x) - (x^2 + k^2)v(x) = 0.$$

This differential equation is the modified Bessel differential equation formerly presented in Definition 10 and the solutions to this equation are the modified Bessel functions of the first kind (I_k) and second kind (K_k). We select then I_k and K_k as the two independent solutions to our ODE. Using the change of variables we performed, $x = |\xi|r$, we obtain a solution of the following form

$$\begin{cases} \hat{u}_k(r) = C_1^k I_k(|\xi|r) + C_2^k K_k(|\xi|r) & \text{in } (0, r_t), \\ \hat{u}_k(r) = C_3^k I_k(|\xi|r) + C_4^k K_k(|\xi|r) & \text{in } (r_t, r_0), \end{cases}$$

where C_1^k , C_2^k , C_3^k , and C_4^k are coefficients (independent of r) to be determined thanks to the following transmission and boundary conditions

$$\begin{cases} \hat{u}_k(r_t^-) = \hat{u}_k(r_t^+), \\ \partial_r \hat{u}_k(r_t^+) - \partial_r \hat{u}_k(r_t^-) = \frac{A}{2\pi\sigma_{\text{int}}r_t}, \\ \hat{u}_k(r_0) = 0. \end{cases} \quad (5.11)$$

We have to take into account that function K_k tends to infinity when r tends to zero, we conclude that $C_2^k = 0$, since the Fourier modes \hat{u}_k are bounded around the z axis. Then, employing the transmission and boundary conditions (5.11), we obtain the following set of equations for the coefficients C_1^k , C_3^k and C_4^k

$$\begin{cases} I_k(|\xi|r_t) C_1^k - I_k(|\xi|r_t) C_3^k - K_k(|\xi|r_t) C_4^k = 0, \\ - I_k'(|\xi|r_t) C_1^k + I_k'(|\xi|r_t) C_3^k + K_k'(|\xi|r_t) C_4^k = \frac{A}{2\pi\sigma_{\text{int}}r_t|\xi|}, \\ I_k(|\xi|r_0) C_3^k + K_k(|\xi|r_0) C_4^k = 0. \end{cases}$$

Solving this linear system we obtain the values for the coefficients C_1^k , C_3^k and C_4^k , which have been shown in Proposition 11. Now that we have made explicit the expression of \widehat{u}_k we employ the inverse Fourier transform (5.3) to obtain the expression of function u .

□

5.4 Robin conditions

In this section, we derive semi-analytical solutions for a problem with robin boundary conditions. We cite the work [39] related to this topic, where semi-analytical solutions are derived for the Helmholtz equation in a cylinder. We adopt the second approach developed in Chapter 1 to derive approximate models of the second class in a 3D cylindrical domain Ω . Doing so, we obtain the following second-order asymptotic model

$$\begin{cases} \sigma_{\text{int}} \Delta u_{\text{int}} = f_{\text{int}} & \text{in } \Omega_{\text{int}}, \\ u_{\text{int}} = \frac{\varepsilon}{2} \partial_r u_{\text{int}} & \text{on } \Gamma, \\ u_{\text{int}} = 0 & \text{on } \partial\Omega \cap \partial\Omega_{\text{int}}, \end{cases}$$

$$\begin{cases} \sigma_{\text{ext}} \Delta u_{\text{ext}} = f_{\text{ext}} & \text{in } \Omega_{\text{ext}}, \\ u_{\text{ext}} = -\frac{\varepsilon}{2} \partial_r u_{\text{ext}} & \text{on } \Gamma, \\ u_{\text{ext}} = 0 & \text{on } \partial\Omega \cap \partial\Omega_{\text{ext}}, \end{cases}$$

where the domains Ω_{int} and Ω_{ext} are the same of the previous section. This model can be seen as a generalization to a problem defined over a 3D cylindrical domain of Problem (1.85) we have derived in Section 1.6.5. We consider the right-hand side (5.4) we introduced in the previous section. With this right-hand side, once again we deduce that the solution vanishes inside domain Ω_{ext} . Then, the problem set inside an infinite domain along the z direction is written as in Equation (5.6), along with the following boundary condition

$$u(r_0, \theta, z) = \frac{\varepsilon}{2} \partial_r u(r_0, \theta, z) \quad (\theta, z) \in [0, 2\pi) \times (-\infty, \infty). \quad (5.12)$$

The main result of this section is the following proposition:

Proposition 12. *The differential problem composed of Equation (5.6), together with the boundary condition (5.12), admits a decomposition in Fourier series of the form (5.3), where the Fourier modes \widehat{u}_k are bounded around the z axis and have the following form*

$$\begin{cases} \widehat{u}_k(r, \xi) = C_1^k(|\xi|)I_k(|\xi|r), & r \in (0, r_t), \\ \widehat{u}_k(r, \xi) = C_3^k(|\xi|)I_k(|\xi|r) + C_4^k(|\xi|)K_k(|\xi|r), & r \in (r_t, r_0). \end{cases}$$

The coefficients C_1^k , C_3^k , C_4^k are defined as

$$\begin{cases} C_1^k(|\xi|) = \frac{A(2K_k(|\xi|r_t)I_k(|\xi|r_0) - 2K_k(|\xi|r_0)I_k(|\xi|r_t))}{\sigma_{int}|\xi|\Delta_k(\xi)(-2I_k(|\xi|r_0) + \varepsilon|\xi|I_k'(|\xi|r_0))} \\ \quad + \frac{A(-\varepsilon|\xi|K_k(|\xi|r_t)I_k'(|\xi|r_0) + \varepsilon|\xi|K_k'(|\xi|r_0)I_k(|\xi|r_t))}{\sigma_{int}|\xi|\Delta_k(\xi)(-2I_k(|\xi|r_0) + \varepsilon|\xi|I_k'(|\xi|r_0))}, \\ C_3^k(|\xi|) = \frac{AI_k(|\xi|r_t)(-2K_k(|\xi|r_0) + \varepsilon|\xi|K_k'(|\xi|r_0))}{\sigma_{int}|\xi|\Delta_k(\xi)(-2I_k(|\xi|r_0) + \varepsilon|\xi|I_k'(|\xi|r_0))}, \\ C_4^k(|\xi|) = \frac{-AI_k(|\xi|r_t)}{\sigma_{int}|\xi|\Delta_k(\xi)}. \end{cases}$$

Remark 6. *It is worth noting that if we apply $\varepsilon = 0$ to the expression of the coefficients obtained in Proposition 12, we obtain the expression of the coefficients obtained in Proposition 11.*

Proof. If we apply Fourier transform (5.2) to Equation (5.6), we obtain the ordinary differential equation in the variable r (5.8). We employ the same reasoning as in Section 5.3 to deduce the behaviour at the point r_t , obtaining the transmission conditions (5.9) and (5.10). The main difference between this configuration and the configuration of Section 5.3, corresponds to the following boundary condition, obtained by applying the Fourier transform (5.2) to Equation (5.12)

$$\widehat{u}_k(r_0) = \frac{\varepsilon}{2}\partial_r\widehat{u}_k(r_0). \quad (5.13)$$

Following the same reasoning as in Section 5.3, we conclude that the solution to the volumic equation (5.8) has the following form

$$\begin{cases} \widehat{u}_k(r) = C_1^k I_k(|\xi|r) + C_2^k K_k(|\xi|r) & \text{in } (0, r_t), \\ \widehat{u}_k(r) = C_3^k I_k(|\xi|r) + C_4^k K_k(|\xi|r) & \text{in } (r_t, r_0), \end{cases}$$

where C_1^k , C_2^k , C_3^k , and C_4^k are coefficients (independent of r) to be determined thanks to the transmission and boundary conditions (5.9), (5.10), and (5.13)

$$\left\{ \begin{array}{l} \hat{u}_k(r_t^-) = \hat{u}_k(r_t^+), \\ \partial_r \hat{u}_k(r_t^+) - \partial_r \hat{u}_k(r_t^-) = \frac{A}{2\pi\sigma_{\text{int}}r_t}, \\ \hat{u}_k(r_0) = \frac{\varepsilon}{2}\partial_r \hat{u}_k(r_0). \end{array} \right. \quad (5.14)$$

Again as function K_k tends to infinity when r tends to zero, we will consider $C_2^k = 0$. Then, employing the transmission and boundary conditions (5.14), we obtain the following set of equations for the coefficients C_1^k , C_3^k , and C_4^k

$$\left\{ \begin{array}{l} I_k(|\xi|r_t)C_1^k - I_k(|\xi|r_t)C_3^k - K_k(|\xi|r_t)C_4^k = 0, \\ -I'_k(|\xi|r_t)C_1^k + I'_k(|\xi|r_t)C_3^k + K'_k(|\xi|r_t)C_4^k = \frac{A}{2\pi\sigma_{\text{int}}r_t|\xi|}, \\ \left(I_k(|\xi|r_0) - \frac{\varepsilon}{2}|\xi|I'_k(|\xi|r_0) \right) C_3^k + \left(K_k(|\xi|r_0) - \frac{\varepsilon}{2}|\xi|K'_k(|\xi|r_0) \right) C_4^k = 0. \end{array} \right.$$

Solving these equations we obtain the values for the coefficients C_1^k , C_3^k , and C_4^k which have been given in Proposition 12. Now that we have made explicit the expression of \hat{u}_k we employ the inverse Fourier transform (5.3) to obtain the expression of function u .

□

5.5 Impedance Transmission conditions

In this section we derive semi-analytical solutions for a problem with transmission conditions. We adopt the first approach developed in Chapter 1 to derive approximate models of the first class in a 3D domain $\Omega^\varepsilon = \Omega_{\text{int}}^\varepsilon \cup \Omega_{\text{ext}}^\varepsilon$. Doing so, we obtain the following fourth-order asymptotic model

$$\left\{ \begin{array}{ll} \sigma_{\text{int}}\Delta u_{\text{int}} = f_{\text{int}} & \text{in } \Omega_{\text{int}}^\varepsilon, \\ \sigma_{\text{ext}}\Delta u_{\text{ext}} = f_{\text{ext}} & \text{in } \Omega_{\text{ext}}^\varepsilon, \\ [u]_{\Gamma^\varepsilon} = 0, & \\ \varepsilon^2 \frac{1}{\hat{\sigma}_0} [\sigma \partial_r u]_{\Gamma^\varepsilon} + \varepsilon^3 \frac{1}{\hat{\sigma}_0 r_0} \{ \sigma \partial_r u \}_{\Gamma^\varepsilon} = -\Delta_\Gamma \{ u \}_{\Gamma^\varepsilon}, & \\ u = 0 & \text{on } \partial\Omega \cap \partial\Omega^\varepsilon, \end{array} \right. \quad (5.15)$$

where $\Delta_\Gamma = \partial_z^2 + \frac{1}{r_0^2} \partial_\theta^2$. This model can be seen as a generalization to a 3D cylindrical domain of Problem (1.77) we have derived in Section 1.6.3. We remind that domains $\Omega_{\text{int}}^\varepsilon$ and $\Omega_{\text{ext}}^\varepsilon$ have been defined in (5.1). We consider again the right-hand side (5.4). Then, the problem set inside an infinite domain along the z direction is written as follows

$$\sigma_{\text{int}} \Delta u(r, \theta, z) = \frac{A}{2\pi r} \delta(r - r_t) \delta(\theta) \delta(z) \quad (5.16)$$

for

$$(r, \theta, z) \in \left(0, r_0 - \frac{\varepsilon}{2}\right) \times [0, 2\pi) \times (-\infty, \infty),$$

and

$$\Delta u(r, \theta, z) = 0 \quad (5.17)$$

for

$$(r, \theta, z) \in \left(r_0 + \frac{\varepsilon}{2}, R_0\right) \times [0, 2\pi) \times (-\infty, \infty).$$

These equations are coupled with the following transmission conditions

$$\begin{cases} [u]_{\Gamma^\varepsilon} = 0, \\ \varepsilon^2 \frac{1}{\widehat{\sigma}_0} [\sigma \partial_r u]_{\Gamma^\varepsilon} + \varepsilon^3 \frac{1}{\widehat{\sigma}_0 r_0} \{\sigma \partial_r u\}_{\Gamma^\varepsilon} = -\Delta_\Gamma \{u\}_{\Gamma^\varepsilon}, \end{cases} \quad (5.18)$$

and the following boundary condition

$$u(R_0, \theta, z) = 0, \quad (\theta, z) \in [0, 2\pi) \times (-\infty, \infty). \quad (5.19)$$

For the sake of simplicity we introduce the following notation

$$\begin{cases} r_{0,\varepsilon}^+ = r_0 + \frac{\varepsilon}{2}, \\ r_{0,\varepsilon}^- = r_0 - \frac{\varepsilon}{2}. \end{cases}$$

The main result of this section is the following proposition:

Proposition 13. *The differential problem composed of Equations (5.16) and (5.17), together with transmission conditions (5.18) and the boundary condition (5.19), admits a decomposition in Fourier series of the form (5.3), where the Fourier modes \widehat{u}_k are bounded around the z axis and have the following form*

$$\begin{cases} \widehat{u}_k(r, \xi) = C_1^k(|\xi|) I_k(|\xi| r), & r \in (0, r_t), \\ \widehat{u}_k(r, \xi) = C_3^k(|\xi|) I_k(|\xi| r) + C_4^k(|\xi|) K_k(|\xi| r), & r \in (r_t, r_{0,\varepsilon}^-), \\ \widehat{u}_k(r, \xi) = C_5^k(|\xi|) I_k(|\xi| r) + C_6^k(|\xi|) K_k(|\xi| r), & r \in (r_{0,\varepsilon}^+, R_0). \end{cases}$$

The coefficients C_1^k , C_3^k , C_4^k , C_5^k , and C_6^k are defined as

$$C_i^k(|\xi|) = \frac{C_{i1}^k(|\xi|)}{C_{i2}^k(|\xi|)}, \quad i = 1, 3, 4, 5, 6,$$

where

$$\begin{aligned} C_{11}^k(|\xi|) = & -2A \left(K_k(|\xi|R_0)I_k(|\xi|r_{0,\varepsilon}^+) - K_k(|\xi|r_{0,\varepsilon}^+)I_k(|\xi|R_0) \right) \\ & \left(K_k(|\xi|r_t)I_k(|\xi|r_{0,\varepsilon}^-) - K_k(|\xi|r_{0,\varepsilon}^-)I_k(|\xi|r_t) \right) \left(k^2 + \xi^2 r_0^2 \right) \hat{\sigma}_0 \\ & - 2A\varepsilon^2 \left[\left(-K_k(|\xi|R_0)I_k'(|\xi|r_{0,\varepsilon}^+) + K_k'(|\xi|r_{0,\varepsilon}^+)I_k(|\xi|R_0) \right) \right. \\ & \left. \left(K_k(|\xi|r_t)I_k(|\xi|r_{0,\varepsilon}^-) - K_k(|\xi|r_{0,\varepsilon}^-)I_k(|\xi|r_t) \right) |\xi|r_0^2 \sigma_{ext} \right. \\ & \left. - \left(-K_k(|\xi|R_0)I_k(|\xi|r_{0,\varepsilon}^+) + K_k(|\xi|r_{0,\varepsilon}^+)I_k(|\xi|R_0) \right) \left(K_k(|\xi|r_t)I_k'(|\xi|r_{0,\varepsilon}^-) \right. \right. \\ & \left. \left. - K_k'(|\xi|r_{0,\varepsilon}^-)I_k(|\xi|r_t) \right) |\xi|r_0^2 \sigma_{int} \right] - A\varepsilon^3 \left(\left(-K_k(|\xi|R_0)I_k'(|\xi|r_{0,\varepsilon}^+) \right. \right. \\ & \left. \left. + K_k'(|\xi|r_{0,\varepsilon}^+)I_k(|\xi|R_0) \right) \left(K_k(|\xi|r_t)I_k(|\xi|r_{0,\varepsilon}^-) - K_k(|\xi|r_{0,\varepsilon}^-)I_k(|\xi|r_t) \right) \right. \\ & \left. |\xi|r_0 \sigma_{ext} + \left(-K_k(|\xi|R_0)I_k(|\xi|r_{0,\varepsilon}^+) + K_k(|\xi|r_{0,\varepsilon}^+)I_k(|\xi|R_0) \right) \right. \\ & \left. \left(K_k(|\xi|r_t)I_k'(|\xi|r_{0,\varepsilon}^-) - K_k'(|\xi|r_{0,\varepsilon}^-)I_k(|\xi|r_t) \right) |\xi|r_0 \sigma_{int} \right), \end{aligned}$$

$$\begin{aligned}
C_{12}^k(|\xi|) &= 2I_k(|\xi|r_{0,\varepsilon}^-) \left(K_k(|\xi|R_0)I_k(|\xi|r_{0,\varepsilon}^+) - K_k(|\xi|r_{0,\varepsilon}^+)I_k(|\xi|R_0) \right) \\
&\quad |\xi|\Delta_k(\xi) \left(k^2 + \xi^2 r_0^2 \right) \widehat{\sigma}_0 \sigma_{int} + |\xi|\Delta_k(\xi) \varepsilon^2 \sigma_{int} \left[- 2I_k(|\xi|r_{0,\varepsilon}^-) \right. \\
&\quad \left. \left(K_k(|\xi|R_0)I_k'(|\xi|r_{0,\varepsilon}^+) - K_k'(|\xi|r_{0,\varepsilon}^+)I_k(|\xi|R_0) \right) |\xi|r_0^2 \sigma_{ext} + 2I_k'(|\xi|r_{0,\varepsilon}^-) \right. \\
&\quad \left. \left(K_k(|\xi|R_0)I_k(|\xi|r_{0,\varepsilon}^+) - K_k(|\xi|r_{0,\varepsilon}^+)I_k(|\xi|R_0) \right) |\xi|r_0^2 \sigma_{int} \right] + |\xi|\Delta_k(\xi) \varepsilon^3 \sigma_{int} \\
&\quad \left[- I_k(|\xi|r_{0,\varepsilon}^-) \left(K_k(|\xi|R_0)I_k'(|\xi|r_{0,\varepsilon}^+) - K_k'(|\xi|r_{0,\varepsilon}^+)I_k(|\xi|R_0) \right) |\xi|r_0 \sigma_{ext} \right. \\
&\quad \left. - I_k'(|\xi|r_{0,\varepsilon}^-) \left(K_k(|\xi|R_0)I_k(|\xi|r_{0,\varepsilon}^+) - K_k(|\xi|r_{0,\varepsilon}^+)I_k(|\xi|R_0) \right) |\xi|r_0 \sigma_{int} \right],
\end{aligned}$$

$$\begin{aligned}
C_{31}^k(|\xi|) &= 2AK_k(|\xi|r_{0,\varepsilon}^-) \left(K_k(|\xi|R_0)I_k(|\xi|r_{0,\varepsilon}^+) - K_k(|\xi|r_{0,\varepsilon}^+)I_k(|\xi|R_0) \right) \\
&\quad I_k(|\xi|r_t) \left(k^2 + \xi^2 r_0^2 \right) \widehat{\sigma}_0 + AI_k(|\xi|r_t) \varepsilon^2 \left[- 2K_k(|\xi|r_{0,\varepsilon}^-) \right. \\
&\quad \left. \left(K_k(|\xi|R_0)I_k'(|\xi|r_{0,\varepsilon}^+) - K_k'(|\xi|r_{0,\varepsilon}^+)I_k(|\xi|R_0) \right) |\xi|r_0^2 \sigma_{ext} + 2K_k'(|\xi|r_{0,\varepsilon}^-) \right. \\
&\quad \left. \left(K_k(|\xi|R_0)I_k(|\xi|r_{0,\varepsilon}^+) - K_k(|\xi|r_{0,\varepsilon}^+)I_k(|\xi|R_0) \right) |\xi|r_0^2 \sigma_{int} \right] + AI_k(|\xi|r_t) \varepsilon^3 \\
&\quad \left[- K_k(|\xi|r_{0,\varepsilon}^-) \left(K_k(|\xi|R_0)I_k'(|\xi|r_{0,\varepsilon}^+) - K_k'(|\xi|r_{0,\varepsilon}^+)I_k(|\xi|R_0) \right) |\xi|r_0 \sigma_{ext} \right. \\
&\quad \left. - K_k'(|\xi|r_{0,\varepsilon}^-) \left(K_k(|\xi|R_0)I_k(|\xi|r_{0,\varepsilon}^+) - K_k(|\xi|r_{0,\varepsilon}^+)I_k(|\xi|R_0) \right) |\xi|r_0 \sigma_{int} \right],
\end{aligned}$$

$$\begin{aligned}
C_{32}^k(|\xi|) &= 2I_k(|\xi|r_{0,\varepsilon}^-) \left(K_k(|\xi|R_0)I_k(|\xi|r_{0,\varepsilon}^+) - K_k(|\xi|r_{0,\varepsilon}^+)I_k(|\xi|R_0) \right) \\
&\quad |\xi|\Delta_k(\xi) \left(k^2 + \xi^2 r_0^2 \right) \widehat{\sigma}_0 \sigma_{int} + |\xi|\Delta_k(\xi) \varepsilon^2 \sigma_{int} \left[-2I_k(|\xi|r_{0,\varepsilon}^-) \right. \\
&\quad \left. \left(K_k(|\xi|R_0)I_k'(|\xi|r_{0,\varepsilon}^+) - K_k'(|\xi|r_{0,\varepsilon}^+)I_k(|\xi|R_0) \right) |\xi|r_0^2 \sigma_{ext} + 2I_k'(|\xi|r_{0,\varepsilon}^-) \right. \\
&\quad \left. \left(K_k(|\xi|R_0)I_k(|\xi|r_{0,\varepsilon}^+) - K_k(|\xi|r_{0,\varepsilon}^+)I_k(|\xi|R_0) \right) |\xi|r_0^2 \sigma_{int} \right] + |\xi|\Delta_k(\xi) \varepsilon^3 \sigma_{int} \\
&\quad \left[-I_k(|\xi|r_{0,\varepsilon}^-) \left(K_k(|\xi|R_0)I_k'(|\xi|r_{0,\varepsilon}^+) - K_k'(|\xi|r_{0,\varepsilon}^+)I_k(|\xi|R_0) \right) |\xi|r_0 \sigma_{ext} \right. \\
&\quad \left. - I_k'(|\xi|r_{0,\varepsilon}^-) \left(K_k(|\xi|R_0)I_k(|\xi|r_{0,\varepsilon}^+) - K_k(|\xi|r_{0,\varepsilon}^+)I_k(|\xi|R_0) \right) |\xi|r_0 \sigma_{int} \right],
\end{aligned}$$

$$C_{41}^k(|\xi|) = -AI_k(|\xi|r_t),$$

$$C_{42}^k(|\xi|) = |\xi|\Delta_k(\xi)\sigma_{int},$$

$$\begin{aligned}
C_{51}^k(|\xi|) &= -2AK_k(|\xi|R_0) \left(K_k(|\xi|r_{0,\varepsilon}^-)I_k'(|\xi|r_{0,\varepsilon}^-) - K_k'(|\xi|r_{0,\varepsilon}^-)I_k(|\xi|r_{0,\varepsilon}^-) \right) \\
&\quad I_k(|\xi|r_t) \varepsilon^2 r_0^2 + AK_k(|\xi|R_0) \left(K_k(|\xi|r_{0,\varepsilon}^-)I_k'(|\xi|r_{0,\varepsilon}^-) \right. \\
&\quad \left. - K_k'(|\xi|r_{0,\varepsilon}^-)I_k(|\xi|r_{0,\varepsilon}^-) \right) I_k(|\xi|r_t) \varepsilon^3 r_0,
\end{aligned}$$

$$\begin{aligned}
C_{52}^k(|\xi|) &= 2I_k(|\xi|r_{0,\varepsilon}^-) \left(K_k(|\xi|R_0)I_k(|\xi|r_{0,\varepsilon}^+) - K_k(|\xi|r_{0,\varepsilon}^+)I_k(|\xi|R_0) \right) \\
&\quad \Delta_k(\xi) \left(k^2 + \xi^2 r_0^2 \right) \hat{\sigma}_0 + \Delta_k(\xi) \varepsilon^2 \left[-2I_k(|\xi|r_{0,\varepsilon}^-) \right. \\
&\quad \left. \left(K_k(|\xi|R_0)I_k'(|\xi|r_{0,\varepsilon}^+) - K_k'(|\xi|r_{0,\varepsilon}^+)I_k(|\xi|R_0) \right) |\xi|r_0^2 \sigma_{ext} + 2I_k'(|\xi|r_{0,\varepsilon}^-) \right. \\
&\quad \left. \left(K_k(|\xi|R_0)I_k(|\xi|r_{0,\varepsilon}^+) - K_k(|\xi|r_{0,\varepsilon}^+)I_k(|\xi|R_0) \right) |\xi|r_0^2 \sigma_{int} \right] + \Delta_k(\xi) \varepsilon^3 \\
&\quad \left[-I_k(|\xi|r_{0,\varepsilon}^-) \left(K_k(|\xi|R_0)I_k'(|\xi|r_{0,\varepsilon}^+) - K_k'(|\xi|r_{0,\varepsilon}^+)I_k(|\xi|R_0) \right) |\xi|r_0 \sigma_{ext} \right. \\
&\quad \left. - I_k'(|\xi|r_{0,\varepsilon}^-) \left(K_k(|\xi|R_0)I_k(|\xi|r_{0,\varepsilon}^+) - K_k(|\xi|r_{0,\varepsilon}^+)I_k(|\xi|R_0) \right) |\xi|r_0 \sigma_{int} \right],
\end{aligned}$$

$$\begin{aligned}
C_{61}^k(|\xi|) &= 2A \left(K_k(|\xi|r_{0,\varepsilon}^-)I_k'(|\xi|r_{0,\varepsilon}^-) - K_k'(|\xi|r_{0,\varepsilon}^-)I_k(|\xi|r_{0,\varepsilon}^-) \right) \\
&\quad I_k(|\xi|R_0)I_k(|\xi|r_t) \varepsilon^2 r_0^2 - A \left(K_k(|\xi|r_{0,\varepsilon}^-)I_k'(|\xi|r_{0,\varepsilon}^-) \right. \\
&\quad \left. - K_k'(|\xi|r_{0,\varepsilon}^-)I_k(|\xi|r_{0,\varepsilon}^-) \right) I_k(|\xi|R_0)I_k(|\xi|r_t) \varepsilon^3 r_0,
\end{aligned}$$

$$\begin{aligned}
C_{62}^k(|\xi|) &= 2I_k(|\xi|r_{0,\varepsilon}^-) \left(K_k(|\xi|R_0)I_k(|\xi|r_{0,\varepsilon}^+) - K_k(|\xi|r_{0,\varepsilon}^+)I_k(|\xi|R_0) \right) \\
&\quad \Delta_k(\xi) \left(k^2 + \xi^2 r_0^2 \right) \hat{\sigma}_0 + \Delta_k(\xi) \varepsilon^2 \left[-2I_k(|\xi|r_{0,\varepsilon}^-) \right. \\
&\quad \left. \left(K_k(|\xi|R_0)I_k'(|\xi|r_{0,\varepsilon}^+) - K_k'(|\xi|r_{0,\varepsilon}^+)I_k(|\xi|R_0) \right) |\xi|r_0^2 \sigma_{ext} + 2I_k'(|\xi|r_{0,\varepsilon}^-) \right. \\
&\quad \left. \left(K_k(|\xi|R_0)I_k(|\xi|r_{0,\varepsilon}^+) - K_k(|\xi|r_{0,\varepsilon}^+)I_k(|\xi|R_0) \right) |\xi|r_0^2 \sigma_{int} \right] + \Delta_k(\xi) \varepsilon^3 \\
&\quad \left[-I_k(|\xi|r_{0,\varepsilon}^-) \left(K_k(|\xi|R_0)I_k'(|\xi|r_{0,\varepsilon}^+) - K_k'(|\xi|r_{0,\varepsilon}^+)I_k(|\xi|R_0) \right) |\xi|r_0 \sigma_{ext} \right. \\
&\quad \left. - I_k'(|\xi|r_{0,\varepsilon}^-) \left(K_k(|\xi|R_0)I_k(|\xi|r_{0,\varepsilon}^+) - K_k(|\xi|r_{0,\varepsilon}^+)I_k(|\xi|R_0) \right) |\xi|r_0 \sigma_{int} \right],
\end{aligned}$$

Remark 7. *It is worth noting that if we apply $\varepsilon = 0$ to the expression of the coefficients obtained in Proposition 13, we obtain the expression of the coefficients obtained in Proposition 11.*

Proof. If we apply Fourier transform (5.2) to Equations (5.16) and (5.17), we obtain the following ordinary differential equations in the variable r

$$\partial_r^2 \hat{u}_k + \frac{1}{r} \partial_r \hat{u}_k - \left(\xi^2 + \frac{k^2}{r^2} \right) \hat{u}_k = \frac{A}{2\pi\sigma_{\text{int}} r} \delta(r - r_t) \quad r \in \left(0, r_0 - \frac{\varepsilon}{2} \right), \quad (5.20)$$

and

$$\partial_r^2 \hat{u}_k + \frac{1}{r} \partial_r \hat{u}_k - \left(\xi^2 + \frac{k^2}{r^2} \right) \hat{u}_k = 0 \quad r \in \left(r_0 + \frac{\varepsilon}{2}, R_0 \right). \quad (5.21)$$

We employ the same reasoning as in Section 5.3 to deduce the behaviour at the point r_t , obtaining the transmission conditions (5.9) and (5.10). The main difference with the previous sections corresponds to the following transmission and boundary conditions, obtained by applying the Fourier transform (5.2) to Equations (5.18), and (5.19)

$$\left\{ \begin{array}{l} \hat{u}_k \left(r_0 - \frac{\varepsilon}{2} \right) = \hat{u}_k \left(r_0 + \frac{\varepsilon}{2} \right), \\ \varepsilon^2 \frac{1}{\hat{\sigma}_0} [\sigma \partial_r \hat{u}_k]_{\Gamma^\varepsilon} + \varepsilon^3 \frac{1}{\hat{\sigma}_0 r_0} \{ \sigma \partial_r \hat{u}_k \}_{\Gamma^\varepsilon} = \left(\xi^2 + \frac{k^2}{r_0^2} \right) \{ \hat{u}_k \}_{\Gamma^\varepsilon}, \\ \hat{u}_k(R_0) = 0. \end{array} \right. \quad (5.22)$$

Here, for the sake of simplicity, we keep the same notation for the jump and mean values, even though the meaning now is the following

$$\left\{ \begin{array}{l} [\hat{u}_k]_{\Gamma^\varepsilon}(\xi) = \hat{u}_k(r_{0,\varepsilon}^+, \xi) - \hat{u}_k(r_{0,\varepsilon}^-, \xi), \\ \{ \hat{u}_k \}_{\Gamma^\varepsilon}(\xi) = \frac{1}{2} \left(\hat{u}_k(r_{0,\varepsilon}^+, \xi) + \hat{u}_k(r_{0,\varepsilon}^-, \xi) \right). \end{array} \right.$$

Following the reasoning of Section 5.3, the solution to volumic Equations (5.20) and (5.21) have the following form

$$\left\{ \begin{array}{l} \hat{u}_k(r) = C_1^k I_k(|\xi|r) + C_2^k K_k(|\xi|r) \quad \text{in} \quad (0, r_t), \\ \hat{u}_k(r) = C_3^k I_k(|\xi|r) + C_4^k K_k(|\xi|r) \quad \text{in} \quad \left(r_t, r_0 - \frac{\varepsilon}{2} \right), \\ \hat{u}_k(r) = C_5^k I_k(|\xi|r) + C_6^k K_k(|\xi|r) \quad \text{in} \quad \left(r_0 + \frac{\varepsilon}{2}, R_0 \right), \end{array} \right.$$

where $C_1^k, C_2^k, C_3^k, C_4^k, C_5^k$, and C_6^k are coefficients (independent of r) to be determined thanks to the transmission and boundary conditions (5.9), (5.10) and (5.22)

$$\left\{ \begin{array}{l} \hat{u}_k(r_t^-) = \hat{u}_k(r_t^+), \\ \partial_r \hat{u}_k(r_t^+) - \partial_r \hat{u}_k(r_t^-) = \frac{A}{2\pi\sigma_{\text{int}}r_t}, \\ \hat{u}_k\left(r_0 - \frac{\varepsilon}{2}\right) = \hat{u}_k\left(r_0 + \frac{\varepsilon}{2}\right), \\ \varepsilon^2 \frac{1}{\hat{\sigma}_0} [\sigma \partial_r \hat{u}_k]_{\Gamma^\varepsilon} + \varepsilon^3 \frac{1}{\hat{\sigma}_0 r_0} \{\sigma \partial_r \hat{u}_k\}_{\Gamma^\varepsilon} = \left(\xi^2 + \frac{k^2}{r_0^2}\right) \{\hat{u}_k\}_{\Gamma^\varepsilon}, \\ \hat{u}_k(R_0) = 0. \end{array} \right. \quad (5.23)$$

Again, as function K_k tends to infinity when r tends to zero, we will consider $C_2^k = 0$. Then, employing the transmission and boundary conditions (5.23), we obtain the following set of equations for the coefficients $C_1^k, C_3^k, C_4^k, C_5^k$, and C_6^k

$$\left\{ \begin{array}{l} I_k(|\xi|r_t)C_1^k - I_k(|\xi|r_t)C_3^k - K_k(|\xi|r_t)C_4^k = 0, \\ -I_k'(|\xi|r_t)C_1^k + I_k'(|\xi|r_t)C_3^k + K_k'(|\xi|r_t)C_4^k = \frac{A}{2\pi\sigma_{\text{int}}r_t|\xi|}, \\ I_k(|\xi|r_{0,\varepsilon}^-)C_3^k + K_k(|\xi|r_{0,\varepsilon}^-)C_4^k - I_k(|\xi|r_{0,\varepsilon}^+)C_5^k - K_k(|\xi|r_{0,\varepsilon}^+)C_6^k = 0, \\ B_3^k C_3^k + B_4^k C_4^k + B_5^k C_5^k + B_6^k C_6^k = 0, \\ J_k(|\xi|R_0)C_5^k + K_k(|\xi|R_0)C_6^k = 0, \end{array} \right.$$

where the coefficients B_3^k, B_4^k, B_5^k , and B_6^k are defined as

$$B_3^k = \frac{\varepsilon^2 \sigma_{\text{int}} |\xi|}{\hat{\sigma}_0} I_k'(|\xi|r_{0,\varepsilon}^-) - \frac{\varepsilon^3 \sigma_{\text{int}} |\xi|}{2\hat{\sigma}_0 r_0} I_k'(|\xi|r_{0,\varepsilon}^-) + \frac{1}{2} \left(\xi^2 + \frac{k^2}{r_0^2}\right) I_k(|\xi|r_{0,\varepsilon}^-),$$

$$B_4^k = \frac{\varepsilon^2 \sigma_{\text{int}} |\xi|}{\hat{\sigma}_0} K_k'(|\xi|r_{0,\varepsilon}^-) - \frac{\varepsilon^3 \sigma_{\text{int}} |\xi|}{2\hat{\sigma}_0 r_0} K_k'(|\xi|r_{0,\varepsilon}^-) + \frac{1}{2} \left(\xi^2 + \frac{k^2}{r_0^2}\right) K_k(|\xi|r_{0,\varepsilon}^-),$$

$$B_5^k = -\frac{\varepsilon^2 \sigma_{\text{ext}} |\xi|}{\hat{\sigma}_0} I_k'(|\xi|r_{0,\varepsilon}^+) - \frac{\varepsilon^3 \sigma_{\text{ext}} |\xi|}{2\hat{\sigma}_0 r_0} I_k'(|\xi|r_{0,\varepsilon}^+) + \frac{1}{2} \left(\xi^2 + \frac{k^2}{r_0^2}\right) I_k(|\xi|r_{0,\varepsilon}^+),$$

$$B_6^k = -\frac{\varepsilon^2 \sigma_{\text{ext}} |\xi|}{\hat{\sigma}_0} K_k'(|\xi|r_{0,\varepsilon}^+) - \frac{\varepsilon^3 \sigma_{\text{ext}} |\xi|}{2\hat{\sigma}_0 r_0} K_k'(|\xi|r_{0,\varepsilon}^+) + \frac{1}{2} \left(\xi^2 + \frac{k^2}{r_0^2}\right) K_k(|\xi|r_{0,\varepsilon}^+).$$

Solving this equation we obtain the values for the coefficients C_1^k , C_3^k , C_4^k , C_5^k , and C_6^k , which have been shown in Proposition 13. Now that we have made explicit the expression of \hat{u}_k we employ the inverse Fourier transform (5.3) to obtain the expression of function u .

□

CONCLUSIONS AND FUTURE WORK

In this work, we have studied the problem of the acquisition of borehole through-casing resistivity measurements by employing the electric potential. We have mainly considered configurations which include boreholes for performing these resistivity measurements. These boreholes are surrounded by a highly conductive metallic casing. The thickness and high conductivity of the casing give rise to difficulties and an increase of the computational cost when performing numerical simulations. The aim of this study has been to develop approximate models to deal with the numerical instabilities this metallic casing creates. In this framework, we have obtained results in four main directions.

First we have derived approximate models. Here, we have worked on 2D and on 3D axi-symmetric configurations with different external boundary conditions. We have also considered both static and frequency dependent problems. For all these diverse scenarios, we have obtained two different classes of asymptotic models by employing two different approaches. Each of them has delivered several models with different characteristics, like coupled and uncoupled models or different orders of convergence.

The second set of results consists of a mathematical analysis of the new approximate models. In this aspect, we have derived the corresponding suitable variational formulations for these models. Then, we have obtained stability results by proving the existence and uniqueness of a solution to these problems, together with uniform estimates. Moreover, we have proved the convergence of the approximate models with a determined order of convergence.

The third direction we have worked on is related to the numerical simulations of the different reference models we have considered and the different approximate models we have derived. For this purpose, we have developed a code in Matlab and C programming languages to numerically solve such models by using a classical Finite Element Method. Thanks to this, we have obtained several numerical results and we have been able to assess the numerical performance of the models.

Moreover, we have also performed several applications to our models concerning the acquisition of resistivity measurements.

Lastly, we have constructed semi-analytical solutions for the approximate models. We have applied a Fourier transform involving two dimensions of the problem, to transform it from a 3D problem into a 1D problem. Then, we have obtained the analytical solution of this 1D problem and applied the inverse Fourier transform to obtain a 3D semi-analytical solution. These semi-analytical solutions provide a less expensive way for evaluating the solutions to our asymptotic models as compared to full numerical solutions.

There are several natural directions in which we could advance concerning this problem. A possible step forward would be to analyze the possible singularities of the problem and observe their impact in the performance of the ITCs. Related to this, it would also be interesting to study the case of deviated wells. This case is specially challenging due to the corners that appear in the configuration, which are known to reduce the performance of the ITCs and require a special treatment.

Another continuation of this work could be to keep on working in the direction of 3D Electromagnetism. Here we have presented some preliminary numerical simulations for assessing the numerical performance of a limit problem. Regarding this subject it would be interesting to perform a thorough derivation of approximate models by finding a suitable *Ansatz* for the asymptotic expansion.

In the same way, the continuation on the semi-analytical solutions is another suitable research line. Here we have presented the derivation of these solutions. The natural step forward in this direction would be the implementation of these solutions and the acquisition of several numerical results. Then, a comparison between these results and the results we have obtained with fully numerical solutions could be done regarding aspects like the performance and the accuracy of the solutions.

Finally it would also be interesting to perform a study of this problem, depicted in Figure 5.1, by performing a different expansion of the solution than the one we have considered in this document. Here, we have performed an expansion in powers of the thickness of the casing. As the conductivity in the casing is several magnitudes bigger than the conductivity in the rock formations, we could investigate an expansion in powers of the conductivity contrast of these two values. The expansion would have the following form

$$u \approx \sum_{k \geq 0} \delta^k u^k, \quad \text{where} \quad \delta = \frac{\sigma_{\text{ext}}}{\sigma_{\text{lay}}}.$$

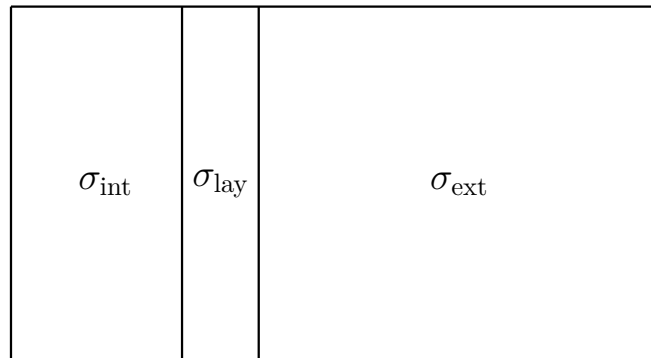


Figure 5.1: Domain with different conductivities, where $\sigma_{\text{lay}} \gg \sigma_{\text{ext}}, \sigma_{\text{int}}$.

CONCLUSIONS ET TRAVAIL FUTUR

Dans ce travail, on a étudié le problème d'acquisitions des mesures de résistivité en forage à travers un tube métallique, en utilisant le potentiel électrique. On a considéré en général des configurations qui incluent des forages pour réaliser ces mesures de résistivité. Les forages sont couverts par un tube métallique hautement conducteur. La faible épaisseur et la haute conductivité du tube induisent une augmentation du coût de calcul lors de simulations numériques, ainsi que des instabilités numériques. Le but de ce travail a été de développer des modèles approchés pour traiter les difficultés créées par ce tube. Dans ce contexte, on a obtenu des résultats dans quatre directions principales.

Tout d'abord on a obtenu des modèles approchés. Ici on a travaillé avec des configurations 2D et 3D axisymétriques, avec diverses conditions de bord. On a considéré le problème pour le potentiel électrique statique, aussi bien que le problème à fréquence non-nulle. Pour toutes ces configurations, on a obtenu deux classes différentes de modèles asymptotiques en utilisant deux approches différentes. Chacune d'elles a délivré plusieurs modèles de caractéristiques différentes, comme des modèles couplés ou non-couplés, ou des modèles de différents ordres de convergence.

Le deuxième groupe de résultats consiste en une analyse mathématique des modèles approchés. On a explicité les formulations variationnelles pour ces modèles. Ensuite, on a obtenu des résultats de stabilité en démontrant des estimations uniformes. De plus, on a prouvé la convergence des modèles approchés avec un ordre de convergence déterminé.

La troisième direction dans laquelle on a travaillé est liée aux simulations numériques des différents problèmes modèles qu'on a considéré, et les différents modèles approchés qu'on a obtenu. À cet effet, on a développé un code en Matlab et en C pour résoudre numériquement ces modèles, en utilisant la méthode des éléments finis. On a obtenu ainsi plusieurs illustrations numériques et on a évalué la performance numérique des modèles. De plus, on a aussi implémenté plusieurs applications pour nos modèles, concernant l'acquisition de mesures de résistivité.

Enfin, on a construit des solutions semi-analytiques pour les modèles approchés. On a utilisé une transformé de Fourier pour transformer le problème 3D en un problème 1D. Ensuite, on a obtenu la solution analytique de ce problème 1D et on a utilisé la transformé de Fourier inverse pour obtenir une solution semi-analytique 3D. Ces solutions semi-analytiques permettent d'évaluer les solutions de nos modèles asymptotiques de façon moins coûteuse, par rapport aux solutions purement numériques.

Il y a plusieurs directions naturelles dans lesquelles on pourrait poursuivre l'étude de ce modèle. Un possible pas en avant serait d'analyser les singularités éventuelles du problème et d'observer leur impacte dans la performance des ITCs. À ce sujet, il serait intéressant d'étudier le cas des puits déviés. Ce cas est plus difficile en général à cause des coins qui apparaissent dans la configuration, lesquels réduisent la performance des ITCs et exigent un traitement spécial.

Une autre piste intéressante à poursuivre est l'étude du problème électromagnétique 3D. Ici on a présenté quelques simulations numériques préliminaires pour évaluer la performance numérique d'un modèle limite. Il serait aussi intéressant d'effectuer une dérivation minutieuse des modèles approchés en trouvant un *Ansatz* approprié pour le développement asymptotique.

Une étape suivante consisterait à implanter les solutions semi-analytiques qu'on a calculé. Il serait intéressant de comparer la performance et la précision de ces solutions avec celles des solutions purement numériques.

Enfin, il serait aussi intéressant d'étudier le problème, dont le domaine d'étude est représenté par la Figure 5.2, à l'aide de développements en puissances de δ , où δ représente un contraste de conductivité:

$$u \approx \sum_{k \geq 0} \delta^k u^k, \quad \text{où} \quad \delta = \frac{\sigma_{\text{ext}}}{\sigma_{\text{lay}}}.$$

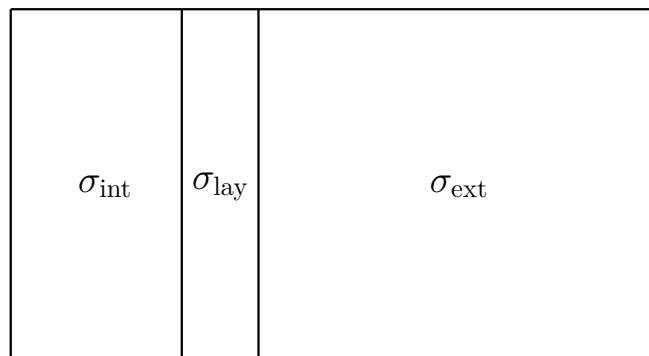


Figure 5.2: Domaine avec des conductivités différentes, où $\sigma_{\text{lay}} \gg \sigma_{\text{ext}}, \sigma_{\text{int}}$.

CONCLUSIONES Y TRABAJO FUTURO

En este trabajo, hemos estudiado el problema de la adquisición de medidas de resistividad en perforaciones a través de un tubo metálico, por medio del potencial eléctrico. En general, hemos considerado configuraciones que incluyen pozos para realizar estas medidas de resistividad. Los pozos están cubiertos de un tubo metálico altamente conductivo. Debido a la finura del tubo y a la alta conductividad del mismo, surgen dificultades y un aumento en el coste de computación, al realizar simulaciones numéricas. El objetivo de este trabajo ha sido desarrollar modelos aproximados para lidiar con las dificultades que crea este tubo metálico. En este contexto, hemos obtenido resultados en cuatro principales direcciones.

Primero de todo, hemos desarrollado modelos aproximados. En este punto, hemos trabajado con configuraciones 2D y 3D con simetría axial, considerando diferentes condiciones de frontera. Asimismo, hemos considerado tanto problemas estáticos, como problemas con frecuencias no nulas. Para todos estos diversos escenarios, hemos obtenido dos clases de modelos asintóticos por medio de dos enfoques diferentes. Cada uno de ellos ha generado varios modelos de características diferentes, como modelos acoplados y desacoplados, o modelos de diferentes órdenes de convergencia.

El segundo conjunto de resultados consiste en un análisis matemático de los modelos asintóticos obtenidos. En este aspecto, hemos obtenido las formulaciones variacionales correspondientes para estos modelos. Igualmente, hemos obtenido resultados sobre la estabilidad, analizando aspectos como la existencia y unicidad de soluciones a estos problemas. Además, hemos demostrado la convergencia de los modelos aproximados con un determinado orden de convergencia.

La tercera dirección en la que hemos trabajado corresponde a las simulaciones numéricas de los diferentes problemas modelo que hemos considerado, y los diferentes modelos aproximados que hemos obtenido. Para ello, hemos desarrollado un

código en Matlab y C para resolver dichos modelos empleando el método de elementos finitos. Gracias a esto, hemos obtenido varios resultados numéricos y hemos podido evaluar el rendimiento numérico de los modelos. Además, hemos considerado varias aplicaciones de nuestros modelos, en lo que respecta a la adquisición de medidas de resistividad.

Por último, hemos construido soluciones semi-analíticas para los modelos aproximados. Hemos utilizado una transformada de Fourier involucrando dos dimensiones del problema, así lo transformamos de un problema 3D a uno 1D. Entonces, hemos obtenido la solución analítica de este problema 1D y hemos empleado la transformada inversa de Fourier para obtener una solución semianalítica 3D. Estas soluciones semianalíticas proporcionan una manera menos costosa de evaluar las soluciones de nuestros modelos asintóticos en comparación con soluciones puramente numéricas.

Existen varias direcciones naturales para avanzar en el estudio de este problema. Un posible paso adelante podría ser el análisis de las posibles singularidades del problema, y una observación de su impacto sobre el rendimiento de las ITCs. En relación con esto, sería también interesante estudiar el caso de perforaciones altamente desviadas. Este caso es especialmente complejo debido a las esquinas que presenta la configuración del problema, las cuales es sabido que reducen el rendimiento de las ITCs y requieren un tratamiento especial.

Otra posible forma de continuar este trabajo podría ser el trabajo realizado en lo que respecta al Electromagnetismo en 3D. Aquí, se han presentado varias simulaciones numéricas preliminares para evaluar el rendimiento numérico de un problema límite. Respecto a este tema, sería interesante realizar una minuciosa derivación de los modelos aproximados encontrando un *Ansatz* apropiado para la expansión asintótica.

Del mismo modo, la continuación de las soluciones semianalíticas es otra línea de investigación apropiada. En el presente documento, hemos presentado la obtención de dichas soluciones. El pasado adelante natural en esta dirección consistiría en la implementación de estas soluciones y la adquisición de varios resultados numéricos. Más tarde, se podría realizar una comparación entre estos resultados y los resultados obtenidos mediante soluciones puramente numéricas, analizando aspectos como el rendimiento y la precisión de las soluciones.

Por último, sería también interesante realizar un estudio de este problema, ilustrado en la Figura 5.3, realizando una expansión de la solución diferente de la que se ha presentado en este documento. Aquí, hemos realizado una expansión en potencias del grosor del tubo. Como la conductividad en el tubo es varias magnitudes mayor que la conductividad de las formaciones rocosas, sería apropi-

ado considerar una expansión en potencias del contraste de conductividades. La expansión tendría la forma siguiente

$$u \approx \sum_{k \geq 0} \delta^k u^k, \quad \text{donde} \quad \delta = \frac{\sigma_{\text{ext}}}{\sigma_{\text{lay}}}.$$

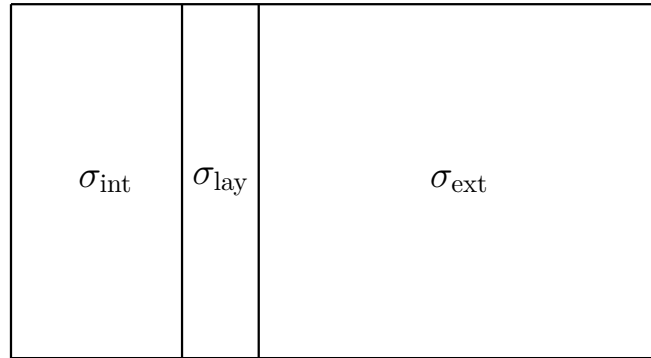


Figura 5.3: Dominio con conductividades diferentes, donde $\sigma_{\text{lay}} \gg \sigma_{\text{ext}}, \sigma_{\text{int}}$.

ONDORIOAK ETA ETORKIZUNERAKO LANA

Lan honetan, potentzial elektrikoa erabiliz, hobietan egindako eroankortasun neurketen problemari ekin diogu. Orokorrean, neurketa hauek egiteko, hodi metaliko batez inguraturiko hobiak kontsideratu ditugu. Hodi metaliko hauen lodiera txikia eta eroankortasun altua direla eta, hainbat zailtasun eta koste konputazionalaren igoera bat ikusi ditzakegu zenbakizko simulazioak egiterako orduan. Lan honen helburua hodi metaliko honek sortzen dituen zailtasunei aurre egiteko eredu hurbilduak garatzea da. Testuinguru honetan, hainbat emaitza lortu ditugu lau norabide nagusitan.

Lehenik eta behin eredu hurbilduak garatu ditugu. Atal honetan 2D eta ardatz bertikalarekiko simetria duten 3D konfigurazioekin lan egin dugu, aldi berean muga baldintza ezberdinak kontsideratu ditugularik. Gainera, bai kasu estatikoa, bai frekuentziarekiko dependentea den problema kontsideratu ditugu. konfigurazio ezberdin hauentzako guztientzako, bi ikuspegi ezberdin erabiliz, bi eredu asintotiko klase ezberdin garatu ditugu. Bietako bakoitzarekin ezaugarri ezberdinak dituzten hainbat eredu garatu ditugu, adibidez, akoplaturiko eta ez akoplaturiko ereduak, edo konbergentzia orden ezberdineko ereduak.

Bigarren emaitza multzoa garaturiko ereduaren analisi matematiko baten ondorioa da. Alde honetatik, erduei dagokien formulazio ahul aproposak garatu ditugu. Ondoren, egonkortasun emaitzak eskuratu ditugu, eredu hauen existentzia eta bakartasuna frogatuz, aldi berean estimazio uniformeak garatu ditugularik. Gainera, eredu hurbilduek orden jakin batekin konbergitzen dutela frogatu dugu.

Lan egin dugun hirugarren norabidea kontsideratu ditugun erreferentzia ereduaren eta garatu dugun eredu hurbilduen zenbakizko simulazioekin erlazionatuta dago. Hau burutzeko Matlab eta C erabiliz kode bat garatu dugu eredu hauek guztiak Elementu Finituen Metodoa erabiliz ebazteko. Honi esker, hainbat zenbakizko emaitza eskuratu ditugu eta ereduaren zenbakizko errendimendua ebaluatzeke gai

izan gara. Halaber, eroankortasun neurketekin erlazionaturiko hainbat aplikazio garatu ditugu.

Azkenik, eredu hurbilduentzako soluzio semi-analitikoak eraiki ditugu. Problemaren bi dimentsio kontuan hartzen dituen Fourierren transformada bat erabiliz, 3D problema 1D problema batean eraldatu dugu. Orduan, 1D problema honen ebazpen analitikoa eraiki dugu eta Fourierren alderantzizko transformada erabili dugu gure 3D problemaren soluzio semi-analitikoa lortzeko. Soluzio semi-analitiko hauek, kostu komputazional txikiago batekin, gure problemaren soluzioak ebaluatze bide bat eskeintzen digute zenbakizko soluzio hutsekin konparatuta.

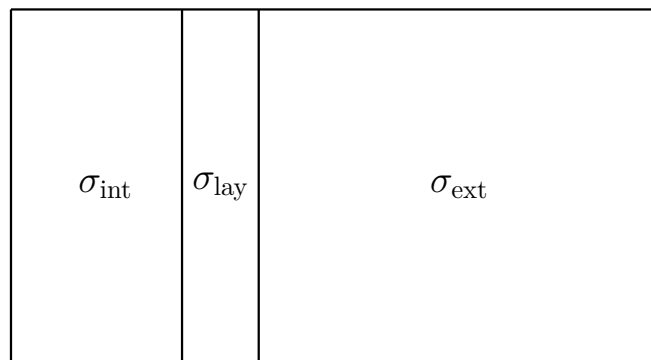
Hainbat norabide natural daude problema honen inguruan aurrera egiteko. Aurrera pausu posible bat, problemaren singularitasun posibleak aztertzea izan liteke, eta aldi berean, hauek eredu hurbilduen errendimenduan duten eragina aztertzea. Honekin erlazionatuta, desbideratutako hobiak aztertzea interesgarria izango litzateke. Kasu honek erronka berezi bat planteatzen du, izan ere konfigurazioan azaltzen diren izkinen eredu hurbiluden errendimendua txikitzeagatik eta arreta berezia eskatzeagatik ezagunak dira.

Lan honen beste jarraipen posible bat 3D elektromagnetismoaren inguruan lan egiten jarraitzea izango litzateke. Lan honetan haibat zenbakizko simulazio aurkeztu ditugu problema limite baten zenbakizko errendimendua azterteko. Arlo honetan, eredu hurbilduen garapen sakon bat egitea interesgarria izango litzateke, hedapen asintotikoarentzako *Ansatz* apropos bat bilatuz.

Era berean, soluzio semi-analitikoen norabidean lan egiten jarraitu beharko litzateke. Hemen, soluzio hauen garapena aurkeztu dugu. Norabide honetan, aurrera pausu naturala, soluzio hauen inplementazioa eta hainbat zenbakizko emaitza lortzea izango litzateke. Orduan, emaitza hauen eta zenbakizko soluzio hutsekin eskuratutako emaitzen konparazio bat egitea posible izango litzateke, errendimendua eta zehaztasuna bezalako alderdiak aztertuz.

Azkenik, Irudi 5.4-ean erakusten den problemaren analisi bat egitea posible izango litzateke beste ikuspuntu bat erabiliz. Dokumentu honetan hedapen asintotiko bat garatu dugu hodi metalikoaren lodieraren berreturetan. Jodien eroankortasuna lur geruzen eroankortasuna baino hainbat magnitude altuagoa denez, posible izango litzateke hedapen asintotiko berri bat aztertzea, zeina eroankortasun hauen kontrastearen berreturetan egin izango litzateke. Hedapenak ondorengo forma edukiko luke

$$u \approx \sum_{k \geq 0} \delta^k u^k, \quad \text{non} \quad \delta = \frac{\sigma_{\text{ext}}}{\sigma_{\text{lay}}}.$$



Irudi 5.4: Eroankortasun ezberdinetako eremua, non $\sigma_{\text{lay}} \gg \sigma_{\text{ext}}, \sigma_{\text{int}}$.

ADDITIONAL RESULTS

A.1 Introduction

In this Appendix we present several additional results related to the models obtained in the previous chapters. We begin by presenting the derivation of the 3D axi-symmetric asymptotic models we have employed in chapter 5. Then we show the variational formulations for the time-harmonic problems obtained in section 1.5. In the same way, we continue by giving the variational formulations for the problems set in the 3D axisymmetric configuration considered in section 1.6. Then, we show some steps towards an extension of the results obtained in the previous chapters to a 3D electromagnetic problem. The next section is devoted to a unified notation for the different asymptotic models we have derived. Finally, we compare our models with several similar models that can be found in the literature.

A.2 3D axisymmetric configuration

The main objective of this section is the derivation of approximate models in a 3D axisymmetric configuration. The plan of the section is the following. First we set the model problem we are interested in. Then, we develop a multiscale expansion in powers of ε for the solution to the model problem and we obtain the equations for the first terms of the expansion adopting the first approach. Finally, we derive the desired approximate models. We then address the second class of problems, and for avoiding repetition with the previous sections only the main results are presented.

A.2.1 Model problem and scaling

Let $\Omega \subset \mathbb{R}^3$ be the domain of interest described at Figure A.1. The Domain Ω is a cylinder shaped domain and is decomposed into three subdomains: $\Omega_{\text{int}}^\varepsilon$, $\Omega_{\text{ext}}^\varepsilon$, and $\Omega_{\text{lay}}^\varepsilon$. Subdomain $\Omega_{\text{lay}}^\varepsilon$ is a thin layer of uniform thickness $\varepsilon > 0$. We denote by $\Gamma_{\text{int}}^\varepsilon$ the interface between $\Omega_{\text{int}}^\varepsilon$ and $\Omega_{\text{lay}}^\varepsilon$, and by $\Gamma_{\text{ext}}^\varepsilon$ the interface between $\Omega_{\text{lay}}^\varepsilon$ and $\Omega_{\text{ext}}^\varepsilon$. In this domain, we study the static electric potential equation, which read as follows

$$\operatorname{div}(\sigma \nabla u) = f. \quad (\text{A.1})$$

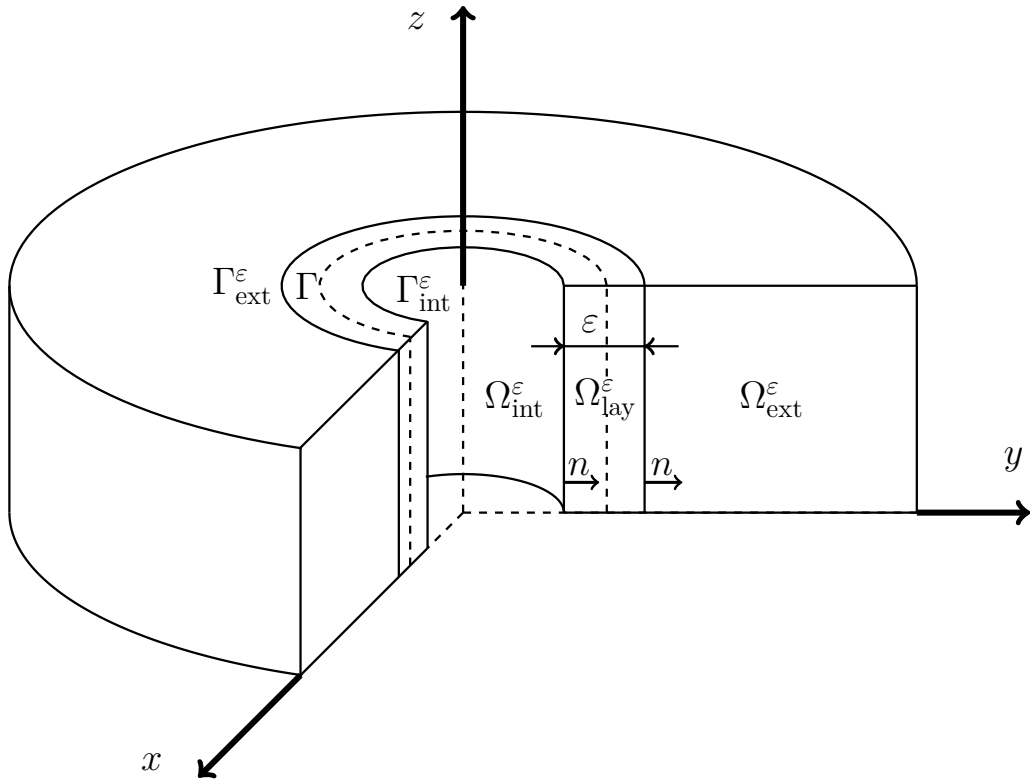


Figure A.1: Sectioned three dimensional domain for the model problem and asymptotic models of the first class.

Here, u represents the electric potential, σ stands for the conductivity and f is the right-hand side, which corresponds to a current source. The conductivity is a piecewise constant function, with a different value in each subdomain. Specifically, the value of the conductivity inside the thin layer $\Omega_{\text{lay}}^\varepsilon$ is much larger than the one in the other subdomains and we assume that it depends on parameter ε . We

consider a conductivity of the following form

$$\sigma = \begin{cases} \sigma_{\text{int}} & \text{in } \Omega_{\text{int}}^\varepsilon, \\ \sigma_{\text{lay}} = \widehat{\sigma}_0 \varepsilon^{-3} & \text{in } \Omega_{\text{lay}}^\varepsilon, \\ \sigma_{\text{ext}} & \text{in } \Omega_{\text{ext}}^\varepsilon, \end{cases}$$

where $\widehat{\sigma}_0 > 0$ is a given constant. We assume the right-hand side f is a piecewise smooth function that is independent of ε and vanishes inside the layer.

$$f = \begin{cases} f_{\text{int}} & \text{in } \Omega_{\text{int}}^\varepsilon, \\ f_{\text{lay}} = 0 & \text{in } \Omega_{\text{lay}}^\varepsilon, \\ f_{\text{ext}} & \text{in } \Omega_{\text{ext}}^\varepsilon. \end{cases}$$

We assume that we have a solution $u \in H^1(\Omega)$ to (A.1). Then, denoting the solution u by

$$u = \begin{cases} u_{\text{int}} & \text{in } \Omega_{\text{int}}^\varepsilon, \\ u_{\text{lay}} & \text{in } \Omega_{\text{lay}}^\varepsilon, \\ u_{\text{ext}} & \text{in } \Omega_{\text{ext}}^\varepsilon, \end{cases}$$

Problem (A.1) becomes

$$\left\{ \begin{array}{ll} \sigma_{\text{int}} \Delta u_{\text{int}} = f_{\text{int}} & \text{in } \Omega_{\text{int}}^\varepsilon, \\ \sigma_{\text{ext}} \Delta u_{\text{ext}} = f_{\text{ext}} & \text{in } \Omega_{\text{ext}}^\varepsilon, \\ \Delta u_{\text{lay}} = 0 & \text{in } \Omega_{\text{lay}}^\varepsilon, \\ u_{\text{int}} = u_{\text{lay}} & \text{on } \Gamma_{\text{int}}^\varepsilon, \\ u_{\text{lay}} = u_{\text{ext}} & \text{on } \Gamma_{\text{ext}}^\varepsilon, \\ \sigma_{\text{int}} \partial_n u_{\text{int}} = \widehat{\sigma}_0 \varepsilon^{-3} \partial_n u_{\text{lay}} & \text{on } \Gamma_{\text{int}}^\varepsilon, \\ \widehat{\sigma}_0 \varepsilon^{-3} \partial_n u_{\text{lay}} = \sigma_{\text{ext}} \partial_n u_{\text{ext}} & \text{on } \Gamma_{\text{ext}}^\varepsilon, \\ u = 0 & \text{on } \partial\Omega, \end{array} \right. \quad (\text{A.2})$$

where ∂_n represents the normal derivative in the direction of the normal vector, which is interior to $\Omega_{\text{ext}}^\varepsilon$ on $\Gamma_{\text{ext}}^\varepsilon$, and exterior to $\Omega_{\text{int}}^\varepsilon$ on $\Gamma_{\text{int}}^\varepsilon$, as shown at Figure A.1. Due to the cylindrical shape of the considered domain, we consider these equations to be written in cylindrical coordinates. Thus, the Laplacian operators of equation (A.2) have the following form

$$\Delta = \frac{1}{r} \partial_r (r \partial_r) + \frac{1}{r^2} \partial_\theta^2 + \partial_z^2.$$

A key point for the derivation of a multiscale expansion for the solution to Problem (A.2) consists in performing a scaling along the direction normal to the thin layer. We begin by describing domain $\Omega_{\text{lay}}^\varepsilon$ in the following way

$$\Omega_{\text{lay}}^\varepsilon = \left\{ \gamma(\theta, z) + \varepsilon R n : \gamma(z) \in \Gamma, R \in \left(-\frac{1}{2}, \frac{1}{2} \right) \right\},$$

where γ is a parametrization of the interface Γ (see Figure A.1), which in cylindrical coordinates is defined as

$$\gamma(\theta, z) = (r_0, \theta, z), \text{ for all } \theta \in [0, 2\pi), z \in (0, z_0),$$

and $n = (1, 0, 0)$ is the normal vector to the curve Γ . This domain geometry induces the following scaling

$$r = r_0 + \varepsilon R \quad \Leftrightarrow \quad R = \varepsilon^{-1} (r - r_0).$$

As a consequence, we have

$$\partial_R^k = \varepsilon^k \partial_r^k, \quad k \in \mathbb{N}.$$

This scaling allows us to write the scalar operator $\frac{1}{r} \partial_r (r \partial_r) + \frac{1}{r^2} \partial_\theta^2 + \partial_z^2$ in the following way

$$\varepsilon^{-2} \partial_R^2 + \varepsilon^{-1} \frac{1}{r_0 + \varepsilon R} \partial_R + \frac{1}{(r_0 + \varepsilon R)^2} \partial_\theta^2 + \partial_z^2.$$

Now we perform an expansion of the terms $\frac{1}{r_0 + \varepsilon R}$ and $\frac{1}{(r_0 + \varepsilon R)^2}$ in powers of ε so that we obtain the following expression

$$\varepsilon^{-2} \partial_R^2 + \sum_{k=0}^{\infty} \varepsilon^{k-1} \frac{(-R)^k}{r_0^{k+1}} \partial_R + \sum_{k=0}^{\infty} \varepsilon^k \frac{(-R)^k}{r_0^{k+2}} \partial_\theta^2 + \partial_z^2.$$

We also notice that on the interfaces $\Gamma_{\text{int}}^\varepsilon$ and $\Gamma_{\text{ext}}^\varepsilon$ we rewrite the normal derivative in the following form $\partial_n = \partial_r = \varepsilon^{-1} \partial_R$. Finally we denote by U the function that satisfies

$$u_{\text{lay}}(r, \theta, z) = u_{\text{lay}}(r_0 + \varepsilon R, \theta, z) = U(R, \theta, z), \quad (R, \theta, z) \in \left(-\frac{1}{2}, \frac{1}{2} \right) \times [0, 2\pi) \times (0, z_0).$$

We rewrite Equations (A.2) with the newly defined variables and functions and they satisfy the following equations outside the thin layer

$$\begin{cases} \sigma_{\text{int}} \Delta u_{\text{int}} = f_{\text{int}} & \text{in } \Omega_{\text{int}}^\varepsilon, \\ \sigma_{\text{ext}} \Delta u_{\text{ext}} = f_{\text{ext}} & \text{in } \Omega_{\text{ext}}^\varepsilon, \end{cases} \quad (\text{A.3})$$

the following equation inside the thin layer

$$\begin{aligned} \varepsilon^{-2} \partial_R^2 U + \sum_{k=0}^{\infty} \varepsilon^{k-1} \frac{(-R)^k}{r_0^{k+1}} \partial_R U + \sum_{k=0}^{\infty} \varepsilon^k (k+1) \frac{(-R)^k}{r_0^{k+2}} \partial_\theta^2 U + \partial_z^2 U = 0 \\ \text{in } \left(-\frac{1}{2}, \frac{1}{2}\right) \times [0, 2\pi) \times (0, z_0), \end{aligned} \quad (\text{A.4})$$

and the following transmission and boundary conditions

$$\begin{cases} u_{\text{int}} \left(r_0 - \frac{\varepsilon}{2}, \theta, z \right) = U \left(-\frac{1}{2}, \theta, z \right) & (\theta, z) \in [0, 2\pi) \times (0, z_0), \\ u_{\text{ext}} \left(r_0 + \frac{\varepsilon}{2}, \theta, z \right) = U \left(\frac{1}{2}, \theta, z \right) & (\theta, z) \in [0, 2\pi) \times (0, z_0), \\ \sigma_{\text{int}} \partial_n u_{\text{int}} \left(r_0 - \frac{\varepsilon}{2}, \theta, z \right) = \hat{\sigma}_0 \varepsilon^{-4} \partial_R U \left(-\frac{1}{2}, \theta, z \right) & (\theta, z) \in [0, 2\pi) \times (0, z_0), \\ \sigma_{\text{ext}} \partial_n u_{\text{ext}} \left(r_0 + \frac{\varepsilon}{2}, \theta, z \right) = \hat{\sigma}_0 \varepsilon^{-4} \partial_R U \left(\frac{1}{2}, \theta, z \right) & (\theta, z) \in [0, 2\pi) \times (0, z_0), \\ u = 0 & \text{on } \partial\Omega. \end{cases} \quad (\text{A.5})$$

A.2.2 First class of ITCs: construction of a multiscale expansion

We now derive the asymptotic expansion. To begin with, we perform an *Ansatz* in the form of power series of ε for the solution to Problems (A.3), (A.4) and (A.5). We look for solutions

$$\begin{cases} u_{\text{int}}(r, \theta, z) \approx \sum_{k \geq 0} \varepsilon^k u_{\text{int}}^k(r, \theta, z) & \text{in } \Omega_{\text{int}}^\varepsilon, \\ u_{\text{ext}}(r, \theta, z) \approx \sum_{k \geq 0} \varepsilon^k u_{\text{ext}}^k(r, \theta, z) & \text{in } \Omega_{\text{ext}}^\varepsilon, \\ U(R, \theta, z) \approx \sum_{k \geq 0} \varepsilon^k U^k(R, \theta, z) & \text{in } \left(-\frac{1}{2}, \frac{1}{2}\right) \times [0, 2\pi) \times (0, z_0). \end{cases} \quad (\text{A.6})$$

Equations for the coefficients of the electric potential

Substituting the previous expressions into Equations (A.3), (A.4), and (A.5), and collecting the terms with the same powers in ε , for every $k \in \mathbb{N}$, we obtain the following set of equations outside the layer

$$\begin{cases} \sigma_{\text{int}} \Delta u_{\text{int}}^k = f_{\text{int}} \delta_k^0 & \text{in } \Omega_{\text{int}}^\varepsilon, & \text{(A.7a)} \\ \sigma_{\text{ext}} \Delta u_{\text{ext}}^k = f_{\text{ext}} \delta_k^0 & \text{in } \Omega_{\text{ext}}^\varepsilon, & \text{(A.7b)} \end{cases}$$

and the following equations inside the layer

$$\begin{aligned} \partial_R^2 U^k + \sum_{l=0}^{k-1} \frac{(-R)^{k-l-1}}{r_0^{k-l}} \partial_R U^l + \sum_{l=0}^{k-2} (k-l-1) \frac{(-R)^{k-l-2}}{r_0^{k-l}} \partial_\theta^2 U^l + \partial_z^2 U^{k-2} = 0 \\ \text{in } \left(-\frac{1}{2}, \frac{1}{2}\right) \times [0, 2\pi) \times (0, z_0), \end{aligned} \quad \text{(A.8)}$$

along with the following transmission conditions

$$\begin{cases} U^k \left(-\frac{1}{2}, \theta, z\right) = u_{\text{int}}^k \left(r_0 - \frac{\varepsilon}{2}, \theta, z\right) & (\theta, z) \in [0, 2\pi) \times (0, z_0), & \text{(A.9a)} \\ U^k \left(\frac{1}{2}, \theta, z\right) = u_{\text{ext}}^k \left(r_0 + \frac{\varepsilon}{2}, \theta, z\right) & (\theta, z) \in [0, 2\pi) \times (0, z_0), & \text{(A.9b)} \\ \partial_R U^k \left(-\frac{1}{2}, \theta, z\right) = \frac{\sigma_{\text{int}}}{\widehat{\sigma}_0} \partial_n u_{\text{int}}^{k-4} \left(r_0 - \frac{\varepsilon}{2}, \theta, z\right) & (\theta, z) \in [0, 2\pi) \times (0, z_0), & \text{(A.9c)} \\ \partial_R U^k \left(\frac{1}{2}, \theta, z\right) = \frac{\sigma_{\text{ext}}}{\widehat{\sigma}_0} \partial_n u_{\text{ext}}^{k-4} \left(r_0 + \frac{\varepsilon}{2}, \theta, z\right) & (\theta, z) \in [0, 2\pi) \times (0, z_0), & \text{(A.9d)} \end{cases}$$

and the following boundary conditions

$$\begin{cases} u^k(R_0, \theta, z) = 0 & (\theta, z) \in [0, 2\pi) \times (0, z_0), & \text{(A.10a)} \\ u^k(r, \theta, 0) = u^k(r, \theta, z_0) = 0 & (r, \theta) \in \left(0, r_0 - \frac{\varepsilon}{2}\right) \cup \left(r_0 + \frac{\varepsilon}{2}, R_0\right) \\ & \times [0, 2\pi), & \text{(A.10b)} \\ U^k(R, \theta, 0) = U^k(R, \theta, z_0) = 0 & (R, \theta) \in \left(-\frac{1}{2}, \frac{1}{2}\right) \times [0, 2\pi). & \text{(A.10c)} \end{cases}$$

For determining the elemental problem satisfied by each of the terms of the expansion, we will also need the following equation obtained by applying the fundamental theorem of calculus for a smooth function U^k ,

$$\int_{-\frac{1}{2}}^{\frac{1}{2}} \partial_R^2 U^k(R, z) dR = \partial_R U^k\left(\frac{1}{2}, z\right) - \partial_R U^k\left(-\frac{1}{2}, z\right).$$

If we substitute Equation (A.8) to the left-hand side and Equations (A.9c) and (A.9d) to the right-hand side, we obtain the following compatibility condition

$$\int_{-\frac{1}{2}}^{\frac{1}{2}} \left(\partial_z^2 U^{k-2}(R, \theta, z) + \sum_{l=0}^{k-1} \frac{(-R)^{k-1-l}}{r_0^{k-l}} \partial_R U^l(R, \theta, z) + \sum_{l=0}^{k-2} (k-l-1) \frac{(-R)^{k-2-l}}{r_0^{k-l}} \partial_\theta^2 U^l(R, \theta, z) \right) dR = \frac{-1}{\hat{\sigma}_0} \left[\sigma \partial_n u^{k-4} \right]_{\Gamma^\varepsilon}(z). \quad (\text{A.11})$$

We adopt the convention that the terms with negative indices in Equations (A.7)-(A.11) are equal to 0. Employing Equations (A.7) - (A.11) we deduce the elementary problems satisfied outside and inside the layer for any $k \in \mathbb{N}$. For that purpose we employ the following algorithm composed of three steps.

Algorithm for the determination of the coefficients

Initialization of the algorithm:

Before showing the different steps to obtain function U^k and u^k for every k , we need to determine function U^0 up to a function in the variables θ and z , denoted by φ_0^0 . For that purpose we consider Equations (A.8), (A.9c), and (A.9d), and we build the following differential problem in the variable R for U^0 (the variables θ and z play the role of a parameter)

$$\begin{cases} \partial_R^2 U^0(R, \theta, z) = 0 & R \in \left(-\frac{1}{2}, \frac{1}{2}\right), \\ \hat{\sigma}_0 \partial_R U^0\left(-\frac{1}{2}, \theta, z\right) = 0, \\ \hat{\sigma}_0 \partial_R U^0\left(\frac{1}{2}, \theta, z\right) = 0. \end{cases}$$

From these equations we deduce that U^0 has the following form $U^0(R, \theta, z) = \varphi_0^0(\theta, z)$, where function φ_0^0 has yet to be determined and this will be done during the

first step of the algorithm. After these preliminary steps, we move onto determining U^k and u^k for any k .

We assume that the first terms of the expansion (A.6) up to the order ε^{k-1} have already been calculated and we calculate the equations for the k -th term. We also assume that at rank k we know the form of U^k up to a function in the variables θ and z , denoted by φ_0^k . We obtain the expression of U^k at rank $k-1$. The first step consists in determining the expression of function U^{k+1} up to function φ_0^{k+1} . Then, at the second step we determine function φ_0^k involved in the expression of function U^k . Finally, we determine u_{int}^k and u_{ext}^k at the third step. For every $k = 0, 1, 2, \dots$, we perform the following steps:

First step:

We select Equations (A.8), (A.9c), and (A.9d), and we build the following differential problem in the variable R for U^{k+1} (the variables θ and z play the role of a parameter)

$$\begin{cases} \partial_R^2 U^{k+1}(R, \theta, z) = g^{k+1}(R, \theta, z) & R \in \left(-\frac{1}{2}, \frac{1}{2}\right), \\ \hat{\sigma}_0 \partial_R U^{k+1}\left(-\frac{1}{2}, \theta, z\right) = \sigma_{\text{int}} \partial_n u_{\text{int}}^{k-3}\left(r_0 - \frac{\varepsilon}{2}, \theta, z\right), \\ \hat{\sigma}_0 \partial_R U^{k+1}\left(\frac{1}{2}, \theta, z\right) = \sigma_{\text{ext}} \partial_n u_{\text{ext}}^{k-3}\left(r_0 + \frac{\varepsilon}{2}, \theta, z\right), \end{cases} \quad (\text{A.12})$$

where

$$g^{k+1}(R, \theta, z) = - \sum_{l=0}^k \frac{(-R)^{k-l}}{r_0^{k-l+1}} \partial_R U^l(R, \theta, z) - \sum_{l=0}^{k-1} (k-l) \frac{(-R)^{k-l-1}}{r_0^{k-l+1}} \partial_\theta^2 U^l(R, \theta, z) - \partial_z^2 U^{k-1}(R, \theta, z).$$

There exists a solution U^{k+1} to (A.12) provided the compatibility condition (A.11) is satisfied. We deduce the expression of U^{k+1} up to a function in the variables θ and z , denoted by $\varphi_0^{k+1}(\theta, z)$. The function U^{k+1} has the following form

$$U^{k+1}(R, \theta, z) = V^{k+1}(R, \theta, z) + \varphi_0^{k+1}(\theta, z),$$

where V^{k+1} represents the part of U^{k+1} that is determined at this step and has the form (see Proposition 14)

$$V^k(R, \theta, z) = \begin{cases} 0 & \text{if } k = 0, 1, 2, 3 \\ \varphi_{k-2}^k(\theta, z) R^{k-2} + \varphi_{k-3}^k(\theta, z) R^{k-3} + \dots + \varphi_1^k(\theta, z) R & \text{if } k > 3. \end{cases}$$

Function φ_0^{k+1} represents the part of U^{k+1} that is determined at the following rank.

Second step:

We employ the compatibility condition (A.11) (at rank $k + 2$), along with Equation (A.10c) to write the following differential problem in the variables θ and z for function φ_0^k , present in the expression of U^k .

$$\left\{ \begin{array}{l} \partial_z^2 \varphi_0^k(\theta, z) + \frac{1}{r_0^2} \partial_\theta^2 \varphi_0^k(\theta, z) = h^k(\theta, z) \quad (\theta, z) \in [0, 2\pi) \times (0, z_0), \\ \varphi_0^k(\theta, 0) = 0 \quad \theta \in [0, 2\pi), \\ \varphi_0^k(\theta, z_0) = 0 \quad \theta \in [0, 2\pi), \end{array} \right. \quad (\text{A.13})$$

where

$$h^k(\theta, z) = - \int_{-\frac{1}{2}}^{\frac{1}{2}} \left(\partial_z^2 V^k(R, \theta, z) + \sum_{l=0}^{k+1} \frac{(-R)^{k+1-l}}{r_0^{k+2-l}} \partial_R U^l(R, \theta, z) \right. \\ \left. + \sum_{l=0}^{k-1} (k-l+1) \frac{(-R)^{k-l}}{r_0^{k+2-l}} \partial_\theta^2 U^l(R, \theta, z) + \frac{1}{r_0^2} \partial_\theta^2 V^k(R, \theta, z) \right) dR - \frac{1}{\hat{\sigma}_0} [\sigma \partial_n u^{k-2}]_{\Gamma^\varepsilon}(\theta, z).$$

Solving this differential equation we obtain function φ_0^k and thus, the complete expression of U^k .

Third step:

We derive the equations outside the layer by employing Equations (A.7a), (A.7b), (A.9a), (A.9b), (A.10a), and (A.10b). We infer that u_{int}^k and u_{ext}^k are

defined independently in the two subdomains $\Omega_{\text{int}}^\varepsilon$ and $\Omega_{\text{ext}}^\varepsilon$.

$$\left\{ \begin{array}{ll} \sigma_{\text{int}} \Delta u_{\text{int}}^k = 0 & \text{in } \Omega_{\text{int}}^\varepsilon, \\ u_{\text{int}}^k \left(r_0 - \frac{\varepsilon}{2}, \theta, z \right) = U^k \left(-\frac{1}{2}, \theta, z \right), & \\ u_{\text{int}}^k = 0 & \text{on } \partial\Omega \cap \partial\Omega_{\text{int}}^\varepsilon. \end{array} \right. \quad (\text{A.14})$$

$$\left\{ \begin{array}{ll} \sigma_{\text{ext}} \Delta u_{\text{ext}}^k = 0 & \text{in } \Omega_{\text{ext}}^\varepsilon, \\ u_{\text{ext}}^k \left(r_0 + \frac{\varepsilon}{2}, \theta, z \right) = U^k \left(\frac{1}{2}, \theta, z \right), & \\ u_{\text{ext}}^k = 0 & \text{on } \partial\Omega \cap \partial\Omega_{\text{ext}}^\varepsilon. \end{array} \right.$$

We will now employ this algorithm to obtain the equations for the first terms of the expansion.

First terms of the asymptotics

Terms of order zero

Thanks to the preliminary steps formerly performed during the initialization of the algorithm we already know that U^0 has the form $U^0(R, \theta, z) = \varphi_0^0(\theta, z)$. In the same way we consider Problem (A.12) for U^1

$$\left\{ \begin{array}{l} \partial_R^2 U^1(R, \theta, z) = 0 \quad R \in \left(-\frac{1}{2}, \frac{1}{2} \right), \\ \partial_R U^1 \left(-\frac{1}{2}, \theta, z \right) = 0, \\ \partial_R U^1 \left(\frac{1}{2}, \theta, z \right) = 0. \end{array} \right.$$

We deduce that the solution to this equation has the form $U^1(R, \theta, z) = \varphi_0^1(\theta, z)$. Then, we employ (A.13) and we build the following problem for φ_0^0

$$\left\{ \begin{array}{l} \partial_z^2 \varphi_0^0(\theta, z) + \frac{1}{r_0^2} \partial_\theta^2 \varphi_0^0(\theta, z) = 0 \quad (\theta, z) \in [0, 2\pi) \times (0, z_0), \\ \varphi_0^0(\theta, 0) = 0, \\ \varphi_0^0(\theta, z_0) = 0. \end{array} \right.$$

We conclude that $\varphi_0^0(\theta, z) = 0$ and thus, $U^0(R, \theta, z) = 0$. Finally, employing (A.14), we obtain that the limit solution u^0 satisfies homogeneous Dirichlet boundary conditions on $\Gamma_{\text{int}}^\varepsilon$ and $\Gamma_{\text{ext}}^\varepsilon$. Thus, the problem satisfied by u^0 reads as

$$\begin{cases} \sigma_{\text{int}} \Delta u_{\text{int}}^0 = f_{\text{int}} & \text{in } \Omega_{\text{int}}^\varepsilon, \\ u_{\text{int}}^0 = 0 & \text{on } \partial\Omega_{\text{int}}^\varepsilon. \end{cases} \quad (\text{A.15})$$

$$\begin{cases} \sigma_{\text{ext}} \Delta u_{\text{ext}}^0 = f_{\text{ext}} & \text{in } \Omega_{\text{ext}}^\varepsilon, \\ u_{\text{ext}}^0 = 0 & \text{on } \partial\Omega_{\text{ext}}^\varepsilon. \end{cases}$$

Terms of order one

We consider Problem (A.12) for U^2

$$\begin{cases} \partial_R^2 U^2(R, \theta, z) = 0 & R \in \left(-\frac{1}{2}, \frac{1}{2}\right), \\ \partial_R U^2\left(-\frac{1}{2}, \theta, z\right) = 0, \\ \partial_R U^2\left(\frac{1}{2}, \theta, z\right) = 0. \end{cases}$$

We deduce that the solution to this equation has the form $U^2(R, \theta, z) = \varphi_0^2(\theta, z)$. Then, we employ (A.13) and we obtain the following problem for φ_0^1

$$\begin{cases} \partial_z^2 \varphi_0^1(\theta, z) + \frac{1}{r_0^2} \partial_\theta^2 \varphi_0^1(\theta, z) = 0 & (\theta, z) \in [0, 2\pi) \times (0, z_0), \\ \varphi_0^1(0, \theta) = 0, \\ \varphi_0^1(z_0, \theta) = 0. \end{cases}$$

We conclude that $\varphi_0^1(\theta, z) = 0$ and thus, $U^1(R, \theta, z) = 0$. Finally, employing (1.68) we write the problem satisfied outside the layer by u^1 as two uncoupled problems

$$\begin{cases} \Delta u_{\text{int}}^1 = 0 & \text{in } \Omega_{\text{int}}^\varepsilon, \\ u_{\text{int}}^1 = 0 & \text{on } \partial\Omega_{\text{int}}^\varepsilon. \end{cases} \quad (\text{A.16})$$

$$\begin{cases} \Delta u_{\text{ext}}^1 = 0 & \text{in } \Omega_{\text{ext}}^\varepsilon, \\ u_{\text{ext}}^1 = 0 & \text{on } \partial\Omega_{\text{ext}}^\varepsilon. \end{cases}$$

We deduce that $u^1 \equiv 0$.

Terms of order two

We consider Problem (A.12) for U^3

$$\begin{cases} \partial_R^2 U^3(R, \theta, z) = 0 & R \in \left(-\frac{1}{2}, \frac{1}{2}\right), \\ \partial_R U^3\left(-\frac{1}{2}, \theta, z\right) = 0, \\ \partial_R U^3\left(\frac{1}{2}, \theta, z\right) = 0. \end{cases}$$

We deduce that the solution to this equation has the form $U^3(R, \theta, z) = \varphi_0^3(\theta, z)$. Then, we employ (A.13) and φ_0^2 satisfies

$$\begin{cases} \partial_z^2 \varphi_0^2(\theta, z) + \frac{1}{r_0^2} \partial_\theta^2 \varphi_0^2(\theta, z) = -\frac{1}{\bar{\sigma}_0} [\sigma \partial_r u^0]_{\Gamma^\varepsilon}(\theta, z) & (\theta, z) \in [0, 2\pi) \times (0, z_0), \\ \varphi_0^2(\theta, 0) = 0, \\ \varphi_0^2(\theta, z_0) = 0. \end{cases} \quad (\text{A.17})$$

Solving this problem we obtain the function $\varphi_0^2(\theta, z)$ and thus, the complete expression of $U^2(R, \theta, z)$. Finally, employing (A.14) we write the problem satisfied by u^2 outside the layer as two uncoupled problems

$$\begin{cases} \Delta u_{\text{int}}^2 = 0 & \text{in } \Omega_{\text{int}}^\varepsilon, \\ u_{\text{int}}^2\left(r_0 - \frac{\varepsilon}{2}, \theta, z\right) = \varphi_0^2(\theta, z), \\ u_{\text{int}}^2 = 0 & \text{on } \partial\Omega \cap \partial\Omega_{\text{int}}^\varepsilon. \end{cases} \quad (\text{A.18})$$

$$\begin{cases} \Delta u_{\text{ext}}^2 = 0 & \text{in } \Omega_{\text{ext}}^\varepsilon, \\ u_{\text{ext}}^2\left(r_0 + \frac{\varepsilon}{2}, \theta, z\right) = \varphi_0^2(\theta, z), \\ u_{\text{ext}}^2 = 0 & \text{on } \partial\Omega \cap \partial\Omega_{\text{ext}}^\varepsilon. \end{cases}$$

Terms of order three

We consider Problem (A.12) for U^4

$$\begin{cases} \partial_R^2 U^4(R, \theta, z) = -\partial_z^2 U^2(\theta, z) - \frac{1}{r_0^2} \partial_\theta^2 \varphi_0^2(\theta, z) & R \in \left(\frac{-1}{2}, \frac{1}{2}\right), \\ \widehat{\sigma}_0 \partial_R U^4\left(-\frac{1}{2}, \theta, z\right) = \sigma_{\text{int}} \partial_n u_{\text{int}}^0\left(r_0 - \frac{\varepsilon}{2}, \theta, z\right), \\ \widehat{\sigma}_0 \partial_R U^4\left(\frac{1}{2}, \theta, z\right) = \sigma_{\text{ext}} \partial_n u_{\text{ext}}^0\left(r_0 + \frac{\varepsilon}{2}, \theta, z\right). \end{cases}$$

We deduce that the solution to this equation has the form

$$U^4(R, \theta, z) = \frac{1}{\widehat{\sigma}_0} [\sigma \partial_n u^0]_{\Gamma^\varepsilon}(\theta, z) \frac{R^2}{2} + \frac{1}{\widehat{\sigma}_0} \{\sigma \partial_n u^0\}_{\Gamma^\varepsilon}(\theta, z) R + \varphi_0^4(\theta, z).$$

Then, we employ (A.13) and we build the following problem for φ_0^3

$$\begin{cases} \partial_z^2 \varphi_0^3(\theta, z) + \frac{1}{r_0^2} \partial_\theta^2 \varphi_0^3(\theta, z) = -\frac{1}{\widehat{\sigma}_0 r_0} \{\sigma \partial_n u^0\}_{\Gamma^\varepsilon}(\theta, z) & (\theta, z) \in [0, 2\pi) \times (0, z_0), \\ \varphi_0^3(\theta, 0) = 0, \\ \varphi_0^3(\theta, z_0) = 0. \end{cases} \quad (\text{A.19})$$

Solving this problem we obtain the function $\varphi_0^3(\theta, z)$, and thus, the complete expression of $U^2(R, \theta, z)$. Finally, employing (A.14) we write the problem satisfied outside the layer by u^3 as two uncoupled problems

$$\begin{cases} \Delta u_{\text{int}}^3 = 0 & \text{in } \Omega_{\text{int}}^\varepsilon, \\ u_{\text{int}}^3\left(r_0 - \frac{\varepsilon}{2}, \theta, z\right) = U^3\left(-\frac{1}{2}, \theta, z\right), \\ u_{\text{int}}^3 = 0 & \text{on } \partial\Omega \cap \partial\Omega_{\text{int}}^\varepsilon. \end{cases} \quad (\text{A.20})$$

$$\begin{cases} \Delta u_{\text{ext}}^3 = 0 & \text{in } \Omega_{\text{ext}}^\varepsilon, \\ u_{\text{ext}}^3\left(r_0 + \frac{\varepsilon}{2}, \theta, z\right) = U^3\left(\frac{1}{2}, \theta, z\right), \\ u_{\text{ext}}^3 = 0 & \text{on } \partial\Omega \cap \partial\Omega_{\text{ext}}^\varepsilon. \end{cases}$$

Recapitulation of the asymptotic expansion

Proposition 14. *The asymptotic expansion (A.6), has the following form*

$$\left\{ \begin{array}{l} u_{int}(r, \theta, z) = u_{int}^0(r, \theta, z) + \varepsilon^2 u_{int}^2(r, \theta, z) + \varepsilon^3 u_{int}^3(r, \theta, z) + O(\varepsilon^4) \quad \text{in } \Omega_{int}^\varepsilon, \\ u_{ext}(r, \theta, z) = u_{ext}^0(r, \theta, z) + \varepsilon^2 u_{ext}^2(r, \theta, z) + \varepsilon^3 u_{ext}^3(r, \theta, z) + O(\varepsilon^4) \quad \text{in } \Omega_{ext}^\varepsilon, \\ U(R, \theta, z) = \varepsilon^2 \varphi_0^2(\theta, z) + \varepsilon^3 \varphi_0^3(\theta, z) + O(\varepsilon^4) \quad \text{in } \left(-\frac{1}{2}, \frac{1}{2}\right) \\ \qquad \qquad \qquad \qquad \qquad \qquad \qquad \qquad \qquad \qquad \qquad \qquad \qquad \qquad \qquad \times [0, 2\pi) \times (0, z_0), \end{array} \right.$$

where functions u^0 , u^2 , u^3 , φ_0^2 , and φ_0^3 are defined by Equations (A.15), (A.18), (A.20), (A.17), and (A.19) respectively. For $k \in \mathbb{N}$, the solution U^k to Equation (A.12) has the following form

$$U^k(R, z) = \begin{cases} 0 & \text{if } k = 0, 1, \\ \varphi_0^k(\theta, z) & \text{if } k = 2, 3, \\ \sum_{j=0}^{k-2} \varphi_j^k(\theta, z) R^j & \text{if } k \geq 4, \end{cases}$$

Proof. We conduct the proof by induction on k . For $k = 0, 1, 2, 3$, we have already calculated the expressions of u^k and U^k in the previous section. Now let us assume that for any number $i \in \mathbb{N}$, such that $i < k$, function U^i has the form

$$U^i(R, \theta, z) = \varphi_{i-2}^i(\theta, z) R^{i-2} + \varphi_{i-3}^i(\theta, z) R^{i-3} + \dots + \varphi_1^i(\theta, z) R + \varphi_0^i(\theta, z),$$

We begin by considering Problem (A.12) for U^k . Solving this problem we obtain a solution of the form

$$U^k(R, \theta, z) = \varphi_{k-2}^k(\theta, z) R^{k-2} + \varphi_{k-3}^k(\theta, z) R^{k-3} + \dots + \varphi_1^k(\theta, z) R + \varphi_0^k(\theta, z),$$

In the above expression of U^k we find function V^k , defined as

$$V^k(R, \theta, z) = \varphi_{k-2}^k(\theta, z) R^{k-2} + \varphi_{k-3}^k(\theta, z) R^{k-3} + \dots + \varphi_1^k(\theta, z) R$$

at the first step of the algorithm.

□

A.2.3 First class of ITCs: equivalent models

Now that we know the expressions for the first terms of the expansion, we truncate the series and we identify a simpler problem satisfied by

$$u^{(k)} = u^0 + \varepsilon u^1 + \dots + \varepsilon^k u^k \quad \text{in} \quad \Omega_{\text{int}}^\varepsilon \cup \Omega_{\text{ext}}^\varepsilon$$

up to a residual term of order ε^{k+1} . We neglect the residual term of order ε^{k+1} to obtain an approximate model satisfied by function $u^{[k]}$. We formally derive three approximate models of second, third, and fourth order respectively.

Second-order model

For deriving the model of order two, we truncate the series from the second term and we define $u^{(1)}$ as

$$u^{(1)} = u^0 + \varepsilon u^1 = u^0 \quad \text{in} \quad \Omega_{\text{int}}^\varepsilon \cup \Omega_{\text{ext}}^\varepsilon \quad (\text{see Proposition 3}).$$

From (A.15), we deduce that $u^{(1)}$ solves the following uncoupled problem

$$\begin{cases} \sigma_{\text{int}} \Delta u_{\text{int}}^{(1)} = f_{\text{int}} & \text{in} \quad \Omega_{\text{int}}^\varepsilon, \\ u_{\text{int}}^{(1)} = 0 & \text{on} \quad \partial\Omega_{\text{int}}^\varepsilon. \end{cases} \quad (\text{A.21})$$

$$\begin{cases} \sigma_{\text{ext}} \Delta u_{\text{ext}}^{(1)} = f_{\text{ext}} & \text{in} \quad \Omega_{\text{ext}}^\varepsilon, \\ u_{\text{ext}}^{(1)} = 0 & \text{on} \quad \partial\Omega_{\text{ext}}^\varepsilon. \end{cases}$$

In this case, we have $u^{[1]} = u^{(1)}$ as $u^{(1)}$ does not depend on ε . We infer a second-order model satisfied by $u^{[1]}$ solution to Problem (A.21).

Third-Order model

For deriving the model of order three, we truncate the series from the third term and we define $u^{(2)}$ as

$$u^{(2)} = u^0 + \varepsilon u^1 + \varepsilon^2 u^2 = u^0 + \varepsilon^2 u^2 \quad \text{in} \quad \Omega_{\text{int}}^\varepsilon \cup \Omega_{\text{ext}}^\varepsilon \quad (\text{see Proposition 3}).$$

From (A.15), (A.16), and (A.18) we deduce that $u^{(2)}$ satisfies the following equations

$$\left\{ \begin{array}{ll} \sigma_{\text{int}} \Delta u_{\text{int}}^{(2)} = f_{\text{int}} & \text{in } \Omega_{\text{int}}^{\varepsilon}, \\ \sigma_{\text{ext}} \Delta u_{\text{ext}}^{(2)} = f_{\text{ext}} & \text{in } \Omega_{\text{ext}}^{\varepsilon}, \\ [u^{(2)}]_{\Gamma^{\varepsilon}} = 0, \\ \Delta_{\Gamma} \{u^{(2)}\}_{\Gamma^{\varepsilon}} = -\varepsilon^2 \frac{1}{\widehat{\sigma}_0} [\sigma \partial_n u^0]_{\Gamma^{\varepsilon}} \\ u^{(2)} = 0 & \text{on } \partial\Omega \cap \partial\Omega^{\varepsilon}. \end{array} \right.$$

where $\Delta_{\Gamma} = \partial_z^2 + \frac{1}{r_0^2} \partial_{\theta}^2$. Following the same procedure as in Section 1.3.2, we obtain the following third-order asymptotic model for $u^{[2]}$

$$\left\{ \begin{array}{ll} \sigma_{\text{int}} \Delta u_{\text{int}}^{[2]} = f_{\text{int}} & \text{in } \Omega_{\text{int}}^{\varepsilon}, \\ \sigma_{\text{ext}} \Delta u_{\text{ext}}^{[2]} = f_{\text{ext}} & \text{in } \Omega_{\text{ext}}^{\varepsilon}, \\ [u^{[2]}]_{\Gamma^{\varepsilon}} = 0, \\ \Delta_{\Gamma} \{u^{[2]}\}_{\Gamma^{\varepsilon}} = -\varepsilon^2 \frac{1}{\widehat{\sigma}_0} [\sigma \partial_n u^{[2]}]_{\Gamma^{\varepsilon}} \\ u^{[2]} = 0 & \text{on } \partial\Omega \cap \partial\Omega^{\varepsilon}. \end{array} \right. \quad (\text{A.22})$$

Fourth-order model

For deriving the model of order four, we truncate the series from the fourth term and we define $u^{(3)}$ as

$$u^{(3)} = u^0 + \varepsilon u^1 + \varepsilon^2 u^2 + \varepsilon^3 u^3 = u^0 + \varepsilon^2 u^2 + \varepsilon^3 u^3 \quad \text{in } \Omega_{\text{int}}^{\varepsilon} \cup \Omega_{\text{ext}}^{\varepsilon} \quad (\text{see Proposition 3}).$$

From (A.15), (A.16), (A.18), and (A.20), we deduce that $u^{(3)}$ satisfies the following equations

$$\left\{ \begin{array}{ll} \sigma_{\text{int}} \Delta u_{\text{int}}^{(3)} = f_{\text{int}} & \text{in } \Omega_{\text{int}}^{\varepsilon}, \\ \sigma_{\text{ext}} \Delta u_{\text{ext}}^{(3)} = f_{\text{ext}} & \text{in } \Omega_{\text{ext}}^{\varepsilon}, \\ [u^{(3)}]_{\Gamma^{\varepsilon}} = 0, \\ \Delta_{\Gamma} \{u^{(3)}\}_{\Gamma^{\varepsilon}} = g, \\ u^{(3)} = 0 & \text{on } \partial\Omega \cap \partial\Omega^{\varepsilon}, \end{array} \right.$$

where

$$g = -\varepsilon^2 \frac{1}{\hat{\sigma}_0} [\sigma \partial_n u^0]_{\Gamma^\varepsilon} - \varepsilon^3 \frac{1}{\hat{\sigma}_0} [\sigma \partial_n u^1]_{\Gamma^\varepsilon} - \varepsilon^3 \frac{1}{\hat{\sigma}_0 r_0} \{ \sigma \partial_n u^0 \}_{\Gamma^\varepsilon}.$$

Following the same procedure as in Section 1.3.2 we obtain the following fourth-order asymptotic model for $u^{[3]}$

$$\left\{ \begin{array}{ll} \sigma_{\text{int}} \Delta u_{\text{int}}^{[3]} = f_{\text{int}} & \text{in } \Omega_{\text{int}}^\varepsilon, \\ \sigma_{\text{ext}} \Delta u_{\text{ext}}^{[3]} = f_{\text{ext}} & \text{in } \Omega_{\text{ext}}^\varepsilon, \\ [u^{[3]}]_{\Gamma^\varepsilon} = 0, & \\ \Delta_\Gamma \{u^{[3]}\}_{\Gamma^\varepsilon} = -\frac{\varepsilon^2}{\hat{\sigma}_0} [\sigma \partial_n u^{[3]}]_{\Gamma^\varepsilon} - \frac{\varepsilon^3}{\hat{\sigma}_0 r_0} \{ \sigma \partial_n u^{[3]} \}_{\Gamma^\varepsilon}, & \\ u^{[3]} = 0 & \text{on } \partial\Omega \cap \partial\Omega^\varepsilon. \end{array} \right. \quad (\text{A.23})$$

A.2.4 Second class of ITCs: equivalent models

In this section we show the asymptotic models we obtain when we write the asymptotic conditions across the interface Γ . We expand the solution in power series of ε . Then, by truncating this series and neglecting higher order terms in ε , we derive approximate models coupled with equivalent transmission conditions across interface Γ . Since we use the same procedure as in the previous sections, we will concentrate on presenting the obtained results, regarding the multiscale expansion and the derivation of the asymptotic models. The domain where the approximate models are defined is depicted at Figure A.2.

Here, we formally derive two approximate models of order one and order two respectively.

First-order model

$$\left\{ \begin{array}{ll} \sigma_{\text{int}} \Delta u_{\text{int}}^{[0]} = f_{\text{int}} & \text{in } \Omega_{\text{int}}, \\ u_{\text{int}}^{[0]} = 0 & \text{on } \partial\Omega_{\text{int}}. \end{array} \right. \quad (\text{A.24})$$

$$\left\{ \begin{array}{ll} \sigma_{\text{ext}} \Delta u_{\text{ext}}^{[0]} = f_{\text{ext}} & \text{in } \Omega_{\text{ext}}, \\ u_{\text{ext}}^{[0]} = 0 & \text{on } \partial\Omega_{\text{ext}}. \end{array} \right.$$

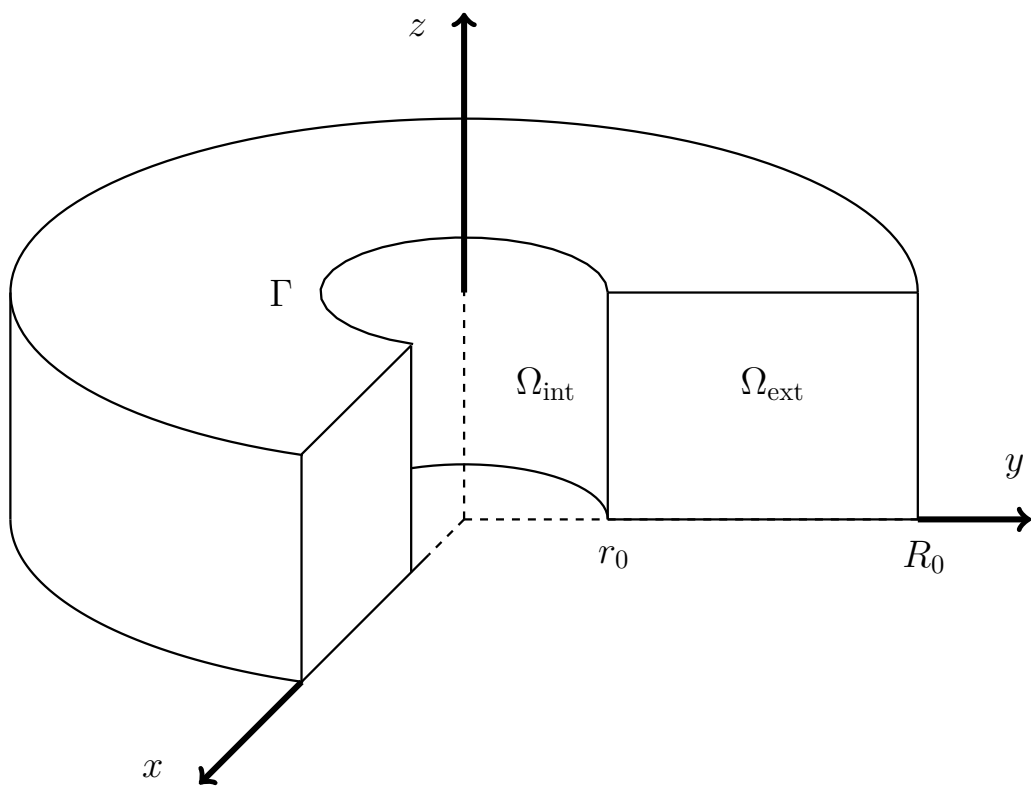


Figure A.2: Sectioned domain for the asymptotic models of the second class.

Second-order model

$$\left\{ \begin{array}{ll} \sigma_{\text{int}} \Delta u_{\text{int}}^{[1]} = f_{\text{int}} & \text{in } \Omega_{\text{int}}, \\ u_{\text{int}}^{[1]} = \frac{\varepsilon}{2} \partial_n u_{\text{int}}^{[1]} & \text{on } \Gamma, \\ u_{\text{int}}^{[1]} = 0 & \text{on } \partial\Omega \cap \partial\Omega_{\text{int}}. \end{array} \right. \quad (\text{A.25})$$

$$\left\{ \begin{array}{ll} \sigma_{\text{ext}} \Delta u_{\text{ext}}^{[1]} = f_{\text{ext}} & \text{in } \Omega_{\text{ext}}, \\ u_{\text{ext}}^{[1]} = -\frac{\varepsilon}{2} \partial_n u_{\text{ext}}^{[1]} & \text{on } \Gamma, \\ u_{\text{ext}}^{[1]} = 0 & \text{on } \partial\Omega \cap \partial\Omega_{\text{ext}}. \end{array} \right.$$

A.3 Variational formulations for the time-harmonic problem

In this section we focus on presenting the resulting variational formulation for the different models we have considered.

A.3.1 Reference model

We write the variational formulation of Problem (1.45). Assuming $f \in L^2(\Omega_{\text{int}})$, we look for $u \in H_0^1(\Omega)$, such that for all $w \in H_0^1(\Omega)$

$$\begin{aligned} & (\sigma_{\text{int}} - i\epsilon_0\omega) \int_{\Omega_{\text{int}}^\varepsilon} \nabla u \cdot \nabla \bar{w} \, dx + (\sigma_{\text{ext}} - i\epsilon_0\omega) \int_{\Omega_{\text{ext}}^\varepsilon} \nabla u \cdot \nabla \bar{w} \, dx \\ & + (\hat{\sigma}_0 \varepsilon^{-3} - i\epsilon_0\omega) \int_{\Omega_{\text{lay}}^\varepsilon} \nabla u \cdot \nabla \bar{w} \, dx = - \int_{\Omega_{\text{int}}^\varepsilon} f_{\text{int}} \bar{w} \, dx - \int_{\Omega_{\text{ext}}^\varepsilon} f_{\text{ext}} \bar{w} \, dx. \end{aligned}$$

A.3.2 First class of ITCs

Second-order model

Here we deal with the variational formulation for the second-order asymptotic model we have derived in Section 1.5.3. Problem (1.49) is uncoupled into two

independent problems, therefore we write two variational formulations, one for each problem. Assuming $f_{\text{int}} \in L^2(\Omega_{\text{int}}^\varepsilon)$ and $f_{\text{ext}} \in L^2(\Omega_{\text{ext}}^\varepsilon)$, the variational formulations consist in finding $u_{\text{int}} \in H_0^1(\Omega_{\text{int}}^\varepsilon)$, such that for all $w_{\text{int}} \in H_0^1(\Omega_{\text{int}}^\varepsilon)$

$$-\int_{\Omega_{\text{int}}^\varepsilon} f_{\text{int}} \bar{w}_{\text{int}} \, dx = \int_{\Omega_{\text{int}}^\varepsilon} (\sigma_{\text{int}} - i\varepsilon_0 \omega) \nabla u_{\text{int}} \cdot \nabla \bar{w}_{\text{int}} \, dx,$$

and finding $u_{\text{ext}} \in H_0^1(\Omega_{\text{ext}}^\varepsilon)$ such that for all $w_{\text{ext}} \in H_0^1(\Omega_{\text{ext}}^\varepsilon)$

$$-\int_{\Omega_{\text{ext}}^\varepsilon} f_{\text{ext}} \bar{w}_{\text{ext}} \, dx = \int_{\Omega_{\text{ext}}^\varepsilon} (\sigma_{\text{ext}} - i\varepsilon_0 \omega) \nabla u_{\text{ext}} \cdot \nabla \bar{w}_{\text{ext}} \, dx.$$

Fourth-order model

The fourth-order asymptotic model (1.50) has been derived in Section 1.5.3. The corresponding functional space V_4 has been defined in Definition 6. Assuming $f_{\text{int}} \in L^2(\Omega_{\text{int}}^\varepsilon)$ and $f_{\text{ext}} \in L^2(\Omega_{\text{ext}}^\varepsilon)$, the variational problem reduces to finding $u \in V_4$, such that for all $w \in V_4$,

$$\begin{aligned} & (\sigma_{\text{int}} - i\varepsilon_0 \omega) \int_{\Omega_{\text{int}}^\varepsilon} \nabla u \cdot \nabla \bar{w} \, dx + (\sigma_{\text{int}} - i\varepsilon_0 \omega) \int_{\Omega_{\text{ext}}^\varepsilon} \nabla u \cdot \nabla \bar{w} \, dx \\ & + \widehat{\sigma}_0 \varepsilon^{-2} \int_{\Gamma^\varepsilon} \nabla_{\Gamma^\varepsilon} \{u\}_{\Gamma^\varepsilon} \nabla_{\Gamma^\varepsilon} \{\bar{w}\}_{\Gamma^\varepsilon} \, ds = - \int_{\Omega_{\text{int}}^\varepsilon} f_{\text{int}} \bar{w} \, dx - \int_{\Omega_{\text{ext}}^\varepsilon} f_{\text{ext}} \bar{w} \, dx. \end{aligned}$$

A.3.3 Second class of ITCs

First-order model

Here we write a variational formulation for the first-order asymptotic model (1.54) we have derived in Section 1.5.5. Problem (1.54) is uncoupled into two independent problems, which explain why we have two variational formulations, one for each problem. Assuming $f_{\text{int}} \in L^2(\Omega_{\text{int}})$ and $f_{\text{ext}} \in L^2(\Omega_{\text{ext}})$, the variational formulations of these problems consist in finding $u_{\text{int}} \in H_0^1(\Omega_{\text{int}})$ such that for all $w_{\text{int}} \in H_0^1(\Omega_{\text{int}})$

$$-\int_{\Omega_{\text{int}}} f_{\text{int}} \bar{w}_{\text{int}} \, dx = \int_{\Omega_{\text{int}}} (\sigma_{\text{int}} - i\varepsilon_0 \omega) \nabla u_{\text{int}} \cdot \nabla \bar{w}_{\text{int}} \, dx,$$

and finding $u_{\text{ext}} \in H_0^1(\Omega_{\text{ext}})$ such that for all $w_{\text{ext}} \in H_0^1(\Omega_{\text{ext}})$

$$-\int_{\Omega_{\text{ext}}} f_{\text{ext}} \bar{w}_{\text{ext}} \, dx = \int_{\Omega_{\text{ext}}} (\sigma_{\text{ext}} - i\epsilon_0\omega) \nabla u_{\text{ext}} \cdot \nabla \bar{w}_{\text{ext}} \, dx.$$

Second-order Model

In this section we introduce a variational formulation for the second-order asymptotic model (1.55) we have derived in Section 1.5.5. Again, Problem (1.55) is uncoupled into two independent problems, thus, we derive two variational formulations, one for each problem. The spaces V_{int} and V_{ext} are the functional spaces, which have been defined in (3.27). Assuming $f_{\text{int}} \in L^2(\Omega_{\text{int}})$ and $f_{\text{ext}} \in L^2(\Omega_{\text{ext}})$, the variational formulations reduce to looking for $u_{\text{int}} \in V_{\text{int}}$, such that for all $w_{\text{int}} \in V_{\text{int}}$

$$\begin{aligned} -\int_{\Omega_{\text{int}}} f_{\text{int}} \bar{w}_{\text{int}} \, dx &= \int_{\Omega_{\text{int}}} (\sigma_{\text{int}} - i\epsilon_0\omega) \nabla u_{\text{int}} \cdot \nabla \bar{w}_{\text{int}} \, dx \\ &\quad - \int_{\Gamma} \frac{2(\sigma_{\text{int}} - i\epsilon_0\omega)}{\varepsilon} u_{\text{int}} \bar{w}_{\text{int}} \, ds, \end{aligned}$$

and looking for $u_{\text{ext}} \in V_{\text{ext}}$, such that for all $w_{\text{ext}} \in V_{\text{ext}}$

$$\begin{aligned} -\int_{\Omega_{\text{ext}}} f_{\text{ext}} \bar{w}_{\text{ext}} \, dx &= \int_{\Omega_{\text{ext}}} (\sigma_{\text{ext}} - i\epsilon_0\omega) \nabla u_{\text{ext}} \cdot \nabla \bar{w}_{\text{ext}} \, dx \\ &\quad - \int_{\Gamma} \frac{2(\sigma_{\text{ext}} - i\epsilon_0\omega)}{\varepsilon} u_{\text{ext}} \bar{w}_{\text{ext}} \, ds. \end{aligned}$$

A.4 Variational formulations for the problem in the 3D axisymmetric configuration

A.4.1 Reference model

In this section we derive the variational formulation for the reference model (1.57). This is used when doing the performance assessment with our finite element method. We begin by introducing the functional framework.

Definition 11. For $\alpha \in \mathbb{R}$, space $L^2_\alpha(\Omega)$ is defined as

$$L^2_\alpha(\Omega) = \left\{ v \text{ measurable} : \|v\|_{L^2_\alpha(\Omega)} < \infty \right\},$$

where

$$\|v\|_{L^2_\alpha(\Omega)} = \int_{\Omega} |v|^2 r^\alpha \, dr \, dz.$$

Definition 12. For $m \in \mathbb{N}$, the spaces $H_1^m(\Omega)$ and $V_{1,0}^1$ are defined as

$$H_1^m(\Omega) = \left\{ v \in L_1^2(\Omega) \mid \partial_r^l \partial_z^{m-l} v \in L_1^2(\Omega), l \in [0, m] \right\},$$

$$V_{1,0}^m(\Omega) = \left\{ v \in H_1^m(\Omega) \mid v = 0 \text{ on } \partial\Omega - \Gamma_0 \right\}.$$

We select $V_{1,0}^1(\Omega)$ as the suitable functional space. We assume that $f_{\text{int}} \in L_1^2(\Omega_{\text{int}}^\varepsilon)$ and $f_{\text{ext}} \in L_1^2(\Omega_{\text{ext}}^\varepsilon)$, and we select a test function $w \in V_{1,0}^1(\Omega)$. We multiply the equations in $\Omega_{\text{int}}^\varepsilon$, $\Omega_{\text{ext}}^\varepsilon$ and $\Omega_{\text{lay}}^\varepsilon$ with this test function and we integrate over the domain. Then, we integrate by parts and we apply the transmission and boundary conditions. We obtain the following variational formulation, find $u \in V_{1,0}^1(\Omega)$ such that for all $w \in V_{1,0}^1(\Omega)$,

$$\begin{aligned} & - \int_{\Omega_{\text{int}}^\varepsilon} f_{\text{int}} w r \, dr \, dz - \int_{\Omega_{\text{ext}}^\varepsilon} f_{\text{ext}} w r \, dr \, dz = \int_{\Omega_{\text{int}}^\varepsilon} \sigma_{\text{int}} \partial_r u_{\text{int}} \partial_r w r \, dr \, dz \\ & + \int_{\Omega_{\text{ext}}^\varepsilon} \sigma_{\text{ext}} \partial_r u_{\text{ext}} \partial_r w r \, dr \, dz + \int_{\Omega_{\text{lay}}^\varepsilon} \hat{\sigma}_0 \varepsilon^{-3} \partial_r u_{\text{lay}} \partial_r w r \, dr \, dz \\ & + \int_{\Omega_{\text{int}}^\varepsilon} \sigma_{\text{int}} \partial_z u_{\text{int}} \partial_z w r \, dr \, dz + \int_{\Omega_{\text{ext}}^\varepsilon} \sigma_{\text{ext}} \partial_z u_{\text{ext}} \partial_z w r \, dr \, dz \\ & + \int_{\Omega_{\text{lay}}^\varepsilon} \hat{\sigma}_0 \varepsilon^{-3} \partial_z u_{\text{lay}} \partial_z w r \, dr \, dz. \end{aligned}$$

A.4.2 First class of ITCs

Second-order model

This section is devoted to the derivation of a variational formulation for the second-order asymptotic model we have derived in Section 1.6.3. Problem (1.75) is uncoupled into two independent problems, therefore, we write two variational formulations, one for each problem. We introduce functional spaces $V_{1,0}^1(\Omega_{\text{int}}^\varepsilon)$ and $V_{1,0}^1(\Omega_{\text{ext}}^\varepsilon)$ as the functional framework.

We select the test functions $w_{\text{int}} \in V_{1,0}^1(\Omega_{\text{int}}^\varepsilon)$ and $w_{\text{ext}} \in V_{1,0}^1(\Omega_{\text{ext}}^\varepsilon)$, we multiply the equations in $\Omega_{\text{int}}^\varepsilon$ and $\Omega_{\text{ext}}^\varepsilon$ in Problem (1.75) with these test functions and we integrate over the domains. Then, we integrate by parts and we apply the boundary conditions. Assuming $f_{\text{int}} \in L_1^2(\Omega_{\text{int}}^\varepsilon)$ and $f_{\text{ext}} \in L_1^2(\Omega_{\text{ext}}^\varepsilon)$, we obtain the following variational formulations, find $u_{\text{int}} \in V_{1,0}^1(\Omega_{\text{int}}^\varepsilon)$, such that for all $w_{\text{int}} \in V_{1,0}^1(\Omega_{\text{int}}^\varepsilon)$

$$- \int_{\Omega_{\text{int}}^\varepsilon} f_{\text{int}} w_{\text{int}} r \, dr \, dz = \int_{\Omega_{\text{int}}^\varepsilon} \sigma_{\text{int}} \partial_r u_{\text{int}} \partial_r w_{\text{int}} r \, dr \, dz + \int_{\Omega_{\text{int}}^\varepsilon} \sigma_{\text{int}} \partial_z u_{\text{int}} \partial_z w_{\text{int}} r \, dr \, dz.$$

and find $u_{\text{ext}} \in V_{1,0}^1(\Omega_{\text{ext}}^\varepsilon)$, such that for all $w_{\text{ext}} \in V_{1,0}^1(\Omega_{\text{ext}}^\varepsilon)$

$$- \int_{\Omega_{\text{ext}}^\varepsilon} f_{\text{ext}} w_{\text{ext}} r \, dr \, dz = \int_{\Omega_{\text{ext}}^\varepsilon} \sigma_{\text{ext}} \partial_r u_{\text{ext}} \partial_r w_{\text{ext}} r \, dr \, dz + \int_{\Omega_{\text{ext}}^\varepsilon} \sigma_{\text{ext}} \partial_z u_{\text{ext}} \partial_z w_{\text{ext}} r \, dr \, dz.$$

Fourth-order model

In this section we derive a variational formulation for the fourth-order asymptotic model we have derived in Section 1.6.3. We remark the problem is governed by Equations (1.77), which define the problem. Using V_4 as the functional space of the problem, and defined by

Definition 13. We define the Hilbert functional space V_4 in the following way

$$V_4 = \left\{ w : w_{\text{int}} \in H_1^1(\Omega_{\text{int}}^\varepsilon), w_{\text{ext}} \in H_1^1(\Omega_{\text{ext}}^\varepsilon), \frac{d}{dz} \{w\} \in L^2(\Gamma^\varepsilon), \right. \\ \left. w|_{\Gamma_{\text{int}}^\varepsilon} = w|_{\Gamma_{\text{ext}}^\varepsilon}, w|_{\partial\Omega \cap \partial\Omega_{\text{int}}^\varepsilon} = 0, w|_{\partial\Omega \cap \partial\Omega_{\text{ext}}^\varepsilon} = 0 \right\}$$

provided with the norm

$$\|w\|_{V_4} = \left(\|w\|_{H_1^1(\Omega^\varepsilon)}^2 + \left\| \frac{d}{dz} \{w\} \right\|_{0,\Gamma^\varepsilon}^2 \right)^{\frac{1}{2}}.$$

We obtain the variational formulation

$$- \int_{\Omega_{\text{int}}^\varepsilon} f_{\text{int}} w r \, dr \, dz - \int_{\Omega_{\text{ext}}^\varepsilon} f_{\text{ext}} w r \, dr \, dz = \int_{\Omega_{\text{int}}^\varepsilon} \sigma_{\text{int}} \partial_r u_{\text{int}} \partial_r w r \, dr \, dz \\ + \int_{\Omega_{\text{ext}}^\varepsilon} \sigma_{\text{ext}} \partial_r u_{\text{ext}} \partial_r w r \, dr \, dz + \int_{\Omega_{\text{int}}^\varepsilon} \sigma_{\text{int}} \partial_z u_{\text{int}} \partial_z w r \, dr \, dz \\ + \int_{\Omega_{\text{ext}}^\varepsilon} \sigma_{\text{ext}} \partial_z u_{\text{ext}} \partial_z w r \, dr \, dz - \int_{\partial\Omega_{\text{int}}^\varepsilon} \sigma_{\text{int}} \partial_n u_{\text{int}} w \, ds - \int_{\partial\Omega_{\text{ext}}^\varepsilon} \sigma_{\text{ext}} \partial_n u_{\text{ext}} w \, ds.$$

We rewrite the traces of u_{int} and u_{ext} employing the jump and mean value expressions, whose definitions have been set in Definition 1.

$$\begin{cases} \sigma_{\text{int}} \partial_n u_{\text{int}} \left(x_0 - \frac{\varepsilon}{2}, y \right) = \{\sigma \partial_n u\}_{\Gamma^\varepsilon}(y) - \frac{1}{2} [\sigma \partial_n u]_{\Gamma^\varepsilon}(y), \\ \sigma_{\text{ext}} \partial_n u_{\text{ext}} \left(x_0 + \frac{\varepsilon}{2}, y \right) = \{\sigma \partial_n u\}_{\Gamma^\varepsilon}(y) + \frac{1}{2} [\sigma \partial_n u]_{\Gamma^\varepsilon}(y). \end{cases}$$

We also take into account that

$$\begin{cases} r = x_0 - \frac{\varepsilon}{2} & \text{in } \Gamma_{\text{int}}^\varepsilon, \\ r = x_0 + \frac{\varepsilon}{2} & \text{in } \Gamma_{\text{ext}}^\varepsilon. \end{cases}$$

Substituting these expressions in the previous equation, we derive an identity as follows

$$\begin{aligned} & - \int_{\Omega_{\text{int}}^\varepsilon} f_{\text{int}} w r \, dr \, dz - \int_{\Omega_{\text{ext}}^\varepsilon} f_{\text{ext}} w r \, dr \, dz = \int_{\Omega_{\text{int}}^\varepsilon} \sigma_{\text{int}} \partial_r u_{\text{int}} \partial_r w r \, dr \, dz \\ & + \int_{\Omega_{\text{ext}}^\varepsilon} \sigma_{\text{ext}} \partial_r u_{\text{ext}} \partial_r w r \, dr \, dz + \int_{\Omega_{\text{int}}^\varepsilon} \sigma_{\text{int}} \partial_z u_{\text{int}} \partial_z w r \, dr \, dz \\ & + \int_{\Omega_{\text{ext}}^\varepsilon} \sigma_{\text{ext}} \partial_z u_{\text{ext}} \partial_z w r \, dr \, dz - \int_{\partial\Omega \cap \partial\Omega_{\text{int}}^\varepsilon} \sigma_{\text{int}} \partial_n u_{\text{int}} w \, ds \\ & - \int_{\partial\Omega \cap \partial\Omega_{\text{ext}}^\varepsilon} \sigma_{\text{ext}} \partial_n u_{\text{ext}} w \, ds + \int_{\Gamma^\varepsilon} x_0 \{ \sigma \partial_n u \}_{\Gamma^\varepsilon} [w]_{\Gamma^\varepsilon} \, ds \\ & + \int_{\Gamma^\varepsilon} \varepsilon \{ \sigma \partial_n u \}_{\Gamma^\varepsilon} \{ w \}_{\Gamma^\varepsilon} \, ds - \int_{\Gamma^\varepsilon} x_0 [\sigma \partial_n u]_{\Gamma^\varepsilon} \{ w \}_{\Gamma^\varepsilon} \, ds \\ & - \int_{\Gamma^\varepsilon} \frac{\varepsilon}{4} [\sigma \partial_n u]_{\Gamma^\varepsilon} [w]_{\Gamma^\varepsilon} \, ds. \end{aligned} \tag{A.26}$$

Taking into account the properties of the test functions, we directly deduce the variational formulation for Problem (1.77) from Equation (A.26). Assuming $f_{\text{int}} \in L_1^2(\Omega_{\text{int}}^\varepsilon)$ and $f_{\text{ext}} \in L_1^2(\Omega_{\text{ext}}^\varepsilon)$, it reduces to finding $u \in V_4$ such that for all $w \in V_4$

$$\begin{aligned} & - \int_{\Omega_{\text{int}}^\varepsilon} f_{\text{int}} w r \, dr \, dz - \int_{\Omega_{\text{ext}}^\varepsilon} f_{\text{ext}} w r \, dr \, dz = \int_{\Omega_{\text{int}}^\varepsilon} \sigma_{\text{int}} \partial_r u_{\text{int}} \partial_r w r \, dr \, dz \\ & + \int_{\Omega_{\text{ext}}^\varepsilon} \sigma_{\text{ext}} \partial_r u_{\text{ext}} \partial_r w r \, dr \, dz + \int_{\Omega_{\text{int}}^\varepsilon} \sigma_{\text{int}} \partial_z u_{\text{int}} \partial_z w r \, dr \, dz \\ & + \int_{\Omega_{\text{ext}}^\varepsilon} \sigma_{\text{ext}} \partial_z u_{\text{ext}} \partial_z w r \, dr \, dz + \int_{\Gamma^\varepsilon} \hat{\sigma}_0 x_0 \varepsilon^{-2} \frac{d}{dz} \{u\} \frac{d}{dz} \{w\} \, ds. \end{aligned} \tag{A.27}$$

A.4.3 Second class of ITCs

First-order model

This section is devoted to the derivation of a variational formulation for the first-order asymptotic model we have derived in Section 1.6.5. Problem (1.84) is uncoupled into two independent problems, therefore, we write two variational formulations, one for each problem. We define first functional spaces $V_{1,0}^1(\Omega_{\text{int}})$ and $V_{1,0}^1(\Omega_{\text{ext}})$ which are well-suited for the analysis of the problem.

We select the test functions $w_{\text{int}} \in V_{1,0}^1(\Omega_{\text{int}})$ and $w_{\text{ext}} \in V_{1,0}^1(\Omega_{\text{ext}})$, we multiply the equations in Ω_{int} and Ω_{ext} in Problem (1.75) with these test functions and we integrate over the domains. Then, we integrate by parts and we apply the boundary conditions. Assuming $f_{\text{int}} \in L^2(\Omega_{\text{int}})$ and $f_{\text{ext}} \in L^2(\Omega_{\text{ext}})$, we obtain the following variational formulations, find $u_{\text{int}} \in V_{1,0}^1(\Omega_{\text{int}})$, such that for all $w_{\text{int}} \in V_{1,0}^1(\Omega_{\text{int}})$

$$-\int_{\Omega_{\text{int}}} f_{\text{int}} w_{\text{int}} r \, dr \, dz = \int_{\Omega_{\text{int}}} \sigma_{\text{int}} \partial_r u_{\text{int}} \partial_r w_{\text{int}} r \, dr \, dz + \int_{\Omega_{\text{int}}} \sigma_{\text{int}} \partial_z u_{\text{int}} \partial_z w_{\text{int}} r \, dr \, dz,$$

and find $u_{\text{ext}} \in V_{1,0}^1(\Omega_{\text{ext}})$, such that for all $w_{\text{ext}} \in V_{1,0}^1(\Omega_{\text{ext}})$,

$$-\int_{\Omega_{\text{ext}}} f_{\text{ext}} w_{\text{ext}} r \, dr \, dz = \int_{\Omega_{\text{ext}}} \sigma_{\text{ext}} \partial_r u_{\text{ext}} \partial_r w_{\text{ext}} r \, dr \, dz + \int_{\Omega_{\text{ext}}} \sigma_{\text{ext}} \partial_z u_{\text{ext}} \partial_z w_{\text{ext}} r \, dr \, dz.$$

Second-order model

In this section we derive a variational formulation for the fourth-order asymptotic model we have derived in Section 1.6.5. The Equations governing the problem are given at (1.85).

We introduce functional spaces V_{int} and V_{ext} as the functional framework, which are defined as follows

$$V_{\text{int}} = \left\{ w \in H_1^1(\Omega_{\text{int}}) : w|_{\partial\Omega \cap \partial\Omega_{\text{int}}} = 0 \right\},$$

$$V_{\text{ext}} = \left\{ w \in H_1^1(\Omega_{\text{ext}}) : w|_{\partial\Omega \cap \partial\Omega_{\text{ext}}} = 0 \right\}.$$

We select as test functions $w_{\text{int}} \in V_{\text{int}}$ and $w_{\text{ext}} \in V_{\text{ext}}$, and we multiply the equations in Ω_{int} and Ω_{ext} in Problem (1.85) with these test functions. Integrating by parts over the domain of interest we obtain the variational formulation for both uncoupled problems (1.85). Assuming $f_{\text{int}} \in L^2(\Omega_{\text{int}})$ and $f_{\text{ext}} \in L^2(\Omega_{\text{ext}})$,

the variational formulations consist in looking for $u_{\text{int}} \in V_{\text{int}}$, such that for all $w_{\text{int}} \in V_{\text{int}}$

$$\begin{aligned} - \int_{\Omega_{\text{int}}} f_{\text{int}} w_{\text{int}} r \, dr \, dz &= \int_{\Omega_{\text{int}}} \sigma_{\text{int}} \partial_r u_{\text{int}} \partial_r w_{\text{int}} r \, dr \, dz + \int_{\Omega_{\text{int}}} \sigma_{\text{int}} \partial_z u_{\text{int}} \partial_z w_{\text{int}} r \, dr \, dz \\ &\quad - \int_{\Gamma} \frac{2\sigma_{\text{int}}}{\varepsilon} u_{\text{int}} w_{\text{int}} \, ds. \end{aligned}$$

and looking for $u_{\text{ext}} \in V_{\text{ext}}$, such that for all $w_{\text{ext}} \in V_{\text{ext}}$

$$\begin{aligned} - \int_{\Omega_{\text{ext}}} f_{\text{ext}} w_{\text{ext}} r \, dr \, dz &= \int_{\Omega_{\text{ext}}} \sigma_{\text{ext}} \partial_r u_{\text{ext}} \partial_r w_{\text{ext}} r \, dr \, dz + \int_{\Omega_{\text{ext}}} \sigma_{\text{ext}} \partial_z u_{\text{ext}} \partial_z w_{\text{ext}} r \, dr \, dz \\ &\quad - \int_{\Gamma} \frac{2\sigma_{\text{ext}}}{\varepsilon} u_{\text{ext}} w_{\text{ext}} \, ds. \end{aligned}$$

A.5 Numerical results for 3D Electromagnetism

A.5.1 Introduction

In this section we show some steps towards an extension of the techniques employed in this document to a 3D electromagnetic problem. We consider a thin layer problem in the framework of a borehole shaped domain with a thin casing of uniform thickness and the objective is to derive equivalent transmission conditions for replacing this thin layer. The equations that govern Electromagnetism are the Maxwell's equations. This is a set of four equations that explain the behaviour of the electric and magnetic fields. The first of these equations is Gauss' Law, which explain how the Electric field behaves under the influence of electric charges. Gauss' Law is written as follows,

$$\operatorname{div} E = \frac{\rho}{\epsilon_0}, \quad (\text{A.28})$$

where E represents the electric field, ρ represents the electric charge density, and ϵ_0 represents the permittivity of the medium we are measuring the field at. The second equation corresponds to the Gauss' Law for the Magnetic Field. This equation explains the behaviour of the magnetic field H and is written as follows,

$$\operatorname{div} H = 0. \quad (\text{A.29})$$

The third equation is called Faraday's Law and it shows that the magnetic and electric fields are in fact related to each other,

$$\operatorname{curl} E = -\mu \frac{\partial H}{\partial t}, \quad (\text{A.30})$$

where μ represents the permeability. Finally, the last equation that compose Maxwell's equation is Ampere's Law, which is expressed as

$$\text{curl } H = \epsilon_0 \frac{\partial E}{\partial t} + \sigma E + j, \quad (\text{A.31})$$

where σ represents the conductivity and j represents the free current densities. These two last laws show how a varying electric field produces a magnetic field and also how a varying magnetic field produces an electric field. Putting all these equations together we obtain the time-domain Maxwell equations.

$$\left\{ \begin{array}{l} \text{div } E = \frac{\rho}{\epsilon_0}, \\ \text{div } H = 0, \\ \text{curl } E = -\mu \frac{\partial H}{\partial t}, \\ \text{curl } H = \epsilon_0 \frac{\partial E}{\partial t} + \sigma E + j. \end{array} \right. \quad (\text{A.32})$$

In this text, we are interested in the time-harmonic Maxwell equations, which eliminate the time derive ∂_t by introducing the frequency ω . Time-harmonic Maxwell equations can be written as follows

$$\left\{ \begin{array}{l} \text{div } E = \frac{\rho}{\epsilon_0}, \\ \text{div } H = 0, \\ \text{curl } E = \mu i \omega H, \\ \text{curl } H = -\epsilon_0 i \omega E + \sigma E + j. \end{array} \right. \quad (\text{A.33})$$

Employing these equations, we obtain a second-order equation where only the electric field appears. Taking the curl in both sides of time-harmonic Faraday's Law and substituting it in the time-harmonic Ampere's Law, we obtain the following differential equation for the electric field

$$\text{curl curl } E - k^2 E = i \omega \mu j \quad (\text{A.34})$$

where k is the wave number defined as $k^2 = \mu \omega^2 \left(\epsilon_0 + \frac{\sigma}{\omega} i \right)$, $\text{Im}(k) \geq 0$.

A.5.2 Model problem

Let $\Omega \subset \mathbb{R}^3$ be the domain of interest described in Figure A.3. This domain is a cylinder shaped domain which is composed of three subdomains $\Omega_{\text{int}}^\varepsilon$, $\Omega_{\text{ext}}^\varepsilon$, and $\Omega_{\text{lay}}^\varepsilon$. In particular, the subdomain $\Omega_{\text{lay}}^\varepsilon$ is a thin layer of uniform thickness $\varepsilon > 0$. We denote by $\Gamma_{\text{int}}^\varepsilon$ the interface between $\Omega_{\text{int}}^\varepsilon$ and $\Omega_{\text{lay}}^\varepsilon$, and as $\Gamma_{\text{ext}}^\varepsilon$ the interface between $\Omega_{\text{ext}}^\varepsilon$ and $\Omega_{\text{lay}}^\varepsilon$. In this domain, we study the equation for the electric field (A.34) we presented in the introduction.

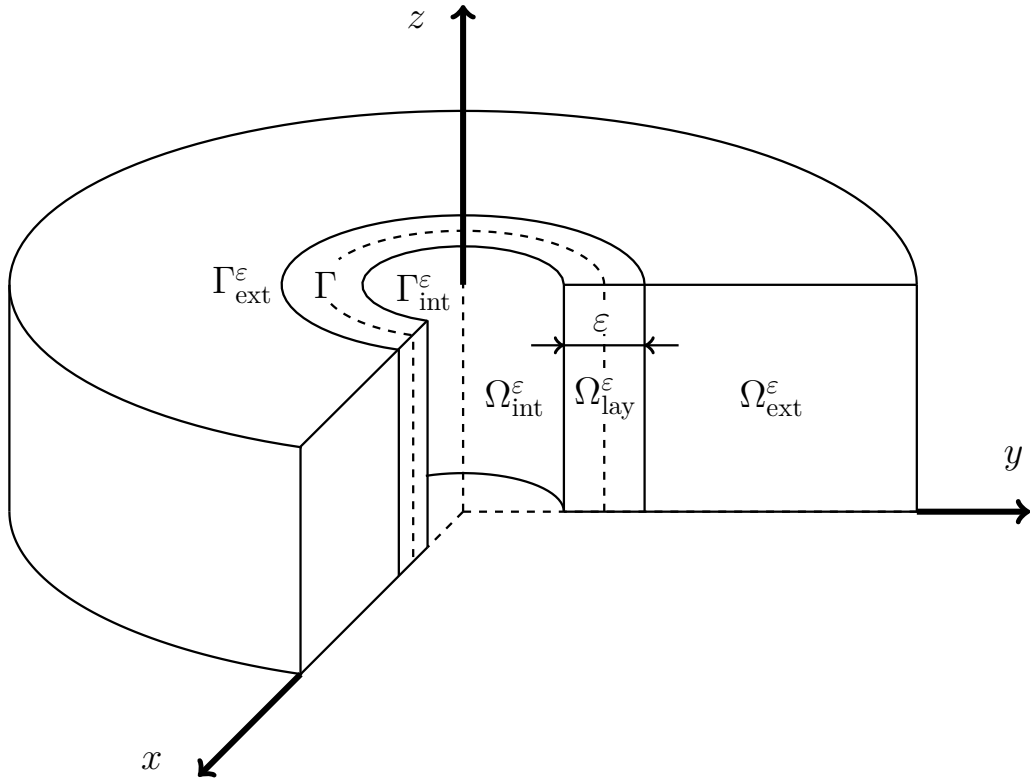


Figure A.3: Sectioned three dimensional domain.

Here, E represents the electric field, k is the wave number, ω stands for the frequency, μ is the permeability, and j represents the free current densities. Like in the previous chapters, the conductivity, involved in the expression of the wave number, is a piecewise constant function, which takes a different value inside each subdomain, and in particular, inside the casing, it depends on ε

$$\sigma = \begin{cases} \sigma_{\text{int}} & \text{in } \Omega_{\text{int}}^\varepsilon, \\ \sigma_{\text{lay}} = \hat{\sigma}_0 \varepsilon^{-3} & \text{in } \Omega_{\text{lay}}^\varepsilon, \\ \sigma_{\text{ext}} & \text{in } \Omega_{\text{ext}}^\varepsilon, \end{cases}$$

where $\hat{\sigma}_0 > 0$ is a given constant. The rest of the physical parameters are also constant piecewise functions, which take different values inside each of the subdomains, we denote them as follows

$$k = \begin{cases} k_{\text{int}} & \text{in } \Omega_{\text{int}}^\varepsilon, \\ k_{\text{lay},\varepsilon} & \text{in } \Omega_{\text{lay}}^\varepsilon, \\ k_{\text{ext}} & \text{in } \Omega_{\text{ext}}^\varepsilon, \end{cases} \quad \mu = \begin{cases} \mu_{\text{int}} & \text{in } \Omega_{\text{int}}^\varepsilon, \\ \mu_{\text{lay}} & \text{in } \Omega_{\text{lay}}^\varepsilon, \\ \mu_{\text{ext}} & \text{in } \Omega_{\text{ext}}^\varepsilon, \end{cases} \quad j = \begin{cases} j_{\text{int}} & \text{in } \Omega_{\text{int}}^\varepsilon, \\ j_{\text{lay}} & \text{in } \Omega_{\text{lay}}^\varepsilon, \\ j_{\text{ext}} & \text{in } \Omega_{\text{ext}}^\varepsilon. \end{cases}$$

We remark that as the wave number depends on the conductivity, and this last one depends on ε inside the casing, the wave number also depends on ε inside the casing. To express this fact we have denoted as $k_{\text{lay},\varepsilon}$ the wave number inside the casing. We denote the electric field in the following way for each subdomain

$$E = \begin{cases} E_{\text{int}} & \text{in } \Omega_{\text{int}}^\varepsilon, \\ E_{\text{lay}} & \text{in } \Omega_{\text{lay}}^\varepsilon, \\ E_{\text{ext}} & \text{in } \Omega_{\text{ext}}^\varepsilon. \end{cases}$$

Employing these notations, we rewrite Equation (A.34) inside each subdomain so that the resulting problem can be written as follows

$$\left\{ \begin{array}{ll} \text{curl curl } E_{\text{int}} - k_{\text{int}}^2 E_{\text{int}} = i\omega\mu_{\text{int}}j_{\text{int}} & \text{in } \Omega_{\text{int}}^\varepsilon, \\ \text{curl curl } E_{\text{lay}} - k_{\text{lay},\varepsilon}^2 E_{\text{lay}} = i\omega\mu_{\text{lay}}j_{\text{lay}} & \text{in } \Omega_{\text{lay}}^\varepsilon, \\ \text{curl curl } E_{\text{ext}} - k_{\text{ext}}^2 E_{\text{ext}} = i\omega\mu_{\text{ext}}j_{\text{ext}} & \text{in } \Omega_{\text{ext}}^\varepsilon, \\ E_{\text{int}} \times n = E_{\text{lay}} \times n & \text{on } \Gamma_{\text{int}}^\varepsilon, \\ E_{\text{ext}} \times n = E_{\text{lay}} \times n & \text{on } \Gamma_{\text{ext}}^\varepsilon, \\ \frac{1}{\mu_{\text{int}}}\text{curl } E_{\text{int}} \times n = \frac{1}{\mu_{\text{lay}}}\text{curl } E_{\text{lay}} \times n & \text{on } \Gamma_{\text{int}}^\varepsilon, \\ \frac{1}{\mu_{\text{ext}}}\text{curl } E_{\text{ext}} \times n = \frac{1}{\mu_{\text{lay}}}\text{curl } E_{\text{lay}} \times n & \text{on } \Gamma_{\text{ext}}^\varepsilon, \\ E \times n = 0 & \text{on } \partial\Omega. \end{array} \right. \quad (\text{A.35})$$

where n represents the normal vector exterior to $\Omega_{\text{int}}^\varepsilon$ on $\Gamma_{\text{int}}^\varepsilon$ and interior to $\Omega_{\text{ext}}^\varepsilon$ on $\Gamma_{\text{ext}}^\varepsilon$. We will consider these equations to be written in cylindrical coordinates (r, θ, z) because it is much more suitable for the shape of the domain we are dealing with. Thus, the expression of the curl operator in this equations is the following

$$\text{curl } E = \left(\frac{1}{r}\partial_\theta E_z - \partial_z E_\theta \right) \hat{r} + \left(\partial_z E_r - \partial_r E_z \right) \hat{\theta} + \left(\frac{1}{r}E_\theta + \partial_r E_\theta - \frac{1}{r}\partial_\theta E_r \right) \hat{z}.$$

A.5.3 Approximate model

Following the same path employed in the previous chapters it is natural to consider the following limit problems as approximate models for Problem (A.35)

$$\begin{cases} \operatorname{curl} \operatorname{curl} E_{\text{int}} - k_{\text{int}}^2 E_{\text{int}} = i\omega\mu_{\text{int}}j_{\text{int}} & \text{in } \Omega_{\text{int}}^\varepsilon, \\ E_{\text{int}} \times n = 0 & \text{on } \partial\Omega_{\text{int}}^\varepsilon, \end{cases} \quad (\text{A.36})$$

$$\begin{cases} \operatorname{curl} \operatorname{curl} E_{\text{ext}} - k_{\text{ext}}^2 E_{\text{ext}} = i\omega\mu_{\text{ext}}j_{\text{ext}} & \text{in } \Omega_{\text{ext}}^\varepsilon, \\ E_{\text{ext}} \times n = 0 & \text{on } \partial\Omega_{\text{ext}}^\varepsilon. \end{cases}$$

The order of convergence of this model is not yet established, and in the following section we perform a numerical study of its performance.

A.5.4 Numerical results

Here we present some numerical tests regarding model Problem (A.35) and approximate model (A.36). domain Ω employed for these simulations is the following cylinder

$$\Omega = \{(r, \theta, z) : 0 \leq r < 1, 0 \leq \theta < 2\pi, -1 < z < 1\},$$

which is composed of the following subdomains

$$\Omega_{\text{int}}^\varepsilon = \left\{ (r, \theta, z) : 0 \leq r < r_0 - \frac{\varepsilon}{2}, 0 \leq \theta < 2\pi, -1 < z < 1 \right\},$$

$$\Omega_{\text{lay}}^\varepsilon = \left\{ (r, \theta, z) : r_0 - \frac{\varepsilon}{2} < r < r_0 + \frac{\varepsilon}{2}, 0 \leq \theta < 2\pi, -1 < z < 1 \right\},$$

$$\Omega_{\text{ext}}^\varepsilon = \left\{ (r, \theta, z) : r_0 + \frac{\varepsilon}{2} < r < 1, 0 \leq \theta < 2\pi, -1 < z < 1 \right\},$$

where $r_0 = 0.35$. We consider a toroidal source term in the form of a Gaussian function of the following form

$$j(x, y, z) = \begin{pmatrix} e^{-7(\sqrt{x^2+y^2}-0.2)^2} & 0 & 0 \end{pmatrix}.$$

Under this configuration and with these parameters we solve problems (A.35) and (A.36) by employing the Finite Element Code Montjoie developed by professor

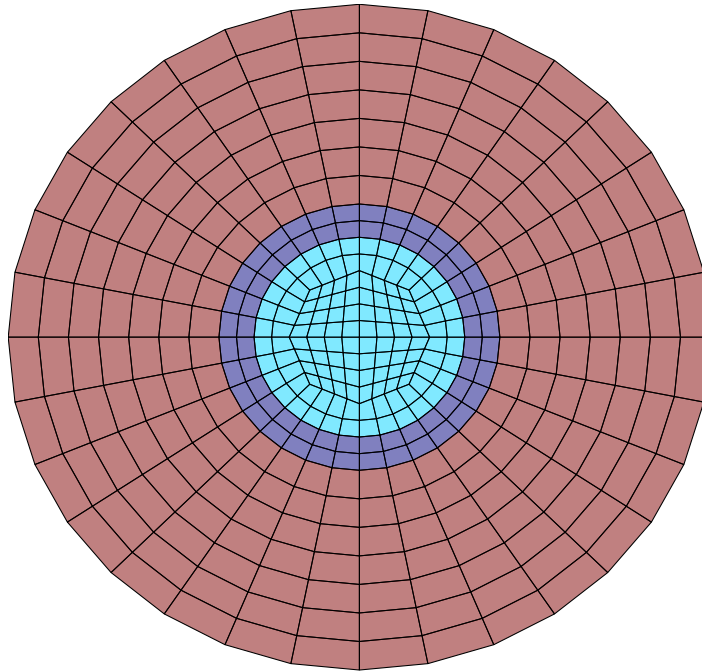


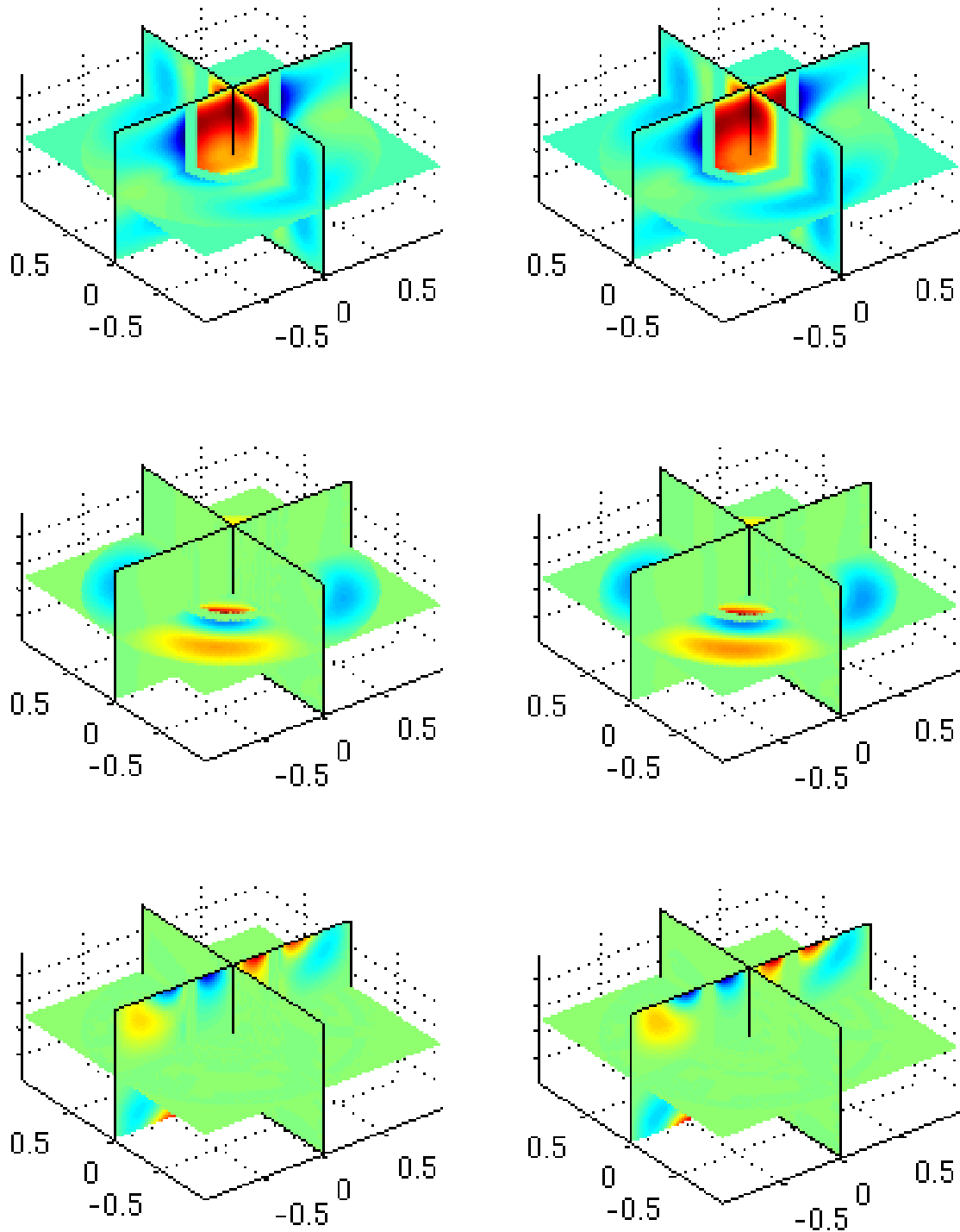
Figure A.4: Example of a mesh (x-y axis view) employed to solve Problem (A.35)

Marc Duruflé. For discretizing the domain, we use curved hexahedral shaped elements as illustrated in Figure A.4. We observe the numerical solution to problems (A.35) and (A.36) in Figure A.5.

Now we proceed to perform a more quantitative comparison of the models we have presented here. For that purpose, we calculate the L^2 error between these two models for different thicknesses of the thin layer, in order to observe a numerical order of convergence for the approximate model (A.36). The results are depicted in Figure A.6, from which we deduce that this model has a numerical convergence of order two.

A.6 Unified notation for Equivalent Conditions

The objective of this section is to introduce a unified notation for the different asymptotic models we have derived. In this way, it is easier to compare and observe the differences between these models. However, there are some drawbacks with this way of writing the models. For example, some of the derived models are uncoupled, whereas some are transmission problems, and with a unified notation this property is difficult to highlight, as all the models will be written as coupled problems.



(a) First, second, and third component of the solution to model Problem (A.35).

(b) First, second, and third component of the solution to approximate model (A.36).

Figure A.5: Solution for the model Problem (A.35) and the approximate model (A.36).

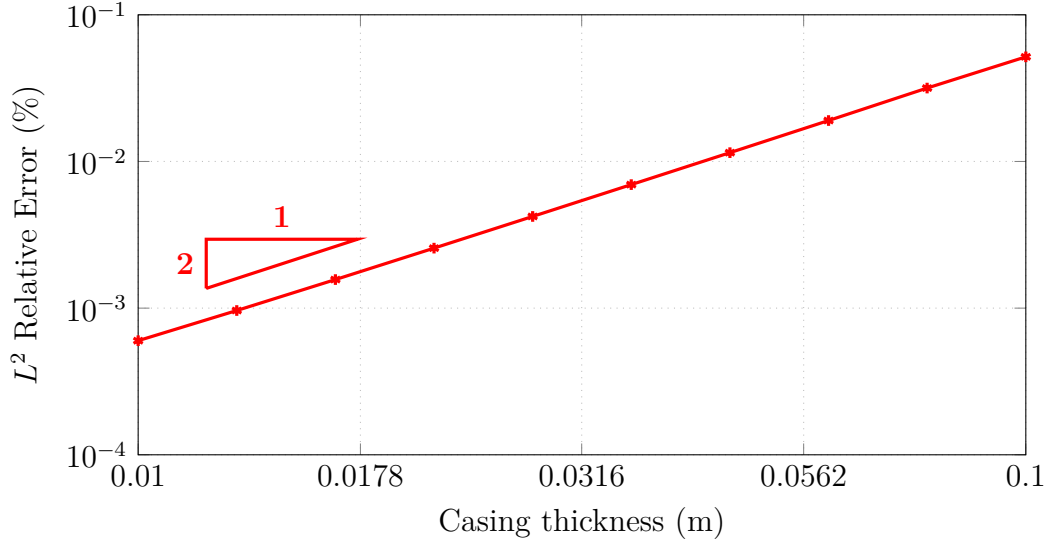


Figure A.6: L^2 relative error between problems (A.35) and (A.36) for different values of ε .

2D configuration

We begin by rewriting the asymptotic models of the first class in the following way

$$\begin{pmatrix} [u]_{\Gamma^\varepsilon} \\ \{u\}_{\Gamma^\varepsilon} \end{pmatrix} = \begin{pmatrix} 0 & 0 \\ 0 & m_{\varepsilon,k}^{2D} \end{pmatrix} \begin{pmatrix} \{\sigma \partial_n u\}_{\Gamma^\varepsilon} \\ [\sigma \partial_n u]_{\Gamma^\varepsilon} \end{pmatrix},$$

where the operator $m_{\varepsilon,k}^{2D}$ is defined as

Order two (first class)

$$m_{\varepsilon,1}^{2D} = 0,$$

Order four (first class)

$$m_{\varepsilon,3}^{2D} = -\frac{\varepsilon^2}{\widehat{\sigma}_0} \left(d_{\varepsilon,1}^{2D} \right)^{-1},$$

and

$$d_{\varepsilon,1}^{2D} = \Delta_\Gamma = \partial_y^2.$$

Before presenting the asymptotic conditions derived for the second class of problems, we introduce the following notation for the mean value and jump of the

conductivity in order to simplify the equations for these conditions.

$$\begin{cases} \{\bar{\sigma}\} = \frac{1}{2}(\sigma_{\text{ext}} + \sigma_{\text{int}}), \\ [\bar{\sigma}] = \sigma_{\text{ext}} - \sigma_{\text{int}}. \end{cases}$$

The asymptotic conditions derived for the second class of problems are summarized as follows

$$\begin{pmatrix} [u]_{\Gamma} \\ \{u\}_{\Gamma} \end{pmatrix} = E_{\varepsilon,k}^{2D} \begin{pmatrix} \{\sigma \partial_n u\}_{\Gamma} \\ [\sigma \partial_n u]_{\Gamma} \end{pmatrix},$$

where $E_{\varepsilon,k}^{2D}$ is defined as

Order one: (second class)

$$E_{\varepsilon,0}^{2D} = \begin{pmatrix} 0 & 0 \\ 0 & 0 \end{pmatrix},$$

Order two: (second class)

$$E_{\varepsilon,1}^{2D} = \begin{pmatrix} -\frac{\varepsilon \{\bar{\sigma}\}}{\sigma_{\text{int}} \sigma_{\text{ext}}} & \frac{\varepsilon [\bar{\sigma}]}{4\sigma_{\text{int}} \sigma_{\text{ext}}} \\ \frac{\varepsilon [\bar{\sigma}]}{4\sigma_{\text{int}} \sigma_{\text{ext}}} & -\frac{\varepsilon \{\bar{\sigma}\}}{4\sigma_{\text{int}} \sigma_{\text{ext}}} \end{pmatrix},$$

Order three: (second class)

$$E_{\varepsilon,2}^{2D} = \begin{pmatrix} -\frac{\varepsilon \{\bar{\sigma}\}}{\sigma_{\text{int}} \sigma_{\text{ext}}} (d_{\varepsilon,2}^{2D})^{-1} & \frac{\varepsilon [\bar{\sigma}]}{4\sigma_{\text{int}} \sigma_{\text{ext}}} (d_{\varepsilon,2}^{2D})^{-1} \\ \frac{\varepsilon [\bar{\sigma}]}{4\sigma_{\text{int}} \sigma_{\text{ext}}} (\partial_y^2 d_{\varepsilon,2}^{2D})^{-1} & \left(-\frac{\varepsilon^2}{\bar{\sigma}_0} - \frac{\varepsilon \{\bar{\sigma}\}}{4\sigma_{\text{int}} \sigma_{\text{ext}}} \right) (\partial_y^2 d_{\varepsilon,2}^{2D})^{-1} \end{pmatrix},$$

where $d_{\varepsilon,2}^{2D} = 1 - \frac{\varepsilon^2}{8} \partial_y^2$,

Order four: (second class)

$$E_{\varepsilon,3}^{2D} = \begin{pmatrix} (E_{\varepsilon,3}^{2D})_{1,1} & (E_{\varepsilon,3}^{2D})_{1,2} \\ (E_{\varepsilon,3}^{2D})_{2,1} & (E_{\varepsilon,3}^{2D})_{2,2} \end{pmatrix},$$

where

$$\left\{ \begin{array}{l} (E_{\varepsilon,3}^{2D})_{1,1} = \left(-\frac{\varepsilon \{\bar{\sigma}\}}{\sigma_{\text{int}}\sigma_{\text{ext}}} + \frac{\varepsilon^3 \{\bar{\sigma}\}}{24\sigma_{\text{int}}\sigma_{\text{ext}}} \partial_y^2 \right) (d_{\varepsilon,2}^{2D})^{-1}, \\ (E_{\varepsilon,3}^{2D})_{1,2} = \left(\frac{\varepsilon [\bar{\sigma}]}{4\sigma_{\text{int}}\sigma_{\text{ext}}} - \frac{\varepsilon^3 [\bar{\sigma}]}{96\sigma_{\text{int}}\sigma_{\text{ext}}} \partial_y^2 \right) (d_{\varepsilon,2}^{2D})^{-1}, \\ (E_{\varepsilon,3}^{2D})_{2,1} = \left(-\frac{\varepsilon^2}{\hat{\sigma}_0} - \frac{\varepsilon \{\bar{\sigma}\}}{4\sigma_{\text{int}}\sigma_{\text{ext}}} \partial_y^2 + \frac{\varepsilon^3 \{\bar{\sigma}\}}{96\sigma_{\text{int}}\sigma_{\text{ext}}} \partial_y^4 \right) (\partial_y^2 d_{\varepsilon,2}^{2D})^{-1}, \\ (E_{\varepsilon,3}^{2D})_{2,2} = \left(-\frac{\varepsilon^3}{\hat{\sigma}_0} + \frac{\varepsilon [\bar{\sigma}]}{4\sigma_{\text{int}}\sigma_{\text{ext}}} \partial_y^2 - \frac{\varepsilon^3 [\bar{\sigma}]}{96\sigma_{\text{int}}\sigma_{\text{ext}}} \partial_y^4 \right) \partial_y^4 (\partial_y^2 d_{\varepsilon,2}^{2D})^{-1}. \end{array} \right.$$

3D axisymmetric configuration

As we have done for the 2D case, we rewrite the models derived for the 3D axisymmetric configuration employing a unified notation. The asymptotic conditions we have derived for the first class of problems can be summarized in the following way

$$\begin{pmatrix} [u]_{\Gamma^\varepsilon} \\ \{u\}_{\Gamma^\varepsilon} \end{pmatrix} = M_{\varepsilon,k}^{3D} \begin{pmatrix} [\sigma \partial_n u]_{\Gamma^\varepsilon} \\ \{\sigma \partial_n u\}_{\Gamma^\varepsilon} \end{pmatrix},$$

where $M_{\varepsilon,k}^{3D}$ is defined as

Order two (first class)

$$M_{\varepsilon,1}^{3D} = \begin{pmatrix} 0 & 0 \\ 0 & 0 \end{pmatrix},$$

Order three (first class)

$$M_{\varepsilon,2}^{3D} = \begin{pmatrix} 0 & 0 \\ m_{\varepsilon,2}^{3D} & 0 \end{pmatrix},$$

where

$$m_{\varepsilon,2}^{3D} = -\frac{\varepsilon^2}{\widehat{\sigma}_0} \left(d_\varepsilon^{3D} \right)^{-1},$$

$$d_\varepsilon^{3D} = \Delta_\Gamma = \partial_z^2.$$

Order four (first class)

$$M_{\varepsilon,3}^{3D} = \begin{pmatrix} 0 & 0 \\ m_{\varepsilon,2}^{3D} & m_{\varepsilon,3}^{3D} \end{pmatrix},$$

where

$$m_{\varepsilon,3}^{3D} = -\frac{\varepsilon^3}{\widehat{\sigma}_0} \left(d_\varepsilon^{3D} \right)^{-1} = \varepsilon m_{\varepsilon,2}^{3D}$$

On the other hand, the asymptotic conditions derived for the second class of problems are summarized as follows

$$\begin{pmatrix} [u]_\Gamma \\ \{u\}_\Gamma \end{pmatrix} = E_{\varepsilon,k}^{3D} \begin{pmatrix} \{\sigma \partial_n u\}_\Gamma \\ [\sigma \partial_n u]_\Gamma \end{pmatrix},$$

where $E_{\varepsilon,k}^{3D}$ is defined as

Order one (second class)

$$E_{\varepsilon,0}^{3D} = \begin{pmatrix} 0 & 0 \\ 0 & 0 \end{pmatrix},$$

Order two (second class)

$$E_{\varepsilon,1}^{3D} = \begin{pmatrix} -\frac{\varepsilon \{\bar{\sigma}\}}{\sigma_{\text{int}} \sigma_{\text{ext}}} & \frac{\varepsilon [\bar{\sigma}]}{4\sigma_{\text{int}} \sigma_{\text{ext}}} \\ \frac{\varepsilon [\bar{\sigma}]}{4\sigma_{\text{int}} \sigma_{\text{ext}}} & -\frac{\varepsilon \{\bar{\sigma}\}}{4\sigma_{\text{int}} \sigma_{\text{ext}}} \end{pmatrix}.$$

A.7 Comparison with other models

Similar models to ours have been derived in the literature regarding 2D thin layer problems for the electric potential. In our approach, the conductivity inside the layer σ_{lay} depends on the thickness of the thin layer ε . If we consider a constant conductivity, without any dependence on ε , and applying the second approach, we obtain the following models. A first-order asymptotic model, composed of the following transmission conditions

$$\begin{cases} [u^{[0]}]_{\Gamma} = 0, \\ [\sigma \partial_n u^{[0]}]_{\Gamma} = 0. \end{cases}$$

We observe this model differs from model (1.54). A main difference comes from the fact that model (1.54) is uncoupled, whereas this model is coupled. Then, we obtain a second-order asymptotic model composed of the following transmission conditions

$$\begin{cases} [u^{[1]}]_{\Gamma} = \frac{\varepsilon}{\sigma_{\text{lay}}} \{ \sigma \partial_n u^{[1]} \}_{\Gamma} - \varepsilon \{ \partial_n u^{[1]} \}_{\Gamma}, \\ [\sigma \partial_n u^{[1]}]_{\Gamma} = -\varepsilon \sigma_{\text{lay}} \partial_y^2 \{ u^{[1]} \}_{\Gamma} - \varepsilon \{ \sigma \partial_n^2 u^{[1]} \}_{\Gamma} \end{cases}$$

Again we observe that this model differs from model (1.55), the main difference being that this model is coupled and model (1.55) is uncoupled. In this framework we can mention [7, 59], where this approach is considered for the 2D electric potential. These models are not directly comparable with the ones presented in this document because the authors consider a model composed of two subdomains, one of which is a thin layer, whereas in this document, we consider three subdomains. In [47], the author considers the Helmholtz equation

$$\operatorname{div} \left(\frac{1}{\mu} \nabla u \right) + qu = 0 \quad \text{in } \Omega,$$

where domain Ω , showed in Figure A.7, has the shape of a biological cell. This domain is composed of three subdomains, one of which is a thin layer of uniform thickness ε and is situated between the two other subdomains. This equation is directly comparable to ours by applying $q = 0$. The author derives equivalent conditions across the interface that separates the thin layer and the interior domain, which matches exactly none of the two approaches considered in this document, but is not far from the second class of problems we consider. Due to these similarities, even though the configuration and the considered approach are not exactly the

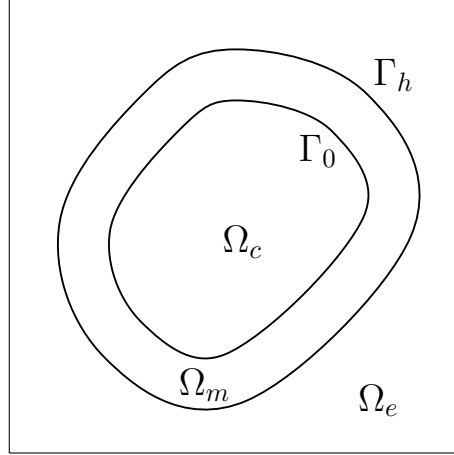


Figure A.7: Biological cell.

same, it is logical to compare these models with the ones we present in this work. One of the main differences with our work is that the thin layer is curved and it does not touch any boundary, whereas in our configuration, the thin layer is straight and it touches the boundary. Two models of first and third order are presented in [47], whose equivalent conditions can be summarized as follows. The first-order asymptotic transmission conditions write as

$$\begin{cases} [u^{[0]}]_{\Gamma_0} = 0, \\ [\sigma \partial_n u^{[0]}]_{\Gamma_0} = 0, \end{cases}$$

and the second-order asymptotic transmission conditions read as

$$\begin{cases} [u^{[1]}]_{\Gamma_0} = \varepsilon \frac{\mu_e - \mu_m}{\mu_c} \partial_n u_c^{[1]}|_{\Gamma_0}, \\ [\sigma \partial_n u^{[1]}]_{\Gamma_0} = \varepsilon \left(\frac{1}{\mu_m} - \frac{1}{\mu_e} \right) \partial_t^2 u_c^{[1]}|_{\Gamma_0}. \end{cases}$$

A.8 Asymptotic expansion in a geometry independent of ε

A.8.1 Introduction

In the first approach considered in Section 1.3, the elementary terms of the asymptotic expansion have a dependence on ε due to the geometry being dependent on

ε . This way, the estimates proved in Chapter 3 are not completely justified, even though the results have been validated numerically. This approach is not new in the literature, we can find for example the works [10, 12] which adopt the same approach.

In this section, we propose a more rigorous procedure for deriving a different asymptotic expansion than the one presented in Section 1.3. We perform a scaling in the thin layer, but we also apply a change of variables in the exterior and interior domains. This way, we transform these domains, which were dependent on ε , and we obtain a geometry independent of epsilon.

The section is structured as follows. Section A.8.1 presents the change of variable we perform as a first step towards deriving a multiscale expansion in terms of powers of ε for the solution to the model problem. Then, Section A.8.2 tackles the construction of the multiscale expansion. Here, we explicit the equations satisfied by the first terms of the expansion. Finally, in Section A.8.3, we compare the expansion developed in this section with the one obtained in Section 1.4.1.

Change of variables

We adopt the same configuration as in Section 1.2. Here, we propose to perform a different change of variables in each of the three subdomains that compose Ω . These changes of variables have the following form

$$\left\{ \begin{array}{ll} X_{\text{lay}} = \varepsilon^{-1} (x - x_0) & x \in \left(x_0 - \frac{\varepsilon}{2}, x_0 + \frac{\varepsilon}{2} \right), \\ X_{\text{int}} = \frac{x_0}{x_0 - \frac{\varepsilon}{2}} x & x \in \left(0, x_0 - \frac{\varepsilon}{2} \right), \\ X_{\text{ext}} = \frac{x_0 - L}{x_0 + \frac{\varepsilon}{2} - L} x + L \left(1 - \frac{x_0 - L}{x_0 + \frac{\varepsilon}{2} - L} \right) & x \in \left(x_0 + \frac{\varepsilon}{2}, L \right), \end{array} \right.$$

As a consequence, we have

$$\left\{ \begin{array}{l} \partial_x = \varepsilon^{-1} \partial_{X_{\text{lay}}}, \\ \partial_x = \frac{x_0}{x_0 - \frac{\varepsilon}{2}} \partial_{X_{\text{int}}}, \\ \partial_x = \frac{x_0 - L}{x_0 + \frac{\varepsilon}{2} - L} \partial_{X_{\text{ext}}}. \end{array} \right.$$

For $y \in (0, y_0)$, $X_{\text{lay}} \in \left(-\frac{1}{2}, \frac{1}{2}\right)$, $X_{\text{int}} \in (0, x_0)$, and $X_{\text{ext}} \in (x_0, L)$, we denote by U_{lay} , U_{int} and U_{ext} the functions that satisfy

$$\begin{cases} u_{\text{lay}}(x, y) = u_{\text{lay}}(x_0 + \varepsilon X_{\text{lay}}, y) = U_{\text{lay}}(X_{\text{lay}}, y), \\ u_{\text{int}}(x, y) = u_{\text{int}}\left(\frac{x_0 - \frac{\varepsilon}{2}}{x_0} X_{\text{int}}, y\right) = U_{\text{int}}(X_{\text{int}}, y), \\ u_{\text{ext}}(x, y) = u_{\text{ext}}\left(\left(X_{\text{ext}} - L \left(1 - \frac{x_0 - L}{x_0 + \frac{\varepsilon}{2} - L}\right)\right) \frac{x_0 + \frac{\varepsilon}{2} - L}{x_0 - L}, y\right) = U_{\text{ext}}(X_{\text{ext}}, y), \end{cases}$$

We define the domains Ω_{int} and Ω_{ext} as follows

$$\begin{cases} \Omega_{\text{int}} = \{(x, y) \in \mathbb{R}^2 : 0 < x < x_0, 0 < y < y_0\}, \\ \Omega_{\text{ext}} = \{(x, y) \in \mathbb{R}^2 : x_0 < x < L, 0 < y < y_0\}. \end{cases}$$

We rewrite System (1.2) with the newly defined variables and functions. Then, we expand the terms $\frac{x_0}{x_0 - \frac{\varepsilon}{2}}$ and $\frac{x_0 - L}{x_0 + \frac{\varepsilon}{2} - L}$ in powers of ε , and we perform a Taylor expansion of the right-hand sides f_{int} and f_{ext} . we obtain the following problem

$$\begin{cases} \sum_{k=0}^{\infty} \frac{k+1}{2^k x_0^k} \varepsilon^k \partial_{X_{\text{int}}}^2 U_{\text{int}} + \partial_y^2 U_{\text{int}} = \frac{1}{\sigma_{\text{int}}} \sum_{k=0}^{\infty} \frac{\varepsilon^k X_{\text{int}}^k}{k! (-2x_0)^k} \partial_{X_{\text{int}}}^k f_{\text{int}} & \text{in } \Omega_{\text{int}}, \\ \sum_{k=0}^{\infty} \frac{(k+1)(-1)^k}{2^k (x_0 - L)^k} \varepsilon^k \partial_{X_{\text{ext}}}^2 U_{\text{ext}} + \partial_y^2 U_{\text{ext}} = \frac{1}{\sigma_{\text{ext}}} \sum_{k=0}^{\infty} \frac{\varepsilon^k (X_{\text{ext}} - L)^k}{k! 2^k (x_0 - L)^k} \partial_{X_{\text{ext}}}^k f_{\text{ext}} & \text{in } \Omega_{\text{ext}}, \\ \varepsilon^{-2} \partial_{X_{\text{lay}}}^2 U_{\text{lay}} + \partial_y^2 U_{\text{lay}} = 0 & \left(-\frac{1}{2}, \frac{1}{2}\right) \times (0, y_0), \\ U_{\text{int}}(x_0, y) = U_{\text{lay}}\left(-\frac{1}{2}, y\right) & y \in (0, y_0), \\ U_{\text{ext}}(x_0, y) = U_{\text{lay}}\left(\frac{1}{2}, y\right) & y \in (0, y_0), \\ \sigma_{\text{int}} \sum_{k=0}^{\infty} \frac{1}{2^k x_0^k} \varepsilon^k \partial_{X_{\text{int}}} U_{\text{int}}(x_0, y) = \hat{\sigma}_0 \varepsilon^{-4} \partial_{X_{\text{lay}}} U\left(-\frac{1}{2}, y\right) & y \in (0, y_0), \\ \sigma_{\text{ext}} \sum_{k=0}^{\infty} \frac{(-1)^k}{2^k (x_0 - L)^k} \varepsilon^k \partial_{X_{\text{ext}}} U_{\text{ext}}(x_0, y) = \hat{\sigma}_0 \varepsilon^{-4} \partial_{X_{\text{lay}}} U_{\text{lay}}\left(\frac{1}{2}, y\right) & y \in (0, y_0). \\ U = 0 & \text{on } \partial\Omega. \end{cases} \quad (\text{A.37})$$

These functions represent the new unknowns of the problem.

A.8.2 Construction of a multiscale expansion

In the following, we asymptotically expand the solution in a power series of ε . We first perform an *Ansatz* in the form of power series expansion of ε for the solution to Problem (A.37), i.e. we look for solutions

$$\left\{ \begin{array}{l} U_{\text{int}}(X_{\text{int}}, y) \approx \sum_{k \geq 0} \varepsilon^k U_{\text{int}}^k(X_{\text{int}}, y) \quad \text{in } \Omega_{\text{int}}, \\ U_{\text{ext}}(X_{\text{ext}}, y) \approx \sum_{k \geq 0} \varepsilon^k U_{\text{ext}}^k(X_{\text{ext}}, y) \quad \text{in } \Omega_{\text{ext}}, \\ U_{\text{lay}}(X_{\text{lay}}, y) \approx \sum_{k \geq 0} \varepsilon^k U_{\text{lay}}^k(X_{\text{lay}}, y) \quad \text{in } \left(-\frac{1}{2}, \frac{1}{2}\right) \times (0, y_0). \end{array} \right. \quad (\text{A.38})$$

Equations for the coefficients of the electric potential

Substituting the previous Expressions (A.38), into the Equations (A.37) and collecting the terms with the same powers in ε , for every $k \in \mathbb{N}$ we obtain the following set of equations

$$\left\{ \begin{array}{l} \sum_{j=0}^k \frac{j+1}{2^k x_0^j} \partial_{X_{\text{int}}}^2 U_{\text{int}}^{k-j} + \partial_y^2 U_{\text{int}}^k = \frac{X_{\text{int}}^k \partial_{X_{\text{int}}}^k f_{\text{int}}}{\sigma_{\text{int}} k! (-2x_0)^k} \quad \text{in } \Omega_{\text{int}}, \\ \sum_{j=0}^k \frac{(j+1)(-1)^j}{2^j (x_0 - L)^j} \partial_{X_{\text{ext}}}^2 U_{\text{ext}}^{k-j} + \partial_y^2 U_{\text{ext}}^k = \frac{(X_{\text{ext}} - L)^k \partial_{X_{\text{ext}}}^k f_{\text{ext}}}{\sigma_{\text{ext}} k! 2^k (x_0 - L)^k} \quad \text{in } \Omega_{\text{ext}}, \\ \partial_{X_{\text{lay}}}^2 U_{\text{lay}}^k + \partial_y^2 U_{\text{lay}}^{k-2} = 0 \quad \left(-\frac{1}{2}, \frac{1}{2}\right) \times (0, y_0), \end{array} \right. \quad (\text{A.39a})$$

$$(\text{A.39b})$$

$$(\text{A.39c})$$

along with the following transmission conditions

$$\left\{ \begin{array}{ll} U_{\text{lay}}^k \left(-\frac{1}{2}, y \right) = U_{\text{int}}^k (x_0, y) & y \in (0, y_0), \\ U_{\text{lay}}^k \left(\frac{1}{2}, y \right) = U_{\text{ext}}^k (x_0, y) & y \in (0, y_0), \\ \partial_X U_{\text{lay}}^k \left(-\frac{1}{2}, y \right) = \frac{\sigma_{\text{int}}}{\widehat{\sigma}_0} \sum_{j=0}^{k-4} \frac{1}{2^j x_0^j} \partial_{X_{\text{int}}} U_{\text{int}}^{k-j} (x_0, y) & y \in (0, y_0), \\ \partial_X U_{\text{lay}}^k \left(\frac{1}{2}, y \right) = \frac{\sigma_{\text{ext}}}{\widehat{\sigma}_0} \sum_{j=0}^{k-4} \frac{(-1)^j}{2^j (x_0 - L)^j} \partial_{X_{\text{ext}}} U_{\text{ext}}^{k-j} (x_0, y) & y \in (0, y_0), \end{array} \right. \quad (\text{A.40a})$$

$$(\text{A.40b})$$

$$(\text{A.40c})$$

$$(\text{A.40d})$$

and the following boundary conditions

$$\left\{ \begin{array}{ll} U_{\text{int}}^k (0, y) = U_{\text{ext}}^k (L, y) = 0 & y \in (0, y_0), \quad (\text{A.41a}) \\ U_{\text{int}}^k (X_{\text{int}}, 0) = U_{\text{int}}^k (X_{\text{int}}, y_0) = 0 & X_{\text{int}} \in (0, x_0), \quad (\text{A.41b}) \\ U_{\text{ext}}^k (X_{\text{ext}}, 0) = U_{\text{ext}}^k (X_{\text{ext}}, y_0) = 0 & X_{\text{ext}} \in (x_0, L), \quad (\text{A.41c}) \\ U_{\text{lay}}^k (X_{\text{lay}}, 0) = U_{\text{lay}}^k (X_{\text{lay}}, y_0) = 0 & X_{\text{lay}} \in \left(-\frac{1}{2}, \frac{1}{2} \right), \quad (\text{A.41d}) \end{array} \right.$$

where δ_0^k represents the Kronecker symbol. For determining the elemental problem satisfied by each of the terms of the expansion, we will also need the following equation obtained by applying the fundamental theorem of calculus for a smooth

function U^k , along with equations (A.39c), (A.40c) and (A.40d)

$$\begin{aligned}
& - \int_{-\frac{1}{2}}^{\frac{1}{2}} \partial_y^2 U_{\text{lay}}^{k-2}(X_{\text{lay}}, y) \, dX_{\text{lay}} = \\
& \frac{1}{\widehat{\sigma}_0} \left(\sigma_{\text{ext}} \sum_{j=0}^{k-4} \frac{(-1)^j}{2^j (x_0 - L)^j} \partial_{X_{\text{ext}}} U_{\text{ext}}^{k-j-4}(x_0, y) - \sigma_{\text{int}} \sum_{j=0}^{k-4} \frac{1}{2^j x_0^j} \partial_{X_{\text{ext}}} U_{\text{int}}^{k-j-4}(x_0, y) \right).
\end{aligned} \tag{A.42}$$

We adopt the convention that the terms with negative indices in Equations (A.39) - (A.42) are equal to zero. Employing equations (A.39) - (A.42) we deduce the elementary problems satisfied outside and inside the layer for any $k \in \mathbb{N}$. For that purpose, we employ the following algorithm composed of three steps.

First terms of the asymptotics

Terms of order zero

We consider Problem (A.39c), along with conditions (A.40c) and (A.40d) for U^0

$$\left\{ \begin{array}{l} \partial_{X_{\text{lay}}}^2 U_{\text{lay}}^0(X_{\text{lay}}, y) = 0 \quad X_{\text{lay}} \in \left(-\frac{1}{2}, \frac{1}{2} \right), \\ \partial_{X_{\text{lay}}} U_{\text{lay}}^0 \left(-\frac{1}{2}, y \right) = 0, \\ \partial_{X_{\text{lay}}} U_{\text{lay}}^0 \left(\frac{1}{2}, y \right) = 0. \end{array} \right.$$

The solution to the above equation has the form $U_{\text{lay}}^0(X_{\text{lay}}, y) = \varphi_0^0(y)$. Then, we employ Equation (A.42) and Conditions (A.41d) to build the following problem for φ_0^0

$$\left\{ \begin{array}{l} \frac{d^2}{dy^2} \varphi_0^0(y) = 0 \quad y \in (0, y_0), \\ \varphi_0^0(0) = 0, \\ \varphi_0^0(y_0) = 0. \end{array} \right.$$

We deduce that $\varphi_0^0(y) = 0$ and thus, $U_{\text{lay}}^0(X_{\text{lay}}, y) = 0$. Finally, employing Equations (A.39a) and (A.39b), along with Transmission Conditions (A.40a) and (A.40b), and Boundary Conditions (A.41a), (A.41b), and (A.41c), we obtain that the limit solution U^0 satisfies homogeneous Dirichlet boundary conditions. Thus, we write

the problem satisfied by U^0 as

$$\begin{cases} \partial_{X_{\text{int}}}^2 U_{\text{int}}^0 + \partial_y^2 U_{\text{int}}^0 = \frac{f_{\text{int}}}{\sigma_{\text{int}}} & \text{in } \Omega_{\text{int}}, \\ U_{\text{int}}^0 = 0 & \text{on } \partial\Omega_{\text{int}}. \end{cases} \quad (\text{A.43})$$

$$\begin{cases} \partial_{X_{\text{ext}}}^2 U_{\text{ext}}^0 + \partial_y^2 U_{\text{ext}}^0 = \frac{f_{\text{ext}}}{\sigma_{\text{ext}}} & \text{in } \Omega_{\text{ext}}, \\ U_{\text{ext}}^0 = 0 & \text{on } \partial\Omega_{\text{ext}}. \end{cases}$$

Terms of order one

We consider Problem (A.39c), along with conditions (A.40c) and (A.40d) for U^1

$$\begin{cases} \partial_{X_{\text{lay}}}^2 U_{\text{lay}}^1(X_{\text{lay}}, y) = 0 & X_{\text{lay}} \in \left(-\frac{1}{2}, \frac{1}{2}\right), \\ \partial_{X_{\text{lay}}} U_{\text{lay}}^1\left(-\frac{1}{2}, y\right) = 0, \\ \partial_{X_{\text{lay}}} U_{\text{lay}}^1\left(\frac{1}{2}, y\right) = 0. \end{cases}$$

The solution to the above equation has the form $U_{\text{lay}}^1(X_{\text{lay}}, y) = \varphi_0^1(y)$. Then, we employ Equation (A.42) and Conditions (A.41d) to build the following problem for φ_0^1

$$\begin{cases} \frac{d^2}{dy^2} \varphi_0^1(y) = 0 & y \in (0, y_0), \\ \varphi_0^1(0) = 0, \\ \varphi_0^1(y_0) = 0. \end{cases}$$

We deduce that $\varphi_0^1(y) = 0$ and thus, $U_{\text{lay}}^1(X_{\text{lay}}, y) = 0$. Finally, employing Equations (A.39a) and (A.39b), along with Transmission Conditions (A.40a) and (A.40b), and Boundary Conditions (A.41a), (A.41b), and (A.41c), we obtain that the limit solution U^0 satisfies homogeneous Dirichlet boundary conditions. Thus, we write

the problem satisfied by U^1 as

$$\begin{cases} \partial_{X_{\text{int}}}^2 U_{\text{int}}^1 + \partial_y^2 U_{\text{int}}^1 = \frac{-1}{x_0} \partial_{X_{\text{int}}}^2 U_{\text{int}}^0 - \frac{X_{\text{int}}}{2x_0 \sigma_{\text{int}}} \partial_{X_{\text{int}}} f_{\text{int}} & \text{in } \Omega_{\text{int}}, \\ U_{\text{int}}^1 = 0 & \text{on } \partial\Omega_{\text{int}}. \end{cases}$$

$$\begin{cases} \partial_{X_{\text{ext}}}^2 U_{\text{ext}}^1 + \partial_y^2 U_{\text{ext}}^1 = \frac{1}{x_0 - L} \partial_{X_{\text{ext}}}^2 U_{\text{ext}}^0 + \frac{(X_{\text{ext}} - L)}{2(x_0 - L) \sigma_{\text{ext}}} \partial_{X_{\text{ext}}} f_{\text{ext}} & \text{in } \Omega_{\text{ext}}, \\ U_{\text{ext}}^1 = 0 & \text{on } \partial\Omega_{\text{ext}}. \end{cases} \quad (\text{A.44})$$

A.8.3 Comparison

In this section we compare the expansion performed in the previous section with the one considered in Section 1.4. In this case, the elemental problems are defined over ε -independent domains Ω_{int} and Ω_{ext} . In this sense, we could expect this expansion to have similarities with the second approach considered in Section 1.4, or even coincide. We concentrate on the part of the solution defined over Ω_{int} . We have an asymptotic expansion of the following form

$$U_{\text{int}}(X_{\text{int}}, y) = U_{\text{int}}^0(X_{\text{int}}, y) + \varepsilon U_{\text{ext}}^1(X_{\text{int}}, y) + \varepsilon^2 U_{\text{int}}^2(X_{\text{int}}, y) + \dots$$

If we consider only the first term of the expansion, thanks to Problem (A.43), we deduce that the obtained model coincides with the first-order model of the second class (1.30). Then, if we also consider the second term and we neglect the terms of order two or higher in ε , we obtain:

$$\begin{aligned} (U_{\text{int}}^0 + \varepsilon U_{\text{int}}^1)(X_{\text{int}}, y) &= (U_{\text{int}}^0 + \varepsilon U_{\text{int}}^1) \left(\frac{1}{1 - \frac{\varepsilon}{2x_0}} x, y \right) \\ &= (U_{\text{int}}^0 + \varepsilon U_{\text{int}}^1) \left(\left(1 + \frac{\varepsilon}{2x_0} + O(\varepsilon^2) \right) x, y \right) \\ &= U_{\text{int}}^0(x, y) + \varepsilon \left(\frac{x}{2x_0} \partial_x U_{\text{int}}^0 + U_{\text{int}}^1 \right) (x, y) + O(\varepsilon^2). \end{aligned}$$

If we evaluate the first order term, $\frac{x}{2x_0} \partial_x U_{\text{int}}^0 + U_{\text{int}}^1$ at $x = x_0$ we obtain the condition

$$U_{\text{int}}^1(x_0, y) = -\frac{1}{2} \partial_x U_{\text{int}}^0(x_0, y),$$

which coincides with the condition obtained for the first order term (1.30). Then, if we calculate the Laplacian over Ω_{int} , we obtain

$$\Delta \left(\frac{x}{2x_0} \partial_x U_{\text{int}}^0(x_0, y) + U_{\text{int}}^1(x_0, y) \right) = 0,$$

which also coincides with the equation obtained for the first order term of the second approach (1.30).

FINITE ELEMENT METHOD IMPLEMENTATION

B.1 Introduction

Chapters 1 and 2 were devoted to the derivation of several asymptotic models, which after have been numerically analyzed in Chapter 4. These tests are useful to numerically validate the derived models and to illustrate the convergence results proved in Chapter 3.

For obtaining such numerical results, a classical Finite Element Method code has been implemented. The code is based on straight triangular elements for discretizing the domain of the problem and piecewise polynomials of any given degree for representing the numerical solution. Such polynomials correspond to the Lagrange Polynomials.

This appendix provides a brief explanation about how this code has been implemented. We set the model problem solved by the code from the strong formulation of the differential problem and we explain how we derive a weak formulation on which the Finite Element Method is applied. We also describe how the weak formulation is discretized and also how to proceed when we consider Dirichlet and Robin type boundary conditions. To provide a self-contained description of the code, we also give some details on the construction of the mesh and the creation of the corresponding data structures.

In this appendix, one can also find information on the construction of the shape functions and on the different data structures which are used for getting a numerical solution.

The code is divided into two main parts. The first one consists in the assembling of a linear system and the second one deals with solving such linear system. The code is implemented in C and Matlab programming languages, where the part corresponding to the assembling is mainly coded in C and the part corresponding

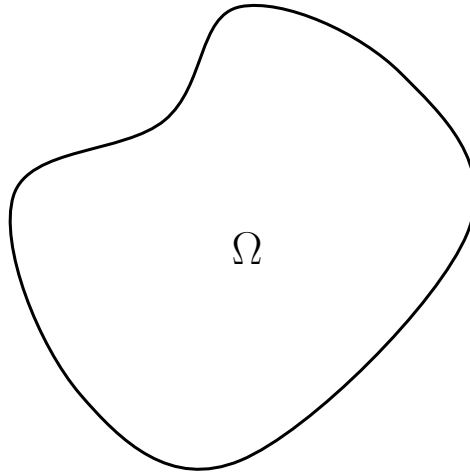


Figure B.1: Geometry of the problem: A smooth domain Ω .

to the resolution of the linear system is mainly coded in Matlab. Moreover, Matlab is used for the post processing of the solution, including tasks like the visualization of the solution or the calculus of the error in different norms.

B.2 Model problem: strong and weak formulations

Here we explain the configuration and model problem we are interested in solving. As stated before, the code is developed to discretize the models we have derived in chapters 1 and 2. The configurations we are interested in have already been explained in the previous chapters. They are quite complex, composed of several subdomains, whose physical parameters take different values and include different types of boundary conditions and also transmission conditions between the different subdomains. Our code is adapted to deal with these kinds of complex configurations, but for the sake of simplicity, here we will concentrate on explaining how the code works for simple configurations. This is why we consider the Poisson equation

$$\sigma \Delta u = f,$$

where constant σ and the right-hand side function f are given data. This problem is set in a smooth domain $\Omega \subset \mathbb{R}^2$, which can be observed in Figure B.1.

Remark 8. *The code is also capable of working with the 3D Laplace equation in an axisymmetric configuration, when everything in the configuration, including the*

right-hand side function f , has a symmetry with an axis, and thus, we simplify the 3D problem to a 2D problem. In such a configuration the problem is solved in the meridian domain and the 3D Laplace operator takes the following form

$$\Delta = \frac{1}{r} \partial_r (r \partial_r) + \partial_z^2.$$

We consider two types of boundary conditions to complement the Poisson equation: Dirichlet or Robin boundary conditions. Each boundary condition requires a different procedure, thus, in the following we will explain both separately.

B.2.1 Homogeneous Dirichlet boundary conditions

We begin with Dirichlet homogeneous boundary conditions because this case is slightly simpler and its handling is a required passage to deal with non-homogeneous conditions. In this case, the continuous problem writes as follows

$$\begin{cases} \sigma \Delta u = f & \text{in } \Omega, \\ u = 0 & \text{on } \partial\Omega. \end{cases} \tag{B.1}$$

When using finite element discretization, it is usual to derive a variational formulation for the problem. For that purpose, we consider functional space $H_0^1(\Omega)$ and we assume that Problem (B.1) admits a solution regular enough (for instance $H^2(\Omega)$). The source is supposed to be in $L^2(\Omega)$. We deduce the following variational formulation: find $u \in H_0^1(\Omega)$, such that for all $w \in H_0^1(\Omega)$

$$\int_{\Omega} \sigma \nabla u \cdot \nabla w \, dx = - \int_{\Omega} f w \, dx. \tag{B.2}$$

This is the variational formulation for the problem when we consider a Dirichlet type boundary condition. The derivation of such a variational formulation is necessary for deriving a numerical Finite Element solution and represents the first step towards obtaining such a solution.

B.2.2 Non-homogeneous Dirichlet boundary conditions

In the case of non-homogeneous Dirichlet conditions, the strong problem writes as follows

$$\begin{cases} \sigma \Delta u = f & \text{in } \Omega, \\ u = g & \text{on } \partial\Omega. \end{cases} \tag{B.3}$$

It is no more possible to take the boundary condition directly inside the functional space. This is why we are going to introduce a lifting operator allowing us to modify the problem into a problem set in $H_0^1(\Omega)$. We begin by defining the Dirichlet trace operator γ as

$$\begin{aligned}\gamma : H^1(\Omega) &\longrightarrow H^{\frac{1}{2}}(\partial\Omega) \\ w &\longmapsto \gamma(w) := w|_{\partial\Omega}.\end{aligned}$$

Now, as the Dirichlet trace operator γ is surjective, if $g \in H^{1/2}(\partial\Omega)$, there exists a function $u_g \in H^1(\Omega)$, for which we assume $\Delta u_g \in L^2(\Omega)$, such that $\gamma(u_g) = g$. This function u_g is a Dirichlet trace lifting of g in Ω . From u_g we define function \hat{u} as

$$\hat{u} := u - u_g.$$

Function \hat{u} satisfies the following problem

$$\begin{cases} \sigma\Delta\hat{u} = f - \sigma\Delta u_g & \text{in } \Omega, \\ \hat{u} = 0 & \text{on } \partial\Omega. \end{cases}$$

Function \hat{u} satisfies a homogeneous Dirichlet problem, which can be solved with the variational formulation formerly introduced. We then end up with the solution through the formula:

$$u = \hat{u} + u_g.$$

B.2.3 Robin boundary conditions

The second type of boundary conditions we are going to consider are Robin type boundary conditions. When these conditions are considered, both the solution and its derivative take part in the formulation. In this case, the continuous problem is written as follows

$$\begin{cases} \sigma\Delta u = f & \text{in } \Omega, \\ au + b\partial_n u = g & \text{on } \partial\Omega, \end{cases} \quad (\text{B.4})$$

where the right-hand side function g and the two coefficients a and b are data. We also write a variational formulation for the problem. For that purpose, we assume the solution to the continuous problem is regular enough (for instance $H^2(\Omega)$). we select a test function $w \in \mathcal{D}(\overline{\Omega})$, we multiply the equation in Ω with this test function, and assuming that $f \in L^2(\Omega)$ and that $g \in H^{\frac{1}{2}}(\Omega)$, we integrate over

the domain. Then, we obtain

$$\int_{\Omega} \sigma \nabla u \cdot \nabla w \, dx - \langle \sigma \partial_n u, w \rangle_{\partial\Omega} = - \int_{\Omega} f w \, dx.$$

We apply the Robin boundary condition to the integral over $\partial\Omega$ and from the density of $\mathcal{D}(\overline{\Omega})$ into $H^1(\Omega)$, we obtain the following variational formulation: find $u \in H^1(\Omega)$, such that for all $w \in H^1(\Omega)$

$$\int_{\Omega} \sigma \nabla u \cdot \nabla w \, dx + \frac{a}{b} \int_{\partial\Omega} \sigma u w \, ds = - \int_{\Omega} f w \, dx - \frac{1}{b} \int_{\partial\Omega} \sigma g w \, ds. \quad (\text{B.5})$$

Remark 9. We infer the weak formulation for Neumann type boundary conditions

$$\partial_n u = g \quad \text{on} \quad \partial\Omega,$$

by just employing the formulation for Robin type boundary conditions if we apply $a = 0$ and $b = 1$. We could consider the formulation for Neumann type conditions as a particular case of the formulation for Robin type conditions.

Remark 10. We can also consider a mix of the different boundary conditions presented here. When we impose two different boundary conditions on two different parts of the boundary, we say that we consider mixed boundary conditions. In general, the problem needs at least a Dirichlet boundary condition on one part of the boundary to be well posed, so often the problems we consider have the following form

$$\begin{cases} \sigma \Delta u = f & \text{in } \Omega, \\ \partial_n u = g & \text{on } \Gamma^N, \\ u = 0 & \text{on } \Gamma^D, \end{cases}$$

where $\partial\Omega = \Gamma^D \cup \Gamma^N$, and Γ^D represents the part of the boundary where Dirichlet boundary conditions are imposed, and Γ^N represents the part of the boundary where Neumann conditions are imposed. In such a case, the variational formulation writes: Find $u \in V$, such that for all $w \in V$

$$\int_{\Omega} \sigma \nabla u \cdot \nabla w \, dx = - \int_{\Omega} f w \, dx - \int_{\Gamma^N} \sigma g w \, ds,$$

where

$$V = \{w \in H^1(\Omega) : w|_{\Gamma^D} = 0\}.$$

B.3 Discrete formulation

Let us denote by V_h the discrete space and let us assume that $\text{Dim}(V_h)=N$. This space, in which we will search for our numerical solution, is called the trial space. As it is a finite dimensional space, it is possible to find a set of functions $\{e_1, \dots, e_N\}$ which form a basis of such space and as we want to search for a solution inside this space, we will look for an approximate solution u_h of the form

$$u_h(x, y) = \sum_{i=1}^N U_i e_i(x, y) = U_1 e_1(x, y) + \dots + U_N e_N(x, y). \quad (\text{B.6})$$

The choice of the approximate space V_h and its basis functions $\{e_1, \dots, e_N\}$ is arbitrary, we are free to choose them as we wish, but it has of course to be coherent with the regularity problem you are solving. In this implementation, we have selected basis functions to be piecewise polynomials of a given degree p . This is a rather classical approach and we will explain better how to build the discrete space in the following sections. Now that we know what kind of approximate solution we are seeking, we are willing to set the discrete variational formulations by substituting $u = u_h$.

B.3.1 Dirichlet boundary conditions

If we consider a solution of the form (B.6) and we substitute it in (B.2), we obtain

$$\sum_{i=1}^N U_i \int_{\Omega} \sigma \nabla e_i \cdot \nabla w \, dx = - \int_{\Omega} f w \, dx.$$

Now we need to select a finite dimensional functional space containing the test functions. This space takes the name of test space and in the same way as for the trial space, we have are free to choose it. In this implementation we choose the same test space as the trial one, but this choice is not at all mandatory. Thus, using functions e_1, \dots, e_N as test functions and substituting them into the variational formulation we obtain

$$\sum_{i=1}^N U_i \int_{\Omega} \sigma \nabla e_i \cdot \nabla e_j \, dx = - \int_{\Omega} f e_j \, dx \quad j = 1, \dots, N.$$

If we denote by A the $N \times N$ matrix composed by the entries

$$a_{i,j} = \int_{\Omega} \sigma \nabla e_i \cdot \nabla e_j \, dx, \quad i = 1, \dots, N, \quad j = 1, \dots, N,$$

and we denote F the vector with components

$$F_j = - \int_{\Omega} f e_j \, dx, \quad j = 1, \dots, N,$$

we obtain the following linear system

$$AU = F.$$

The matrix A is called the stiffness matrix and the vector F is the force vector. This is a linear system that can be solved to obtain the coefficients $U = (U_1, \dots, U^N)^t$, and thus, obtain our approximate solution u_h .

B.3.2 Robin boundary conditions

We proceed in the same way for Robin boundary conditions. We consider a solution of the form (B.6) and we substitute it into (B.5) to obtain

$$\sum_{i=1}^N U_i \int_{\Omega} \sigma \nabla e_i \cdot \nabla w \, dx + \sum_{i=1}^N U_i \frac{a}{b} \int_{\partial\Omega} \sigma e_i w \, ds = - \int_{\Omega} f w - \frac{1}{b} \int_{\partial\Omega} \sigma g w \, ds.$$

Now we select again the same test space and basis functions we selected for the trial space, e_1, \dots, e_N , and we substitute them into the variational formulation. We then have

$$\sum_{i=1}^N U_i \int_{\Omega} \sigma \nabla e_i \cdot \nabla e_j \, dx + \sum_{i=1}^N U_i \frac{a}{b} \int_{\partial\Omega} \sigma e_i e_j \, ds = - \int_{\Omega} f e_j \, dx - \frac{1}{b} \int_{\partial\Omega} \sigma g e_j \, ds,$$

for $j = 1, \dots, N$. If we denote by A the stiffness matrix with coefficients

$$a_{i,j} = \int_{\Omega} \sigma \nabla e_i \cdot \nabla e_j \, dx + \frac{a}{b} \int_{\partial\Omega} \sigma e_i e_j \, ds, \quad i = 1, \dots, N, \quad j = 1, \dots, N,$$

and if F stands for the force vector with components

$$F_j = - \int_{\Omega} f e_j \, dx - \frac{1}{b} \int_{\partial\Omega} \sigma g e_j \, ds, \quad j = 1, \dots, N,$$

we obtain again a linear system represented by the stiffness matrix A and the right hand side F

$$AU = F.$$

The system can be solved to obtain the coefficients $U = (U_1, \dots, U^N)^t$, which define our approximate solution u_h .

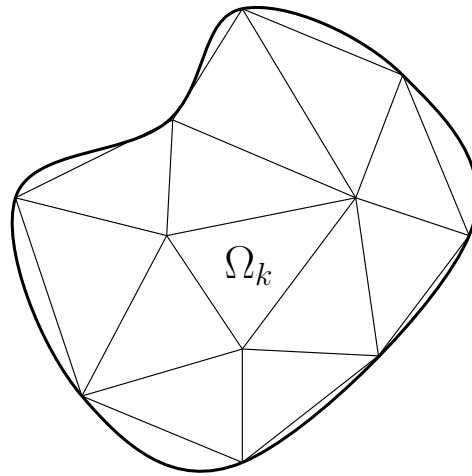


Figure B.2: An example of a triangular mesh for domain Ω .

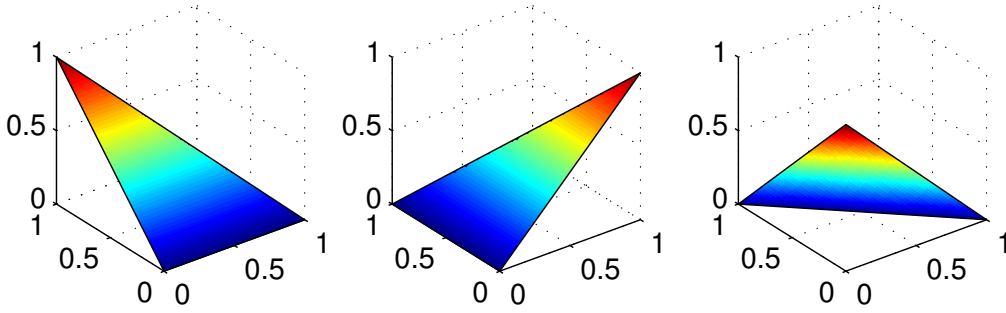
B.4 Domain discretization

Here we explain how we proceed to discretize domain Ω . This step is not mandatory when employing the finite element method as you could consider trial and test functions whose support takes the whole domain Ω , but in such a case the resulting linear system would have a full matrix which would be very costly to invert. As stated before, in this implementation we employ piecewise polynomials of a given degree p , which have support only in certain parts of the domain. This choice is rather classical and it makes the basis functions interact only with a limited number of basis functions, thus, inducing a more sparse stiffness matrix.

For accomplishing this, it is necessary to discretize domain Ω by dividing it in several pieces, Ω_k , $k = 1, \dots, N_e$, called elements, inside of which we will define our basis functions. The shape of these elements can be chosen among different options, different shapes leading to different solutions and each one having their advantages and drawbacks. For this implementation, we have chosen to implement straight triangular shaped elements, which offer a simple solution to discretize complex shaped domains. Then, the first step towards this discretization consists in building a mesh composed of triangular shaped elements so that we approximate the shape of domain Ω . We observe an example of such a mesh in Figure B.2.

The implementation includes a mesh generator for discretizing rectangular shaped domains in triangular shaped elements, which are the most used in this study, but it can easily be used with any other mesh generator for more complex domains.

Once the domain is discretized we have to build the basis functions. As stated before, we select these basis functions to be piecewise polynomials of degree p . We impose them to take the value 1 at one node of the mesh and the value 0 at the rest of the nodes that compose the mesh. For defining these basis functions, we employ the so-called shape functions, whose support is defined only over one element. Instead of directly defining them over the physical elements, the standard procedure to define the shape functions is to define them over the triangle of vertices $(0,0)$, $(1,0)$, and $(0,1)$, which we refer to as the master element and denote by T . We observe the shape functions of first degree defined over the master element in Figure B.3. Then, we define a map from the master element to every element, which allows us to perform all the integrations over the master element instead of performing them over each of the elements. Let Ω_k , $k \in 1, \dots, N_e$, be a given element of physical vertices (x_1^k, y_1^k) , (x_2^k, y_2^k) , and (x_3^k, y_3^k) , see Figure B.4, we explicit this map \bar{X}_k employing the following equations

Figure B.3: Shape functions for $p = 1$.

$$\bar{X}_k : \begin{cases} x_k(\alpha, \beta) = x_1^k + (x_2^k - x_1^k) \alpha + (x_3^k - x_1^k) \beta, \\ y_k(\alpha, \beta) = y_1^k + (y_2^k - y_1^k) \alpha + (y_3^k - y_1^k) \beta, \end{cases} \quad (\text{B.7})$$

whose Jacobian matrix has the following form

$$J = \begin{pmatrix} x_2^k - x_1^k & y_2^k - y_1^k \\ x_3^k - x_1^k & y_3^k - y_1^k \end{pmatrix},$$

and its inverse

$$Q = J^{-1} = \frac{1}{(x_2^k - x_1^k)(y_3^k - y_1^k) - (x_3^k - x_1^k)(y_2^k - y_1^k)} \begin{pmatrix} x_2^k - x_1^k & y_2^k - y_1^k \\ x_3^k - x_1^k & y_3^k - y_1^k \end{pmatrix}.$$

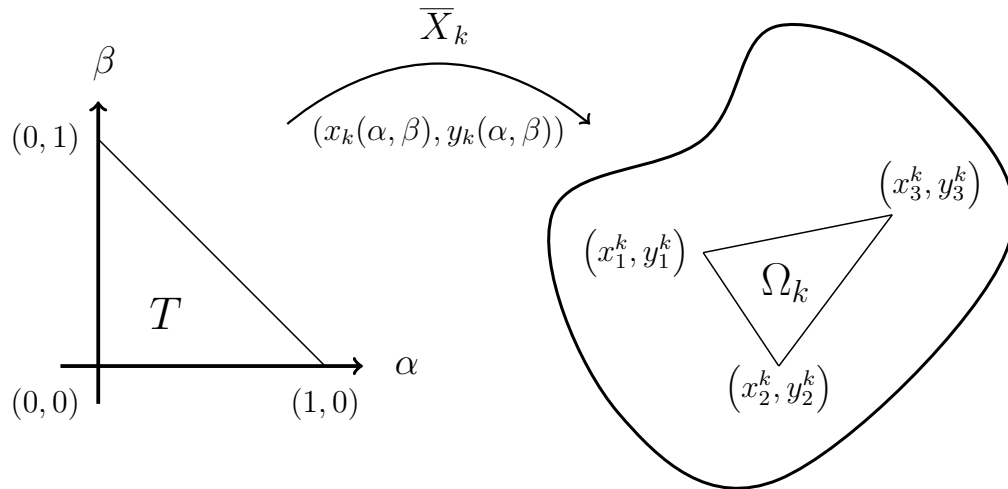


Figure B.4: Map from the master element to the physical element.

Finally, the Jacobian takes the following value

$$|J| = (x_2^k - x_1^k)(y_3^k - y_1^k) - (x_3^k - x_1^k)(y_2^k - y_1^k).$$

These expressions will be useful when applying this map to the calculi of the integrals of the stiffness matrix and force vector, which will be presented later.

B.5 Meshes

Even though the code works with complex geometries, we mostly employ it for solving rectangular shaped problems. Thus, most of the time we employ structured meshes like the one showed in Figure B.5 for a $[0, 0.75] \times [0, 0.5]$ rectangle.

In order to create this kind of meshes, we need several data structures. In the following sections we will use the example of figure B.5 to explain how these data structures work.

B.5.1 Nodes coordinates

The first data structure we need is a matrix containing the coordinates of all the nodes composing the mesh. Following the example of Figure B.5, for this case the

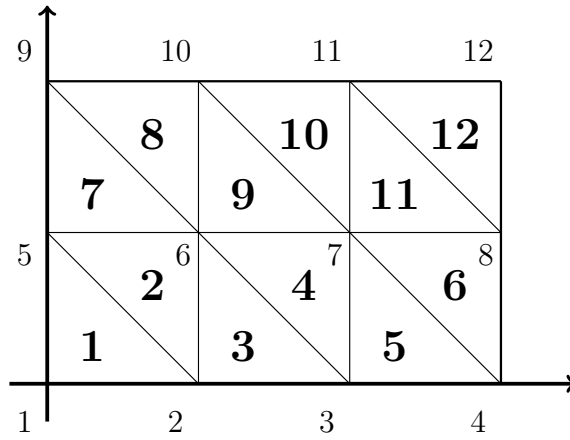


Figure B.5: Structured mesh for a rectangular domain.

coordinate matrix would be the following

$$\begin{pmatrix} 0 & , & 0 \\ 0.25 & , & 0 \\ 0.5 & , & 0 \\ 0.75 & , & 0 \\ 0 & , & 0.25 \\ 0.25 & , & 0.25 \\ 0.5 & , & 0.25 \\ 0.75 & , & 0.25 \\ 0 & , & 0.5 \\ 0.25 & , & 0.5 \\ 0.5 & , & 0.5 \\ 0.75 & , & 0.5 \end{pmatrix} .$$

B.5.2 Connectivity matrix

The second data structure we need is the connectivity matrix. This is a matrix employed to connect each basis functions with its corresponding shape functions inside every element. We denote it as C and the values inside it indicate that basis function $C_{i,j}$ corresponds to shape functions j inside element i , for $i = 1, \dots, N_e$ and $j = 1, \dots, \frac{(p+1)(p+2)}{2}$. Continuing with the example of Figure B.5, in this

case, considering we are dealing with polynomials of degree $p = 1$, we would have the following connectivity matrix

$$C = \begin{pmatrix} 1 & 2 & 5 \\ 6 & 5 & 2 \\ 2 & 3 & 6 \\ 7 & 6 & 3 \\ 3 & 4 & 7 \\ 8 & 7 & 4 \\ 5 & 6 & 9 \\ 10 & 9 & 6 \\ 6 & 7 & 10 \\ 11 & 10 & 7 \\ 7 & 8 & 11 \\ 12 & 11 & 8 \end{pmatrix}.$$

The main utility of this matrix is that it can be employed to assemble the global stiffness matrix and global force vector in the following way. For $k \in \{1, \dots, N_e\}$ and $i, j \in \left\{1, \dots, \frac{(p+1)(p+2)}{2}\right\}$, we have

$$A_{C_{k,i}, C_{k,j}} = A_{C_{k,i}, C_{k,j}} + a_{i,j}^k,$$

$$F_{C_{k,j}} = F_{C_{k,j}} + F_j^k,$$

where the terms $a_{i,j}^k$ and F_j^k are the elements composing the local stiffness matrix and local stiffness vector. We will explain how to calculate these values more in details in Section B.7 and Section B.8

B.5.3 Robin nodes

If we have a Robin boundary condition on some part of the boundary, we need a matrix that stores the nodes that touch such part of the boundary, and also what elements are in touch with such boundary. For the example of Figure B.5, assuming we have Robin boundary conditions all over the boundary, this matrix would look

as follows,

$$\begin{pmatrix} 1 & 1 & 2 \\ 3 & 2 & 3 \\ 5 & 3 & 4 \\ 6 & 4 & 8 \\ 12 & 8 & 12 \\ 12 & 12 & 11 \\ 10 & 11 & 10 \\ 8 & 10 & 9 \\ 7 & 9 & 5 \\ 1 & 5 & 1 \end{pmatrix},$$

where we store the number of the element that is in contact with the boundary with a Robin condition on the first column, and the two nodes of such element which are over the boundary in the second and third column.

B.5.4 Dirichlet nodes

When we consider a Dirichlet boundary condition over some part of the boundary, we need a matrix that stores the nodes that touch such part of the boundary. In this case we do not need to know what elements touch the boundary, only which nodes. Following the example of Figure B.5, assuming we have Dirichlet boundary conditions in all the boundary, this matrix would have the following form,

$$\begin{pmatrix} 1 \\ 2 \\ 3 \\ 4 \\ 8 \\ 12 \\ 11 \\ 10 \\ 9 \\ 5 \end{pmatrix}.$$

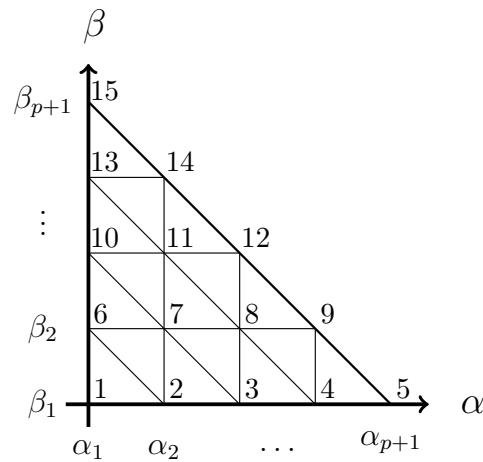


Figure B.6: Nodes inside the master element for defining shape functions of degree p .

B.6 Shape functions of degree p and basis functions

In this section we explain how to build the desired shape functions as piecewise polynomials of any degree. For a given degree p , this makes a total of $\frac{(p+1)(p+2)}{2}$ shape functions defined over the master element. We build a grid over the master element by dividing each axis in p pieces of the same length. This creates $\frac{(p+1)(p+2)}{2}$ nodes, as we show in Figure B.6. The shape functions must take the value 1 at one of those nodes, and 0 at the rest of them. We number shape functions starting from node $(0,0)$ and moving from left to right and from bottom to top, as we show in Figure B.6.

Thus, the shape functions are defined in the following way, for a shape function that takes the value 1 at a node (α_i, β_j) and 0 at the rest of nodes, shape function number $s = ((p+1) + (p-j+3)) \frac{j-1}{2} + i$, we employ the following expression

$$\begin{aligned}
 \psi_s(\alpha, \beta) &= \prod_{l=1}^{i-1} \frac{\alpha - \alpha_l}{\alpha_i - \alpha_l} \prod_{l=1}^{j-1} \frac{\beta - \beta_l}{\beta_j - \beta_l} \prod_{l=i+1}^{p+1} \frac{\alpha + \beta - \alpha_l}{\alpha_i + \beta_j - \alpha_l} \\
 &= \frac{\alpha - \alpha_1}{\alpha_i - \alpha_1} \frac{\alpha - \alpha_2}{\alpha_i - \alpha_2} \cdots \frac{\alpha - \alpha_{i-1}}{\alpha_i - \alpha_{i-1}} \\
 &\quad \frac{\beta - \beta_1}{\beta_j - \beta_1} \frac{\beta - \beta_2}{\beta_j - \beta_2} \cdots \frac{\beta - \beta_{j-1}}{\beta_j - \beta_{j-1}} \\
 &\quad \frac{\alpha + \beta - \alpha_{i+1}}{\alpha_i + \beta_j - \alpha_{i+1}} \frac{\alpha + \beta - \alpha_{i+2}}{\alpha_i + \beta_j - \alpha_{i+2}} \cdots \frac{\alpha + \beta - \alpha_{p+1}}{\alpha_i + \beta_j - \alpha_{p+1}}.
 \end{aligned}$$

This is the expression of the shape function defined over the master element. Employing this expression and the map (B.7), $\bar{X}_k(\alpha, \beta) = (x(\alpha, \beta), y(\alpha, \beta))$, we obtain the shape functions defined over the physical elements. We will denote the shape function defined over the physical element corresponding to ψ_s as φ_s :

$$\varphi_s(x, y) = \varphi_s(x(\alpha, \beta), y(\alpha, \beta)) = \psi_s(\alpha, \beta).$$

We define the basis functions by employing these physical shape functions. As stated before, this basis functions will be piecewise linear polynomials that take the value 1 at one node and the value 0 at the rest of the nodes. Thus, we will count with as many basis functions as nodes we have on the mesh. In general we find three different types of basis functions.

The first ones are the basis functions corresponding to a node interior to an element, like the nodes 7, 8, and 11 on the example of Figure B.6. These basis functions will have support only inside that element and will vanish outside of it.

The second type of basis functions are the ones corresponding to a node which is placed over the side of two elements that touch each other. In this case, these basis functions will have support over those two elements and will vanish outside them. In the example of Figure B.6, the nodes 2, 3, 4, 6, 10, 13, 9, 12, and 14 could correspond to basis functions of this type.

Finally, the last type of basis functions are the ones corresponding to a node which is placed over a vertex of several elements that touch each other just at that point. In this case, these basis functions will have support over all those elements which touch the given node and will vanish outside of them. Nodes 1, 5, and 15 in the example of Figure B.6 could correspond to basis functions of this type.

B.7 Local stiffness matrix

Here we explain how to calculate the local stiffness matrices. For every element Ω_k , $k = 1, \dots, N_e$, we will calculate the matrices

$$a_{i,j}^k = \int_{\Omega_k} \sigma \nabla \varphi_i^k(x, y) \cdot \nabla \varphi_j^k(x, y) \, dx \, dy, \quad i, j = 1, \dots, \frac{(p+1)(p+2)}{2}.$$

Then, we can employ these matrices to calculate the global stiffness matrix A by employing the connectivity matrix. For calculating these local stiffness matrices, we employ the following formula with the help of the map the map (B.7) to perform the integration over the master element T ,

$$\begin{aligned} a_{i,j}^k &= \int_{\Omega_k} \sigma \nabla \varphi_i^k(x, y) \cdot \nabla \varphi_j^k(x, y) \, dx \, dy \\ &= \int_{\Omega_k} \sigma (\partial_x, \partial_y) \varphi_i^k(x, y) \cdot (\partial_x, \partial_y)^t \varphi_j^k(x, y) \, dx \, dy \\ &= \int_T \sigma (\partial_\alpha, \partial_\beta) J^{-1} \varphi_i^k(x_k(\alpha, \beta), y_k(\alpha, \beta)) \cdot \left((\partial_\alpha, \partial_\beta) J^{-1} \right)^t \varphi_j^k(x(\alpha, \beta), y(\alpha, \beta)) |J| \, d\alpha \, d\beta \\ &= \int_T \sigma (\partial_\alpha, \partial_\beta) J^{-1} \psi_i(\alpha, \beta) \cdot J^{-t} (\partial_\alpha, \partial_\beta)^t \psi_j(\alpha, \beta) |J| \, d\alpha \, d\beta. \end{aligned}$$

After calculating these integrals, we assemble them into the global stiffness matrix A by using the connectivity matrix C ,

$$A_{C_{k,i}, C_{k,j}} = A_{C_{k,i}, C_{k,j}} + a_{i,j}^k.$$

B.8 Local force vector

In the same way, we calculate the local force vector thanks to the following formula

$$\begin{aligned} F_j^k &= \int_{\Omega_k} f(x, y) \varphi_j^k(x, y) \, dx \, dy \\ &= \int_T f(x_k(\alpha, \beta), y_k(\alpha, \beta)) \varphi_j^k(x_k(\alpha, \beta), y_k(\alpha, \beta)) |J| \, d\alpha \, d\beta \\ &= \int_T f(x_k(\alpha, \beta), y_k(\alpha, \beta)) \psi_j(\alpha, \beta) |J| \, d\alpha \, d\beta, \quad j = 1, \dots, \frac{(p+1)(p+2)}{2}. \end{aligned}$$

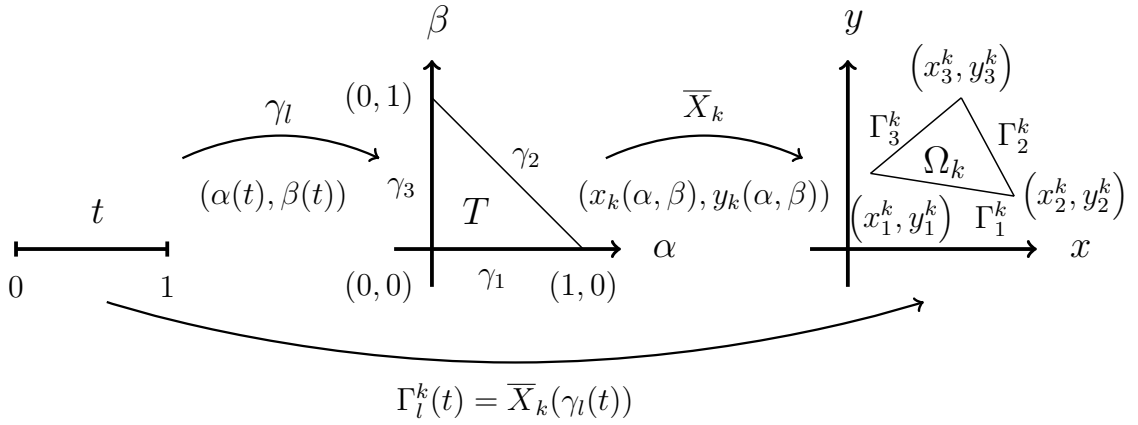


Figure B.7: Maps employed to calculate the integrals of the Robin boundary conditions.

After calculating these integrals, we assemble them into the global force vector F by employing the connectivity matrix C ,

$$F_{C_{k,j}} = F_{C_{k,j}} + F_j^k.$$

B.9 Robin boundary conditions

When the problem includes Robin type boundary conditions, like Problem (B.1), we need to calculate some extra integrals over $\partial\Omega$. Thanks to the data structures we have defined we already know which elements touch this boundary and which vertices of these elements are placed over it. Let Ω_k be an element and let us assume that one of its edges is in contact with the part of the boundary where we have imposed Robin boundary conditions. We denote such side of the element as Γ^k . Then, we have to calculate integrals of the following form

$$N_j^k = \int_{\Gamma^k} \sigma g \varphi_j^k ds, \quad j = 1, \dots, \frac{(p+1)(p+2)}{2},$$

$$R_{i,j}^k = \int_{\Gamma^k} \sigma \varphi_i^k \varphi_j^k ds, \quad i, j = 1, \dots, \frac{(p+1)(p+2)}{2}.$$

For calculating these integrals we employ the map $\bar{X}_k = (x(\alpha, \beta), y(\alpha, \beta))$ defined in Section B.4, along with another map that goes from the $[0, 1]$ to the sides of the master element T . We observe this configuration in Figure B.7.

We have to separate three possible cases for defining this map, depending on which edge of the element touches the boundary, each case corresponding to one of the edges, Γ_1^k , Γ_2^k or Γ_3^k . We then define the map γ_l , $l = 1, 2, 3$, as

$$\gamma_l = \begin{cases} \gamma_1(t) = (t, 0), \\ \gamma_2(t) = (1 - t, t), \\ \gamma_3(t) = (0, 1 - t), \end{cases} \quad t \in (0, 1).$$

Composing this map with the map $\bar{X}_k = (x(\alpha, \beta), y(\alpha, \beta))$ defined in Section B.4, we obtain

$$\Gamma_l = \bar{X}_k(\gamma_l) = \begin{cases} \Gamma_1^k(t) = (x_1^k + (x_2^k - x_1^k)t, y_1^k + (y_2^k - y_1^k)t), \\ \Gamma_2^k(t) = (x_1^k + (x_2^k - x_1^k)(1 - t) + (x_3^k - x_1^k)t, \\ \quad y_1^k + (y_2^k - y_1^k)(1 - t) + (y_3^k - y_1^k)t), \\ \Gamma_3^k(t) = (x_1^k + (x_3^k - x_1^k)(1 - t), y_1^k + (y_3^k - y_1^k)(1 - t)). \end{cases}$$

We deduce

$$\|\Gamma_l^{k'}\| = \begin{cases} \|\Gamma_1^{k'}\| = \sqrt{(x_2^k - x_1^k)^2 + (y_2^k - y_1^k)^2}, \\ \|\Gamma_2^{k'}\| = \sqrt{(x_3^k - x_2^k)^2 + (y_3^k - y_2^k)^2}, \\ \|\Gamma_3^{k'}\| = \sqrt{(x_1^k - x_3^k)^2 + (y_1^k - y_3^k)^2}. \end{cases}$$

Now we calculate the integrals by using the following formulas, for $l \in \{1, 2, 3\}$,

$$N_j^k = \int_{\Gamma_l} \sigma g \varphi_j^k ds = \int_0^1 \sigma g(\Gamma_l(t)) \psi_j(\gamma(t)) \|\Gamma_l^{k'}(t)\| dt.$$

$$R_{i,j}^k = \int_{\Gamma_l} \sigma \varphi_i^k \varphi_j^k ds = \int_0^1 \sigma \psi_i(\gamma(t)) \psi_j(\gamma(t)) \|\Gamma_l^{k'}(t)\| dt.$$

We assemble these integrals into the global stiffness matrix and global force vector thanks to the connectivity matrix

$$A_{C_{k,i}, C_{k,j}} = A_{C_{k,i}, C_{k,j}} + R_{i,j}^k,$$

$$F_{C_{k,j}} = F_{C_{k,j}} + N_j^k.$$

B.10 Dirichlet boundary conditions

When a Dirichlet boundary condition is set on a part of the boundary, thanks to the data structures we have defined, we already know what vertices are placed over this boundary. Then, Dirichlet conditions are imposed by directly modifying the global stiffness matrix and global force vector in the linear system

$$AU = F.$$

Let us assume that the node (x_i, y_i) , $i \in \{1, \dots, N\}$ touches the boundary with a Dirichlet boundary condition. Then, we modify row number i in the matrix in the following way

$$\begin{cases} A_{i,j} = 0, & j = 1, \dots, i-1, i+1, \dots, N, \\ A_{i,i} = 1, \end{cases}$$

and we modify the force vector by imposing $F_i = f(x_i, y_i)$. Now when we solve the linear system, with these changes we enforce the solution to take the desired value at the nodes we have a Dirichlet condition. In practice, instead of modifying the global force vector and stiffness matrix, which are going to be very big and sparse in the case of the stiffness matrix, we just avoid adding elements to those rows when performing the assembling.

B.11 Transmission conditions

The models we have to deal with are sometimes composed of transmission conditions between the different subdomains. These transmission conditions often include terms like jumps and mean values of functions or their derivatives. These transmission conditions have to be treated differently depending on the terms that appear in their formulations. Here, to illustrate how we deal with this kind of conditions, let us assume we have an integral of the following form in the variational formulation.

$$\int_{\Gamma} [u] [v] \, ds.$$

The procedure is similar when dealing with mean values instead of jumps. For each pair of elements Ω_k , Ω_l , whose boundaries are connected via a transmission condition written on interface Γ , we have the shape functions φ_i^k , $i = 1, \dots, \frac{(p+1)(p+2)}{2}$ defined over Ω_k and the shape functions φ_i^l , $i =$

$1, \dots, \frac{(p+1)(p+2)}{2}$ defined over Ω_l . Let us denote by Γ^k the part of the boundary that meets $\Gamma^k = \Gamma \cap \bar{\Omega}_k$. Then, we have to calculate the following integrals

$$\int_{\Gamma^k} [\varphi_i^k] [\varphi_j^k] ds, \quad i, j = 1, \dots, \frac{(p+1)(p+2)}{2}.$$

$$\int_{\Gamma^k} [\varphi_i^l] [\varphi_j^l] ds, \quad i, j = 1, \dots, \frac{(p+1)(p+2)}{2}.$$

$$\int_{\Gamma^k} [\varphi_i^l] [\varphi_j^k] ds, \quad i, j = 1, \dots, \frac{(p+1)(p+2)}{2}.$$

$$\int_{\Gamma^k} [\varphi_i^k] [\varphi_j^l] ds, \quad i, j = 1, \dots, \frac{(p+1)(p+2)}{2}.$$

We will concentrate on the last integral since the three others are calculated following the same procedure. We develop the integral in the following way

$$\begin{aligned} \int_{\Gamma^k} [\varphi_i^k] [\varphi_j^l] ds &= \int_{\Gamma^k} \varphi_i^k|_{\Gamma^{k+}} \varphi_j^l|_{\Gamma^{k+}} ds - \int_{\Gamma^k} \varphi_i^k|_{\Gamma^{k+}} \varphi_j^l|_{\Gamma^{k-}} ds \\ &\quad - \int_{\Gamma^k} \varphi_i^k|_{\Gamma^{k-}} \varphi_j^l|_{\Gamma^{k+}} ds + \int_{\Gamma^k} \varphi_i^k|_{\Gamma^{k-}} \varphi_j^l|_{\Gamma^{k-}} ds. \end{aligned}$$

Among these integrals only the third one is non zero due to the shape functions only having support over one element. To calculate this integral, we define the two following maps from the master element T to the two elements Ω_k and Ω_l , and we define another map from the segment $[0, 1]$ to the corresponding side of the master element in the same way we have done in Section B.9. We denote it by γ . Figure B.8 illustrates what is going on with this case.

Now we calculate the integral in the following way

$$\begin{aligned} \int_{\Gamma^k} \varphi_i^k|_{\Gamma^-} \varphi_j^l|_{\Gamma^+} ds &= \int_{\Gamma^k} (\psi_i \circ \bar{X}_k^{-1})|_{\Gamma^{k-}} (\psi_j \circ \bar{X}_l^{-1})|_{\Gamma^{k+}} ds \\ &= \int_{\Gamma^k} (\psi_i \circ \bar{X}_k^{-1})|_{\Gamma^{k-}} (\psi_j \circ \bar{X}_l^{-1} \circ \bar{X}_k \circ \bar{X}_k^{-1})|_{\Gamma^{k+}} ds \\ &= \int_{\Gamma^k} (\psi_i \circ \bar{X}_k^{-1})|_{\Gamma^{k-}} (\psi_j \circ \bar{X}_{lk} \circ \bar{X}_k^{-1})|_{\Gamma^{k+}} ds \\ &= \int_0^1 (\psi_i \circ \gamma)(t) (\psi_j \circ \bar{X}_{lk} \circ \gamma)(t) \|\Gamma'(t)\| dt \end{aligned}$$

where $\bar{X}_{lk} = \bar{X}_l^{-1} \circ \bar{X}_k$.

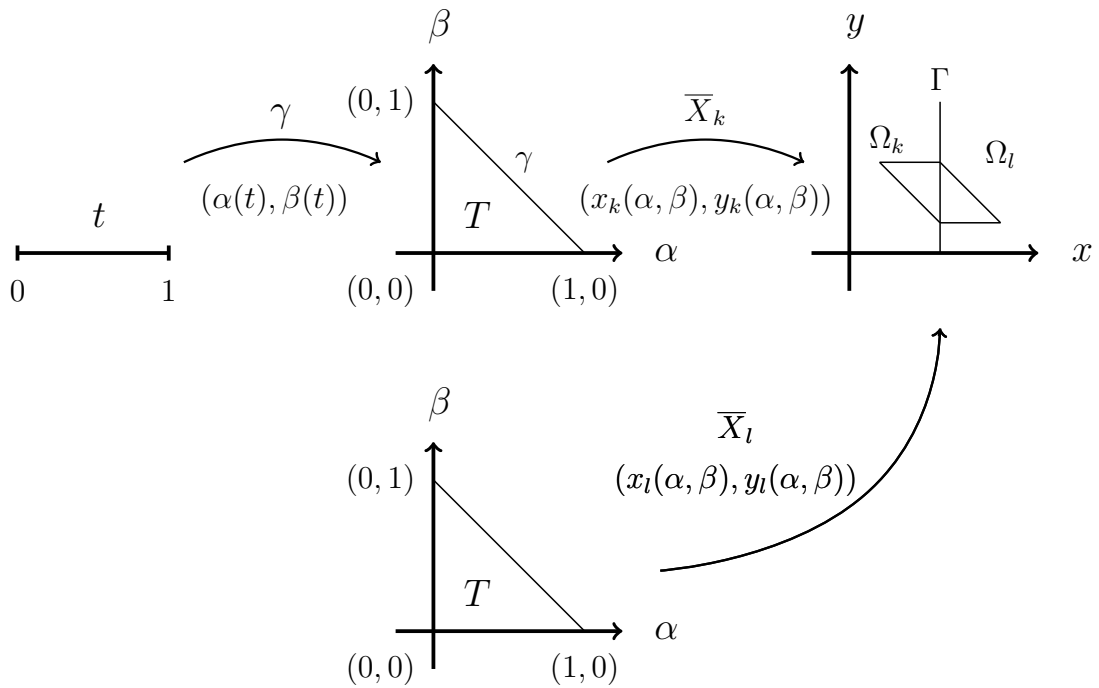


Figure B.8: Maps employed for the jump integrals.

B.12 Numerical intregation

During the whole process of applying the finite element method, we have to perform several integrations. To achieve this goal, we employ the one dimensional Gaussian quadrature points for numerically integrating functions. This quadrature rule is very suitable for integrating over rectangles in two dimensions, but if we want to employ it for integrating over our master triangle T , we have to adapt it.

We consider a map $\bar{\alpha}$ that goes from the square $Q = [0, 1] \times [0, 1]$, to the master element T . We explicit this map as follows

$$\begin{cases} x = \zeta, \\ y = \eta(1 - \zeta). \end{cases}$$

We deduce that the Jacobian matrix has the following form

$$J = \begin{pmatrix} 1 & 0 \\ -1 & 1 - \zeta \end{pmatrix}$$

and the Jacobian

$$|J| = 1 - \zeta.$$

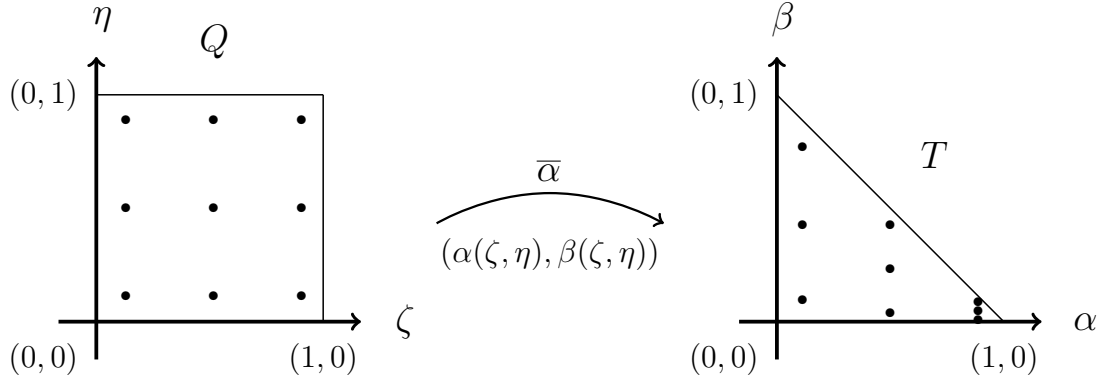


Figure B.9: Map from a square to the master element.

Now we employ this map into our numerical integrations in the following way. Let us assume we want to integrate function h over T , then, we proceed as follows

$$\begin{aligned}
 \int_T h(\alpha, \beta) \, d\alpha \, d\beta &= \int_0^1 \int_0^{1-\alpha} h(\alpha, \beta) \, d\alpha \, d\beta = \int_0^1 \int_0^1 h(\zeta, \zeta(1-\eta)) |J| \, d\zeta \, d\eta \\
 &= \int_Q h(\zeta, \eta(1-\zeta)) (1-\zeta) \, d\zeta \, d\eta \\
 &= \sum_i \sum_j \omega_i \omega_j h(\zeta_i, \eta_j(1-\zeta_i)) (1-\zeta_i),
 \end{aligned}$$

where ζ_i, η_j are the integration points and ω_i, ω_j are the weights of the Gaussian quadrature rule for one dimension. These quadrature points and weights take different values and increase or decrease in number depending on the degree of the polynomials we want to integrate. This quadrature rule is suitable for the type of integrations we want to perform, because if enough points and weights are selected, it can integrate polynomials with no error, and our shape functions are indeed polynomials.

The one dimensional Gaussian quadrature rule is capable of integrating polynomials of degree $2n - 1$ with no error by employing n points and weights. Thus, in our case, if the degree of the shape functions is set to p we need $2p + 1$ points to integrate with no error the integrals of the stiffness matrix.

One of the drawbacks of this technique is that it works very well for squares but when working with triangles it is not so efficient. When creating the map from Q to T the integration points are no longer symmetrically distributed along the domain, therefore, we need more points for integrating with no error polynomials of a given degree. We observe this phenomenon in Figure B.9. The points employed

in the example of the figure are the following for Q

$$\begin{pmatrix} 0.1127 & 0.1127 \\ 0.1127 & 0.5000 \\ 0.1127 & 0.8873 \\ 0.5000 & 0.1127 \\ 0.5000 & 0.5000 \\ 0.5000 & 0.8873 \\ 0.8873 & 0.1127 \\ 0.8873 & 0.5000 \\ 0.8873 & 0.8873 \end{pmatrix}$$

and the following for T

$$\begin{pmatrix} 0.1127 & 0.1000 \\ 0.1127 & 0.4436 \\ 0.1127 & 0.7873 \\ 0.5000 & 0.0563 \\ 0.5000 & 0.2500 \\ 0.5000 & 0.4436 \\ 0.8873 & 0.0127 \\ 0.8873 & 0.0564 \\ 0.8873 & 0.1000 \end{pmatrix}.$$

References

- [1] M. Abramowitz and I. A. Stegun. *Handbook of mathematical functions: with formulas, graphs, and mathematical tables*, volume 55. Courier Corporation, 1964.
- [2] A. Bendali and K. Lemrabet. The effect of a thin coating on the scattering of a time-harmonic wave for the Helmholtz equation. *SIAM Journal on Applied Mathematics*, 56(6):1664–1693, 1996.
- [3] A.-L. Bessoud, F. Krasucki, and M. Serpilli. Asymptotic analysis of shell-like inclusions with high rigidity. *Journal of Elasticity*, 103(2):153–172, 2011.
- [4] H. Brezis. *Functional analysis, Sobolev spaces and partial differential equations*. Springer Science & Business Media, 2010.
- [5] A. Burel. *Contributions à la simulation numérique en élastodynamique: découplage des ondes P et S, modèles asymptotiques pour la traversée de couches minces*. PhD thesis, Université Paris Sud-Paris XI, 2014.
- [6] F. Buret, M. Dauge, P. Dular, L. Krähenbühl, V. Péron, R. Perrussel, C. Poignard, and D. Voyer. Eddy currents and corner singularities. *IEEE Transactions on Magnetics*, 48(2):679–682, Jan. 2012.
- [7] G. Caloz, M. Costabel, M. Dauge, and G. Vial. Asymptotic expansion of the solution of an interface problem in a polygonal domain with thin layer. *Asymptotic Analysis*, 50(1, 2):121–173, 2006.
- [8] G. Caloz, M. Dauge, E. Faou, and V. Péron. On the influence of the geometry on skin effect in electromagnetism. *Computer Methods in Applied Mechanics and Engineering*, 200(9):1053–1068, 2011.
- [9] G. Caloz, M. Dauge, and V. Péron. Uniform estimates for transmission problems with high contrast in heat conduction and electromagnetism. *Journal of Mathematical Analysis and applications*, 370(2):555–572, 2010.
- [10] F. Caubet, H. Haddar, J.-R. Li, and D. V. Nguyen. New Transmission Condition Accounting For Diffusion Anisotropy In Thin Layers Applied To Diffusion MRI. *Modelisation Mathématique et Analyse Numérique*, 2016.
- [11] Q. Chen, D. Pardo, H.-b. Li, and F.-r. Wang. New post-processing method for interpretation of through casing resistivity (TCR) measurements. *Journal of Applied Geophysics*, 74(1):19–25, 2011.
- [12] S. Chun, H. Haddar, and J. S. Hesthaven. High-order accurate thin layer approximations for time-domain electromagnetics. Part II: transmission layers. *Journal of Computational and Applied Mathematics*, 234(8):2587–2608, 2010.

- [13] S. Chun and J. S. Hesthaven. High-order accurate thin layer approximations for time-domain electromagnetics. Part I: General metal backed coatings. *Journal of computational and applied mathematics*, 231(2):598–611, 2009.
- [14] M. Costabel, M. Dauge, and S. Nicaise. Singularities of Maxwell interface problems. *ESAIM: Mathematical Modelling and Numerical Analysis*, 33(03):627–649, 1999.
- [15] B. Delourme. *Modèles et asymptotiques des interfaces fines et périodiques en électromagnétisme*. PhD thesis, Université Pierre et Marie Curie-Paris VI, 2010.
- [16] B. Delourme, H. Haddar, and P. Joly. Approximate models for wave propagation across thin periodic interfaces. *Journal de mathématiques pures et appliquées*, 98(1):28–71, 2012.
- [17] L. F. Demkowicz and J. Gopalakrishnan. A class of discontinuous Petrov–Galerkin methods. Part I: The transport equation. *Computer Methods in Applied Mechanics and Engineering*, 199(23):1558–1572, 2010.
- [18] D. G. Duffy. *Green’s functions with applications*. CRC Press, 2015.
- [19] M. Duruflé, V. Péron, and C. Poinard. Time-harmonic Maxwell equations in biological cells. The differential form formalism to treat the thin layer. *Confluentes Mathematici*, 3(2):325–357, 2011. voir aussi <http://hal.inria.fr/inria-00347971/fr/>.
- [20] M. Duruflé, V. Péron, and C. Poinard. Thin layer models for electromagnetism. *Communications in Computational Physics*, 16:213–238, 2014.
- [21] B. Engquist and J.-C. Nédélec. Effective boundary conditions for acoustic and electromagnetic scattering in thin layers. Technical report, Technical Report of CMAP, 278, 1993.
- [22] H. Haddar and P. Joly. Stability of thin layer approximation of electromagnetic waves scattering by linear and nonlinear coatings. *Journal of computational and applied mathematics*, 143(2):201–236, 2002.
- [23] H. Haddar, P. Joly, and H.-M. Nguyen. Generalized impedance boundary conditions for scattering by strongly absorbing obstacles: the scalar case. *Mathematical Models and Methods in Applied Sciences*, 15(08):1273–1300, 2005.
- [24] H. Haddar, P. Joly, and H.-M. Nguyen. Generalized impedance boundary conditions for scattering problems from strongly absorbing obstacles: the case of Maxwell’s equations. *Mathematical Models and Methods in Applied Sciences*, 18(10):1787–1827, 2008.

- [25] J. Hernandez and A. K. T. Assis. Electric potential due to an infinite conducting cylinder with internal or external point charge. *Journal of electrostatics*, 63(12):1115–1131, 2005.
- [26] T. J. Hughes, J. A. Cottrell, and Y. Bazilevs. Isogeometric analysis: CAD, finite elements, NURBS, exact geometry and mesh refinement. *Computer methods in applied mechanics and engineering*, 194(39):4135–4195, 2005.
- [27] N. Ida and S. Yuferev. Impedance boundary conditions for transient scattering problems. *IEEE Transactions on Magnetics*, 33(2):1444–1447, 1997.
- [28] A. A. Kaufman. The electrical field in a borehole with a casing. *Geophysics*, 55(1):29–38, 1990.
- [29] A. A. Kaufman and W. E. Wightman. A transmission-line model for electrical logging through casing. *Geophysics*, 58(12):1739–1747, 1993.
- [30] I. Muga, D. Pardo, P. J. Matuszyk, and C. Torres-Verdín. Semi-analytical response of acoustic logging measurements in frequency domain. *Computers & Mathematics with Applications*, 70(4):314–329, 2015.
- [31] D. Pardo, L. F. Demkowicz, C. Torres-Verdín, and C. Michler. PML enhanced with a self-adaptive goal-oriented hp-finite element method: Simulation of through-casing borehole resistivity measurements. *SIAM Journal on Scientific Computing*, 30(6):2948–2964, 2008.
- [32] D. Pardo, L. F. Demkowicz, C. Torres-Verdín, and M. Paszynski. Two-Dimensional High-Accuracy Simulation of Resistivity Logging-While-Drilling (LWD) Measurements Using a Self-Adaptive Goal-Oriented hp Finite Element Method. *SIAM Journal on Applied Mathematics*, 66(6):2085–2106, 2006.
- [33] D. Pardo, L. F. Demkowicz, C. Torres-Verdín, and M. Paszynski. A self-adaptive goal-oriented hp-finite element method with electromagnetic applications. Part II: Electrodynamics. *Computer methods in applied mechanics and engineering*, 196(37):3585–3597, 2007.
- [34] D. Pardo, L. F. Demkowicz, C. Torres-Verdín, and L. A. Tabarovsky. A goal-oriented hp-adaptive finite element method with electromagnetic applications. Part I: electrostatics. *International Journal for Numerical Methods in Engineering*, 65(8):1269–1309, 2006.
- [35] D. Pardo, C. Torres-Verdín, and L. F. Demkowicz. Simulation of multifrequency borehole resistivity measurements through metal casing using a goal-oriented hp finite-element method. *Geoscience and Remote Sensing, IEEE Transactions on*, 44(8):2125–2134, 2006.

- [36] D. Pardo, C. Torres-Verdín, and L. F. Demkowicz. Feasibility study for 2D frequency-dependent electromagnetic sensing through casing. *Geophysics*, 72(3):F111–F118, 2007.
- [37] D. Pardo, C. Torres-Verdin, and M. Paszynski. Simulations of 3D DC borehole resistivity measurements with a goal-oriented hp finite-element method. Part II: through-casing resistivity instruments. *Computational Geosciences*, 12(1):83–89, 2008.
- [38] D. Pardo, C. Torres-Verdín, and Z. Zhang. Sensitivity study of borehole-to-surface and crosswell electromagnetic measurements acquired with energized steel casing to water displacement in hydrocarbon-bearing layers. *Geophysics*, 73(6):F261–F268, 2008.
- [39] C. Pérez-Arancibia and M. Durán. On the Green’s function for the Helmholtz operator in an impedance circular cylindrical waveguide. *Journal of computational and applied mathematics*, 235(1):244–262, 2010.
- [40] V. Péron. *Mathematical modeling of electromagnetic phenomena in high contrast media*. Theses, Université Rennes 1, Sept. 2009. date de rédaction: avril 2009.
- [41] V. Péron. Equivalent Boundary Conditions for an Elasto-Acoustic Problem set in a Domain with a Thin Layer. Research Report RR-8163, INRIA, June 2013.
- [42] V. Péron. Equivalent boundary conditions for an elasto-acoustic problem set in a domain with a thin layer. *ESAIM: Mathematical Modelling and Numerical Analysis*, 48(5):1431–1449, 2014.
- [43] V. Péron. Asymptotic expansion for the magnetic potential in the eddy current problem : the ferromagnetic case. working paper or preprint, 2015.
- [44] V. Péron and C. Poignard. Approximate transmission conditions for time-harmonic Maxwell equations in a domain with thin layer. Research Report RR-6775, INRIA, 2008.
- [45] V. Péron, K. Schmidt, and M. Duruflé. Equivalent transmission conditions for the time-harmonic Maxwell equations in 3D for a medium with a highly conductive thin sheet. *SIAM Journal on Applied Mathematics*, 76(3):1031–1052, 2016.
- [46] R. Perrussel and C. Poignard. Asymptotic expansion of steady-state potential in a high contrast medium with a thin resistive layer. *Applied Mathematics and Computation*, 221:48–65, 2013.

- [47] C. Poignard. Rigorous asymptotics for the electric field in TM mode at mid-frequency in a bidimensional medium with thin layer. *arXiv preprint math/0607403*, 2006.
- [48] C. Poignard. Asymptotics for steady-state voltage potentials in a bidimensional highly contrasted medium with thin layer. *Mathematical Methods in the Applied Sciences*, 31(4):443–479, 2008.
- [49] C. Poignard. Approximate transmission conditions through a weakly oscillating thin layer. *Mathematical Methods in the Applied Sciences*, 32(4):435–453, 2009.
- [50] C. Qing, D. Pardo, L. Hong-Bin, and W. Fu-Rong. Compensation effect analysis in DIE method for through-casing measuring formation resistivity. *Journal of Applied Geophysics*, 74(4):287–293, 2011.
- [51] D. Schillinger, S. J. Hossain, and T. J. Hughes. Reduced Bézier element quadrature rules for quadratic and cubic splines in isogeometric analysis. *Computer Methods in Applied Mechanics and Engineering*, 277:1–45, 2014.
- [52] K. Schmidt. *High-order numerical modelling of highly conductive thin sheets*. PhD thesis, ETH Zurich, 2008.
- [53] K. Schmidt and A. Chernov. A unified analysis of transmission conditions for thin conducting sheets in the time-harmonic eddy current model. *SIAM Journal on Applied Mathematics*, 73(6):1980–2003, 2013.
- [54] K. Schmidt and A. Chernov. Robust transmission conditions of high order for thin conducting sheets in two dimensions. *Magnetics, IEEE Transactions on*, 50(2):41–44, 2014.
- [55] K. Schmidt and S. Tordeux. Asymptotic modelling of conductive thin sheets. *Zeitschrift für angewandte Mathematik und Physik*, 61(4):603–626, 2010.
- [56] K. Schmidt and S. Tordeux. High order transmission conditions for thin conductive sheets in magneto-quasistatics. *ESAIM: Mathematical Modelling and Numerical Analysis*, 45(06):1115–1140, 2011.
- [57] T. Senior and J. L. Volakis. Generalized impedance boundary conditions in scattering. *Proceedings of the IEEE*, 79(10):1413–1420, 1991.
- [58] P. Solin, L. Dubcova, J. Cerveny, and I. Dolezel. Adaptive hp-FEM with arbitrary-level hanging nodes for Maxwell’s equations. *Adv. Appl. Math. Mech*, 2(4):518–532, 2010.

- [59] G. Vial. *Analyse multi-échelle et conditions aux limites approchées pour un problème avec couche mince dans un domaine à coin*. PhD thesis, Rennes 1, 2003.
- [60] G. Vial. Efficiency of approximate boundary conditions for corner domains coated with thin layers. *Comptes Rendus Mathématique*, 340(3):215–220, 2005.
- [61] J. Zitelli, I. Muga, L. F. Demkowicz, J. Gopalakrishnan, D. Pardo, and V. M. Calo. A class of discontinuous Petrov–Galerkin methods. Part IV: The optimal test norm and time-harmonic wave propagation in 1D. *Journal of Computational Physics*, 230(7):2406–2432, 2011.